Investigation of the flotation behaviour of ball mill and IsaMill products

Thesis presented for the degree of Masters in the department of Chemical Engineering

By

Tsepang Khonthu

at

University of Cape Town

June 2012

"I know the meaning of plagiarism and declare that all the work in the document, save for which is properly acknowledged is my own."

Acknowledgements

This is not a very easy part for me because I believe that everybody that I have met up to this point has contributed in their own way to me being at this point in my life and hence achieving the things I have so far.

I would like to thank God for the opportunities that I have had, which have gotten me this far in my life.

I would like to thank my mother for the support she offered me throughout my studies. She is a superwoman.

I would like to thank my siblings; you never said much but your eyes said it all.

Thank you to my friends who have believed in me and gave me reason to push to the end; it was pressure but it paid off in the end. Special thanks to my friend who allowed me to stay with him during my thesis writing, Lekometsa Mokhesi. "U entse letsoho la monna, 'meke." God bless you more.

I would like to thank my supervisor Prof. C. T. O'Connor for allowing me to work with him on this project and for his insightful input. I would also like to thank my co-supervisors, Mrs J. Wiese and Dr A. Mainza.

There is not enough thanks to Mr Kenneth Maseko who travelled with me to Mintek and helped with ore screening. Rubin Van Schalkwyk, the trips to iThemba and unblocking the clogged IsaMill pipes could not have been so much fun without you, thank you.

Lorraine Nkemba and Monde Bekaphi, thank you for the induction you gave me on the various equipments in the laboratory. Thank you to the entire CMR staff, you made being part of CMR a prerogative.

I would like to thank staff at Mintek who helped with ore processing: Dr. Johnny Kalala, Tshisikane Patrick, Bongani Mabuza, Teboho Moloane and Amos Sambo, you all did a great job.

I would also like to thank my physics teacher from high school, Mrs Nthabiseng Mobe-Mokhesi, who continues to reaffirm my intelligence.

I would also like to thank the NRF for the bursary through the department of Chemical Engineering.

Finally I would like thank the government of Lesotho for paying my accommodation for the two years of my masters and funding all of my undergraduate studies.

Investigation of the flotation behaviour of ball mill and IsaMill products

Summary

Valuable minerals that are used in various aspects of everyday life are buried in fossilised storages below the ground in the earth's crust. These minerals are mined as rocks which then have to be crushed in order to liberate these minerals of value. The liberated valuable minerals have to be winnowed from the rock powder.

Flotation is the main process which is used in mineral processing to recover valuable minerals. This process uses the differences in surface properties of particles to separate hydrophobic particles from hydrophilic ones.

The strong relationship between the method of crushing the rocks and the amount of valuable minerals which can be reclaimed from the crushed rock has long been realized in mineral processing. The type of mineral, the size to which the rock must be reduced to and the amount of energy needed for this size reduction are among the most important factors which guide the decision on the type of device to be used in pulverising mineral rocks.

Physical properties, with the exception of particle size, of mill products have not been investigated as thoroughly as the chemical properties. Physical properties include surface roughness and particle shape. The differences in shape, between particles produced by different mills, with respect to these properties, have been attributed to differences in the breakage mechanisms in the mills used to grind the particles. There is contradicting literature on the breakage mechanisms that dominate in various mills. This confusion is exacerbated by the fact that different breakage mechanisms occur simultaneously in any one mill.

The definition and determination of particle shape are also difficult. Subsequently, the effect of particle shape on flotation is a subject that is rife with contradictions which add to the complexity of the subject.

This project investigated the flotation behaviour of a base metal sulphide (BMS) ore and a platinum group metal (PGM) ore when these ores were milled using a laboratory horizontal ball mill and an M4 IsaMill. Particle size distribution, shape and mineral composition of the mill products were investigated. Scanning electron microscopy (SEM) and rheology were used to determine the shape of particles produced by the two mills. Batch flotation tests were conducted using mill products obtained after grinding the ores to various degrees of fineness in the mills. The aim was to correlate the flotation behaviour with the physical properties of the mill products.

The particle size distribution of the BMS ore milled in the two mills was similar, with a d_{80} of 57 μm for ore milled for 16 minutes and one pass in a ball mill and IsaMill, respectively; d_{80} of 24 μm for ore milled for 64 minutes and four passes in a ball mill and IsaMill, respectively. Rheological behaviour suggested that the IsaMill products were more irregular in the fine products (4 pass cf. 64 minutes) and rounder in the coarse products (1 pass cf. 16 minutes) compared to ball mill products. Chalcopyrite recovery showed no differences depending on the grinding time within one mill. BMS ore milled in the ball mill (16min) showed higher pentlandite recovery 42 % and grade 1.3 % compared to the same ore milled in the IsaMill (1 pass), with 28 % recovery and 0.7 % grade. The reverse was true for ore milled in the ball mill (64min) and the IsaMill (4 pass). Recoveries were 18 % and 38 % and grades were 0.7 % and 0.8 % for ball mill (64min) and IsaMill (4 pass), respectively.

The IsaMill produced finer PGM ore particles than the ball mill. IsaMill (4 pass) had d_{80} of 26 μm while ball mill (64min) had d_{80} of 43 μm; IsaMill (1 pass) had d_{80} of 80 μm while ball mill (16min) had d_{80} of 89 μm. Rheological behaviour suggested that IsaMill products were more irregular in the fine products and rounder in coarse products than ball mill products. Flotation tests resulted in higher chromite recovery for IsaMill products than for ball mill products, suggesting greater entrainment for IsaMill products than for ball mill products.

The fine IsaMill (4 pass) product of BMS ore showed improved flotation behaviour compared to ball mill (64min). IsaMill product was more irregularly shaped than ball mill product, which indicated the role played by particle shape on flotation. IsaMill (4 pass) product also showed higher Cr_2O_3 entrainment in the flotation of UG2 ore. IsaMill product was still more irregular than ball mill product. This suggests a strong relationship between entrainment and particle shape.

Table of Contents

List of Tables

List of Figures

General Nomenclature

D_i:indicates the size below which a certain i-percentage of solids has accumulated
Mill type (grinding time/ number pass): indicates the mill in which the ore was treated and in brackets is the time for which the ore was milled in case of ball mill or number of passes which ore was passed through the grinding chamber in the case of M4 IsaMill.
Ci: indicates the i^{th} batch concentrate, from i=1 to i=4.
T: indicates bulk tailings
F: indicates the flotation feed
Pi: indicates i^{th} pass of the IsaMill, hence ore milled for i-passes, from i=1 to i=4.
Ch: Chalcopyrite.
Pn: Pentlandite.
Po: Pyrrhotite.

List of Abbreviations

BMS: base metal sulphide
GDP: Gross domestic product
MMZ: Main mineralized zone
PGM: Platinum group metals
PSD: Particle size distribution
SEM: Scanning electron microscopy
SMD: Stirred media detritor
UG2: Upper Group number 2
XRD: X-ray diffraction
XRF: X-ray fluorescence

Chapter 1 NTRODUCTION

1.1 Background

South Africa has a thriving mining industry and is the worlds' largest producer of platinum group minerals (PGM). In 2010, the mining sector contributed 8.6 % of the GDP directly on a nominal basis and employed in excess of 4 980 000 people (Chamber of mines, 2010). PGM and other valuable minerals are embedded in a 65000 km^2 basin located in the Bushveld Igneous Complex which extends from the north-eastern part of the country in Limpopo, north of Pretoria. The complex is a 7 to 9 km thick intrusion of variable mineralisation of the mafic and ultramafic rocks associated with two felsic intrusive suites.

The increasing challenge in mining and mineral processing is the depletion of high grade, coarse-grained ore, leaving low grade and fine-grained ores to be mined and processed. This in turn has raised a challenge to develop new technologies and improve existing technologies in order to grind ores to micron and submicron sizes in order to adequately liberate minerals of value. This challenge mainly affects the regrinding sections of the comminution circuits.

Traditionally ball mills have been used for regrinding purposes. However, ball mills have been observed to have a cut-off size of 40-45 µm. With stirred mills being able to produce particles of smaller sizes with P_{80} of up to 4 µm (George *et al.*, 2004), the choice of ball mills as regrinding mills has been questioned. This has led to various comparative studies between the operation of ball mills and various types of stirred mills. The initial studies focused on the energy consumption when grinding in various mills, with stirred mills shown to be more efficient. Energy is not the only parameter that drives the operation and choice of mills. Ball mills have been shown to be more suitable for coarse grinding while stirred mills are more suitable for fine grinding. Although stirred mills have been shown to be energy efficient, their suitability to coarse grinding and their throughputs have negatively impacted on their choice as a replacement for ball mills in regrinding sections. Therefore numerous studies have investigated the energy expenditure of ball mill operations in fine grinding and stirred mill operations in coarse grinding Shi *et al.* (2009).

These studies showed that energy was not the only indicator of the mill's suitability to a specific grinding operation, and subsequent studies have focused on investigating the impact of the use of different mills during grinding on the downstream processes, especially flotation, which is the main separation process in mineral processing.

Flotation is a complex separation process which uses differences in surface properties of mineral particles to effect separation. The efficiency of the separation is affected by chemical and physical parameters in a flotation cell. The chemical aspects of flotation have been well explored. Various chemicals are used to modify the surface properties of mineral particles in order to enhance separation by flotation. On the other hand, particle size is the only physical parameter which has been extensively researched. As early as 1932, the effect of particle size on flotation performance was already a well-established phenomenon in mineral processing. Gaudin and Malozemoff (1932) postulated the upper particle size limit for which flotation could be efficient as a separation technique. However, they suggested the existence of a lower limit, but stated that the difficulty in establishing such a limit lies within the limitations of the measuring instruments.

Factors which are negligible for coarse and intermediate sized particles become significant for fine and ultra-fine particles. Flocculation and surface charge are among some of the factors that need to be considered in assessing the flotation and comminution performance of fine and ultrafine particles. Particle shape also becomes important in the processing of ultrafine particles as it affects the packing of particles and their rheological behaviour, among other things. In flotation, particle shape has long been suspected to play some behavioural role; however, the determination of its role was difficult due to the lack of definition and measurement of particle shape. Therefore, the phenomenon of particle shape and its implications for flotation have been ignored. However, as particle characterisation in mineral processing has gained importance, researchers have started revisiting past studies and have been making attempts to develop standard definitions of particle shape. These methods defined the size parameters of particles in order to obtain an indication of their shape. The application of scanning electron microscopy (SEM) became common practice in mineral processing whereby particles were imaged using SEM and these images were analysed for size parameters of interest (Hicyilmaz *et al.*, 1995; Hicyilmaz *et al.*, 2004; Yekeler *et al.*, 2004; Hicyilmaz *et al* ,2005)., The results of these studies have, however, been contradictory. Studies have been conducted to investigate the shapes of particles produced by different milling devices and their subsequent impact on flotation performance

The possibility of different mill types producing particles of different shapes has shifted comminution research to a more fundamental level in an attempt to understand the mechanisms of breakage in the various mills. Different operating variables have been investigated to determine their impact on the grinding mechanisms taking place in various mills. Such studies have resulted in different findings by different researchers.

Most of the studies that were undertaken to investigate the characteristics of particles produced by different breakage mechanisms and the effect of these characteristics on flotation performance were performed on pure or synthetic minerals. In this project the behaviour of a base metal sulphide ore and a platinum bearing ore was investigated. The milling devices that were investigated are a laboratory ball mill and a M4 IsaMill.

1.2 Objectives

The objectives of this project were to:

1) Characterise the particles produced by a tumbling ball mill and a stirred bead IsaMill in terms of :
    - Particle size distribution
    - Mineral composition
    - Particle shape which was investigated using Scanning electron microscope (SEM) and rheology.
2) Investigate the flotation behaviour of these particles and
3) Link observed flotation behaviour to particle characteristics.

Chapter 2 LITERATURE REVIEW

2.1 Comminution

The word comminution is derived from the Latin word *comminuere,* meaning 'to make small' (Napier-Munn *et al,* 2005). Crushing and grinding are terms often used in comminution depending on or indicating the size of particles being broken.

Minerals are mined as rocks which need to be broken and ground to fine powders in order to liberate the valuable minerals contained in the ores. A series of size reduction stages occur in order to achieve liberation of valuable minerals. These stages are crushing, conventional grinding (primary and secondary grinding), re-grinding, fine and ultra-fine grinding.

Crushing refers to breaking large rocks. This is achieved using different types of crushers at the first stage of the comminution circuit. Comminution inside impact crushers is dominated by single breakage events. The target size for the crushing stage varies, depending on the ore type and the type of crusher used. Physical principle of impact is widely used in different designs of the impact crushers, such as the vertical shaft impact crusher (VSIC) or the horizontal shaft impact crusher (HSIC). The sizing and design of the impact crushers are based on the feed parameters, such as the material to be crushed, the mass flow, diameter and moisture of the feed material and the desired product parameters such as product particle size and shape distribution. However, often times experience plays a major role in the design of impact crushers (Unland & Al-Khasawneh, 2009). Types of crushing equipment common in size reduction are listed in Table 2.1.1.

Table 2.1.1: Crushing equipment (Coulson *et al.*, 1991))

Coarse crushers	Intermediate crushers	Fine crushers
Stag jaw crusher	Crushing rolls	Buhrstone mill
Dodge jaw crusher	Disc crusher	Roller mill
Gyratory crusher	Edge runner mill	NEI pendulum mill
Other coarse crushers	Hammer mill	Griffin mill
	Single roll crusher	Ring roller mill (Lopculco)
	Single roll crusher	Ball mill
	Pin mill	Tube mill
	Symons disc crusher	Hardinge mill
		Babcock mill

Coulson *et al.* (1991) went further to classify the crushing equipment according to the size of feed and the target product size as shown in Table 2.1.2.

Table 2.1.2: Classification of size reduction equipment (Coulson *et al*, 1991)

Crusher Type	Feed size	Product size
Coarse crushers	1500-40 mm	50-5mm
Intermediate crushers	50-5 mm	5-0.1 mm
Fine crushers	5-2 mm	0.1 mm
Colloid mills	0.2 mm	Down to 0.01 µm

2.1.1 Comminution and energy consumption

Comminution is the biggest energy consumer in the mineral processing operations. As a result, the relationship between the comminution energy and particle size is an important part of minerals processing and a lot of effort has been dedicated to understanding it. As a result, theoretical and empirical equations have been proposed. According to Jankovic *et al.* (2010), Walker *et al.* (1837) proposed a general equation of comminution in 1837, which stated that the energy required for a differential decrease in size is proportional to the size change (*dx*) and inversely proportional to the size to some power.

$$dE = -C\frac{dx}{x^n}$$

In this equation *E* is the net specific energy; *x* is the characteristic dimension of the product; *n* is the exponent; and *C* is a constant related to the material. If *n* is replaced by 2, 1 and 1.5 and then integrated, Walker's equation reduces respectively to the well-known equations of Rittinger, Kick and Bond. Rittinger (1867) as cited in (Stamboliadis, 2007) stated that the energy required for size reduction is proportional to the new surface area generated. This statement is formulated as follows:

$$E = K_1(\frac{1}{x_p} - \frac{1}{x_f})$$

Kick (1885) as cited in (Stamboliadis, 2007) postulated a theory that the equivalent relative reductions in sizes require equal energy. This led to Kick's equation as follows:

$$E = K_2 \ln \left(\frac{x_f}{x_p}\right)$$

Bond (1952) as cited in (Stamboliadis, 2007) proposed the third law of grinding which states that the net energy required in comminution is proportional to the total length of the new cracks formed. This was formulated as follows:

$$E = K_3\left(\frac{1}{\sqrt{x_p}} - \frac{1}{\sqrt{x_f}}\right)$$

The E in these equations is the net specific energy; x_f and x_p are the feed and product size indices, respectively; and K_1, K_1 and K_3 are constants.

Jankovic *et al.* (2010) further stated that in 1962, Hukki evaluated the equations of comminution and concluded that each of them might be applicable for different narrow size fractions. Kick and Bond equations might be applicable for crushing; Rittinger's equation may be used for finer grinding. Hukki (1962) as cited in (Jankovic *et al.*, 2010) then concluded that the exponent in Walker's general equation was not a constant but was dependent on the characteristic dimension of the particle. He then reformulated the equation into the one below:

$$E = -C\left(\frac{dx}{x^{f(x)}}\right)$$

2.1.2 The grinding process

Despite the seeming haphazard nature of grinding, there have been attempts to unravel this process and express it in scientific terms and mathematical models.

One way has been to view grinding as a collection of single stress events, with each event being an action of an applied force on a particle. Therefore, the efficacy of grinding in size reduction depends on the number of stress events, stress number and stress intensity at each event. Stress intensity is the specific energy consumed at each stress event, and the overall energy consumption of the mill is a good measure for the product of stress number and stress intensity. Therefore product fineness can be correlated with either stress number or specific energy input, at constant stress intensity (Kwade, 1999). Stress number can be considered as the number of collisions between grinding media and particle that are necessary to break the particle. The different operating parameters in the mill, especially stirred media mills, affect either stress number or stress intensity and hence mill product fineness. Kwade (1999) stated that viscosity and solids concentration influence grinding media movement and therefore stress number and especially stress intensity, by affecting the probability that one or more particles are stressed at the grinding media contact. Stirrer speed and media size also affect stress intensity and stress number. Higher stirrer speeds at high intensity require small stress numbers to achieve certain product fineness, and vice versa.

Kwade (1999) went further to show that the distribution of the stress number of each individual feed particle and the distribution of the stress intensity, which act at various stress events, determine the product size distribution of the mill. The distribution of the stress intensity is in turn determined by the geometry of the mill, while the distribution of

the stress number is determined mainly by the residence time distribution of the particles in the mill and by the mode of operation (batch mode, circuit mode, one and more passage mode) of the mill.

This shows that the work that has been done on the different types of mills and their operation can be summed up as the differences in distributions of stress numbers and stress intensities in the mills. However, a quantitative diagnosis of these distributions remains a challenge.

Grinding not only reduces particle size, but also changes particle morphology. Frances *et al.* (2001) tracked the changes in the particle morphology with grinding, using four different grinding environments (i.e. four different grinding mills). They used ball mill, jet mill (Alpine 100 AFG), shaker bead mill and stirred bead mill (Drais Perl Mill). The morphological changes were tracked using different quantitative descriptors which characterized shape at different levels, viz., macroscopic, mesoscopic and pseudo 3D descriptors.

Grinding gives a broader size distribution than the starting material, until the grinding limit of the mill is reached, at which point the size distribution narrows (Frances *et al.*, 2001). Frances *et al.* (2001) analysed the changes in the morphological parameters as a function of the median size. For all the mills which they used, they found that circularity and the ratio F_{max}/F_{min} increased with decreasing size, indicating that fragments were more elongated than the initial particles. However stirred bead mill products showed this behaviour only up 10 µm, below which size both circularity and F_{max}/F_{min} decreased, indicating more rounded particles. Ball mill products in the size range 10 – 30 µm were rough, characterized by constant F_{max}/F_{min} and increasing circularity.

Frances *et al.* (2001) performed run-by-run shape analyses of the mill products with time to determine the breakage mode in the mills. The rupture of joints leading to dissociation of crystallites (gibbsite), and chipping and breakage of these crystallites were the primary mechanisms in attrition grinding. Impact stress breakage was a result of sequential rupture and breakage which produced more uniform sized products. Even though they determined the breakage mechanisms for the mills that they used on gibbsite, their results cannot be generally applied as a diagnosis for the mill breakage mechanism, using the mill end product, because their results were based on a synthetic ore. From their work, it can be gathered that grinding mechanism, hence product shape, is dependent on the mill type (Bond, 1954 cited in Frances *et al.*, 2001) and ore being ground and evolves with grinding time in the mill.

2.2 Regrinding technologies

Regrinding a flotation stream avoids sending an overall fine feed to the flotation circuit. This reduces overall energy because only the finely-grained part of the ore is ground to a finer liberation size. Regrinding is considered to produce particles finer than 75 µm down to 30 µm (Jankovic, 2003).

The most common technologies for regrinding flotation streams are the ball mill, tower mill, stirred media detritor and IsaMill. These mills differ in terms of stress and power intensity, media size and flow behaviour.

Ball mills have been used in regrinding for a very long time. However, since the challenge to process fine-grained ores arose, ball mills' suitability to regrind circuits has been challenged. This has resulted in several comparative studies between ball mills and various types of

stirred media mills. The earlier types of these studies were focused chiefly on comparisons of energy consumption and efficiency between ball mills and stirred mills. However, the increasing complexity in ore mineralogy led to studies that investigated the particle characteristics produced by different mill types.

2.3 Fine and Ultra-fine grinding

The stages of grinding can be simply classified according to the target grind size. As a result four stages can be identified: grinding to 80 % passing 75 μm is regarded as conventional grinding since many devices achieve this fineness; grinding finer than 75 μm to about 30 μm, is considered as regrinding; fine grinding produces particles down to 10 μm and grinding below 10 μm is considered ultra-fine grinding (Weller & Gao, 2000; Jankovic, 2003).

On the other hand, the changes that happen to the particles due to grinding can be used to classify the grinding stages. Consequently, the scope of applications of treatment in milling devices can be categorized into three divisions, which are, coarse grinding, fine grinding and mechanical activation. Coarse grinding is mainly a size reduction process while mechanical activation changes structure by mechanical energy. Fine grinding is an intermediate case between the two. Although fine grinding also reduces sizes, it does not allow simple scaling because of its complex physical background. Quantitative changes in particle size bring up qualitative changes in the nature of the process, so producing fine and ultrafine powder particles requires a more fundamental understanding of the physics of mechanical energy relaxation. In this way, fine grinding is analogous to mechanical activation (Boldyrev et al., 1996; Venkataraman & Narayanan, 1998; Pourghahramani & Forssberg, 2005).

Pourghahramani and Forssberg (2005) further indicated that the activation ability of the grinding device is controlled by the frequency of impacts and the modes of stress influence the nature structural changes.

Jankovic (2003) stated a more industrial view of fine grinding:
"The definition of fine grinding varies from one industry to another. For example, the fine grinding criteria for the paint and mining industry are very different. In the paint industry particles finer than 1μm are regarded as "fine" while in minerals processing "fines" are the particles which are difficult to recover in a separation process. Depending on the type of separation process (gravity, flotation, leaching etc.), the size definition of fines ranges from 1mm to below 10 μm."

Fine grinding is becoming increasingly important in comminution because of the depletion of the coarse grained ores and the need to treat the alternative fine-grained, complex ores (Weller & Gao, 2000; Jankovic, 2003; Partyka & Yan, 2007). Main objectives of grinding are to provide material of suitable size for a subsequent chemical or physical process, to provide material with specific surface area and to liberate the constituent minerals in ores as a preparation for downstream separation processes or to promote uniformity of products (Lin, 1998). In fine and ultra-fine grinding, the materials become increasingly resistant to fracture and they tend to aggregate. Most of the grinding device energy input is not utilised for particle size reduction in this region. Size reduction of particles stops at the 'grinding limit', which is determined by the crystalline lattice of particles, preventing formation of any finer particles.

Grinding machines which are suitable for fine and ultra-fine grinding need to have high power intensities to overcome material resistance to breakage and they have to be efficient

so that the power input is used for size reduction. Attrition/abrasion breakage is believed to be responsible for production of fine and ultra-fine particle sizes. These modes of breakage are dominant in stirred media mills. Stirred ball mills combine compressional and torsional stresses, which allow their production of submicron particle sizes (Gao & Forssberg, 1995). Impact breakage is also important for size reduction in tumbling mills. Grinding was traditionally achieved using ball mills. However, with the rising need to deal with fine disseminated ores, traditional mills (ball mills), need to be applied to fine grinding.

2.4 Development of fine grinding technology

Jankovic (2003) said that the mining industry has often been regarded as "conservative" because of its reluctance to accept new ideas. Most of the crushing and grinding equipment used today was developed in the 18th century. Flotation which is the main separation technology in mineral processing was invented in the 19th century. On the other, the introduction of stirred milling technology occurred relatively quickly. The first stirred mills were introduced in 1953 in response to the growing need for fine grinding. Since their introduction, over 400 Tower and Verti mills had been installed around the world by 1999 and the number has been increasing, with stirred mills being the preferred option for regrinding and fine grinding (Jankovic, 2003). The complexity of the ores and depletion of coarse grained has been pushing the mining industry toward fine and ultra-fine grinding regimes. This has led to continual development and improvement of fine grinding technology. Some of the fine grinding equipment used in the mining industry has been adopted from other industries such as cement, paint and pigments.

The most commonly used stirred mills in minerals processing are *tower mills, Vertimills, IsaMills, Svedala detritors, Sala agitated mills* and *ANI-Meprotech SVM mills.* Jankovic (2005) compiled a review paper on regrinding and fine grinding technology. In that paper he outlined a brief history of the development of some of the stirred mills.

2.4.1 VERTIMILL^{R}

Iwasaki Iskoichi invented the Tower mill. Nichitsu Mining Industry Co. Ltd introduced the mill in 1953. . In 1979, two Tower mills were supplied to American Hoosier Power station. The Koppers Company Inc., located in York Pennsylvania adopted the technology in the early 1980's. After that Tower mills were manufactured by MPSI under a license agreement with the Japanese. In 1983, Japan Tower Mill which was founded in 1965 was purchased by Kubota Ironworks Co. Kubota Ironworks Co. then supplied Tower mills as Kubota Tower Mills. In 1991 the MPSI license expired and Svedala Industries got all the rights to the technology but changed the name to Vertimill^{R}.

2.4.2 Stirred Media Detritor (SMD)

SMD is a vertical stirred media mill. A stirred sand mill was developed by English China Clays (ECC) in the 1960's and in 1969 the first production scale machines were installed in a kaolin plant. In 1996, Svedala and ECC signed an agreement which enabled attrition sand mills to be supplied for the Century Zinc Project. The license expanded the following year and allowed Svedala, which is now Metso Minerals Ltd, to manufacture and supply Stirred Media Detritor (SMD^{R}) globally. Over 45 SMD units have been installed in base metal concentrators worldwide since 1998.

2.5 History of Ball mills

Ball mills are one form of tumbling mills. Tumbling mills are horizontal rotating cylinders which contain grinding media and particles to be ground. The mill mass move up the wall of the cylinder as it rotates and falls back to the 'toe' of the mill when the force of gravity exceeds friction and centrifugal forces. Particles are broken in the toe of the mill by collisions between the grinding media and the grinding media and the mill walls. Types of tumbling mills are categorized by the type of grinding media and feed size.

Ball mills are the most common type of tumbling mills. Ball mills are versatile, dominating mineral comminution over a wide size range from a few millimetres to microns. Ball mills are used in primary, secondary, tertiary and regrinding operations. Ball mills have grown steadily in size due to cost and scale factors. Large diameter ball mills used in multi-stage crushers and coarse primary grind in the 1950s and 1960s were replaced by AG/SAG mills in 1970s. However, ball mills are still dominant in the secondary grinding but they are increasingly in competition with closed AG/SAG mill circuits and stirred mills (Nappier-Munn *et al.*, 2005).

2.5.1 Key variables in ball mills

1 Ball mill size and Power:

Ball mill sizes are defined in terms of length to diameter aspect ratios. The most common ratios are 1- 1.5. Ratios of 1:3 to 3:1 are also encountered. Ball mills are among the biggest energy consumers in comminution circuits. Therefore power draw of the mill is an important variable of the mill. Ball mills vary from laboratory mills drawing few watts to big industrial units drawing 10 -12 kW of power. Mill power draw is also dependent on a range of other variables including media surface roughness, mill fill ratio, and slurry density.

2 Ball load and Mill speed:

Ball load is defined as a fraction of the cross sectional area after a grind out (no ore feed) of 10-15 minutes (Napier-Munn *et al.*, 2005). Ball load ranges from 35 to 45 % voidage. Mill speed is expressed as a fraction or percentage of the mill critical speed. The mill reaches critical speed when its centrifugal acceleration balances gravitational acceleration.

3 Media ball size and shape:

The ball size is determined by the hardness of the ore and the size distribution of the feed. Hard ores and coarse feeds require high impact energy and large media. Fine grind sizes require high media surface area and small media (Jankovic, 2003; Napier-Munn *et al.*, 2005; He & Forssberg, 2007; Partyka & Yan, 2007; Shi *et al.*, 2009).

Media shape can be such that to increase media surface area. Shape can also change as media is worn. Media density also affects the grinding efficiency of the mill (Farber *et al.*, 2009). Media with high densities improve the mill's grinding efficiency.

2.6 History of IsaMill

Fine grinding introduces high degree of strain into the mineral lattice, and this in turn improves leaching rates in hydrometallurgical processes (Clark & Burford, 2004). The most commonly used stirred mills are tower mills, manufactured in Japan by Kubota, Verti mill, same design as Kubota tower mill but manufactured by Svedala, IsaMill, developed by

Mount Isa Mines Limited and NETZCH- Feinmahltechnik, Svedala detritor, Sala agitated mill and ANI-Metprotech SVM mills (Jankovic, 2003).

2.6.1 Development of IsaMill

There were a number of operational concerns that arose at Mt Isa which led to the development of the IsaMill. Liberation size was decreasing and amounts of refractory pyrite ore at Mt Isa's lead/zinc concentrator were increasing. Consequently, the metallurgical performance of the concentrator was decreased. From 1975 to 1985, work had been done to regrind ultra-fines to increase mineral liberation using conventional grinding technologies. However, these conventional methods consumed huge amounts of power to grind to the required sizes and the flotation performance was worse than expected. Flotation performance deteriorated because of the iron media that was used to grind. In 1990, test work results showed that horizontal high speed stirred mills would be efficient for grinding up to P_{80} of 7 μm, at laboratory scale. There was also an increase in metallurgical performance. Mt Isa Mines Limited and NETZCH- Feinahltechnik GmbH (NFT) collaborated to develop large scale ultrafine mill. Trial installations at Hilton and Mt Isa lead/zinc were used to test and scale up the mill. In 1994, first full scale IsaMill was installed at the lead/zinc concentrator.

Eleven years since the installation of the first unit at Hilton concentrator, units increased capacity to 13 times from 205kW to 2.6MW. Mill volume had gone up 20 times in this time (Clark & Burford, 2004). On the other hand, autogenous milling technology took 19 years to increase power draw to just 6 times from 1940 to 1959 and this was for a technology that existed since 1907 in the goldfields of South Africa (Weiss, 1985).

In 1998, commercialisation rights were transferred from Mt Isa Mines Limited to MIM technologies. On 14th December 1998, under exclusive agreement with NFT, IsaMill technology was launched to the metal industry as a cheap way of grinding to and below 10 μm (Harbort *et al.*, 1998). There were 27 IsaMills up to 2004, 14 installed in Xstrata mines, McArthur River and Mt Isa and the rest at non Xstrata mines. The mills were installed by Xstrata and Netzsch (Clark & Burford, 2004). IsaMill technology has become industry standard in large scale fine grinding, even though it was only designed to overcome liberation problems at McArthur River. It is suspected that the reason for IsaMill's reception in the mining industry is because it was developed on a mine site.

An approximate 650T/Hr of material was ground by 27 IsaMills worldwide in 2004. This is an equivalent of 5.2 tonnes per annum. Product size ranges from P_{80} of 7 μm to 25 μm for materials lead/zinc sulphides, platinum concentrates, industrial minerals, iron oxide and refractory gold concentrate. 1MT of lead/zinc concentrate is produced by IsaMills in Australia alone, with average material under 15 μm. The IsaMill™ website shows a timeline development of the IsaMill as shown in Table 2.6.1, highlighting the important years in the development of this technology.

Table 2.6.1: IsaMill development

1989	Flotation benefit of inert grinding demonstrated with Netzch 0.75 L mill
1989-1992	Prof. Bill Johnson at MIM worked with Netzch on large horizontal bead mill development
1992	Successful test of 100 litre Netzch mill at McArthur River Mining
1993-1994	Scale up to 3000 litre mill at Mount Isa Mines
1998	Proven, and now essential at MRM and Mount Isa Mines (14 by M3000 IsaMills installed across the two sites)
1999	Commercialisation of the IsaMill™ Technology
2003	Scale up to M10000 IsaMill™ installed at Anglo Platinum's WLTRP
2005	First industrial application of Magotteaux's Keramax MT1™ ceramic media
2009	Development of 8MW M50000 IsaMill™
End of 2009	74th IsaMill™ commissioned with 127 MW of installed power

Once developed, IsaMills were in great demand around the world and they were installed on many concentrators. The cumulative installed power was shown against the years as in Figure 2.6.1.

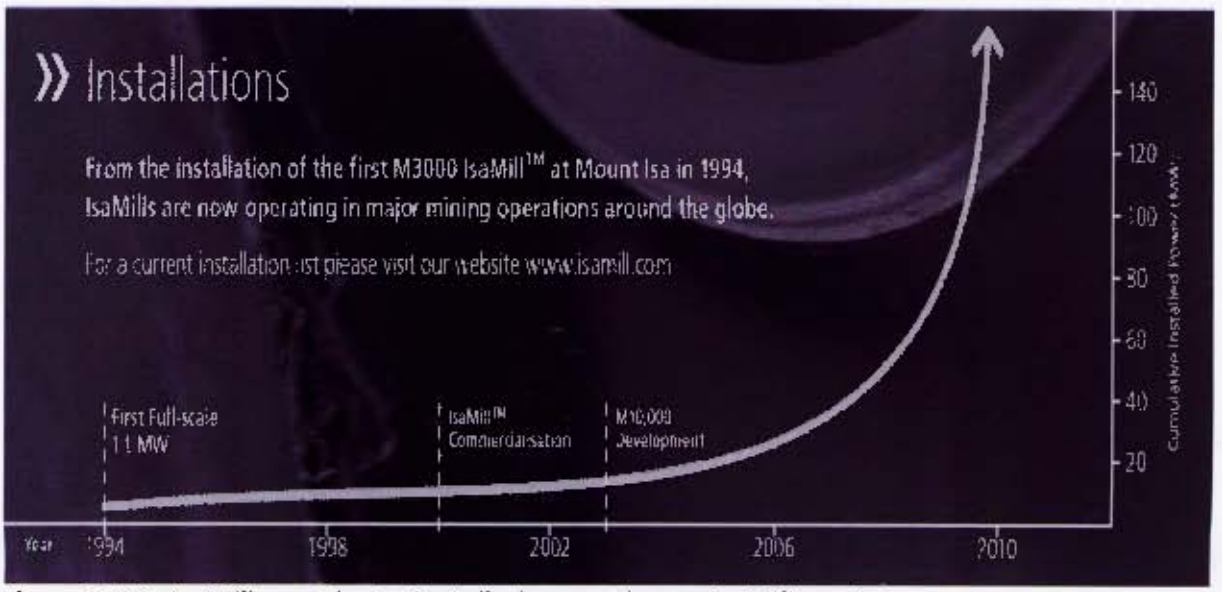

Figure 2.6.1: IsaMill cumulative installed power (www.IsaMill.com)

2.6.2 *IsaMill features and suitability to ultrafine grinding*

IsaMill technology demonstrated its ability for high power efficient grinding to less than 10 µm. The difficulties that needed great investment in time and money were high wear rates characteristic of this kind of operation, and the separation of media from product (Gao *et al.*, 2002).

IsaMill is a large scale, horizontal high-intensity (>300 kW/m^3), compact, continuous ultrafine grinding technology with demonstrated 1:1 scale-up (Harbort *et al.*, 1998). In

comparison ball mills have 20 kW/m^3 power intensities. Inert grinding media are used in the IsaMills. Inert media results in clean mineral surfaces that improve flotation and leach recoveries as compared to grinding with steel media. IsaMill is available in various models which are named according to their net volume in litres, viz. M1000 (355-500 MW), M3000 (1.1-1.5 MW) and M10000 (2.6-3.0 MW).

High power intensities of the IsaMill allow it to process fine particles at high throughput that is important for the economics of the minerals industry. IsaMill has a horizontally mounted grinding chamber shell. The horizontal lay-out allows plug-flow design which avoids short circuiting and makes the mill far less sensitive to process disturbances. The largest shell in 2004 was about 4 m^3. Inside the shell, rotating discs are mounted on a shaft which is coupled to a motor gearbox. The shaft is counter-levelled at the feed inlet end to allow quick and easy removal of grinding chamber to expose the mill internals.

Media and ore particles are continuously agitated by circular grinding discs. The discs of the IsaMill have tip speed of up to 21-23 m/s (Shi *et al.*, 2009). The fine grinding media used in IsaMills make them suited for fine and ultrafine grinding. The size of grinding media which can be used in a laboratory IsaMill is limited to 5 mm by the space between the circumferences of the grinding discs and the mill shell. The fine media increases the probability of collisions between media and ore particles. The mill has been designed to break particles by attrition/abrasion mechanism (Gao *et al.*, 2002). IsaMill is the state of the art in the family of stirred mills that have been developed over time. Various stirred mills are shown in Table 2.6.2.

Table 2.6.2 Power intensity and tip speed of various stirred mills (from Rahal *et al.*, 2011)

Mill Type	Power Intensity (kW/m^3)	Tip speed (m/s)
Tower mill (Vertimill^{TM})	20-40	<3
Vertical Stirred Pin Mill	50-100	<3
Knelson-Deswick Mill	240-765	10-12
Horizontal Stirred Mills	300 1000	>15

Coarse media or ore particles which enter the product separator region are centrifuged towards the shell. The rotor acts like a centrifugal pump, pumping the liquid to the end of the mill. This compresses the media between discs, creating a plug-flow design of 8 consecutive grinding regions which minimises short circuiting. High power intensity yields average residence times of 90 seconds. The short residence times reduce over-grinding of fines. Reduced over-grinding of fines and reduced short circuiting render efficient mill grinding and sharp size distribution in open circuit (Pease *et al.*, 2006). Figure 2.6.2 shows the schematic of the grinding mechanism in the IsaMill.

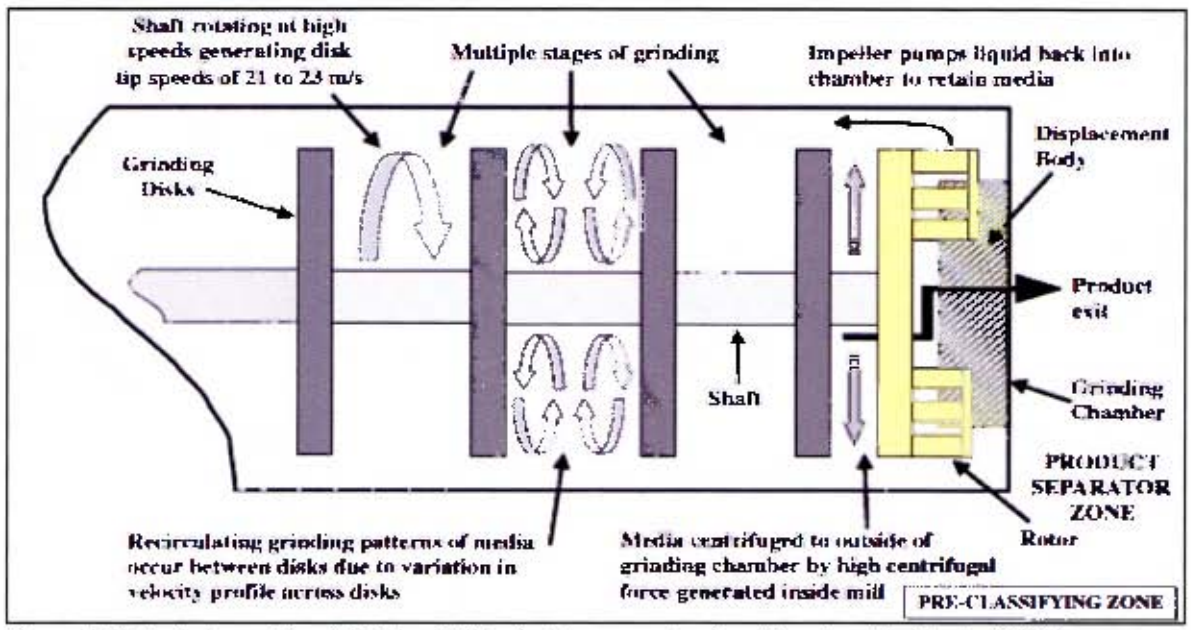

Figure 2.6.2: Schematic of M4 IsaMill grinding mechanism (Burford & Clark, 2007)

2.6.3 Comparison of Ball mill and IsaMill

Comparison of ball mill (tumbling mill) and IsaMill (stirred mill) addresses similarities and differences between these two types of mills. Differences help elucidate on why one and not the other might be suited for a particular operation. Similarities on the other hand, may help on decisions concerning cost and efficiency, if a choice has to be made between the two mills.

Partyka and Yan (2007) proposed the perceived disadvantages that have led to inapplicability of ball mills in fine grinding situations. Firstly, the mill speed has to be less than the centrifugal speed of the mill, otherwise the whole charge body will rotate with the mill and no grinding will occur. This fixes the power draw of the mill, hence reduces efficiency because fine grinding requires high power intensities. Secondly, the empty section of the mill increases as the mill ball size decreases. Finally, a large part of the mill has to be

kept empty to allow the mill charge to tumble. This limits the number of particle-media collisions (impact and attrition events) as opposed to stirred media mills with usual charge of 90% (Weller & Gao, 2000) of the mill volume. However, energy inefficiency was alluded to as the main reason for the inapplicability of ball mills to fine and ultrafine grinding. Despite the perceived disadvantages of ball milling in fine grinding, Partyka and Yan (2007) argued that ball mills still had advantages over stirred media mills. They said that ball mills can be made into large sizes and hence give high throughputs, whereas stirred media mills have size and throughput limitations. On the basis of throughput, they argued that the cost of purchasing, installing and operating one ball mill could be less than that of multiple stirred media mills to achieve similar throughput. Given the long time that ball mills have been used for and the wealth of information available on their operation, Partyka and Yan (2007) believed that ball mills could be made suitable for fine grinding. They gave examples of sites where ball mills were already used for fine grinding in Table 2.6.3.

Table 2.6.3: Some current sites using fine grinding in ball mills (Partyka & Yan, 2007)

Site, Company	Application	Mill dimensions		Media	
		Dia. (m)	Length(m)	Type	Size(mm)
Paging Gold mine, Newmont	Gold (secondary mill) 90 tph, 200-> 38 µm	3.66	4.18	High Cr	25
Germano Iron Ore Concentrator-Samarco, CVRD	Iron Ore 340 tph, 120->32 µm	5.18	10.36	High Cr balls Cylpebs	20-22
Savage River, Savage River Mines	Iron Ore 140 tph, 140-43 µm	3.90	8.80	High Cr balls	25-70
Pena Colorada, Consorcio Minero Benito Juarez	Iron Ore, 125->38 µm	5.00	10.67	30 % Millpeb 70 % ball	4-8 (millpebs)25 (balls)
Beaconsfield, Allstate Exploration	Sulphide conc. Regrind mill 2.5 tph, ->25 µm	1.83	2.44	Cylpebs	22 *22
Tritton copper, Tritton Copper Ltd.	Cu float product, regrind mill 18 tph, 45->30 µm	2.00	3.40	Balls	25
Brunswick Mining, Noranda Mining & Exploration	Cu/Pb/Zn conc. Regrind mill 25 tph, 30->25 µm	3.2OD	4OD	Steel slugs	19
Porgera Gold mine, Placer Done	Pyrite concentrate 80-130 tph, 106->30 µm	3.05 3.05 3.05	4.27 5.40 4.27	Balls	30

High shaft speeds which are common in stirred mills render high energy transfer to mill charge. High speeds that prevail in stirred mills also increase mill capacity (Pilevneli *et al.*, 2004).

Partyka and Yan (2007) studied the effect of ball size on the product size distributions of ball mill in fine grinding situation, for various sizes of feed material. The experiments were conducted with quartz andesite rock. The feeds of 80% passing 55 µm, 100 µm, 500 µm and 1000 µm were used. Sieve sizing was used to get size distributions of the 500 µm and 1000 µm while laser sizing was used for fine feeds. Grinding results were compared according to feed size with the aim of identifying trends. Top ball sizes of 5.5 mm, 9.5 mm, 19 mm and 36 mm were used to the grind the different feeds.

The results showed that all the ball sizes ground the 55 µm and 100 µm to below 40 µm. Small balls of 5.5 mm and 9.5 mm sizes were inefficient for grinding the 500 µm and 1000 µm feeds. They concluded that small ball sizes were suited for fine feeds while larger balls were suited for coarse feeds.

Shi *et al.* (2009) investigated what Partyka and Yan (2007) alluded to as the main reason for ball mills' inapplicability in fine grinding, energy efficiency. They compared the energy

efficiency of ball mills to stirred mills in coarse grinding. Four different ores with four different work indices were used. Batch ball mill and laboratory scale M4 IsaMill were compared for their energy efficiency in coarse grinding. Ball mill non-load and gross power were measured with a digital meter for each test. This determined the specific energy of the ball mill for each grinding cycle. The product size distributions were determined using a combination of sieving sizers and Malvern laser sizer.

Shi *et al.* (2009) presented the "signature plots" for the results they obtained. These are the graphs of net specific energy against grind sizes, P_{80} and P_{98}. The results showed that the laboratory scale IsaMill was inefficient for coarse grinding compared to ball mill. The inefficiency was due to the small grinding media used in the IsaMill, which was only effective for fine grinding by promoting attrition/abrasion grinding.

Ball mills are versatile and typically suited for coarse grinding (Shi *et al.*,2009). When applied to fine grinding, they were inefficient. On the contrary, IsaMill is a horizontal mill which stirs fine inert media at high speed for efficient fine grinding. IsaMill was inefficient for grinding coarse ore. This shows that each mill is efficient only within the range of its design. The comparison of the size and energy consumption of ball mills and stirred mills is shown in Figure 2.6.3.

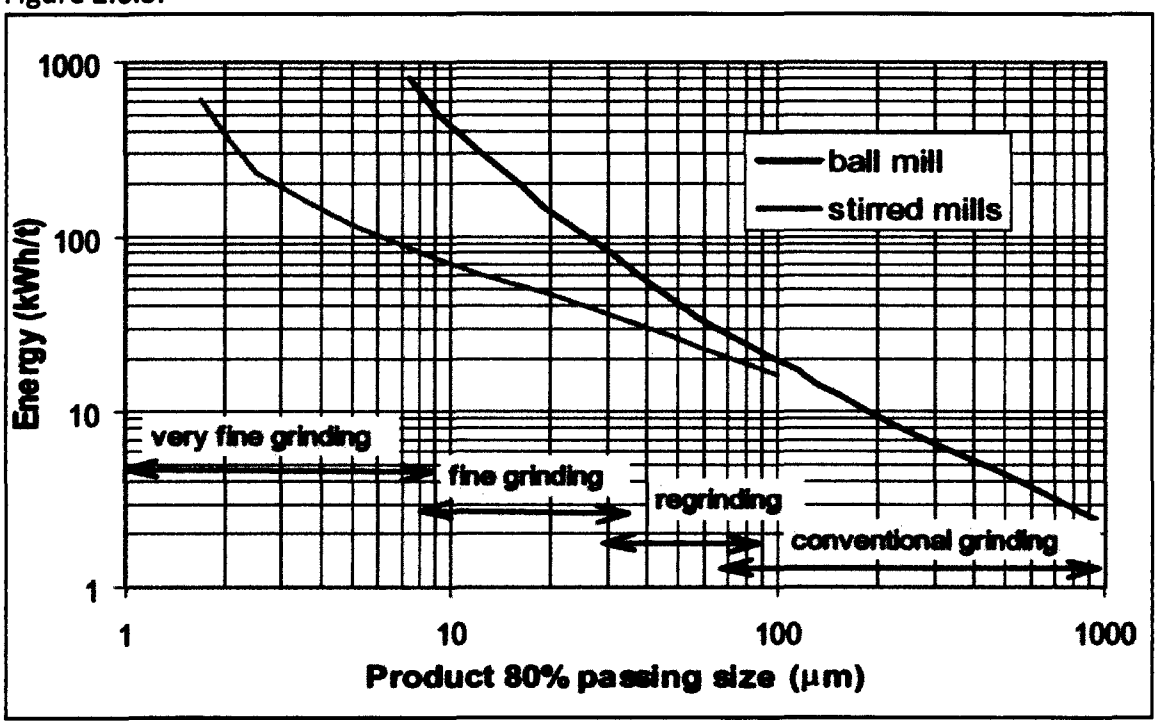

Figure 2.6.3: Size-energy consumption (from Jankovic, 2003)

2.7 Factors affecting the grinding result

The grinding result of a mill is affected by interplay of a myriad of factors. These factors were summarized by (Knieke *et al.*, 2010) in a schematic shown in Figure 2.7.1.

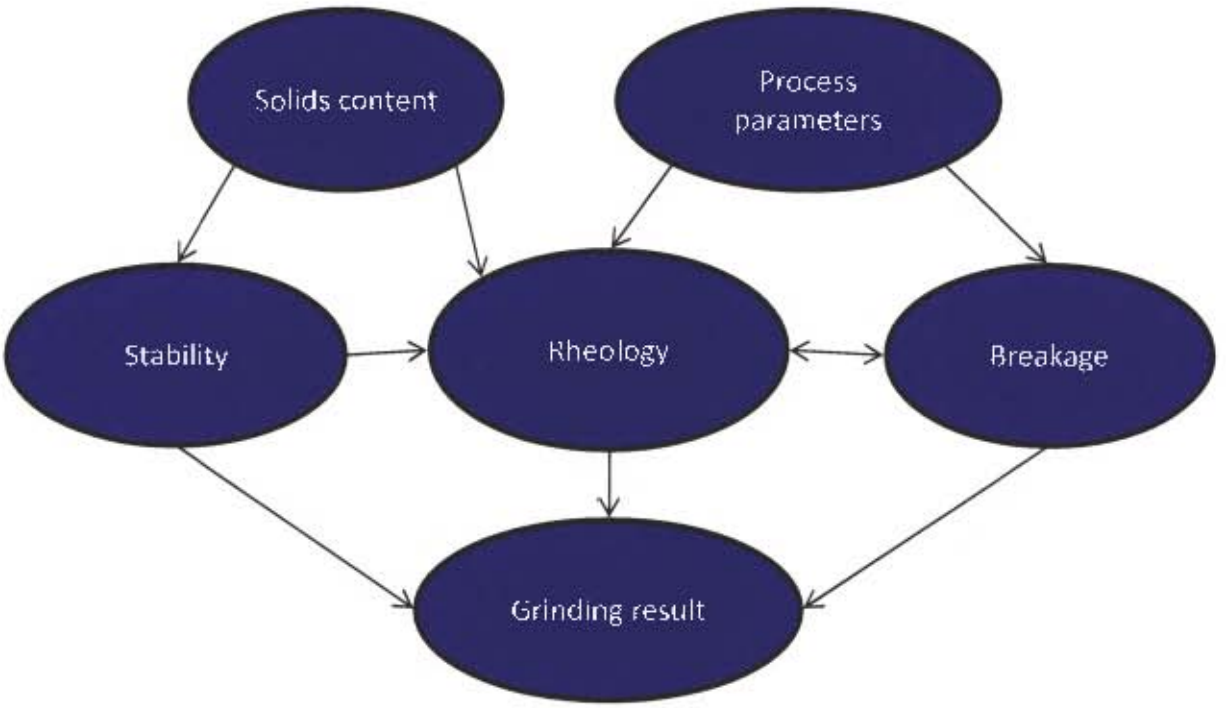

Figure 2.7.1: Factors influencing grinding result (Knieke *et al.*, 2010)

2.7.1 Process parameters

Various process parameters become important, depending on the target product size of the mill. Mill speed is crucial for breakage of coarse particles, while media size becomes very important for the production of fine particles. A brief outline of some of these parameters and how they affect the grinding result follows.

2.7.2 Effect of slurry rheology on grinding

Rheological behaviour of the ground slurry plays an important role in the resulting particle size distribution of the mill product. For a long time, plant operators have observed that controlling slurry flow properties was important for the development of improved wet grinding operating conditions (Klimpel, 1999). Slurry rheology is intimately linked to the solids content of the slurry and the temperature of the slurry. Grinding aids also play a pivotal role in slurry rheology. The effect of grinding aids on grinding result has been mainly explained through two mechanisms. One was based upon the alteration of surface and mechanical properties of the individual particles such as reduction in surface energy and the other was to consider the arrangement of particles and their flow in suspensions (El-Shall, 1984).

Barnes (2000) summarized the interactions that affect viscosity in a suspension in Figure 2.7.2.

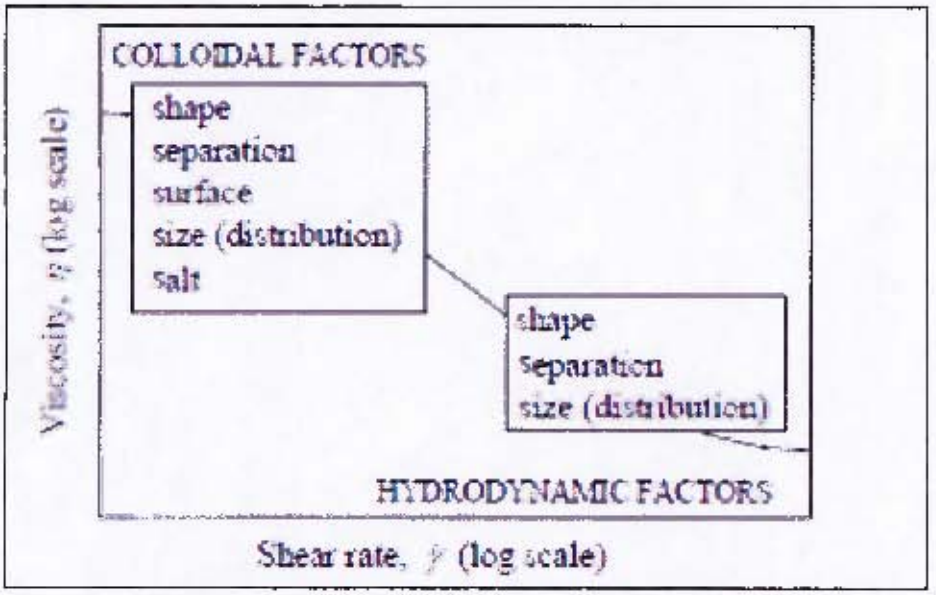

Figure 2.7.2: Flow curve of a suspension of colloidal particles

Factors that are negligible in coarse grinding become controlling in fine and ultrafine grinding. A total of 44 parameters have been identified to affect grinding in stirred media mills (Jankovic, 2003). Most of them are regarded as unimportant. Rheology of the mineral slurry is indicative of the inter-particle interaction or aggregation in the slurry (He *et al.*, 2004; Ding *et al.*, 2007; He & Forssberg, 2007). Rheology describes the relationship between shear stress and shear rate for fluids and slurries (Yue , 2003), with slurry rheology being dependent on the breakage mechanism (He *et al.*, 2004; Ding *et a.l*, 2007).

Rheological behaviour of the slurry is affected by solids concentration, particle size distributions, the chemical environment and the inherent breakage properties of the ore. The work that has been done on the effects of slurry rheology on fine grinding has shown that pseudo plastic slurry behaviour gives "optimum" grinding conditions (Yue, 2003). Dispersants extend the pseudo plastic region and narrow the mill product size distribution. Narrow size distribution has been reported to increase the flotation performance (Pease *et al.*, 2006).

An increased maximum packing fraction of the system leads to lower viscosities and vice versa (Greenwood *et al.*, 1997).

2.7.3 Solids Concentration

The solids content of the slurry in wet grinding affects the particle-particle interactions in the mill during grinding. In fine grinding, multiple particles are simultaneously stressed between collisions of grinding media. The actual number of these particles depends on a number of parameters, for instance, particle concentration, approaching velocity of the grinding media, the fineness and the viscosity of the suspension (Bernhardt *et al.*, 1999).

He and Forssberg (2006) investigated influence of slurry rheology on stirred media milling of limestone. Their results showed that solids concentration in the mill affected viscosity and specific energy input of the mill. Slurry rheological behaviour changed from dilatant to pseudoplastic as solids concentration increased. Their explanation of these results was that in dilute slurry, i.e. low solids concentration, inter-particle distance was so large that the particles were not subjected to attractive forces and they were free to move as individuals.

Higher solids changed slurry flowability to pseudoplastic. This indicated that interparticle forces predominated over hydrodynamic forces in the lower range of shear rates.

Solids concentration was also shown to affect the energy efficiency of the mill. Grinding in a stirred media mill is determined by the number of stress events and the intensity at each stress event. Energy is efficiently used for grinding when the intensity at each event goes into size reduction and this in turn relies on particles being caught between the colliding grinding media. He & Forssberg (2006) observed that the cumulative specific energy input to the mill increased first and then decreased with increasing solids concentration. This was attributed to the fact that at low solids concentration, there were large inter-particle distances which made it difficult for grinding beads to effectively capture particles. This increased possibility of direct collision between beads and hence high energy loss. However, high solids concentrations (high viscosity), above 70 % wt., impeded the motion of grinding beads and decreased velocity and kinetic energy of the beads.

Bernhardt *et al.* (1999) showed that energy utilization of the mill was independent of the energy consumption for low solid concentrations whereas it reached a maximum at higher solid concentrations. The maximum energy utilization at high solid content was at small energy consumption. Jankovic (2003) attributed the increase in efficiency at higher solids percentage to a drop in power draw due to buoyancy effects and the increase in the number of particles in the mill. The maximum was also explained to be a result of two effects: at low energy consumption (short grinding time), the number of particles increased with grinding, the stressing conditions became better and with it thus energy efficiency increased. The number of particles reaches a point where they increase the viscosity of the slurry and retard the motion of the grinding media. This reduces the energy efficiency of the mill. This observation is similar to what He and Gao (2007) found.

Yue (2003) and Ding *et al.* (2007) investigated variation of slurry yield stress with solids concentration. They all found that apparent viscosity varied exponentially with solid content of the slurry. Ding *et al.* (2007) also found that the product particle size decreased with increasing solid concentration, in agreement with Pease *et al.* (2006). The major mode of breakage in stirred media mills is attrition/abrasion particle breakage and it depends on the number of particle-particle and particle-media contact. Therefore slurry particle concentration and media charge are expected to play a big role in the grinding efficiency of stirred mills, since they both increase the probability that a particle will be broken (Jankovic, 2003). The work done shows that grinding efficiency in stirred media mills increase with increasing solid concentration (Bernhardt *et al.*, 1999; Jankovic, 2003; Yue, 2003; Ding *et al.*, 2007; He & Forssberg, 2007). The variations of the respective results are due to the type and concentrations of dispersants. Bernhardt and co-workers concluded that the role of solids concentration in slurry can be used to explain some of the discrepancies in literature on rheology.

2.7.4 Chemical environment (dispersants)

Dispersants are important in ultrafine grinding. A dispersant changes the surface nature of particles in ground slurry, resulting in inter-particle forces being repulsive, thereby increasing slurry flow ability (He & Forssberg, 2007). Smaller amounts of dispersants give higher energy efficiencies and require smaller media sizes at low specific energy input. However, excessive dispersant amounts could form a cushion layer around the milling beads

and therefore lower stress intensities from the collisions of the beads, resulting in inefficient milling operation (He *et al.*, 2006).

2.7.5 Media bead size, density and distribution

Jankovic (2003) investigated the effect of media size on the grinding efficiency, using three narrow media size fractions (-1.7 mm + 1.2 mm, -1.2 mm + 0.85 mm and -0.85 mm + 0.60 mm). These were used to grind coarse (F_{80}~ 46 µm), medium (F_{80} ~ 20 µm) and fine (F_{80} ~ 10.3 µm) feeds, in a high speed Netzch mill. For both coarse and medium feeds, coarse media (-1.7 mm + 1.2 mm) was more energy efficient and fine media (-0.85 mm + 0.60 mm) was the least efficient, with fine media using 40 % and 14 % more energy for coarse and medium feeds respectively to achieve the same P_{80}. On the other hand fine media was more efficient at grinding fine feed, requiring 37 % less energy than the coarse media. The general conclusion was that coarse media was suited for grinding coarse feed and fine media for fine feed (Wang & Forssberg, 2000; Yue, 2003; Partyka & Yan, 2007).

Although there is a general agreement on the effects of media size on ball mill operation, Erdem and Ergün (2009) pointed out that there was no agreement on how ball size affected grinding kinetics. This, they said, was despite a lot of data published in literature, as most of the data was obtained for small diameter laboratory mills. There is doubt surrounding the minimum mill size suitable for studying the effects of media size on grinding kinetics. However, media size effects have been observed to be negligible in mill sizes below 0.2 m.

Farber *et al.* (2009) investigated the grinding efficiency of ceramic media with varying ZrO_2 and Al_2O_3 composition for high energy milling (M4 IsaMill). Additional to the dependence of grinding efficiency on ball size, ball density was also found to play a major role. This shows that the effects of operating parameters, e.g. ball size, are similar across all mill types as the results concur with what Partyka and Yan (2007) observed. Results from studies that investigated different mill operating parameters can be used to design experiments for optimum mill grinding efficiency, especially for comparative studies. Ball mills have been tested for fine grinding applications and size reduction was achieved after long residence times, which impacted negatively on the flotation performance of the product due to steel grinding media (Partyka & Yan, 2007). Farber *et al.* (2009) went further to show that mill power consumption was also affected by the surface roughness of the grinding balls. Balls with smooth surface consumed less power than rough balls. They showed that factors which affect power consumption to a large degree are friction coefficient and bead density. These are the factors that should be considered for efficient grinding which would be conducive for downstream flotation.

Jankovic (2003) showed that the effects of the different parameters on the energy efficiency of the mill were not consistent even in one mill. The inconsistencies are a result of the interactions between the parameters. Stress intensity (SI_m) has been identified as one parameter which encapsulates the effects of mill tip speed, media size and density (Jankovic, 2003).

$$SI_m = D_m^3(\rho_m - \rho)v_t^2$$

Variation of P_{80} with stress intensity for different media size, at 20 kWh/t, is shown in Figure 2.7.3.

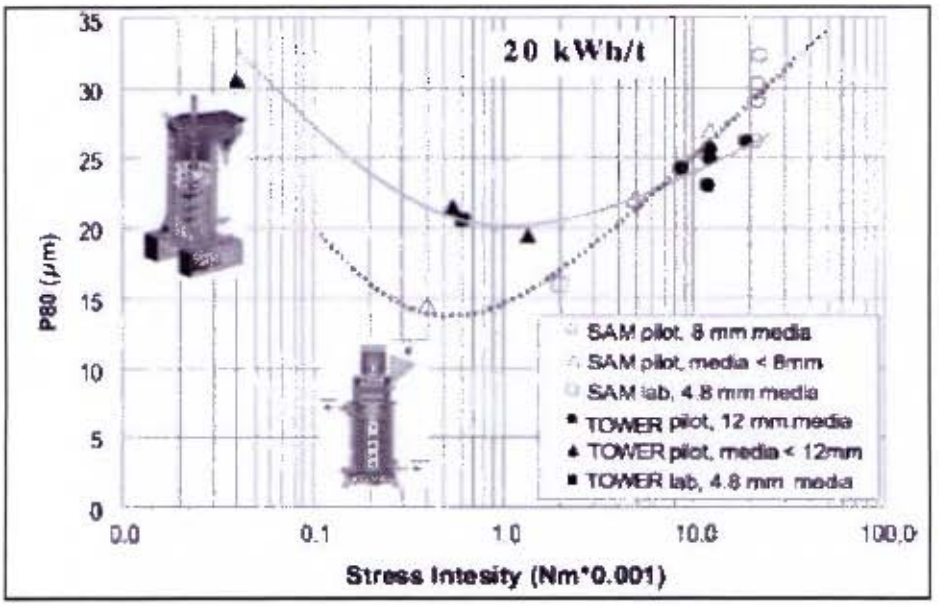

Figure 2.7.3: Variation of P_{80} with stress intensity (from Jankovic, 2003)

Yue (2003) performed tests to investigate the effects of bead size on particle breakage rate, product size and size distribution and agitator power consumption. At constant agitator speed, breakage increased linearly with bead size and at a constant mill power, breakage rate went through a maximum at a particular bead size (2 mm) for the feeds used (F_{80}=32 µm and F_{80}=83 µm).

Media bead size distribution, the choice of which depends on feed size distribution, plays an important role on energy efficiency of grinding. Theoretically, charge load mass can be increased at constant load volume by changing the bead size distribution. The packing density of the grinding media increases when the voids between large beads are filled with smaller beads, resulting in a bimodal bead size distribution (Yue, 2003). Bimodal bead size distribution gives a minimum viscosity of the suspensions at a constant solids concentration, which implies that bimodal bead size distribution would require minimum power draw. Yue (2003) varied bead composition from 0% fine (0.5 mm) and 100 % coarse (2 mm) to 100 % fine and 0 % coarse. The results showed that fine beads in grinding media of stirred mills had negative effects in particle breakage rate, product size and size distribution. He ascribed the effects to the lack of sufficient stress intensity in the stirred mill as beads became smaller. Stirred mills rely on the kinetic energy, high speed and necessary mass of the media to break particles. Therefore small media may not have enough kinetic energy, hence exert enough stress intensity on the particles a certain circumferential speed. On the contrary, fine beads in a ball mill can break through tumbling and rolling.

2.8 Particle shape characterisation

Prasher (1987) gave a comprehensive account of particle shape, referring to available literature on the subject. He started by outlining the importance and role of particle shape in various industrial applications. He then quoted different attempts at the definition of particle shape. Finally he discussed the relative importance of machine and material type in determining shape of the product particles.

Particle shape analysis techniques can be classified into two categories, behavioural and image analysis. In behavioural systems, particle shape is inferred from the behaviour of

particles in some physical system or apparatus, while image analysis techniques rely on examining of two-dimensional image or silhouette of the particle (Clark, 1986). Shape and morphological characterization of particles are based on the analysis of the silhouettes of the particles or their projection (Yekeler *et al.*, 2004). The particle projections are assumed to have elliptical shape and shape factors are defined to describe different aspects of the particle shape. Common shape factors are elongation, flatness, roundness, relative width, circularity, sphericity, chunkiness, external compactness and aspect ratio (Hicyilmaz *et al.*, 1995; Xu & Di Guida, 2003; Yekeler *et al.*, 2004; Ahmed, 2010).

2.8.1 Qualitative definitions of particle shape

Qualitative description of particle shape was adopted from the British standard 2955 of 1958, as shown in Table 2.8.1.

Table 2.8.1: Qualitative definitions of particle shape

Shape	Definition
Acicular	Needle-shaped
Angular	Sharp-edged or having roughly polyhedral shape
Crystalline	Of geometric shape, freely developed in a fluid medium
Dendritic	Having a branched crystalline shape
Fibrous	Regularly or irregularly thread-like
Granular	Having approximately equidimensional but irregular shape
Irregular	Lacking any symmetry
Modular	Having a rounded irregular shape
Spherical	Globule shaped

2.8.2 Quantitative definitions of particle shape

2.8.2.1 Fundamental Concepts

Although qualitative definitions are valuable, scientific shape assessment requires mathematical formulation of the definitions. Prasher (1987) noted that the difficulty of defining particle shape was recognized as early as 1937 by Heywood. The general term 'shape' implies geometrical form and the relative proportions of length L, width W and thickness, which are two distinct characteristics. The size parameters can be normalized into W/L and T/W, which when combined with the geometrical form give three factors essential for definition of shape.

2.8.2.2 Shape Factors

There are many different shape factors. Martin (1923) as cited in Prasher (1987) postulated ideas on some of these factors. Heywood as cited in Prasher (1987) extended these ideas in 1937 and 1947. He brought the idea of spheres of equal volume and equivalent surface to irregular particles. The area of an image of a particle rested on its stable position is assessed and the diameter x_H measured. The volume is defined by:

$$V = k_H x^3$$

k_H is the volume constant for the particles. Surface area is defined as:

$$A = f_H x^2$$

F_H is the surface constant. Volume and surface factors can be combined to give a shape factor which is a ratio of f_H / k_H. Values of some of these factors for square-ended prisms were excerpted from Heywood (1933) as cited in Prasher (1987) and are shown in Table 2.8.2.

Table 2.8.2: Shape factors for square-ended prisms (from Pasher, 1987)

Description	L_2/L_1	F_H	K_H	F_H/k_H
Flat tablet	0.1	1.885	0.0696	27.08
Flat tablet	0.4	2.827	0.2784	10.16
Cube	1.0	4.712	0.6958	6.77
Long prism	5.0	3.454	0.3112	11.10
Long prism	10.0	3.298	0.2202	14.98

Similar results to those in Table 2.8.2 have been obtained for cylinders, spheroids and octahedra of different dimensions. These led to the following general conclusions:

- When the dimensions of a particle are approximately the same in three dimensions, the shape factor has a minimum value.
- When the shape is either elongated or flattened, the shape factor increases.

Prasher went further to explain shape indices such as the flakiness, elongation and angularity, which are not included here.

2.8.3 Image analysis methods of shape characterization

2.8.3.1 Basic principles

The advent of image analysers and the concomitant computer techniques offered tools to the study of particle shape. However the initial studies were bogged down by the number of particles that could be analysed. Analyses of large number of particles required a lot of time and the representativeness of the results obtained was dubious.

The procedure as described by Prasher (1987) was to photographically fix an image of the particle with a microscope and analyse it with a stylus pen (graf pen) digester and a microcomputer. The image could then be transformed into N points and digested in terms of either Cartesian or spherical coordinates.

Despite the acknowledgement of the importance of particle shape, the longstanding difficulty remains with defining particle shape (Riley, 1968; Carter & Yan, 2005).

Meloy *et al.* (1979) as cited in Ulusoy *et al.* (2003) said particle shape characterisation had the potential to become an important analytical technique to virtually all branches of applied science, engineering, metallurgy and ceramic in both academic and industrial environments. Today, various techniques are used to characterise particle shape.

2.8.4 *Effect of Particle Shape on Size Analysis*

Frances *et al.* (2001) noted that particle shape cannot be considered independently of particle size in a grinding process. The interdependence of these physical properties of a particle poses a challenge when determining either parameter. Single parameter descriptions of physical dimensions of micro-particles are insufficient for the stringent quality control requirements in various industries. Often, sizing results from different technologies are compared without acknowledging the effects of the analysis principle of the instrument and particle shape (Xu & Di Guida, 2003).

Different size measurement methods express particle size as an "equivalent sphere diameter". Consequently, different methods, such as sieving, sedimentation and light scattering, give different apparent sizes for the same particle. These discrepancies increase as the particle shape deviates more from a sphere. Particle orientation can also augment these discrepancies (Hogg *et al.*, 2004).

The relationship between particle size and particle shape has been a longstanding challenge. Imaging based approaches have been used in the past to investigate shape quantification. However, it was often assumed that the imaging systems were insensitive to the variations in particle size (in relation to shape), and therefore that shape quantification was independent of particle size (Carter & Yan, 2005).

Xu and Di Guida (2003) sized particles of different shapes using three sizing techniques. The technologies used were laser diffraction (LD), electrical sensing zone (ESZ) and dynamic image analysis. Different sizing techniques use different principles for measurement. These techniques give apparent particle sizes and not the real dimensions of the particle. The common practice in characterizing particulate materials is to compare results obtained from different technologies. Often the results are erroneously expected to be the same, neglecting the differences in analysis principles and the shape effect. They concluded that for spherical and non-spherical particles with small aspect ratios, there was good agreement between the sizing methods. On the other hand, laser diffraction produced oversized size distributions and exaggerated distribution broadness due to particle orientation effects and deviation from the spherical models used in data processing.

2.9 *Breakage Mechanisms*

Mills are classified according to the breakage stress mechanisms in the mill, which are, attrition, compression, shear, impact and internal forces. However, these mechanisms invariably occur in pairs or more in a mill. Hence three modes of breakage are defined, which are abrasion, chipping and impact breakage (Frances *et al*, 2001; Hicyilmaz *et al.*, 2005). The grinding mechanism depends on the material properties, such as the particle tensile strength and size, and on the orientation and intensity of the forces exerted onto the particles (Hennart *et al.*, 2009). Kelly and Spottiswood (1990) and Hennart *et al.*, (2009) represented the different breakage mechanisms and the product size distribution resulting from them, as shown in Figure 2.9.1.

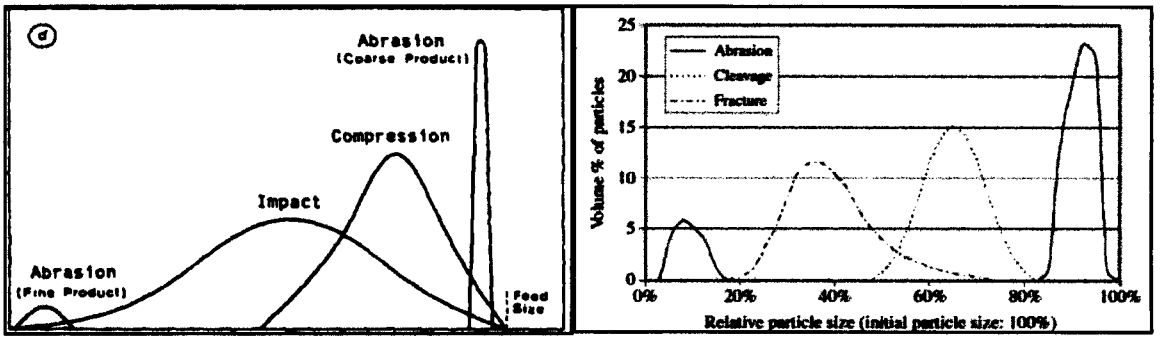

a) b)

Figure 2.9.1: Representation of product size distributions from different mechanisms (a) (Kelly & Spottiswood, 1982), (b) (Hennart et al., 2009).

Literature that relates the particles breakage mechanisms in the mills to the change in mineral surface properties appears to be scarce (Ye *et al.*, 2010). As shown in Figure 2.9.1, the only literature available on this subject is highly qualitative and the qualities of the progeny of different grinding mechanisms are vaguely defined.

2.9.1 Breakage Mechanisms in Stirred Media mills

The fragmentation mechanism in stirred mills results from torsional and compression stresses (Gao & Forssberg, 1995). The dominant breakage mechanisms in a mill play a big role in influencing the properties of the mill products. Bilgili *et al.* (2006) noted that there was a clear and emerging need to understand dynamics of nano-milling processes and the breakage mechanisms involved. This need is not limited to nano-milling but extends to all comminution processes.

Hogg (1999) developed simulations of attrition and massive fracture mechanisms and of the combinations of the two. Massive fracture occurs when the overall stress acting on a particle exceeds some critical value and results in disintegration of the particle into smaller fragments. Attrition is associated with smaller applied stresses for which the critical value is only exceeded on the edges and a particle retains its identity with a slow continuous loss of mass. His results showed that massive fracture broadened the size distribution of the mill product until a certain form, determined by breakage distribution, is reached. However, the distribution shifts to finer sizes as grinding continues. On the other hand, attrition was shown to give bimodal size distributions. The coarse mode shifted slowly toward finer sizes as a result of convective transfer and decreased in magnitude due to loss by direct transfer. When a combination of the two methods was simulated together, the form of the breakage mechanism did not affect the product size distribution. Contribution of attrition to the overall breakage rate led to acceleration of the process and appearance of non-first order breakage. These different breakage mechanisms were explained explicitly in Hogg's (1999) paper. However, a quantitative measure or determination of the dominant mechanism or pair of mechanisms still remains a difficult task.

The main problem regarding a quantitative approach toward determining breakage mechanisms in grinding mills is that the definitions of breakage mechanisms are qualitative. Based on the universal definitions of the different possible breakage mechanisms in mills, image analyses techniques may actually be a suitable approach toward the study of

breakage mechanisms in mills. More conclusive studies of particle shape will depend on the advancement of image analysis techniques.

Yue and Klein (2005) determined the breakage rates on the +97 μm and +64 μm size fractions of quartz in Netzsch LME 4 horizontal stirred bead mill. The results showed first-order breakage kinetics, increasing breakage rate with decreasing solids content and decreasing breakage rate with decreasing particle size. The first-order breakage kinetics imply that the main mechanism in the horizontal mill is massive fracture, with attrition playing a minor role (Kwade, 1999; Yue & Klein, 2005). These results contradict the common perception that ultrafine product in horizontal stirred bead mills is due to attrition, whereas attrition, abrasion and impact were shown to exist in stirred media mills (Kwade, 1999; Kwade & Schwedes, 2002). It is therefore important to determine the dominant breakage mechanism in the mill, since this affects the product shape and the subsequent flotation behaviour. A curve of breakage rate against particle size can be used to determine the different breakage mechanisms in the mill, with linear curve indicating massive fracture and non-linear curve indicating attrition. Yue and Klien (2003) assessed the particle size distributions of the mill product after each cycle for three cycles. Massive fracture was the main mechanism for the first two cycles; attrition became dominant as the grinding limit was approached. Yue (2003) devised experiments to determine the dominant breakage mode in stirred mills between attrition and massive fracture. He used grinding media size of 2mm (coarse) and 0.5 mm (fine). He then varied the composition of the grinding media from 0 % fines and 100 % coarse to 100 % fines and 0 % coarse. He observed that breakage rate decreased as fine media percentage increased, which implied that attrition was not the dominant mechanism. Instead massive fracture was the main mechanism.

Zhang and Kavetsky (1993) developed a mill content size dependent method to investigate particle breakage mechanisms in a batch mill. Their method fitted batch ball milling data better than some of the previously established size-invariant models. Their results went further to show that, not only were different size particles broken by different mechanisms, but also different breakage mechanisms were employed for same size particles of different materials.

Hennart *et al.* (2009) identified the grinding mechanisms and their origin in a stirred ball mill using population balances. They observed that coarse particles (15 μm) were broken by cleavage and some fracture, intermediate particles (0.8 μm) by cleavage and abrasion while fines (< 0.15 μm) were broken by cleavage. On the other hand, Gaudin (1926) as cited in Kaya *et al.* (2002) observed that large particles were often primarily subject to attrition, tending to become more rounded in shape, while finer material underwent massive fracture leading to more angular product particles. This observation concurred with what Durney and Meloy (1986), as cited in Kaya *et al.* (2002), observed in their results. Literature on operative breakage mechanisms inside mills is rife with these contradictions.

Pilevneli *et al.* (2004) held the view that breakage in stirred mills occurs through abrasion. They stated that stirrers transfer their high kinetic energy to surrounding media in radial direction and their rigid structures enhance abrasive and shear forces rather than impact and compression. High stirrer speeds increase both frequency and intensity of the breakage events.

These contradictions on dominant breakage mechanisms, in various mills types, permeate literature on the determination of breakage mechanisms inside grinding mills.

2.9.2 Breakage mechanisms in tumbling mills (ball mills)

Breakage kinetics inside mills play a significant role in studying the kind of breakage mode dominant in that mill. Most of the modelling related to mill operation is concerned with breakage kinetics inside mills (Tangsathitkulchai, 2002; Choi & Choi, 2003; Fuerstenau *et al.*, 2003; Yue & Klein, 2005). Batch grinding is treated as first order chemical reaction. These studies have been based on the linear batch grinding kinetic model for batch milling in tumbling mills. The particle size distribution of the feed to the mill is segmented into n number of size classes starting from the top size to a size below a suitable screen size. The model assumes that the rate of disappearance of particles in a certain size class is proportional to the amount of that size remaining. This is expressed as:

$$\frac{dw_j(t)W}{dt} = -S_j w_j(t)W$$

Where $w_j(t)$ is the mass fraction of size j particles in total powder charge W at time t and S_j is the specific rate of breakage of size j. When a rate-mass balance is performed on the above equation, incorporating the primary breakage distribution, the following equation ensues.

$$\frac{dw_i(t)}{dt} = -S_i w_i(t) + \sum_{j=1}^{i-1} b_{ij} S_j w_j(t), n \geq i \geq 1$$

This is the basic size-mass balance equation for a first-order grinding system. Solution of the resulting n set of differential equations predicts particle size distribution at various grinding times, for a given feed size $w_i(0)$, S_j and b_{ij}.

Tangsathitkulchai (2002) analyzed disappearance kinetics of single size fractions using dry and wet grinding. Plots of weight fraction retained in top size against grinding time had linear relations, suggesting a constant specific breakage rate for dry grinding tests. Similar plots for wet grinding tests showed a deviation from this linear relation, with the top size disappearance rate increasing as fines accumulated in the mill charge.

2.9.3 Effect of breakage mechanisms on particle shape

The shape of particles produced by comminution is affected by the breakage mechanism that is involved. Furthermore, the techniques used to determine product particle size are also influenced by particle shape (Hogg *et al.*, 2004). Frances *et al.* (2001) pointed out that the fragmentation mechanisms, induced by the process used, and the initial texture of the particles determine the particle shape at a given size.

The shape of comminuted particles is affected by the breakage mode/ stress in the mill. But it is often difficult to discriminate between the types of stress since a combination of at least two of them occurs simultaneously in a mill (Ulusoy & Kursun, 2011). Characterisation of particle shape is important not only as a process parameter but also because of potential health hazards of some particle shapes, especially fibres (Pabst *et al.*, 2007).

Frances *et al.* (20001) referred to the conflicting conclusions with regards to the relative importance of material type and machine type on the shape of milled particles. They said that many researchers conclude that mill type is more important in determining the shape of the particles than ore material or character.

Kaya *et al.* (2002) reported that shape of particle was expected to be affected by the type of machine, by the breakage mechanism in a grinding device and by time spent in the grinding environment. Yekeler *et al.* (2004) further stated that character of the material and the type of mill used, determine the shape of particles produced. They used Bleuler ring-and-puck pulveriser and planetary ball mill to investigate effect of grinding device on shape. Grinding times were set so as to give similar extent of grinding for each mill. They found that high energy grinding machines (stirred mills) produced a large proportion of newly created particles. This favoured formation of particles of irregular shape. On the other hand, grinding mills with low energy (tumbling mills) used repeated breakage action to reduce particle size and this promoted round-shaped particles.

As alluded to above, grinding not only reduces particle size, but different grinding mechanisms also induce considerable changes in the morphological properties of the particles (Hicyilmaz *et al.*, 2005). Particle surface area, roughness and particle acuteness are among some of these changes. Hicyilmaz *et al.* (2005) used autogenous mill and ball mill to investigate the effect of grinding mechanism on particle morphology of barite ore. They used BET nitrogen adsorption technique to measure surface roughness and Permaran was used for the measurement of airflow resistance of the powder sample. Acuteness of the particles is defined as ratio of airflow resistance of ground particles to that of reference particles. Ball mill produced particles with higher surface area than autogenous mill for all size fractions considered and surface area increased with decreasing particle size. On the other hand, surface roughness decreased with decreasing particle size. Ball mill product was rougher than autogenous mill product. This was ascribed to the impact breakage which was dominant in the ball mill whereas abrasion was dominant in autogenous grinding. Furthermore, ball mill products were more acute than autogenous mill products, and acuteness decreased with size for both mill products.

Palaniandy *et al.* (2008) investigated effects of operational parameters on the breakage mechanism of silica in a jet mill. Silica was milled under varying parameters, feed rate, classifier rotational speed and grinding pressure. Milled products were analyzed for breakage mechanisms and product shape. At high grinding pressure, particles had high acceleration which led to destructive breakage of particles. Breakage under these conditions was found to be random and particles broke along weak planes, resulting in concave, elongated particles with sharp edges. Conditions of low pressure, high classifier speed and high feed rate promoted abrasion breakage mechanism. High classifier speed increased retention time of particles in the grinding chamber, while high feed rate increased the particle interaction probability. This facilitated production of more spherical and cubical particles. On the other hand, Berthiaux and Dodds (1999) observed that the amount of fine particle fragments increased as the size of mother particles decreased. They said that this suggested a destructive breakage grinding process. Berthiaux and Dodds (1999) and Palaniandy *et al.* (2008) obtained similar results regarding the effect of the breakage mechanisms that prevailed in a jet mill under various operating conditions. However, their deductions differed regarding which breakage mechanism was dominant in which size fractions.

Berthiaux and Dodss (1999) proposed a schematic representation of particle morphology produced by different breakage mechanisms, depending on the operating conditions, in Figure 2.9.2.

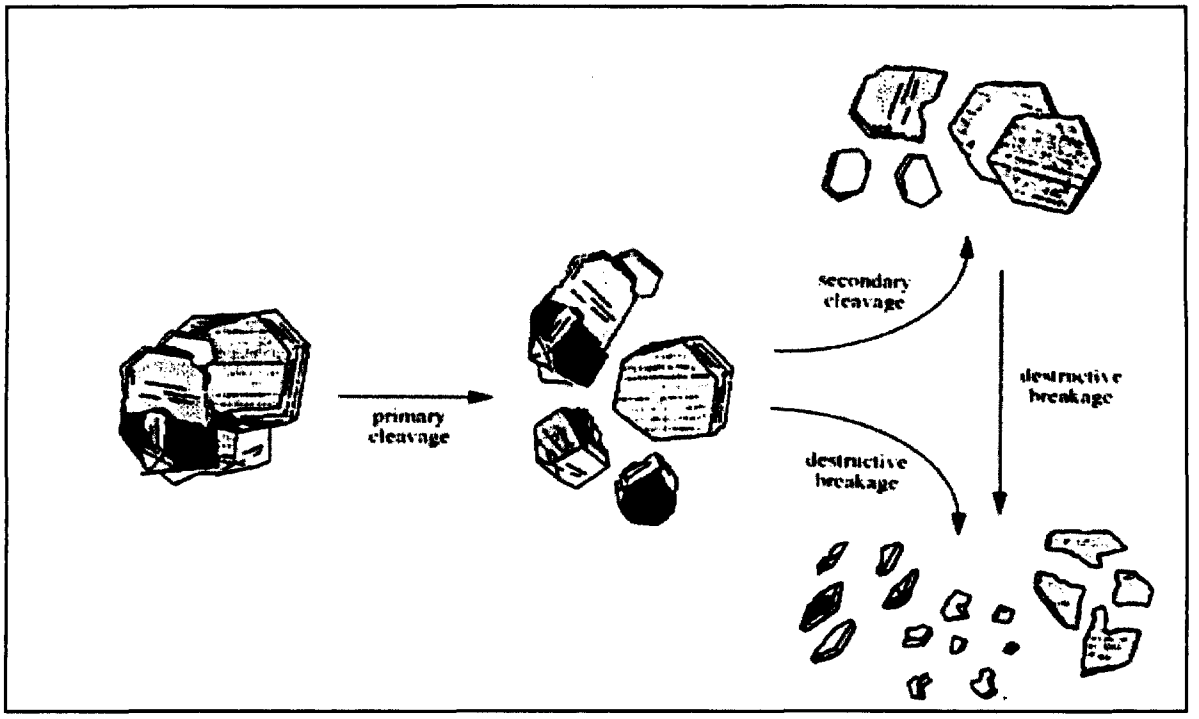

Figure 2.9.2: Schematic representation of the proposed overall breakage mechanism for hydrargillite particles (from Berthiaux & Dodds (1999))

2.9.4 *Effect of breakage mechanisms on mineral liberation*

The differences in stress intensities between different mill types can have significant differences in the properties of the mill products. An ore that has been ground to the same size by different mills may have different liberation profiles due to the different breakage mechanisms in the mills.

Maximum mineral liberation for a given grind size is obtained when breakage occurs along grain boundaries. Andreatidis (1995), as cited in Parry (2006), compared the extent of liberation between the products of ball mill and a bead mill. The results obtained in this study varied with ore types. For some ores, mineral liberation was independent of mill type whereas some ores showed dependence of liberation on the mill type.

2.10 Platinum Group Mineral (PGM) ore types

PGMs are found in different associations in the different ore types available. This association dictates to a large extent the comminution devices to be used and the grind size to which the ore must be ground (liberation size). The types of ores available to the mining industry are a consequence of geological processes that occurred over millennia.

Most of the world's supply of platinum and palladium and associated elements comes from mines within four major layered igneous intrusions, viz., the Bushveld Complex in South Africa, the Stillwater Complex in U.S.A, the Great Dyke in Zimbabwe and the Noril'sk/Talnakh Complexes in Russsia (Schouwstra *et al.*, 2000).

2.10.1 The Bushveld Complex

The complex is a vast repertoire of South Africa's value minerals which spreads over an area of 65000 km^2 and a thickness of 7 to 9 km (Cawthorn, 1999). It is a layered intrusion of variable mineralisation of mafic to ultramafic rocks associated with two felsic intrusive

suites. The rocks were formed by magmas that intruded the Transvaal Supergroup at 2.05 Ga. The Bushveld complex consists of five main limbs, namely, far western limb, western limb, the northern limb which includes Potgietersrus and Villa Nora sections, eastern limb and Bethal limb.

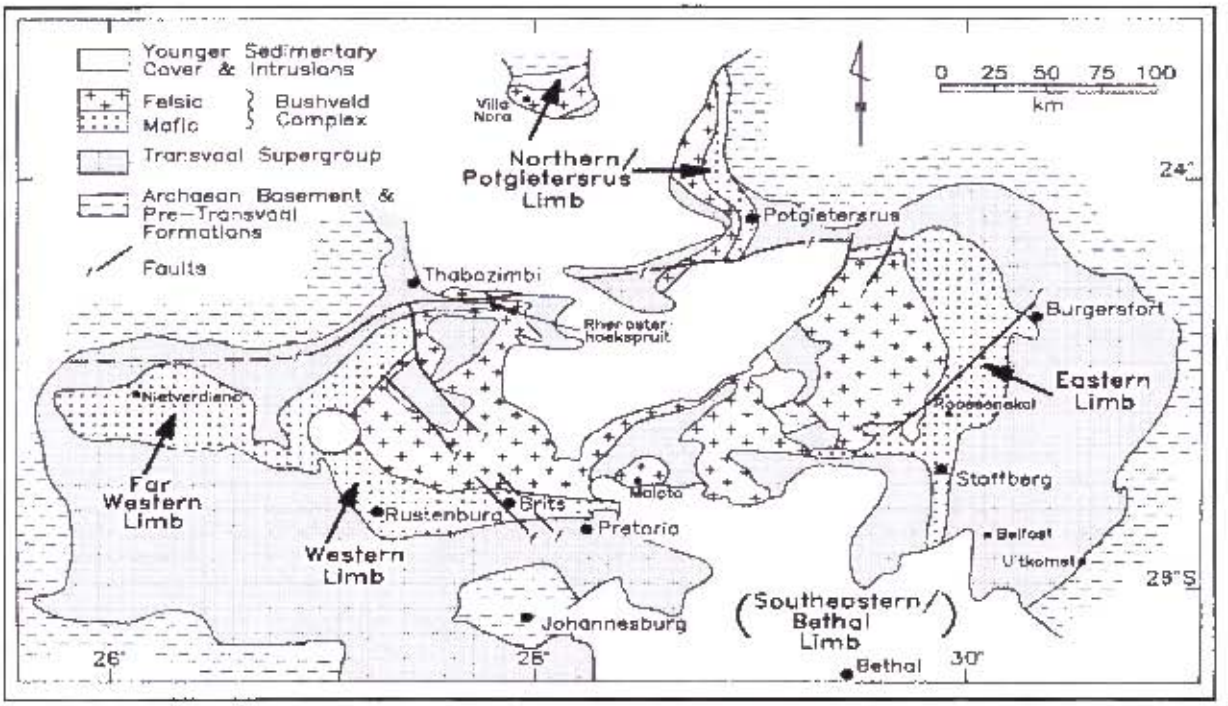

Figure 2.10.1: Geological map of the Bushveld complex, obtained from a compilation by Eales and Cawthorn (1996) as cited in (Cawthorn & Webb, 2001)

This multifaceted intrusion of rocks is divided into three suites. These are the Rustenberg Layered Suite (RLS) comprising mainly of mafic to ultramafic rocks, which are a host to the mineralisation, Lebowa Granite Suite and Rashoop Granophyre Suite.

The Bushveld Complex's upper zone has largest concentration of PGEs. These are the Upper Group Chromitite No.2 (UG2), Merensky reef and Platreef. The mineral ores from these reefs differ according to grain size, association and concentration of PGEs. There are six known PGMs ruthenium (Ru), rhodium (Rh), palladium (Pd), osmium (Os), iridium (Ir) and platinum (Pt) (Xiao & Laplante, 2004).

Terminology based on modal mineral abundance categorises the 'proxenite' unit as a range of rock-types from true pyroxenite to melaronite; however, nomenclature also has to account for the texture of the interstitial nature of the plagioclase. These rocks are conventionally termed pyroxenite or plagioclase-pyroxenite, depending on the amount of interstitial plagioclase present in the rock.

2.10.1.1 The Merensky Reef

Merensky reef is also known as the Merensky pegmatoid. Merensky reef's rock-forming minerals mainly consist of equal amounts of iron-magnesium silicate minerals and lighter calcium-aluminium-sodium silicate minerals (feldspathic pyroxenite). This zone contains base metal sulphide grains and associated platinum group minerals. The rock-forming silicate minerals of the Merensky Reef consist of orthopyrexene (~60 %), plagioglase feldspar (~20%), pyroxene (~15%), phlogopite (~5%) and occasional olivine. Interspersed in

the mineral rock are secondary minerals of talc, serpentine, chlorite and magnetite. The base metal sulphides are pyrrhotite (~40%), pentlandite (~30%), and chalcopyrite (~ 15%) and trace amounts of millerite, troilite, pyrite and cubanite (Pentberthy *et al.*, 2000; Schouwstra *et al.*, 2000).

2.10.1.2 The UG2 Reef

Chromitite layers in the Bushveld complex are localised in the Critical Zone (Mondal & Mathez, 2007). They are further subdivided, according to their height in the Critical Zone, into three groups; Lower Group (LG), Middle Group (MG) and Upper Group (UG). The UG2 chromitite layer presents the second layer of the Upper Group and lies between 20 m to 400 m below the Merensky reef (Schouwstra *et al.*, 2000).

The term "Reef" refers to the economically important zone contained largely within the medium- to coarse-grained plagioclase-pyroxenite and is specifically the mining zone of payable metal values (Wilson & Chunnett, 2006). The thickness and exact location of the economic zone is highly variable and is usually enclosed within the plagioclase-pyroxenite.

UG2's primary characteristics have been shown to be susceptible to modification by several factors, which alter the composition and texture of the chromite grains. Faults, dykes, potholes and Iron-Rich-Ulramafic-Pegmatoids (IRUP) intrusions are the main modifiers (van Schoor, 2005).

Mineralogy of UG2

Two dominant suites of mineralogy constitute UG2, namely, chromite and aluminium silicate-based mineralogy (Nel *et al.*, 2004).

General Mineralogy

UG2 is a platiniferous chromitite layer whose mineralogy varies depending on the geographic location within the complex. UG2 contains chromite (60 to 90 %) with interstitial orthopyrexene (5 to 25 %). Minor amounts, less than 5 %, of subordinate minerals such as clinopyroxene, biotite, phlogopite, talc, chlorite, quartz and serpentine are also present. Ilmenite, magnetite, rutile and calcite may also be present. Chalcopyrite, pyrrhotite, pyrite and pentlandite are the major base-metal sulphide minerals, usually present in trace amounts (< 0.1 %), (Pentberthy *et al.*, 2000; Schouwstra *et al.*, 2000; Mondal & Mathez, 2007).

Platinum group mineralogy

The degree and type of post-magmatic change in the ore determine the assemblages of the platinum-group minerals. These assemblages range from predominantly sulphide minerals to assemblages containing a large portion of non-sulphide minerals. Laurite ($(Ru, Os,Ir)S_2$), cooperate (PtS), malanite ($(Pt, Rh, Ir)_2CuS_4$), braggite ((Pt, Pd)S) and occasionally vysotskite (PdS) and the common PGE sulphides. Non-sulphide PGE minerals include Pt-Fe alloys ((PtFe) and (Pt_3Fe)), tellurides, bismuthinides, and bismuth-tellurides of Pt and or Pd, PGE arsenides and sulpharsenides. Rustenburgite (Pt_3Sn), isomertierite ($Pd_{11}Sb_2As_2$), arsenopalladinite ($Pd_8 (As,Sb)_3$), plumbopalladinite (Pd_3Pb_2), portarite (PdHg) and geversite ($PtSb_2$) also form part of these non-sulphide PGE assemblages.

These assemblages affect the milling and the flotation behavior of UG2 ores. Pentberthy *et al.* (2000) noted that the platinum-group minerals associated with liberated base-metal

sulphides report to faster floating concentrates during flotation. On the other hand, platinum-group minerals which are locked in gangue or associated with locked base-metal suphides report to the slower-floating concentrates and tailings, depending on the degree of liberation. The flotation behaviour of these associations is also affected by the grain size and the type of the base-metal sulphide.

The specific ore that was used in this work was Impala UG2. PGM processing at Impala's UG2 concentrator in Rustenberg was expounded on by Nel *et al.* (2005). Mineralogy of Imapala UG2, in particular, was discussed in their paper. They noted that the feed to Impala's UG2 plant contained 22-24 % Cr_2O_3, or roughly 50 % chromite. Primary alumino-silicates such as feldspars, pyroxenes and chlorite, and hydro-thermally altered silicates such as amphiboles and talc made up the aluminium silicate mineralisation of the ore. Sulphide mineralisatioin was sparse, constituting 0.1 to 0.2 % of the ore. These sulphides were composed of pyrrhotite (roughly 50 % of all sulphides), pentlandite (~ 35 %) and chalcopyrite (~10 %). The mix platinum group elements (PGE) mineralisation of Impala UG2 was also recorded. Platinum constituted roughly 45 %, palladium 25 %, rhodium 10 % and ruthenium 15 %.

However, Nel *et al.* (2005) noted that PGM speciation was a minor issue as it did not dictate floatability; their results showed no hierarchy in mineral floatability of fast-floating, slow-floating and unfloated PGMs. Instead mineral floatability of the finely disseminated PGMs (average grain size of 10 µm) tended to be dictated by grain size, liberation and association. They further noted that platinum group mineral grain size and association could be split into four categories:

- Coarse PGM (roughly 5 % of all PGE)
- PGM associated with base metal and iron sulphides (40 %)
- PGM occurring on host mineral grain boundaries (30 %)
- PGM locked in silicates (25 %)

The floatability of these groups decreases in the listed order, with locked PGMs being almost impossible to float. Milling and flotation behaviour of a UG2 ore are affected by various mineralogical factors such as type, mode of occurrence and grain size of platinum-group minerals and base-metal sulphides, as well as the type and amount of silicate minerals (especially talc), texture and grain of the mineral (Pentberthy *et al.*, 2000).

In their work, Nel and colleagues (2004) gave a brief history of the Impala UG2 processing plant. UG2 ore was first processed by Impala at its Rustenberg operations in 1991. The initial circuit was the mill-float (MF1) configuration. The primary grind was coarse and minimized the risk of chrome entrainment. However this also gave low PGM recoveries. In 1994, the configuration was improved to mill-float-mill-float (MF2) arrangement, which introduced regrind milling and secondary rougher/ cleaner flotation on the plant tails.

2.10.1.3 The Platreef

Platreef is a complex mixture of pyroxenites, serpentinites and calcium-silicates. It has a unique mineralisation and it is found where the Bushveld rocks are in contact with floor rocks (i.e. the Archaean granite and sediments of the Transvaal). Base metal mineralisation and PGE concentrations are irregular, both in distribution and value (Schouwstra *et al.*, 2000).

2.11 Current Practices in Concentration of UG2 ores

The target minerals during UG2 beneficiation are sulphides. However, chromite is a major gangue mineral and accounts for 26 to 50 % of the mass of UG2 ores (Mailula *et al.*, 2003; Nel *et al.*, 2005).

For a long time UG2 ores could not be processed because of their high chrome content. Chrome has been observed to be non-floating by itself. However, fine grinding promotes chrome recovery by entrainment.

Chrome melts at temperatures beyond 1600 ^{0}C and is found in the ore as a chrome spinel with iron oxide. On the other hand, the furnaces used in platinum refineries operate at lower temperatures of around 1400 ^{0}C -1500^{0}C. Chrome in the furnace feeds freezes the furnace, reduces efficiency and damages the equipment. Consequently, limits of around 1.8 % maximum allowable chrome content in the feed to furnaces have been set. There are attempts to improve furnace technology and push the limits higher.

2.12 Nkomati ore

Bulatovic (2007) noted that there were over 45 nickel minerals, but only a few of these have economic importance. The Nkomati ore body is situated in the Mpumalanga province, in South Africa. It is an extensive nickel/copper reserve (Bradford *et al.*, 1998). Nickel-containing ores, including nickel sulfides, nickel arsenides and nickel antimonides, can be classified into three major categories which include:

- Hydrothermal deposits formed as a result of nickel deposition from hydrothermal solution.
- Magmatic mafic deposits with two subtypes: (a) massive sulphide deposits and (b) impregnated deposits.
- Siliceous ore deposits containing mostly nickel silicates.

Bulatovic went further to state that pyrrhotite, chalcopyrite, pentlandite, magnetite and pyrite are the most abundant minerals in nickel and copper-nickel ores. Pyrrhotite, chalcopyrite and pentlandite were also identified as the most important from the processing point of view. The mineralogy of pyrrhotite was said to play the most important role in the treatment of nickel and copper-nickel ores. Pyrrhotite may occur in several crystallographic phases, with monoclinic and hexagonal pyrrhotite being the common types. Monoclinic pyrrhotite is ferromagnetic while hexagonal pyrrhotite is paramagnetic.

Bulatovic (2007) noted that in 2002, only sulphide ores were treated using flotation or a combination of magnetic separation/flotation or reduction roasting flotation. Nickel ores have characteristic low nickel grades in the final concentrates, with grades between 6 % and 11 %, not exceeding 18 %. Nickel minerals contain impurities of other minerals which vary the surface properties of the individual minerals from one deposit to another. Therefore floatability of nickel and copper-nickel minerals varies according the type of gangue minerals present. The reagent scheme to be employed in the treatment of nickel and copper-nickel ores depends on ore mineralogy, flowsheet for treatment of specific ore and the degree of liberation. Pyrrhotite and the amount of nickel in the pyrrhotite play a decisive role in the selection of a reagent scheme. Some important nickel minerals are shown in Table 2.12.1.

Table 2.12.1: List of some important nickel minerals (from Bulatovic, 2007)

Mineral	Chemical formula	Content % Ni	Hardness	Specific Hardness
Millerite	NiS		3-4	5.2-5.6
Pentlandite	$(Fe,Ni)_9S_8$	21-30	3-4	4.6-5.0
Gersdorffite	NiAsS	35.4	5.5	5.6-6.2
Rloanlit	$NiAs_{2-3}$	14.5-21.2	5.0	6.3-7.0
Nickelin	NiAs	43.9	5.5	7.3-7.7
Annabergites	$Ni_3(AsO_4)_2 \cdot 8H_2O$	37.5	2.5-3.0	3.0
Garnierite	$Ni_4(Si_4O_{10})(OH)_4 \cdot 4H_2O$	0-45	-	-
Reevesite	$Ni_6Fe^{3+}_2(CO_3)(OH)_{16} \cdot 4H_2O$	1-15	-	-

Nkomati nickel, copper, cobalt and PGM mineralisation is contained within the Uitkomst Complex which is a layered igneous intrusion between Badplaas and Waterval-Boven in the Mpumalanga Province of South Africa (Bradford *et al.*, 1998). There are four zones of Ni-Cu-Co-PGM sulphide mineralization within the early Bushveld age (two-billion-year-old) Uitkomst Complex, which is a layered, mafic-ultramafic body intruded into the basal sediments of the Transvaal sequence. The four zones of sulphide mineralization comprise:

- The Main Mineralized Zone (MMZ), hosted by Lower Pyroxenite Unit (LrPXT) and containing a variety of pristine to altered hybrid mafic-ultramafic rocks with small very large quartzite and dolomite xenoliths. The MMZ consists of several ore types including net textured, blebby and disseminated sulphides as minor massive and semi-massive sulphide bands and lenses.
- The Chromititic Peridotite Mineralised Zone (PCMZ), which is hosted by talcose and highly altered Chromititic Peridotite Unit (PCR). This zone is less continuous and has lower grade than MMZ.
- The Massive Sulphide Body (MSB), which is mined by Nkomati mine.

- The Basal Mineralized Zone (BMZ) is copper rich. It occurs in very few places in the Basal Gabbro (GAB). This zone has high grade and is continuous with MMZ (Wolmarans & Morgan, 2009).

Pillay *et al.* (2011) determined the minerals present in Nkomati MMZ ore and tabulated them as shown in Table 2.12.1.

Table 2.12.2: List of minerals present in the Nkomati MMZ ore and their average SG (Pillay *et al.*, 2011)

Mineral	Ideal Chemical Formula	SG
Plagioclase	$(Na,Ca)Al(Si,Al)_3O_8$	2.62
Clinopyroxene	$(Ca,Na)(Mg,Fe,Al,Ti)(Si,Al)_2O_6$	3.40
Orthopyroxene	$(Mg,Fe)_2Si_2O_6$	3.55
Olivine	$(Mg,Fe)_2SiO_4$	3.27
Amphibole	$Ca_2(Mg,Fe)_4Al(Si_7Al)O_{22}(OH,F)_2$	3.04
Chlorite	$(Mg,Fe)_3(Si,Al)_4O_{10}(OH)_2$	2.65
Serpentine	$Mg_3Si_2O_5(OH)_4$	2.53
Talc	$Mg_3Si_4O_{10}(OH)_2$	2.75
Dolomite	$CaMg(CO_3)_2$	2.84
Calcite	$CaCO_3$	2.71
Quartz	SiO_2	2.62
Biotite	$K(Mg,Fe)_3AlSi_3O_{10}(OH,F)_2$	3.09
Zoisite	$Ca_2(Al,Fe)Al_2(SiO_4)(SiO_7)(O,OH)_2$	3.40
Ilmenite	$FeTiO_3$	4.72
Magnetite	Fe_3O_4	5.20
Chromite	$FeCr_2O_4$	4.79
Pyrrhotite	$Fe_{1-x}S$	4.61
Chalcopyrite	$CuFeS_2$	4.10
Pentlandite	$(Fe,Ni)_9S_8$	4.80
Sphalerite	ZnS	4.08
Pyrite	FeS_2	5.01
Arsenopyrite	$FeAsS$	6.07

2.13 Mineralogy

Liberation grain sizes differ with the ore type as mentioned in the previous section. Variations in recovery are caused by mineralogical changes in the ore (Pentberthy *et al.*, 2000). Vizcarra *et al.* (2010) said that there was a large scope to investigate the relationship between breakage mechanisms and the resultant liberation properties of both gangue and valuable mineral phases.

Minerals are analysed to obtain information about identities of major, minor and trace minerals, compositions of minerals important to the process, quantities of minerals, particle and grain size distributions and textures of the minerals, minerals liberation and surface coatings.

The usefulness and accuracy of the mineralogical data depends on the equipment used to acquire it. The equipment chosen for analysis depends on the mineralogical information sought after. Petruk (2000) gave a comprehensive list of the equipment used in mineralogical analysis. Optical microscopes, X-Ray Diffractometer, Scanning Electron Microscope (SEM) with Dispersive X-Ray analysers (EDS) and Electron Microscope (MP) are some of the equipments used.

2.13.1 Mineralogical Measurement Integrity

The reliability of the data collected from the different mineralogical analysis equipment depends on the representativeness of the sample at every stage of the analysis, from sample preparation to the data collection and analysis.

Mineralogical analyses are limited by spatial and chemical resolutions. All microbeam systems are limited by the volume of sample material from which x-rays can be generated. This x-ray generation volume is due to internal scattering of high energy electrons, and it is about 1 μm to 2 μm across and beneath the surface of the specimen at 25 kV operating voltage. For phases smaller than 2 μm, the electron beam passes through the phase under observation and a mixture of x-rays is produced from the underlying phases. On the other hand, particles less than 5 μm limit the number of points to be placed on a particle to ensure its accurate representation, at the particle's finest point measurement spacing.

Mineralogical grade distribution, determined by image analysis of sections of size-fractionated particles, is a measure of liberation. However, estimates of the volumetric mineral liberation from measurements of particle sections are estimated because of stereological bias. This is because sectioning of composite particles can result in fully liberated sections, as shown in Figure 2.13.1. Magnitude of stereological error depends on ore texture, with disseminated or complex-textured particles showing less bias than ores with simple intergrowth structures (Gottlieb *et al.*, 2000).

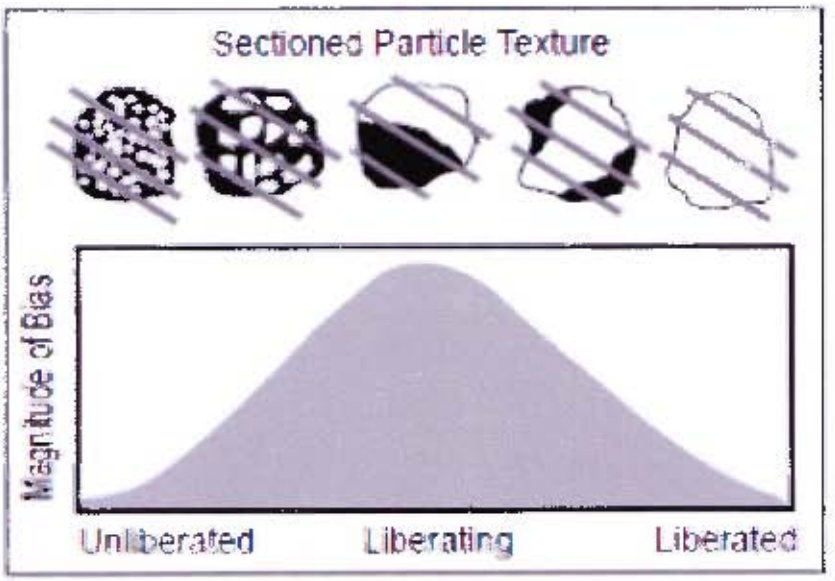

Figure 2.13.1: Schematic of basis of stereological error, with sections through liberated and composite particles of varying texture and the corresponding magnitude of bias (Gottlieb *et al.*, 2000).

2.13.2 Particle size measurements

Particle size measurement techniques define size of particles in different ways and therefore measure different properties of the same material. For instance, the sieve defines particle diameter as the length of the side of a square hole through which the particle can just go. Laser diffraction spectrophotometer on the other hand gives diameter of the particle as the diameter of the sphere that gives the same diffraction as the particle. Projected area of a non-spherical particle averaged over the particle orientation is larger than that of a sphere with equal volume. This leads to coarser results by applying a laser method instead of sieves (Konert & Vandenberghe, 1997).

The amount of material needed for laser analysis depends on the grain size characteristics, typically 100-200 mg for fine samples and 5-10 g for sandy samples.

2.14 Flotation

Costs of industrial comminution forbid complete liberation of value minerals in the ore and therefore some valuable minerals entering a flotation circuit are often locked in gangue. Thus the economics of comminution-flotation plants is tied around the recovery of composite particles and their effect of concentrate grade (Savassi, 2006). This is summarised by Lynch's statement of 1961 which said "many of the complexities of industrial flotation circuits are due to attempts to find the most efficient way to treat composite particles so that the recovery of valuable mineral is maintained at a maximum while the dilution of the concentrate by gangue is minimized".

Froth flotation is used in the mineral processing technologies to separate finely ground value minerals from a mixture with gangue material initially present in the pulp. The separation is achieved when value mineral particles are attached and transported by rising air bubbles (Santana *et al.*, 2008). Particle recovery to the concentrate may be achieved by the following mechanisms: (i) recovery of minerals by true flotation, which is a selective mechanism, transporting only the hydrophobic mineral particles; (ii) recovery of particles by

mechanical entrainment, which is a non-selective mechanism. Entrained particles (value and gangue) are trapped between particles adhered to air bubbles in the froth zone and (iii) recovery of fine particles by hydrophilic dragging (hydrophilic fine particles suspended in the water).

Flotation consists of many sub-processes and interactions which make it difficult to determine the flotation mechanism and assess the relative contribution of each sub-process (Bradshaw *et al.*, 2006; Santana *et al.*, 2008). Inefficiencies in flotation give rise to big losses of revenue and unnecessary waste of platinum reserves (Deglon, 2005). Major flotation inefficiencies are encountered in the fine particle size ranges. However, more platinum group metal ores are becoming fine-grained and they need to be ground to the fine and ultrafine size ranges in order to liberate the value minerals. This need has led to research into the area of fine particles flotation. There are different views on the subject of floatability of fine and ultrafine particles. Some researchers believe that fine particles do not float, and some believe that fine and ultra-fine particles do float when conditions are optimised for their flotation (Pease *et al.*, 2006).

The various sub-processes that constitute flotation include bubble-particle attachment, detachment and entrainment. There are various ways in which researchers are trying to bring together all the parameters that govern flotation. This is done mainly through the use of models.

2.15 Flotation kinetics

Flotation kinetics studies the variation of floated mineral mass with flotation time (Herna´inz & Calero, 2001). Furthermore, flotation kinetics can be considered as the study of flotation problems associated with the kinetics of froth-production step of the flotation process. Schuhmann (1942) reported that kinetics in a flotation cell were hard to determine if the cell was operated in a batch mode because flotation rates decreased by about tenfold in the first minute of the test and by fiftyfold in the first three or four minutes of the test, which made the quantitative measurements of flotation rate, froth composition or other aspects of froth behaviour difficult. The continuous operation of a flotation cell avoided these difficulties. Once steady state in the flotation cell was reached, the underlying assumption in the operation is that the composition of the pulp remains constant, since small mass leaves or enters the pulp during the process. Hence tailings composition was regarded as representative of the pulp composition. However, the proof of this assumption would be impossible without interfering with the operation of the system.

Moreover, Schuhmann (1942) indicated that the specific rate analysis of the different constituents was more logical and catered for the relative abundances of the constituents in the pulp.

$$Q = \frac{r}{c_t V}$$

Specific flotation rate is related to the kinetics of the bubble-particle attachment, through the direct-encounter hypothesis of flotation mechanism, in the following relation.

$$Q = P_c * P_a * F$$

The ratio of concentration (grams per litre of water) of a mineral in the froth to its concentration in the pulp is termed its coefficient of mineralisation. This defines the

floatability of the mineral relative to water. The specific flotation rate and the coefficient of mineralisation are both very sensitive to the changes in the surface properties of the floating mineral.

2.16 Flotation reagents

Flotation reagents enhance the flotation recovery of the value minerals by changing the surface properties of particles. Flotation reagents are categorised into main groups as collectors, frothers and modifiers (activators, depressants and dispersants). Collectors are the most important of the three groups (Laskowski *et al.*, 2007). Flotation reagents modify the particles' surface chemistry by inducing hydrophobicity (collectors) on value mineral surfaces and hydrophilicity (depressants) on gangue minerals.

2.17 Factors affecting flotation behaviour

2.17.1 Effect of grinding chemistry on flotation behaviour

In addition to changes in particle size and morphology, grinding also affects the surface chemistry of the particles, which in turn affects their flotation response (Goncalves *et al.*, 2003). Particle surface chemistry may be affected in various ways during grinding as shown below.

- Eh effect: grinding with steel media creates a reducing environment which decreases Eh and dissolved oxygen of the slurry immediately after grinding (Grano, 2009). Thiol collectors' adsorption is dependent on the Eh. Therefore change (reduction) may reduce mineral floatability if no aeration is provided before flotation.
- Iron hydroxide coatings: iron hydroxide generated from the oxidation of electrochemically reactive steel media may further reduce floatability of value mineral even after aeration and Eh restoration. This is the main factor responsible for reduced fine particle floatability ground in steel media.
- Oxygen reduction: this promotes formation of metal hydroxides on some sulphide minerals.
- Precipitation from solution: during grinding, increases in surface area and pulp temperature promote precipitation from saturated solutions. This has implications on the water composition which is used in the milling process.
- Galvanic coupling of media and sulphide minerals speed up oxidation of the media and oxygen reduction on the sulphide minerals (Huang & Grano, 2006). Galvanic contact is established between minerals and grinding media and among the minerals themselves (Peng *et al.*, 2003; Goncalves *et al.*, 2003). Redox reactions take place on the surfaces of minerals and grinding media due to differences in their rest potentials. The galvanic interactions are represented schematically as in Figure 2.17.1.

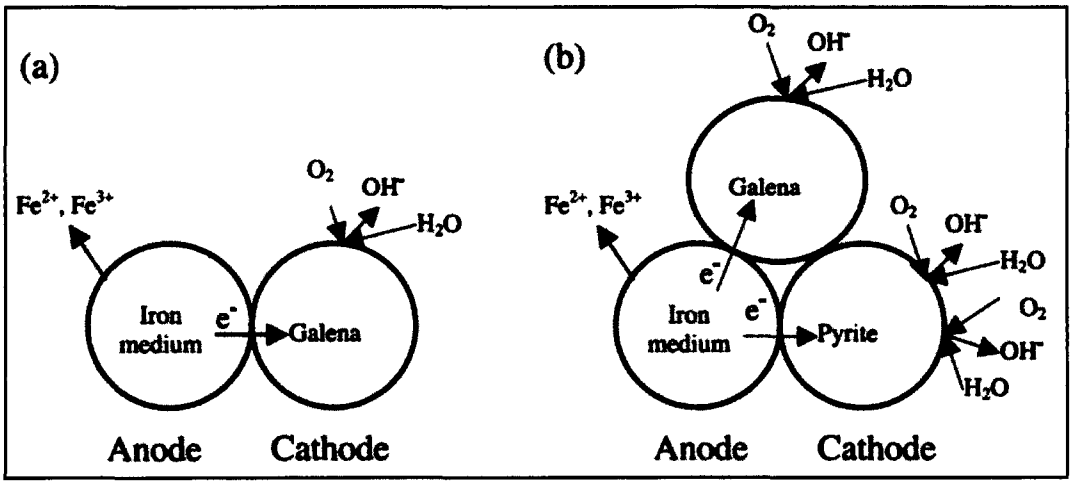

Figure 2.17.1: Schematic representation of galvanic interactions during grinding (Peng *et al*, 2003)

There is confusion in literature as to the exact mechanism which renders the mineral particles hydrophobic.

Ye *et al.* (2010) used a Magotteaux Mill and IsaMill to investigate the effect of stirred mills (IsaMill) and tumbling mills (Magotteaux Mill) on mill products' surface properties and the flotation behaviour. Magotteaux Mill product gave higher recoveries for the coarse size fractons (d_{80} = 60 μm and 40 μm) than IsaMill for the same fractions. However finer size fractions (d_{80} = 20 μm and 10 μm) showed IsaMill products yielding higher recoveries than Magotteaux Mill products. It was hypothesized that the abrasion breakage mechanism dominant in the IsaMill scraped the hydrphobic sites off the coarse particles. These scraped off, hydrophobic sites went directly into the fine size fractions, hence the observed antithetic trends in the coarse and fine fractions. On the contrary, pyrrhotite in both mill products exhibited opposite trends.

On the one hand Vizcarra *et al.* (2010) found that size-by-size liberation properties of both valuable and gangue mineral phases were independent of both the method used to comminute the samples, as well as the size distribution of the final products. They stated that the body of evidence surrounding the effect of breakage mechanism on the degree of libertation is uncertain and conflicting. Furthermore they suggested that detailed investigations between breakage method and resultant liberation properties of both valuable and gangue mineral phases should be conducted using the modern scanning electron microscopy (SEM) based technologies that are currently employed for accurate and reliable liberation analysis.

2.17.2 Effects of particle size on flotation behaviour

The role of particle size in flotation has been a known phenomenon for a long time. In the early stages of the development of the flotation process for concentrating ores, the belief arose that finally a process of ore concentration was available which could treat the finest particles or "slime", in aqueous suspensions (Gaudin & Malozemoff, 1932). Fine mineral particles that could not be recovered by gravity concentration were expected to have equal floatability as long as they had a wide size distribution. Flotation was applicable to a wider size range than any of the three principal methods of gravity separation, jiggling, tabling and vanning. However, the introduction of ball milling made it obvious that floatability and flotation rate of mineral particles was a function of particle size. The presence of an upper

limit beyond which flotation is impossible was recognized even before the advent of selective flotation. The lower size limit beyond which flotation is difficult was suspected, but the limitations of the laboratory sizing techniques made it difficult to do more than just guess that particles of colloidal sizes were not amenable to selective flotation operation. The uncertainty on the existence of this lower limit was sounded off by the following statement made by Gaudin and Malozemoff in 1932.

The size limits within which recovery by flotation is good were found to be more or less peculiar to each mineral. In general, however, the optimum size of mineral particles for concentration by flotation is between 50 and 10 µm, and the recovery is markedly lower for particles finer than 5 µm (Gaudin & Malozemoff, 1932).

The low recovery has been ascribed to a decrease in number of particle-bubble collisions in this size range (Filippov, 1998; Martinez-Carrillo & Uribe-Salas, 2008). This poses a great challenge because this is the size range where liberation of fine-grained ores occurs and a range where stirred media mills grind efficiently.

Furthermore, Gaudin and Malozemoff (1932) stated that the mechanical problem of bringing gas and solid together in flotation was as equally important to the flotation efficacy as the physicochemical properties of the mineral surfaces. This, they said was inherent in the definition of flotation which they stated as:

"Flotation is a process of separation of mixed dissimilar solid particles, applied to the concentration of finely ground ores in aqueous pulp. The separation is caused by the selective adhesion of some species of solids to the gas bubbles and the simultaneous adhesion of other species of solids to the aqueous solution; segregation of the resulting froth from the remaining pulp yields the desired separation."

Simultaneous recovery of value minerals in all size distributions has been identified as the major problem in flotation. Pease *et al.* (2006) stated that fine and coarse particles will never float well in the same cell because the flotation reagents cannot be optimised for these size ranges simultaneously. They stated that surface analysis of fine particles from the tailings showed that they lacked enough hydrophobicity, they had hydrophilic surface coating or did not have enough collector coating.

The conventional view of flotation of different size fractions has shown low recovery for fine and coarse particles as shown in Figure 2.17.2.

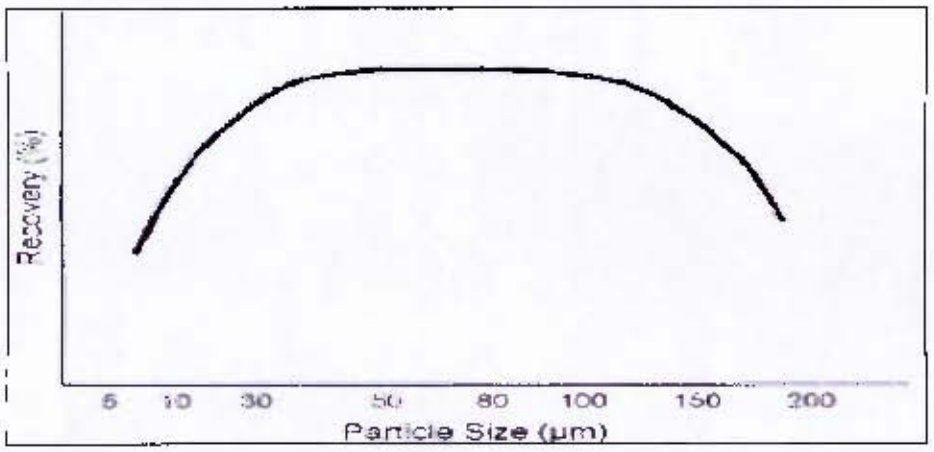

Figure 2.17.2: Typical view of flotation of different size fractions (from Pease *et al.*, 2006)

2.17.2.1 Fine Particles Flotation

Miettinen *et al.* (2010) gave a brief introduction to what they called the milestones of fine particle flotation. They outlined major findings in the study of fine particle flotation, starting from 1942 when Gaudin *et al.* (1942) showed that fine particles had different flotation properties to coarse particles. Gaudin *et al.* (1942) also proposed that the rate of flotation was independent of particle diameter or size up to 4 μm and proportional to particle diameter in the range 4-20 μm. Sutherland (1948) proposed the first theoretical particle-bubble collision model, which stated that the rate of flotation could be found by assuming that the flow around the bubble was a uniform motion of an inviscid fluid. In 1961, Derjaguin and Dukhin, as cited in Miettinen *et al.* (2010) proposed that the overall rate of flotation was equal to the product of bubble-particle collision, attachment and stability. Reay and Ratcliff (1975) as cited in Miettinen *et al.* (2010) suggested two flotation regimes for fine particles, one being where particle-bubble collision efficiency of particles greater than 3 μm increased with increasing particle size and the other being the Brownian motion of particles smaller than 3 μm. Sutherland's theory was first tested by Anfruns and Kitchener (1977) as cited in Miettinen *et al.* (2010), who measured the collection efficiency of fine particles and bubbles under potential flow conditions. The more recent work by Nguyen and Schultze(2004) exposed new limits for the bubble-particle collection efficiency, with a minimum at particle size of around 100 nm or 0.1 μm. Interception and collision controlled the collection of larger particles while diffusion and colloidal forces controlled collection of particles smaller than 100 nm.

The problems associated with fine particles flotation still persist up to today, despite the painstaking effort to understand the flotation mechanism in this area of study. The problems are compounded by the scarce energy and water sources and the complex ore mineralogy and liberation requirements.

Fine and ultra-fine grinding of fine grained ores is important for liberation of value minerals. However, of more importance is the recovery of these minerals by flotation once they are liberated. Most of the published work on fine and ultra-fine grinding leads to a conclusion that flotation performance will increase once the ore is finely ground. However there is no evidence of work done, where flotation performance was used as a measure of the grinding efficiency of the mill. The only instances that are mostly quoted are industrial applications where recoveries increased after installation of IsaMills; 80% recovery at Xstrata's McArthur River Mine (MRM) with 96% of the recovered particles finer than 2.5 μm (Pease *et al.*, 2006), improved lead and zinc recoveries at Mount Isa deposits (Clark & Burford, 2004), to name a few.

Pease *et al.* (2006) identified important properties of fine particles which make them respond differently to flotation, emphasizing that there is nothing special about fines. Fines have higher surface area per unit mass, so they need more reagents. They have less momentum, so they tend to follow water more easily than coarse particles. There is less energy for bubble attachment and higher tendency for entrainment. Therefore flotation rates are slower and cleaning densities are lower or froth washing may be needed to counteract entrainment. Fines tend to be more affected by surface coatings because the high surface area ratio makes them more reactive or because their low momentum makes it difficult for loose surface deposits to be abraded off by other particles. Fines are more affected by water chemistry and ions in solution. The high surface area to volume ratio

makes froths more retentive, making thickening and filtering difficult. Fines have slow flotation kinetics, with rates similar to coarse composite particles. Smaller bubbles increase fines' flotation rates.

Therefore, there is a need to assess the flotation performance of fine and ultra-fine mill products, especially comparing the traditional ball mill and IsaMill products. Flotation is highly dependent on the surface chemistry of the particles. The grinding environment in the mills should be chosen to enhance flotation.

The challenge of fine particles flotation was also alluded to by Rao and Chernyshov (2011) in their paper on the challenges in sulphide mineral processing. They stated that although the problem with fine particles flotation is usually associated with their low mass and high surface area, other factors such as surface composition, oxidation, mineralogical alterations, and dissolved ions concentration can play a decisive role in this phenomenon. The problem of fines flotation needs not be addressed only in attempt to overcome the deleterious effect of sulphide fines but also size-induced alternations in the surface and interior structure of particles should be employed as a novel source of enhanced and selective reactivity of sulphides.

Nguyen and Schulze (2004) summarized the flotation behaviour of fine particles in Figure 2.17.3.

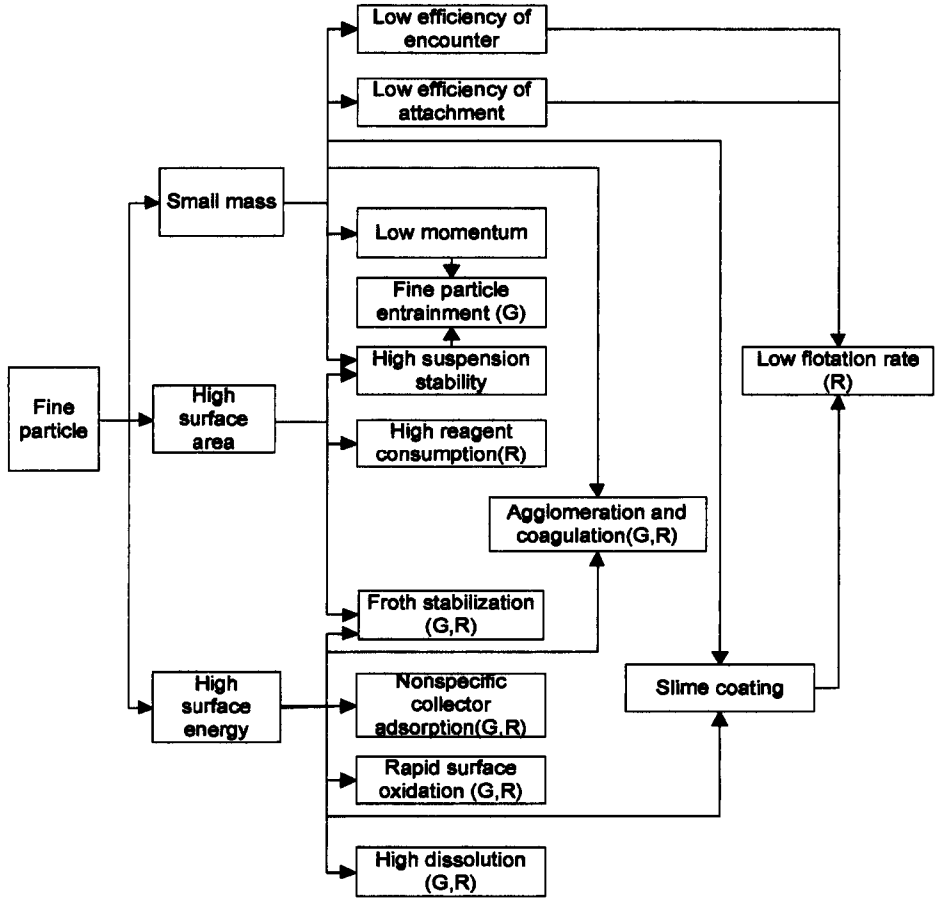

Figure 2.17.3: Schematic diagram showing the relationship between the physical and chemical properties of fine mineral particles and their behaviour in flotation. G and R refer to whether the phenomena affect grade and/or recovery (adapted from Nguyen & Schulze, 2004)

2.17.2.1.1 Problems associated with fine particles flotation

Small mass and high specific surface area, are characteristic of fine and ultrafine particles. Small mass leads to low momentum of the particles through the pulp and this lowers the probability of collision of particles with rising air bubbles. This leads to recovery of fine and ultrafine occurring primarily by water or entrainment rather by true flotation. On the other hand, high specific surface area of fine particles is considered to consume reagents faster and more than coarse particles (Lange *et al.*, 1997).

2.17.2.1.1.1 Entrainment

Entrainment is a non-selective ferrying of fine particles (valuable and gangue minerals) by water to the concentrate. This reduces the grade of the value minerals recovered in the concentrate. Entrainment starts at the pulp-froth interface but depends on the conditions in the pulp phase, such as solids concentration, particle size distribution, bubble size and bubble packing conditions at the pulp-froth interface. Zheng *et al.* (2006) developed a model with entrainment considered as a two step process; transfer of solids from the top of the pulp region just below the pulp-froth interface to the froth and the transfer of the entrained particles in the froth to the concentrate. Entrainment was dominant for fine and ultra-fine particles and was linearly related to water recovery in these size fractions. It then decreased with increase in particle size. Considering the size range in which the IsaMill grinds, entrainment will be an important factor for consideration.

Martinez-Carrillo and Uribe-Salas (2008) developed a rational interpretation of the mass flow of hydrophilic solids to the concentrate in a flotation column. They investigated the degree of entrainment (solids to water recovery ratio) as a function of solids concentration of the flotation slurry, froth depth and air rate.

Zheng *et al.* (2006) observed decreasing degree of entrainment with increasing froth height, using 9.2 cm -24 cm froth height. However, Martinez-Carrillo and Uribe-Salas (2008) found the degree of entrainment to be independent of froth height in the range 10 cm to 30 cm height. They carried their work with hydrophilic silica particles in the absence of any hydrophobic particles. This could be reason for the difference in their results from Zheng *et al.* (2006).

Konopacka and Drzymala (2010) gathered the literature on entrainment of fine particles to identify the different entrainment plots of particles-water recovery, which are useful in flotation research. They presented a schematic of the shapes of entrainment plots in the Fuerstenau upgrading separation plot as shown in Figure 2.17.4.

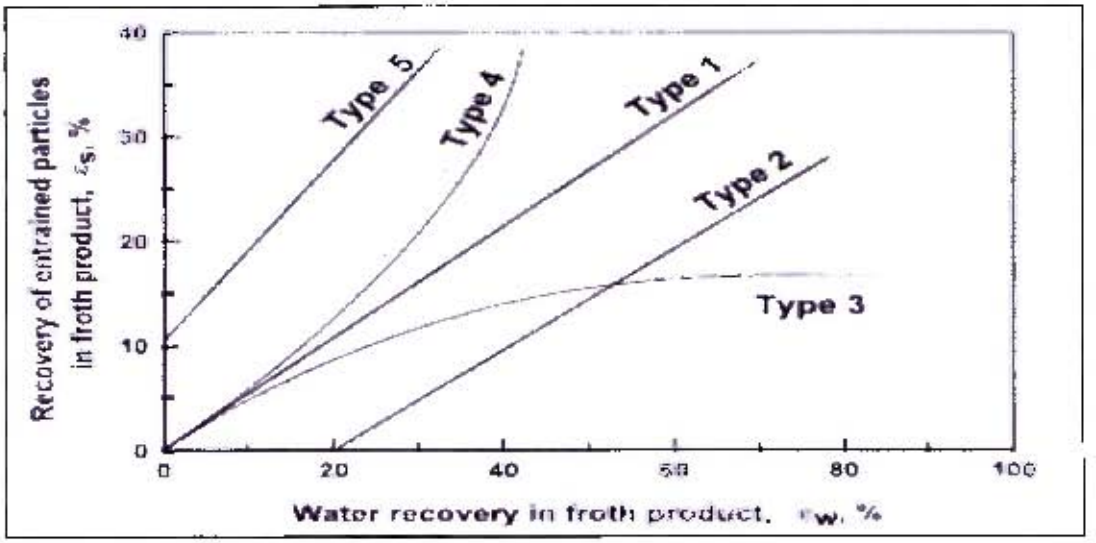

Figure 2.17.4: Shapes of entrainment plots in the Fuerstenau upgrading separation plot (Konopacka & Drzymala, 2010)

2.17.2.1.1.2 Reagent deprivation of coarse particles

High specific surface area of fine particles leads to insufficient reagent (collector or activator) coverage of the larger particles. This in turn results in non-selective activation or collection of fines, reducing overall grades of the valuable minerals. The long grinding times necessary to grind to fine (10 µm -40 µm) and ultrafine (< 10µm) increase the number of cracks, edges and corner sites on the particles surfaces. The high free energies of fine particles are ascribed to the presence of this surface unevenness.

2.17.2.1.1.3 Flotation of base metal sulphides (BMS)

Sulphide minerals are the most important, most diverse, and richest in terms of physical, chemical and structural properties. Such diversity stems from the more complex crystal and electronic structures compared to other materials (Rao & Chernyshov, 2011).

Sulphide minerals are formed in mafic and ultra-mafic rocks (Schouwstra *et al.*, 2000). Flotation of sulphide nickel ores is usually carried out at alkaline pH in order to separate pentlandite selectively from iron sulphides and efficiently depress pyrrhotite and pyrite. Floatability of pentlandite in the nickel ores has been shown to depend strongly on size, with low nickel recovery in coarse and fine fractions. This was said to be a result of iron hydroxide coatings on pentlandite particles (Kirjavanainen *et al.*, 2002).

Platinum group minerals (PGM) follow the flotation of base metal sulphide because of their association with sulphide minerals (Newell *et al.*, 2007; Shackleton *et al.*, 2007a, 2007b). Therefore the effect of different grinding mechanisms (mill types) on a base-metal sulphide ore, like Nkomati ore, provides a good baseline for the comparison of the given grinding mechanisms on the PGM type ores.

The sulphide minerals in nickel ores are easily floatable without a collector in acid pulp due to oxidation, and therefore it is not possible to separate them at low pH. Alkaline pH depresses pyrrhotite and has no significant effect on chalcopyrite Kirjavainen and Heiskanen (2007). Collectorless flotation on a low grade (0.3 % Ni) Enonkoski ore was studied using

ceramic and stainless steel media. Sulphide depression after ceramic grinding was observed and it was attributed to the adsorption of hydrophilic compounds on sulphide surfaces.

Newell *et al.* (2007) said that good flotation was achievable with most sulphide minerals, especially Merensky type ores where chalcopyrite, pentlandite and pyrrhotite were the dominant constituents. However this floatability decreased as sulphide surfaces became oxidised and hydrophilic, with the recovery of the constituents in a decreasing order of chalcopyrite, pentlandite and pyrrhotite.

2.17.3 Effect of shape on the flotation behaviour

Flotation performance is affected by a myriad of factors. Hence some authors have referred to flotation as the encyclopaedia of colloidal science (Nguyen & Schulze, 2004). Among these factors particle size has received a lot of attention in research. On the other hand, particle shape has not been researched as extensively, even though it has been acknowledged that it plays an important role in flotation performance. In addition to its importance to floatability, particle shape has also been found to be very dependent on particle comminution process (Unland & Al-Khasawneh, 2009).

The effects of particle shape on the properties of the bulk material are scarce in mineral processing literature, although it is well known that particle shape plays a role in the behaviour of powdered or granular material during processing and handling. The main problem in the study of particle shape is establishing a suitable definition for particle shape, since most particles encountered in practice are irregular and cannot be described in geometric terms (Riley, 1968). As a result, various contradictions have been pointed out in literature regarding the findings on the subject of the effect of particle shape on flotation performance. Despite these contradictions, the important conclusion has been that particle shape plays an important role in flotation Hicyilmaz *et al.* (1995). Some of the stark contradictions that Hicyilmaz *et al.* (1995) recorded early on in the study of this subject are outlined here. Fahlstrom (1974) found that products of autogenous grinding had lower compactness than conventional milling, which rendered them selectively floatable and improved their concentrate grades. Forssberg and Zhai (1985) found similar results, which showed that autogenous grinding yielded round particles with improved degree of liberation, grade and recovery. Contrary to this, Hoberg and Schneider (1978) found that the round shape of ground ore particles gave low floatability. Huh and Mason (1974) showed that particle shape played a major role on the adhesion force between bubble and particle. They said that Wotruba *et al.* (1991) found that this force was weaker with round particles than with prismatic particles.

Hicyilmaz et *al.* (1995) investigated the shape properties of barite and pyrite particles ground by autogenous and ball mill. Scanning electron Microscope (SEM) was used to analyze the mill products. The results showed that roundness increased flotation recoveries, implying that roundness increased floatability, which they said was in agreement with what Forssberg and Zhai (1985) observed.

Yekeler *et al.* (2004) investigated effects of particle shape on wettability and floatability of ball mill, rod mill and autogenous mill products. In this work, they indicated that Huh and Mason (1974) showed, through numerical calculation, that particle shape and adhesion force between bubble and particle are related. Ball mill product particles had highest roundness and wettability while rod mill products had highest elongation and flatness

values and low wettability. Rod mill products were therefore more hydrophobic since low wettability yields high contact angle and hence high hydrophobicity. The observed poor floatability of round particles was ascribed to their lack of edges, reducing their probability of rupturing the inter-bubble-particle liquid film. Hic¸yilmaz *et al.* (2004) studied effects of shape properties of talc and quartz particles on the wettability based separation processes. This study was similar to the work they did on talc alone, except now both talc and quartz were used. Similar results were observed, showing that flat particles had better hydrophobicity compared to round particles. These results were contrary to results obtained by Hicyilmaz *et al.* (1995). These discrepancies in the literature show that it is important to determine the effects of the shape on particle floatability (flotation response) for the material being dealt with.

Physical and chemical actions occurring on the particle surface during technological processes (e.g. flotation) are highly influenced by the geometry of the particle, and the exact evaluation of this geometry by means of quantified particle parameters is important. The parameters can be used to differentiate between different particles and correlate them with different processes, like flotation (Ahmed, 2010). Particle size, shape and surface roughness are important characteristics used to distinguish between particles (Ahmed, 2010; Yekeler *et al.*, 2004).

Surface properties of the mill products also play an important role in the floatability of the particles. Hicyilmaz *et al.* (2005) found that smooth autogenous mill products had higher floatability than rough ball mill products. Moreover, they found that surface roughness was more effective than acuteness for the flotation responses, since lower flotation recoveries were obtained at coarse size fractions where surface roughness was and high and acuteness low.

Chapter 3 EXPERIMENTAL PROCEDURES

3.1 Ores and ore preparation

The two ores used in this study were Nkomati Main Mineralised Zone (MMZ) ore and Impala UG 2 ore. In this thesis the two ores will be referred to as Nkomati and UG2 ores, respectively.

3.1.1 MMZ Nkomati ore

The first stage of the project was the preparation of the bulk ore sample to produce a feed material. The target size was 80 % passing 106 µm.

A 300 kg sample of Nkomati ore was screened at 1.7 mm using a 760 mm diameter screen mounted on a "SWICO", a vibrating shaker. The material greater than 1.7 mm was crushed using a cone crusher to produce particles less than 1.7 mm, which were of a suitable size for ball milling. As shown in Table 3.1.1 the 300 kg ore was dry milled in batches of 100 kg with a ball charge of 320 kg of ceramic balls in a rubber-lined horizontal ball mill. The size distribution of the ball charge was made up of different sized balls. The mill was cleaned with silica prior to milling the ore.

Table 3.1.1 Milling conditions for Nkomati ore preparation

Sample mass (kg)	100
Ball mass (kg)	320
Ball material	Ceramic

The first 100 kg batch of the ore sample was used to determine the milling time required to achieve a grind of 80 % passing 106 µm. The mill was crash stopped after 30 and 55 minutes of milling. A 100 g sample of milled ore was extracted from the mill after each crash stop. This sample was wet screened at 106 µm and dried. The mass retained on the screen was weighed and from this, the percentage mass passing 106 µm was calculated. This procedure is called "checking the grind".

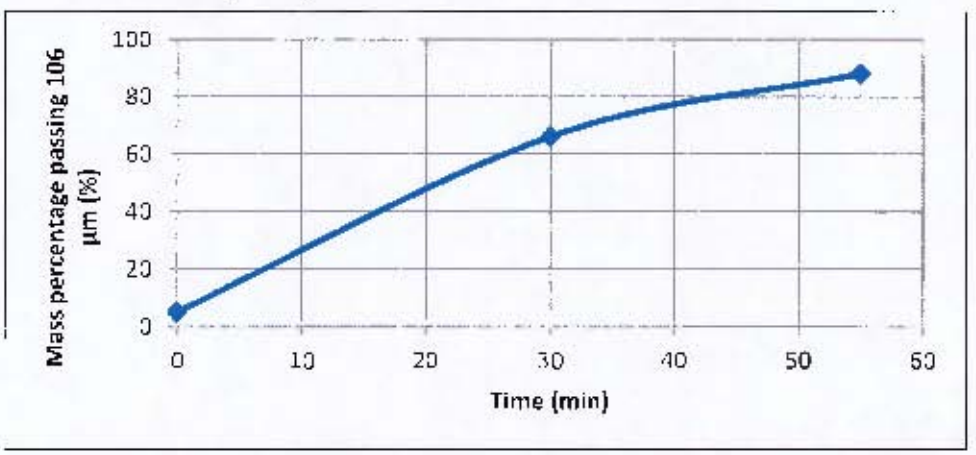

Figure 3.1.1 Milling curve for the horizontal ball mill for Nkomati MMZ ore

Figure 3.1.1 shows the mass percentage of ore passing 106 µm. Interpolation was used to determine that 46 minutes were required to grind 100 kg of Nkomati ore to 80 % passing 106 µm in a rubber-lined, horizontal ball mill. Therefore the other two 100 kg batches were

each milled for 46 minutes. The three milled batches were combined and riffled to provide a homogeneous bulk feed sample. The actual bulk feed size as measured by the Malvern MasterSizer 2000 was 80 % passing 120 µm. This provided the feed material for the M4 IsaMill and the horizontal laboratory ball mill.

3.1.2 Impala UG2 ore

The UG2 ore was prepared by wet milling 4 kg batches of the ore at 66 % solids in a 30.5 cm by 30.5 cm horizontal laboratory ball mill. The ore was milled for 25 minutes using 30 mm, 21 % chrome Magotteaux grinding balls. The product was dried and riffled in a ten way rotary sample riffler. This provided the feed material for the M4 IsaMill and the laboratory ball mill.

Table 3.1.2: Milling conditions for UG2 ore preparation

Diameter (cm)	30.5
Length (cm)	30.5
Ball Size (cm)	30.0
Solids content %	66.0

The various times that were used to determine the time necessary to achieve a grind of 80 % passing 106 µm are shown in Figure 3.1.2.

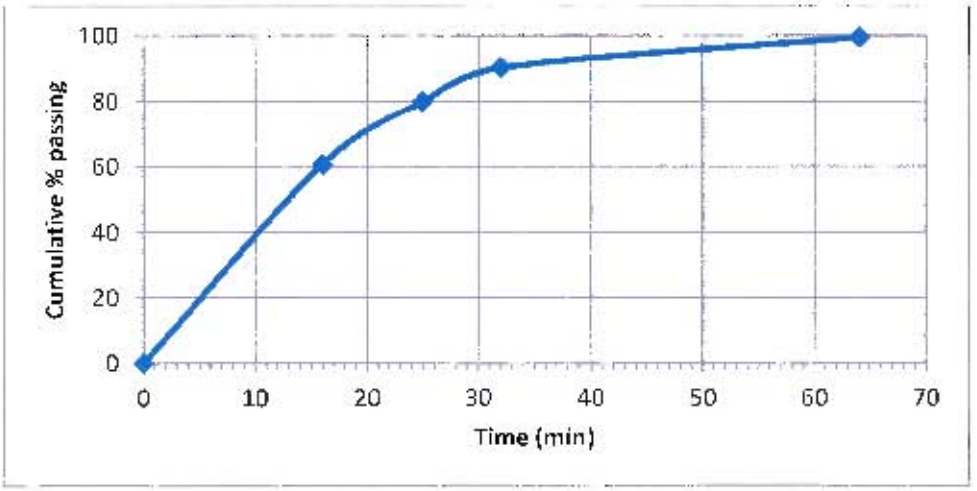

Figure 3.1.2 Milling curve for the laboratory scale horizontal ball mill for Impala UG2 ore

3.2 Milling procedures

3.2.1 M4 IsaMill

In this thesis, the M4 IsaMill will be referred to as just the IsaMill.

3.2.1.1 Equipment and Materials

The IsaMill consisted of six discs mounted on a rotating shaft. The first disc from the feed end of the chamber was 20 mm from the mechanical seal. The discs were spaced 35 mm apart with the last disc 15 mm from the centripetal product separator. The discs were 12 mm thick and 100 mm in diameter. The shaft was 44 mm in diameter. The end of the shaft had six prongs or "fingers" protruding from it. These created a separation area, where media and coarse particles were re-circulated by centrifugal force to the grinding chamber.

The fine product was discharged through the product separator. Each prong was 66.5 mm long and 16 mm in diameter. The interior of the IsaMill grinding chamber is shown in Figure 3.2.1.

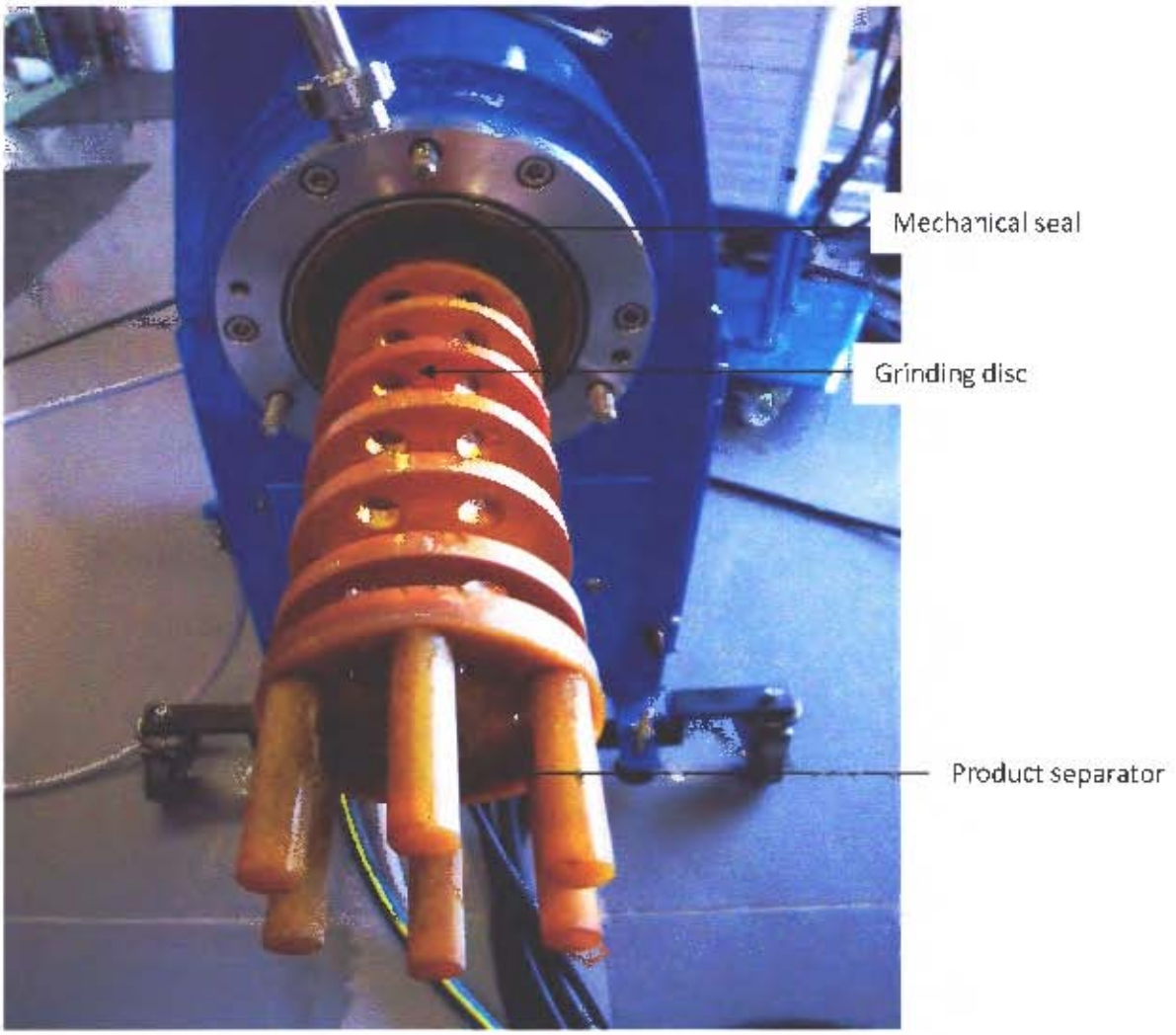

Figure 3.2.1: Interior of M4 IsaMill grinding chamber

3.2.1.2 Procedure

The Xstrata IsaMill procedure was followed to mill the ore. The appropriate masses of water and ore were added to the feed tank to make slurry with 40 % concentration of solids by mass. 2 L of 3.5 mm mono-sized MT1 ceramic media were weighed and added to the grinding chamber and ore samples were wet milled using iThemba laboratory tap water.

3.2.2 Ball Mill

3.2.2.1 Materials and equipment

A 30.5 cm X 30.5 cm laboratory scale cylindrical ball mill was used for the ball mill experiments.

8.615 kg of 11 mm ball bearings were used as the ball charge. The water used in the ball milling experiments was Cape Town tap water.

3.2.2.2 Milling Curve Development for Nkomati ore

66 % solids slurry was prepared by mixing 2 kg Nkomati ore with 1 L of tap water. No reagents were added during milling. The ore was cumulatively milled for a progression of grinding times, viz., 2, 4, 8, 16, 32 and 64 minutes. After each grinding interval, a sample was taken from the mill for laser diffraction particle size analysis.

3.3 Particle Characterization

The mill products were analyzed for particle size distribution by laser diffraction using a Malvern MasterSizer 2000. Initial comparative analyses were done comparing sieve sizing and Malvern particle analysis using the methods described below.

3.3.1 Sieve Sizing

A stack of sieves with appropriate aperture sizes (106, 75, 53, 38, 25 µm) was mounted on a vibrating shaker. A sample of the ore slurry was poured on the top sieve while continually spraying the sample on the screen with tap water from a hose. The spraying was continued until water flowing out from the bottom sieve in the stack was clear. The sieves were removed one by one from the stack, starting with the top size sieve. After removing each sieve water was sprayed onto the subsequent sieve to ensure thorough screening. A clean enamel dish was held under each sieve being removed from the stack to ensure that the water flowing from the sieve was clear of solids.

The sample retained on the sieves was transferred into drying pans and dried in the oven. The -25 µm sample was screened using a 10 µm nitex cloth. Two samples from the ball mill and two IsaMill products were used to compare the size distributions obtained from wet sieving and Malvern particle size analysis.

3.3.2 Malvern Master Sizer 2000

3.3.2.1 Theory

The MasterSizer 2000 particle size analyzer was developed to meet industry's growing need for global comparability of results, traceability, regulatory compliance and efficiency in the laboratory. Software-driven standard operation procedures (SOPs) eliminate user variability. All measurement parameters are automatically embedded in the result files. Wet and dry powders in the size range 0.02 µm to 2000 µm can be measured in a MasterSizer 2000.

Many materials need to be measured as wet dispersions. For this purpose, Hydro G sample dispersion unit is used. The unit is designed to suspend particles in water or other liquid media. The suspension can be optimized through the use of ultrasonics or surfactants. Hydro G has 800 ml holding volume and achieves dispersion through a continuously variable contra-rotating centrifugal pump stirrer to ensure a bubble-free dispersion at high stirrer speeds and a continuously variable ultrasonic probe. Quality and reproducibility of a size measurement, in any size analysis technique, depends on sample dispersion (Tinke *et al.*, 2009).

Malvern MasterSizer 2000 uses laser diffraction to achieve particle size analyses. The technique of laser diffraction is based on the principle that particles passing through a laser beam will scatter light at an angle that is directly related to their size, with small particle scattering at high angles while large particles scatter at low particles. Laser diffraction is a

special branch of electromagnetic scattering theory, and in its classical form it is based on Maxwell equations and its solutions.

Mie theory is the exact classical theory of light scattering with small particles. However, Rayleigh/ Rayleigh-Debye-Gans scattering and Fraunhoffer diffraction are some of the alternative approximate analytical solutions for particles which are much smaller or larger than the wavelength of light. Fraunhoffer is closer to geometrical optics and is commonly used in laser diffraction instruments for particle sizing (Pabst & Gregorová, 2007).

The use of light to measure particle size stems from the interaction between light and matter. Light is electromagnetic radiation in the frequency range (v) from approximately 10^{13} Hz (Infra-Red) to 10^{17} Hz (UV). This corresponds to the wavelengths (λ) from 3 mm to 30 μm. the optical properties of matter (particles) are described by the complex refractive index,

$$N = n + iK$$

The real part accounts for refraction according to Snell's law and the imaginary part is related to the absorption coefficient *a* through the relation,

$$a = \frac{4\pi\kappa}{\lambda}$$

The absorption coefficient occurs in the Lambert-Beer law which describes the exponential attenuation of light intensity (irradiance) *I* as the light wave traverses a medium of thickness *z*, expressed as,

$$I = I_0 exp^{(-az)}$$

I_0 is the intensity of incident light.

3.3.2.2 Experimental Test work

Malvern MasterSizer 2000 uses laser diffraction to analyze the sample aliquot for size distribution. The optical properties (refractive index) of the ore to be analyzed were therefore requisite in order to analyze the ore sample. The unit used in the Malvern MasterSizer 2000 was Hydro 2000G (A).

Table 3.3.1 (from unpublished work of Becker, 2010) shows the composition of Nkomati ore that was used in this study. The composition was used to determine the refractive index (RI) and specific gravity (SG) of the ore.

Table 3.3.1: Mineralogical composition of MMZ Nkomati

Mineral	wt%	RI	SG
Quartz	3	1.55	2.65
Talc	8	1.58	2.82
Chalcopyirite	1	0.00	4.20
Chromite	8	2.12	4.80
Biotite	10	1.61	3.10
Enstatite	18	1.66	3.20
Pyrrhotite	10	0.00	4.62
Lizardite	7	1.55	2.55
Diopside	23	1.68	3.40
Forsterite	6	1.65	3.22
Tremolite	3	1.63	3.17
Olivine	2	1.65	3.81
Pentlandite	1	0.00	4.80

The RI values for the individual minerals were obtained using *minsearch*, a software program containing properties of common minerals. The RI and SG of the ore were used to define the Standard Operating Procedure (SOP) for size analysis tests of that particular ore using the Malvern MasterSizer 2000. These SOPs ensure reproducibility of the Malvern results on an ore samples.

Less than 1 g of material was required for analysis in a Malvern MasterSizer 2000. This amount was obtained by riffling the dry sample in a micro rotary splitter until approximately 1 g mass was obtained. This was to ensure that a representative sample was analyzed in the Malvern. Each test using Malvern particle size analysis was conducted in duplicate.

In addition the Malvern software estimated the specific surface area of the sample being analyzed.

3.3.3 Analysis Techniques

S4 explorer X-ray fluorescence (XRF) spectrophotometer was used to determine the percentage of copper and nickel in the feed, concentrate and tails samples. A LECO S 632 sulphur analyser was used to determine the sulphur content of the feed, concentrate and tails samples.

3.3.4 Particle Shape Analyses

3.3.4.1 Theory

Particle shape analysis has been reported as a major challenge in powder technology due to the lack of a clearly defined shape factor which differentiates between all particle shapes (Podczeck, 1997). The range of shape analysis methods spans from simple methods of

determining aspect and elongation ratios to advanced techniques using Fourier analysis and fractal dimensions.

In theory, particle sizes obtained from different measurement techniques should be similar. However, this is rarely the case because of the shape assumptions inherent in some of these measurement techniques. Correlation between results of different methods is usually achieved through the use of shape factors. Shape factors are usually the ratio of two average sizes rather than the average of the ratio of two sizes (Robins, 1954).

Three common shape factors are commonly used in shape analyses:

Aspect ratio is the maximum to minimum Feret diameters or vice versa. It is a measure of the elongation or flattening of the hull of the particle. Feret diameter is defined as the distance between two parallel tangents of the particle at an arbitrary angle.

$$Aspect\ ratio = \frac{maximumFeretDiameter}{minimumFeretDiameter}$$

Circularity (roundness) is the ratio of the perimeter squared to the projected area.

$$Circularity = \frac{P^2}{4\pi A}$$

Concavity is the diameter of the smallest circumscribed circle (sphere) to the diameter of the largest inscribed circle (sphere) centred in the centre of mass of the particle.

$$Concavity = \frac{diameter\ of\ circumscribed\ circle\ (sphere)}{diameter\ of\ inscribed\ circle\ (sphere)}$$

Scanning electron microscopy (SEM) has been used in most of the shape analysis work that has been conducted. SEM captures 2D images of particles (Ahmad *et al.*, 2008; Yekeler *et al.*, 2004). The images are then analyzed for size and shape parameters of interest using software.

3.3.4.2 Experimental Test work

0.015 g mass of a given size fraction of the ore was weighed out and suspended in 10 ml de-ionized water. The slurry was agitated and solicited for 15 minutes using an ultrasonic bath. Samples were then filtered sequentially through, 10, 1 and 0.1 µm filters.

A scanning electron microscope (SEM) was used to obtain 2-Dimensional images of the mill products. 10 images of each of the samples retained on the filters were captured. The images were analyzed using proprietary image analysis software which calculated the different size parameters from the SEM micrographs.

3.4 Batch Flotation

3.4.1 Batch Flotation Test work

Batch flotation tests were carried out in a 3 L modified Leeds cell.

The mass of the feed used during batch flotation tests conducted in the 0.62 L cell was 200 g and for the 3 L cell 1 kg was used. The flotation feed to the small cell was mill product screened to produce particles which were below 25 µm. The flotation feed to the 3 L cell was the entire mill product. UCT laboratory tap water was used for all batch flotation tests in the two cells.

The impeller speed in the small cell was set at 120 rpm for the flotation experiments. Some experiments were carried out at 240 rpm, to observe the effect changes in impeller speed. Air was fed to the cell at 1 L/min. Air flow rates higher than this resulted in froth spillover under the conditions used in these experiments.

In the 3 L cell, the impeller speed was set at 1200 rpm and the air flow rate was maintained at 7 L/min throughout the test.

Reagent concentrations used in both cells are shown in Table 3.4.1. Solutions of the collector, sodium isobutyl xanthate (SIBX), were freshly prepared before the flotation experiments to prevent xanthate decomposition. Frother (DOW 200) was used "as is" from the laboratory storage. The collector was conditioned for 2 minutes in the slurry, after which point the frother was added and conditioned for 1 minute.

The pH of the pulp in the flotation cell was the natural pH of the ground ore as measured with a pH meter. The meter was calibrated in standard pH 4 and 7 buffer solutions

Four concentrates were collected for every batch flotation test. The first, second, third and fourth concentrates were collected for duration of 2, 4, 6 and 8 minutes, respectively. The froth was scraped into a collecting dish every 15 seconds for all concentrates. This resulted in a total of flotation time of 20 minutes. The masses of the empty concentrate pans were recorded so that the mass of the concentrates collected could be determined. Concentrates were filtered using pre-weighed natron filter papers. The concentrates were dried overnight in a Memmert laboratory oven at a temperature of 70^0C and the masses recorded. The concentrates were riffled in micro rotary splitter to obtain representative samples. Approximately 1 g of the riffled concentrates and tailings samples were weighed and analyzed for particle size analysis. The samples were analyzed for size using a Malvern MasterSizer 2000, with a Hydro 2000 G (A) unit.

Table 3.4.1: Batch Flotation reagent concentrations

Reagent name	Concentration
SIBX	50 g/t
DOW 200	50 g/t
pH	7-8

Batch flotation tests were carried out for both ball mill and IsaMill products. Ore was ground for 16, 32 and 64 minutes in the ball mill. The IsaMill was run for four passes and mill product at the end of each pass was used for the batch flotation tests.

Grades and recoveries were determined on a size by size basis. For this, small portions of the four concentrates and bulk tailings were sampled and mixed to generate one bulk concentrate and a tailings sample respectively. This was done for ball mil (16min) product and the IsaMill (1 pass) product, for both Nkomati and Impala UG2 ores. The aggregate concentrates and tailings samples were wet screened to obtain + 25 µm, - 25 +10 µm and – 10 µm samples, which were dried and assayed for value minerals.

Similarly for IsaMill (4 pass) product and ball mill (64min) product, portions of each of the four concentrates and bulk tailings were collected. However, for these products, these small portions were not combined to create bulk concentrate and tailings samples. Each sub-

sample was screened to generate the same size classes as mentioned previously, retaining the respective concentrate numbers.

3.4.2 Equations to express grade and recovery

The formulae used to calculate grades and recoveries for the batch flotation tests are outlined below together with the notation used to simplify them.

f= assay of valuable element of the feed sample

c= assay of the valuable element in the concentrate

t= assay of valuable element in the tailings

F= mass of feed

C= mass of concentrate

T= mass of tailings

The total mass balance equation is

$$F = C + T$$

Element mass balance is

$$Ff = Cc + Tt$$

Recovery and grade are defined respectively as:

$$R = \frac{Cc}{Ff} * 100$$

$$G = \frac{Cc}{C} * 100$$

Grades and recovery values were reported as cumulative figures.

3.4.3 Rheology

3.4.3.1 Theory

The mathematical packaging of rheology, the general science of fluid flow, is essentially an achievement of the 18th century. It was a field which was spearheaded by the likes of Daniel Bernoulli, Euler and Lagrange. During the second half of the 20th century, the Truesdell-Noll school of rational mechanics revised the non-linear theories of mechanics and summarized virtually all that was known and correct about the theory of rheology and the related experimental issues (Pabst, 2004).

Understanding what properties of particles in a suspension strongly affect bulk rheology is important to a lot of industries dealing with particulate matter. Particle shape has been identified as one of the particle properties that influence bulk suspension rheology (Heine *et al.*, 2010).

This unique rheological behaviour of distinct particle shapes can be used to diagnose the shape distribution in bulk powder samples. However most of the work done on particle rheology and shape is on nanoparticles where the interactions between particles are very strong.

3.4.3.2 Experimental Test work

Rheological tests were performed to detect the behavioural differences of different particle shapes. The apparent viscosities of the ore slurries at varying solids volume percent were measured using an AR 1500 *ex* rheometer, with a vaned plane stirrer.

Mill products were wet screened at 25 µm to provide the -25 µm samples for rheological tests. The samples in the -25 µm fraction were dried and riffled in a rotary micro splitter. Different sample masses were weighed in order to achieve the respective solids volume percent. It should be noted that, a bulk of the material, as will be seen in the particle size distribution results section, was in the -25 µm. Furthermore, the effect of particle shape on rheological behaviour becomes pronounced in slurries containing fine particles. For these reasons, rheology tests were carried out on -25 µm fraction of the mill products.

Slurries were prepared by mixing ore samples with a 0.01 M sodium hydroxide solution which acted as a background electrolyte.

The tests were carried out in duplicate using a fresh slurry sample for each test.

Chapter 4 RESULTS

This chapter presents the results that were obtained in the investigation of the flotation behaviour of ball mill and M4 IsaMill products.

The results are separated into sections which detail the results obtained using each of the mills. The results obtained from using each mill are further subdivided into sections pertaining to each of the two ores, Nkomati ore and Impala UG2 ore.

Results from each ore type are presented in the following manner. Characteristics of particles produced by the mill are outlined. The mill product samples were analysed for particle size distribution. This was done with laser diffraction using Malvern Mastersizer 2000. The scanning electron microscope (SEM) images of the particles are then presented. The images were analysed with proprietary image analysis software to give the relationship between different shape parameters of the same particles. The figures showing these shape parameters are presented in Appendix D. X-Ray diffraction (XRD) analyses of the samples were performed to determine composition of the mill products after different grinding times. XRD analyses can also be used to diagnose changes in crystalline structure due the different milling devices. The results of the XRD analyses follow the rheology results in the subsections.

Rheology was used as a behavioural diagnosis of the differences or similarities in the shape of particles produced by the two mills after various grinding times. The idea is that differently shaped particles affect apparent slurry viscosity to varying extents; rod and needle shaped particles increase slurry viscosity whereas spherical particles decrease slurry viscosity.

A section on batch flotation behaviour then follows after characteristics of particles to float have been presented. Results of the recovery of solids as a function of water recovery are first shown in this subsection. Then copper, nickel and pyrrhotite recoveries are shown as a function of flotation time; grade-recovery curves are also plotted for each of these minerals. Copper grade and recovery indicates to chalcopyrite grade and recovery and nickel flotation behaviour is an indicator of pentlandite flotation behaviour.

Results of the flotation behaviour of different size fractions are presented following the results of the bulk flotation behaviour. These are then followed by the particle size distributions of each of the flotation concentrates.

Batch flotation results for the UG2 ore are presented slightly differently from those of the base metal sulphide ore. They show the solids recovery as a function of water, followed by size by size mass distribution of chromite in the concentrates and tailings. These are then followed by the particle size distributions of the concentrates and tailings.

4.1 Particle size distribution data

4.1.1 Comparison of sieving and laser diffraction (Malvern)

The first stage was to prepare the ores to be fed to the mills. The preparation procedure was outlined in the experimental section, in the previous chapter.

Sieving and laser diffraction were the two sizing methods which could have been used in this project. However, it was necessary to choose one method for all size analysis tests. Size

distributions were obtained using both methods in order to determine how closely the methods correlated with each other.

Samples of Nkomati ore, milled using the IsaMill, were used to compare the results obtained using different sizing techniques i.e. sieving and laser diffraction. Duplicate particle size distributions were determined for samples obtained from each of the four passes of the IsaMill, using each method. The averages for each pass were then compared. Figure 4.1.1 and Figure 4.1.2 show particle size distributions obtained from wet screening and Malvern analysis respectively.

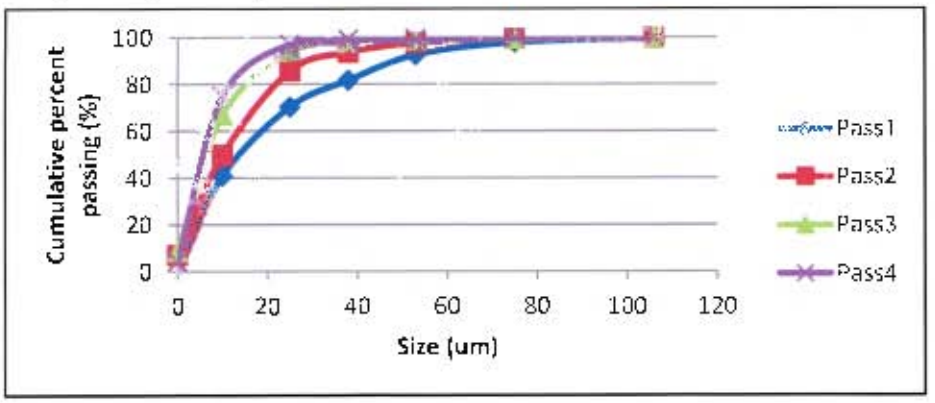

Figure 4.1.1: Sieve size distribution of Nkomati ore milled for four passes in the IsaMill

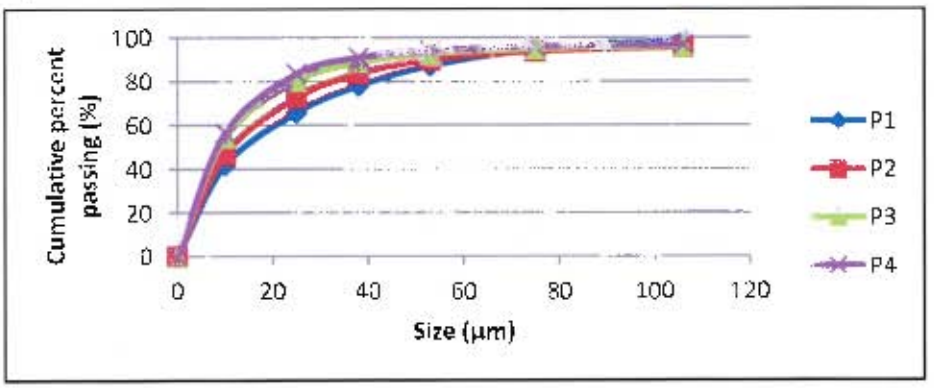

Figure 4.1.2: Malvern size distribution of Nkomati ore milled for four passes in the IsaMill

Table 4.1.1: Size distribution results of Nkomati ore obtained from wet sieving and Malvern sizing (e.g. when i=53 the value shown is the d_{53})

	Sieve Results				Malvern results			
Size class $(\mu m)_i$	d_i Pass1	d_i Pass2	d_i Pass3	d_i Pass4	d_i Pass1	d_i Pass2	d_i Pass3	d_i Pass4
0	0	0	0	0	0	0	0	0
10	41	50	67	75	42	47	54	57
25	70	86	94	97	66	73	80	84
38	82	94	98	99	78	84	88	91
53	93	98	99	99	87	90	92	94
75	98	99	99	100	94	94	95	96
106	100	100	100	100	99	96	96	97

Table 4.1.1 shows the particle size distributions obtained using the sieving and laser diffraction methods. The two sets of results were analysed by ANOVA. The analysis results are given in Table 4.1.2.

Table 4.1.2: P-values to determine the similarity of size distribution results obtained by Malvern and sieve sizing for Nkomati ore

	P-value
Pass1	0.82
Pass2	0.52
Pass3	0.33
Pass4	0.27

Table 4.1.2 shows the *P-values* obtained between sizes distributions of the respective passes. The size distributions obtained from sieving and Malvern sizing for each pass were analysed using Analysis of Variance *(ANOVA), Single-Factor,* to determine if there were any differences in the values obtained by the two methods. This statistical tool assumes the null hypothesis or no difference hypothesis between the sets of data being analysed. *P-value* is the probability that the differences in the data are not random but are a result of a systematic difference between the modes of data investigated. In this case a 95 % confidence interval was chosen, meaning that there was a 5 % probability that the null hypothesis would erroneously be rejected. A *P-value* less than or equal to 0.05 means that there is a systematic difference in the data and the null hypothesis should be rejected.

According to *p-values* in Table 4.1.2, there was no difference between the size distribution measured by sieving and laser diffraction (Malvern) since all the *p-values* are greater than 0.05. It should be noted that the *p-values* decrease as the pass number increases. This shows that the closeness of the results obtained by the two methods decreased as particles became finer. This is as a result of the inherent principles that guide size measurement in the two methods.

Malvern sizing (laser diffraction) has been shown to be suited to measurement of very fine particles (Konert & Vandenberghe, 1997). In their paper, they noted that laser diffraction exaggerated the mean diameter by one or two size classes for particles greater than 2 µm,

which was caused by the non-sphericity of the particles. Compared to laser diffraction, the accuracy and reliability of sieving method reduces for fine particles, with the process becoming very tedious. Malvern sizing method was thus chosen as the sizing method in this project because of the suitability of laser diffraction techniques to fine particles measurement. The bulk of the particles investigated in this project were below 25 µm.

4.1.2 *Determination of Milling Curves for the two ores used in this study*

In order to develop milling curves for Nkomati and UG2 ores milled in the two mills, the bulk mill feed sample was wet milled for different grinding times and number of passes in the ball mill and IsaMill respectively.

The milling results are presented, showing the distribution of the mill product for different grinding times in the case of ball mill and different number of passes in case the IsaMill. Milling curves show a size passed by a given percentage of solids, as a function of milling time or pass number for a ball mill and IsaMill, respectively. In this case, 80% passing size as a function of milling time and pass number was presented as a histogram.

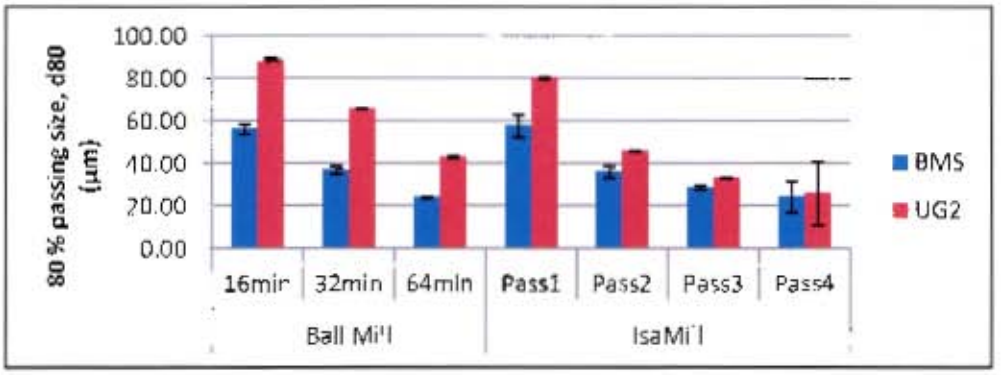

Figure 4.1.3: 80% passing sizes for Nkomati and UG2 ores milled for various grinding times in the ball mill and for four passes in the IsaMill

Figure 4.1.3 shows the P_{80} values after milling Nkomati and UG2 ores in a ball mill and IsaMill. The ores were milled for 16, 32 and 64 minutes in a ball mill and milled for four passes in the IsaMill. It should be noted that milling Nkomati ore in ball mill (16min) and in the IsaMill (1 pass), gave similar P_{80} values, viz. 56 µm and 58 µm respectively. Similarly, ball mill (64 min) and IsaMill (4 pass) material had P_{80} values of 24 µm. For clarity, the d_{80} values of the ore fed to the mills are not included in Figure 4.1.3 but are instead included in Table 4.1.3 and Table 4.1.4.

Table 4.1.3 and Table 4.1.4 show the numerical values of the 50 % and 80 % passing sizes of the mill feed and various products of the ball mill and IsaMill, for Nkomati and UG2 ore respectively. 50 % and 80 % volume of the material are below d_{50} and d_{80} sizes, respectively. The d_{80} values are the same values used to plot Figure 4.1.3.

Table 4.1.3: 50 % and 80 % passing sizes for Nkomati ore milled in the ball mill (16 min, 32min & 64min) and in the IsaMill (1, 2, 3 & 4 pass)

		d50 (μm)	d80 (μm)
Mill Feed	Nkomati feed	37	122
Ball Mill	16 min	19	56
	32 min	14	37
	64 min	9	24
IsaMill	Pass 1	22	58
	Pass 2	14	36
	Pass 3	11	29
	Pass 4	9	24

Table 4.1.4: 50 % and 80 % passing sizes for UG2 milled in the ball mill (16min, 32min & 64min) and in the IsaMill (1, 2, 3 & 4 pass)

		d50 (μm)	d80 (μm)
Mill Feed	UG2 feed	136	246
Ball Mill	16 min	45	89
	32 min	33	66
	64 min	21	43
IsaMill	Pass 1	36	80
	Pass 2	22	46
	Pass 3	15	33
	Pass 4	12	26

4.2 Results obtained for treating ores using the Ball Mill

The results shown in this section present the observations made in the treatment of the two ores, i.e. the base metal sulphide and the UG2 ores, using a ball mill. Section 4.3 will present equivalent results in the case of ore treatment with the IsaMill.

4.2.1 Base metal sulphide ore (Nkomati ore)

This ore sample has been used in earlier studies at UCT. One of these studies investigated the effect of grinding environment on the flotation behaviour of the ore (Mishra, 2011). For this reason this particular ore was chosen to establish a baseline case in the current study.

4.2.1.1 Particle size distribution of ball mill product

It should be noted that the ball mill product is the same as feed to float.

The figures showing size distribution of the mill products (feed to float), i.e. Figure 4.2.1, Figure 4.2.24, Figure 4.3.1 and Figure 4.3.19 display the same data from which Figure 4.1.3 was constructed.

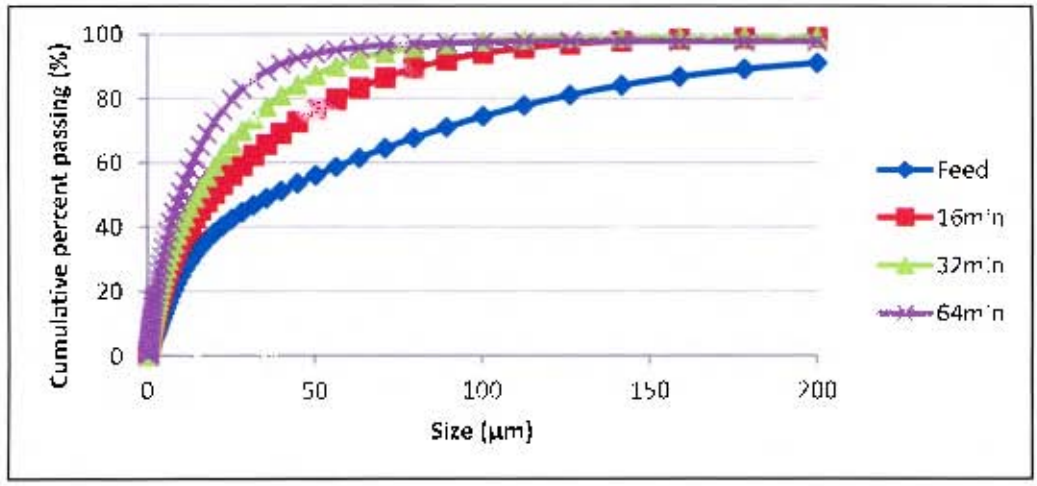

Figure 4.2.1: Size distribution of Nkomati ore milled in the ball mill (16min, 32min and 64min)

4.2.1.2 Particle morphology characterisation

Some aspects of particle morphology were investigated, viz. particle shape. Morphology was characterized by analysing an average of 10 SEM images. The SEM images were then analysed for different shape parameters using proprietary image analysis software. Feret diameter, aspect ratio and roundness were the shape parameters of interest. Feret diameter is defined as the distance between two parallel tangents of the particle at an arbitrary angle. Aspect ratio is defined as the ratio of the particle's longest to its shortest dimension.

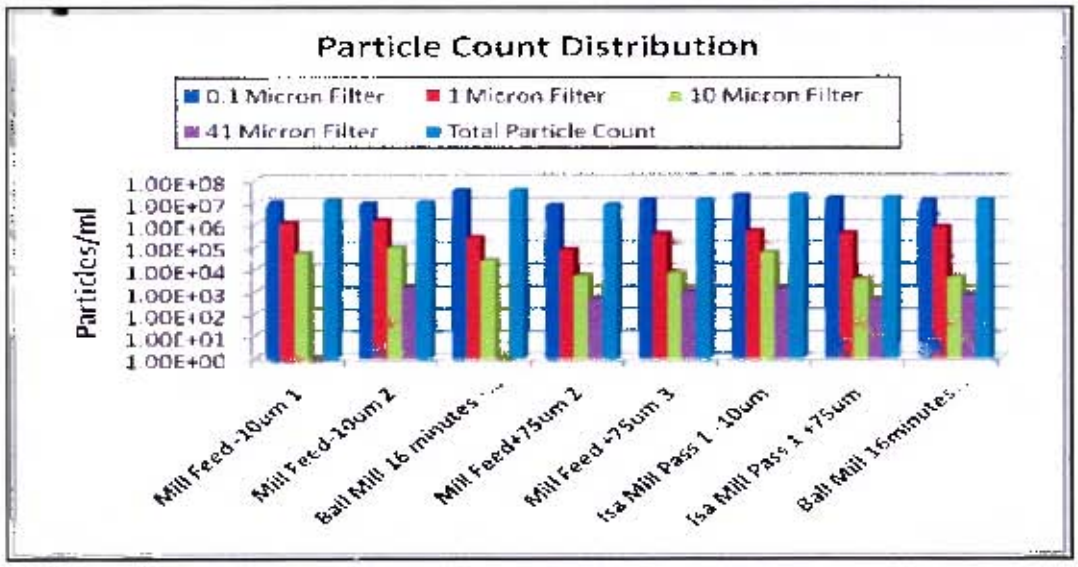

Figure 4.2.2: Number of Nkomati ore particles retained on various filter sizes for mill feed, ball mill 16 minutes and IsaMill pass one products

Figure 4.2.2 shows the number of particles collected on various filter sizes for the different samples. The sample names are shown on the horizontal axis of the histogram. It should be noted from the figure that approximately same number of particles of each sample were retained on each of the different filter sizes. A total of 10 SEM images of the number of particles shown in Figure 4.2.2 were then taken for each sample.

4.2.1.2.1 SEM images

The figures in this section show the SEM images of Nkomati ore milled for a specified time in the ball mill. The images are for samples retained on a 1 micron filter. The figures captions also show the filter size on which the particles were retained.

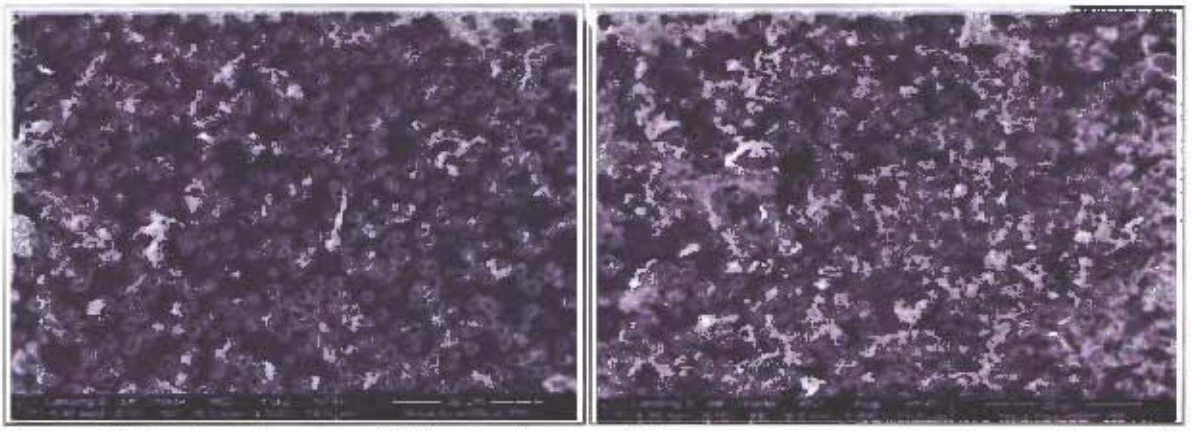

Figure 4.2.3: SEM images of Nkomati ore mill feed samples retained on a 1 µm filter (magnification= 4000 x)

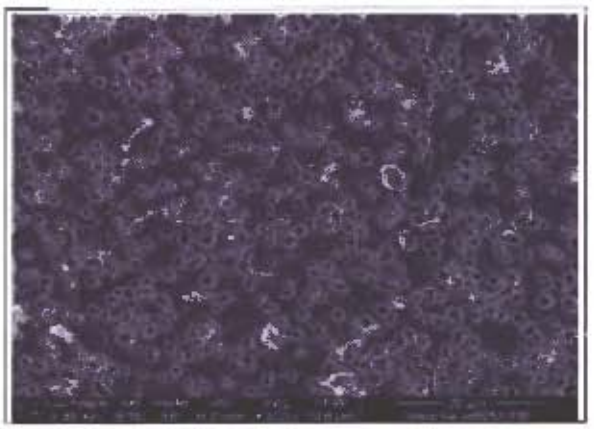

Figure 4.2.4: SEM image of Nkomati ore milled in ball mill (16min), retained on a 1 µm filter (magnification= 4000 x)

4.2.1.2.2 Particle shape characterization

The SEM images were analysed using proprietary image analysis software to calculate the desired shape parameters. Figures from Figure D.1.1 to Figure D.1.4 in Appendix D show the scatter-diagrams of these parameters shown as a function of feret diameter.

It should be noted from Appendix D that the bulk of the particles, milled in ball mill (64min), were distributed around three values of feret diameter. These particles had an aspect ratio between 1 and 5. Roundness values were concentrated between 0.1 and 1. A roundness value of 1 means the particle is perfectly spherical.

4.2.1.2.3 Particle Rheology

The mill products were wet screened at 25 µm; the -25 µm material was dried and riffled. The appropriate masses were weighed out to achieve 10, 20, 30 and 40 volume % in a total slurry volume of 100 ml. The tests were performed using the cup container of the rheometer and a vaned stirrer. Shear rate ranged from 0 to 900/s. The figures that follow

show values of apparent viscosity at a shear rate of 200/s for each of the solids volume concentration mentioned. This procedure was followed for all samples that were analysed for rheology.

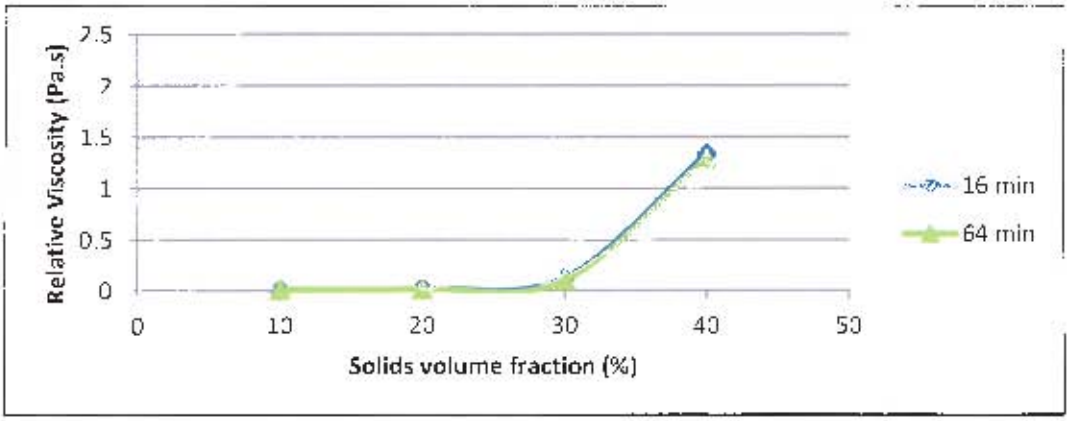

Figure 4.2.5: Relative viscosity as a function of solids volume percentage for -25 µm material of Nkomati ore milled in ball mill (16min and 64 min)

Figure 4.2.5 shows relative viscosity as a function of solids volume percent for Nkomati ore milled in the ball mill (16min & 64 min). The sample names are shown as legends to the right of the figures. These samples had similar relative viscosities for different solids volume concentrations.

Relative viscosity is defined as the ratio of the viscosity of the solution to the ratio of the solvent.

The flow curves at each solids volume concentration for UG2 and Nkomati ores are shown in Appendix F. The flow curves show the apparent slurry viscosity as a function of shear rate for various solids volume fractions.

4.2.1.3 Mineralogy

Table 4.2.1 shows mineral phases present in the Nkomati ore mill feed and the same ore milled in the ball mill (16min & 64min) obtained from XRD analysis. Pyrrhotite is the dominant sulphide. Chalcopyrite and pyrite have roughly similar concentrations, with pentlandite being less than 1 %. The composition of mill feed and ball mill products were similar. Analysis of variance was used to establish that they were similar. The relative amounts of talc and chromite were greater after milling for 64 minutes.

Table 4.2.1: Composition of Nkomati ore determined by XRD

Phase number	Mineral	Weight percent (%)		
		Feed	16 min	64 min
Phase1	Enstatite	15.52	15.72	13.08
Phase2	Pyrite	1.62	1.61	1.52
Phase3	Quartz	2.55	2.40	1.87
Phase4	Talc	3.57	4.09	5.29
Phase5	"Biotite 1M Mica"	15.47	16.61	15.52
Phase6	Chalcopyrite	1.29	0.94	1.40
Phase7	Chromite	5.63	5.24	9.66
Phase8	Pyrrhotite-4C	11.77	11.89	13.18
Phase9	Lizardite 1T	5.60	4.64	5.59
Phase10	Diopsite	22.75	23.36	20.83
Phase11	Tremolite	3.22	2.98	2.70
Phase12	Pentlandite	0.53	0.66	0.70
Phase13	Forsternite iron	10.47	9.87	8.68

4.2.1.4 Batch flotation results

Batch flotation tests were carried out in a 3 L modified Leeds cell as described in the experimental section. The results of the batch flotation tests of Nkomati ore milled in the ball mill are presented in this section.

4.2.1.4.1 Reproducibility of batch flotation tests

Reproducibility is defined as the degree of agreement between measurements or observations conducted on replicate specimens in different locations by different people. Reproducibility also refers to the ability of the whole study to be reproduced by somebody else working independently.

In this case it is taken to mean the degree of agreement between batch flotation tests carried out on the same ore sample at different times. Change in froth stability is one of the most important factors that affect reproducibility of batch flotation tests. Batch flotation tests were conducted to determine reproducibility using Nkomati ore milled in the IsaMill (3 pass), denoted as P3 in the figures, Figure 4.26 to Figure 4.2.9. The reproducibility of the tests was determined for solids, water, copper and nickel recoveries as a function of flotation time.

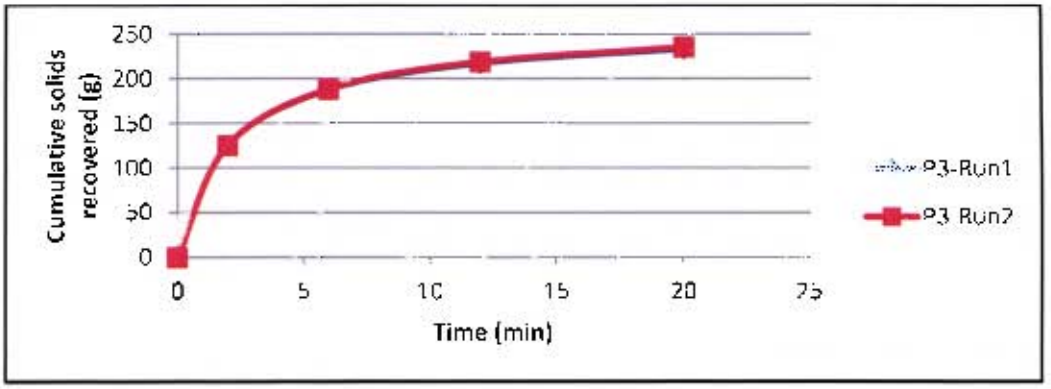

Figure 4.2.6: Solids recovery as a function of time for duplicate batch flotation tests

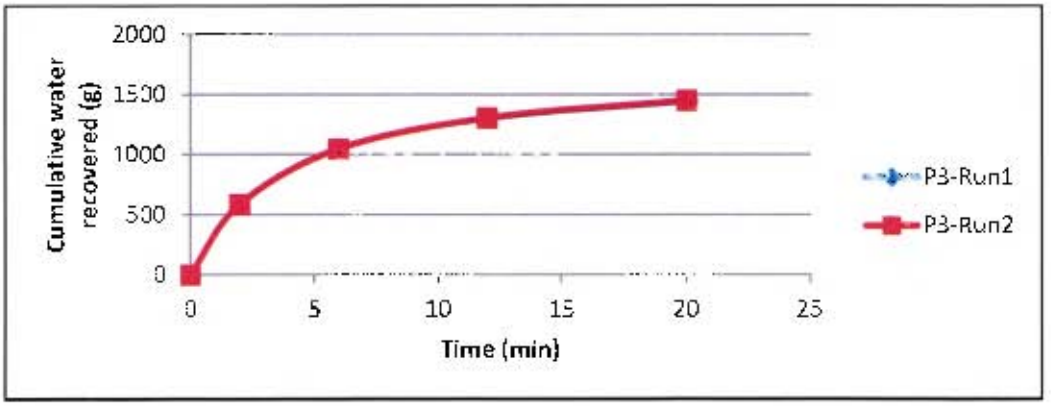

Figure 4.2.7: Water recovery as a function of time for duplicate batch flotation tests

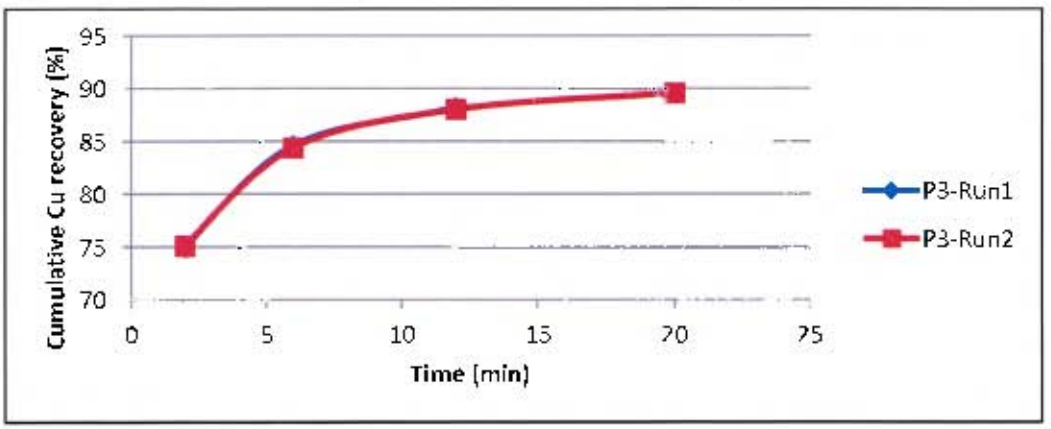

Figure 4.2.8: Cu recovery as a function of time for duplicate batch flotation test

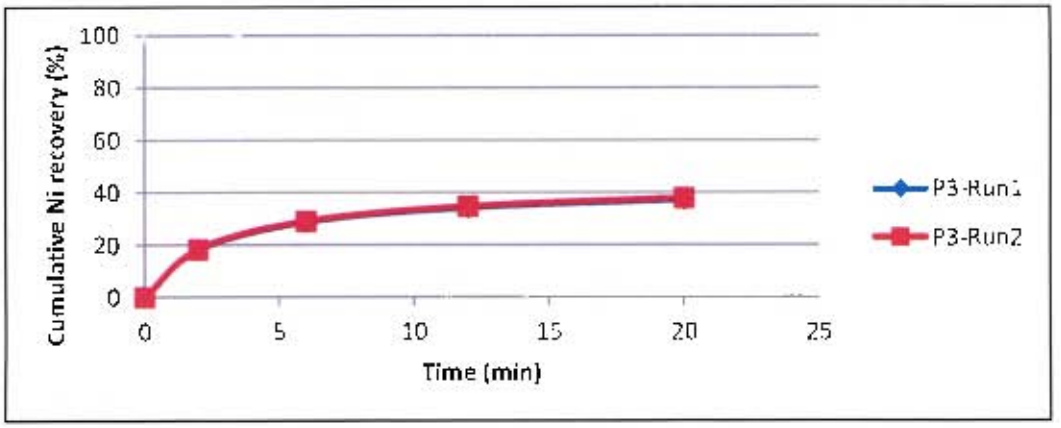

Figure 4.2.9: Ni recovery as a function of time for duplicate batch flotation tests

Figure 4.2.6 to Figure 4.2.9 show that the batch flotation experiments were reproducible. The curves plotted using the results obtained from the two repeats are virtually identical. Same batch flotation procedure which was followed for IsaMill (3 pass) samples was followed for all batch flotation tests.

4.2.1.4.2 Batch flotation results

In this section, batch flotation result on Nkomati ore, figures showing total solids recovery as a function of water recovery are presented first. These are followed by figures showing recovery of each of the sulphide minerals, chalcopyrite, pentlandite and pyrrhotite, as a function of time. Mineral grade-recovery figures then follow.

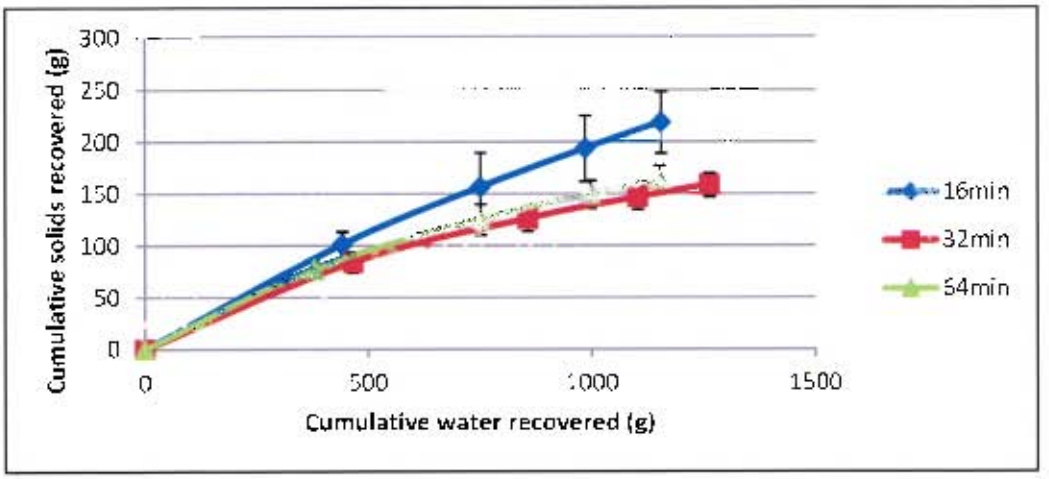

Figure 4.2.10: Solids recovered as a function of water recovery for Nkomati ore milled in ball mill (16min, 32min & 64 min)

Figure 4.2.10 shows the amount of solids and water recovered for batch flotation tests of various ball mill products. It should be noted from this figure that more solids were recovered for the 16 minutes product.

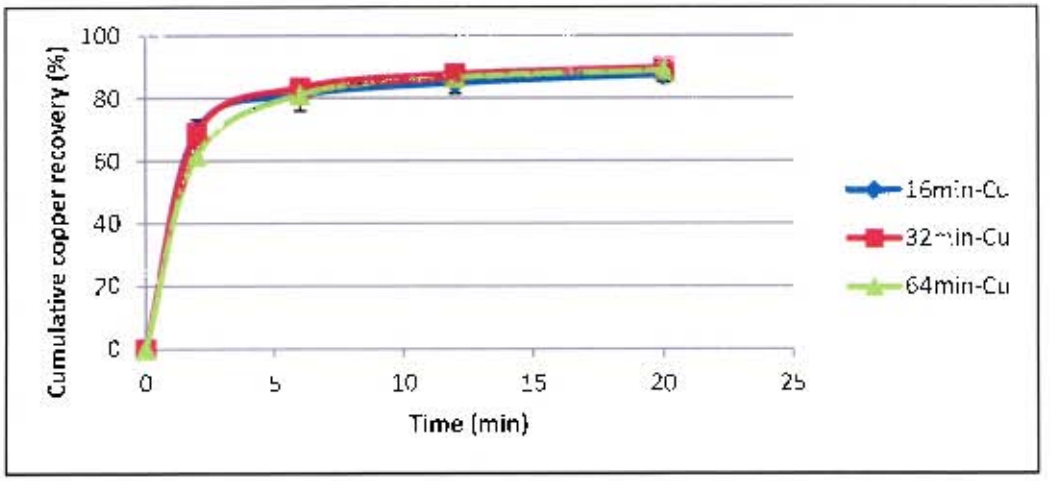

Figure 4.2.11: Cu recovery as a function of flotation time for Nkomati ore ball mill (16min, 32min & 64 min)

Figure 4.2.11 shows the recovery of copper as a function of flotation time for Nkomati ore milled in the ball mill (16min, 32min & 64min). It should be noted that the recovery of copper from the ore was similar despite the variation in the milling time.

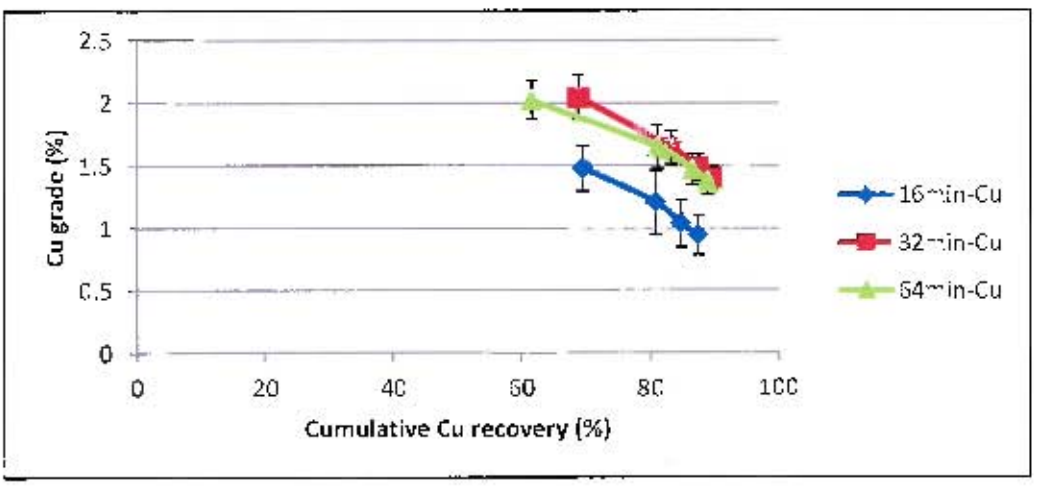

Figure 4.2.12: Cu grade as a function of Cu recovery for Nkomati ore milled in ball mill (16min, 32min & 64 min)

Figure 4.2.12 shows copper grade as a function of copper recovery. There was a decrease in copper grade as copper recovery increased. It should be noted that ball mill (16min) product gave concentrates of lowest grade even though more solids mass was recovered for this sample, as seen in Figure 4.2.10. When the results shown in Figure 4.2.16 are considered, this indicates that the increased solids recovery was almost entirely due to increased gangue (pyrrhotite) recovery.

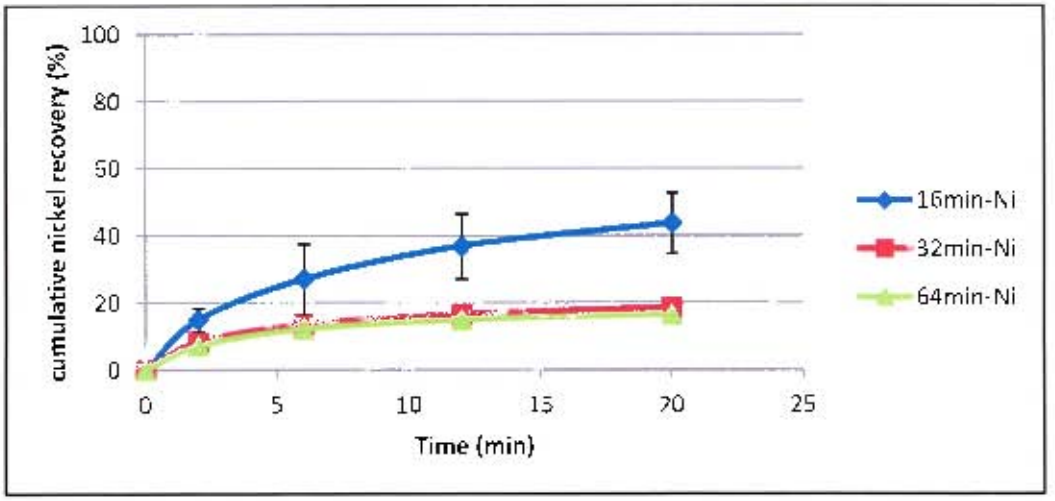

Figure 4.2.13: Ni recovery as a function of flotation time for Nkomati ore milled in a ball mill (16min, 32min & 64 min)

Figure 4.2.13 shows nickel recovery as a function of flotation time for Nkomati ore milled in a ball mill (16min, 32min & 64min). The colour coding matches each curve to the corresponding milling time. Ball mill (32min & 64min) products show similar recoveries with time. Ball mill (16min) product showed a higher recovery. However, it should also be noted that recovery data for ball mill (16min) product had the biggest standard deviation.

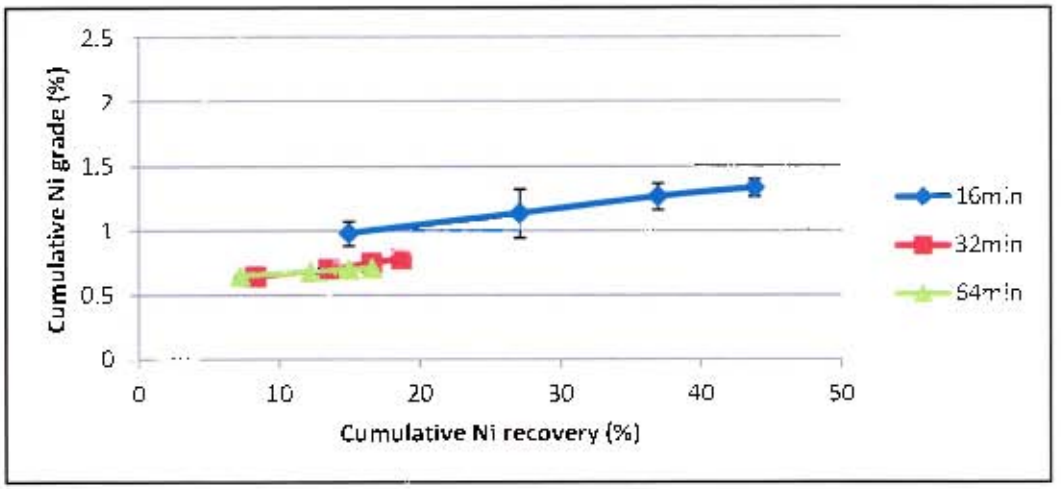

Figure 4.2.14: Ni grade as a function of nickel recovery for Nkomati ore milled in ball mill (16min, 32min & 64 min)

Figure 4.2.14 shows nickel grade as a function of nickel recovery. The figure shows an increase in grade with an increase in recovery. This trend is not typical of grade-recovery behaviour which usually shows a decrease in grade as recovery increases. Furthermore, it should be noted that the highest nickel grade was obtained for ore milled for 16 minutes.

Figure 4.2.15 and Figure 4.2.16 show the results for pyrrhotite grade and recovery. Appendix F explains how pyrrhotite values were obtained from mass balances on copper, iron and sulphur. In this calculation, it was assumed that all the iron in the system reports in either pyrrhotite or chalcopyrite. However, as shown in Table 4.2.1, this is not strictly correct since a small amount of iron is also reporting as pyrite.

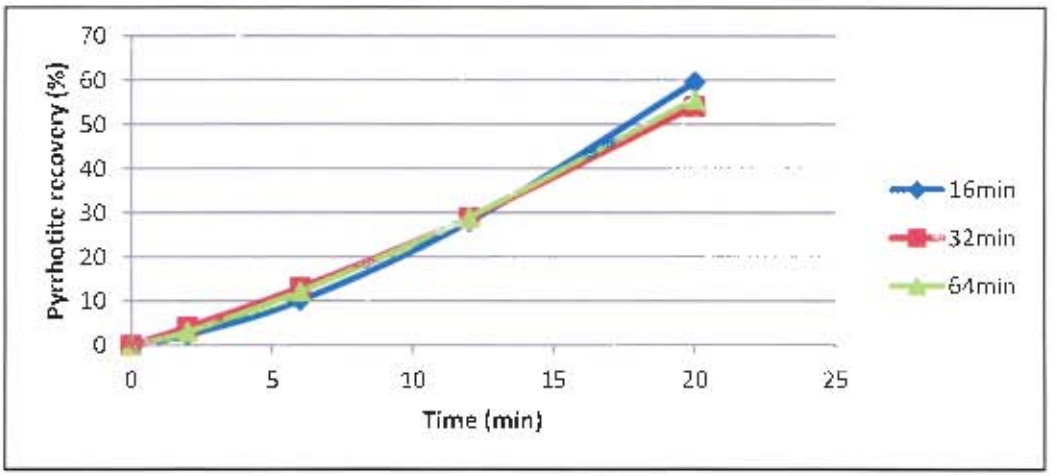

Figure 4.2.15: Pyrrhotite recovery as a function of flotation time for Nkomati ore milled in a ball mill (16min, 32min & 64 min)

Figure 4.2.15 shows the recovery of pyrrhotite as a function of flotation time for Nkomati ore milled in the ball mill (16min, 32min & 64min). The curves show a slight concave upward shape as flotation time increases.

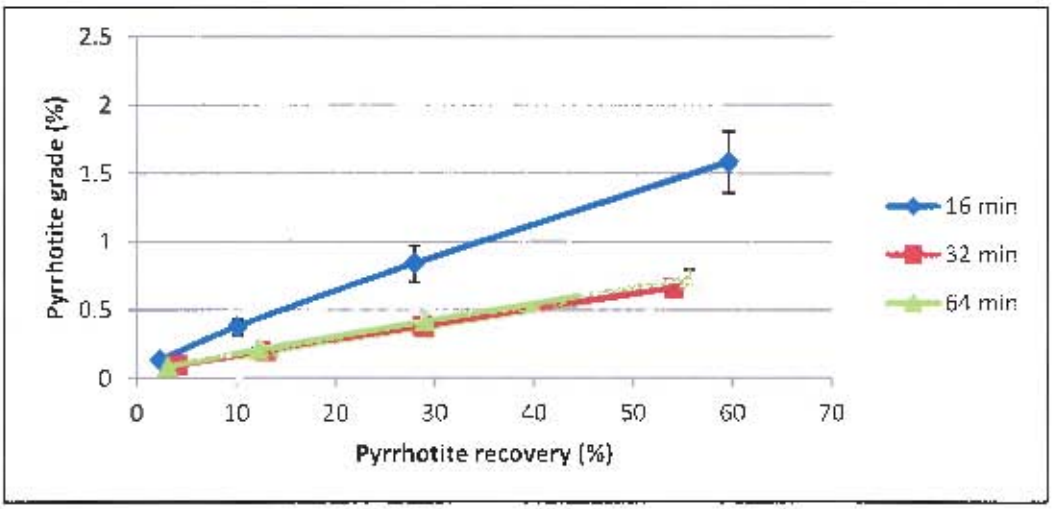

Figure 4.2.16: Pyrrhotite grade as a function of recovery for Nkomati ore milled in a ball mill (16min, 32min & 64 min)

It should be noted that surprisingly the pyrrhotite grade increased with recovery as shown in Figure 4.2.16. Furthermore, pyrrhotite grade for ball mill (16min) product was seen to be significantly higher than for ball mill (32min & 64min) products even though the pyrrhotite recovery as seen in Figure 4.2.15 shows no significant difference between these products.

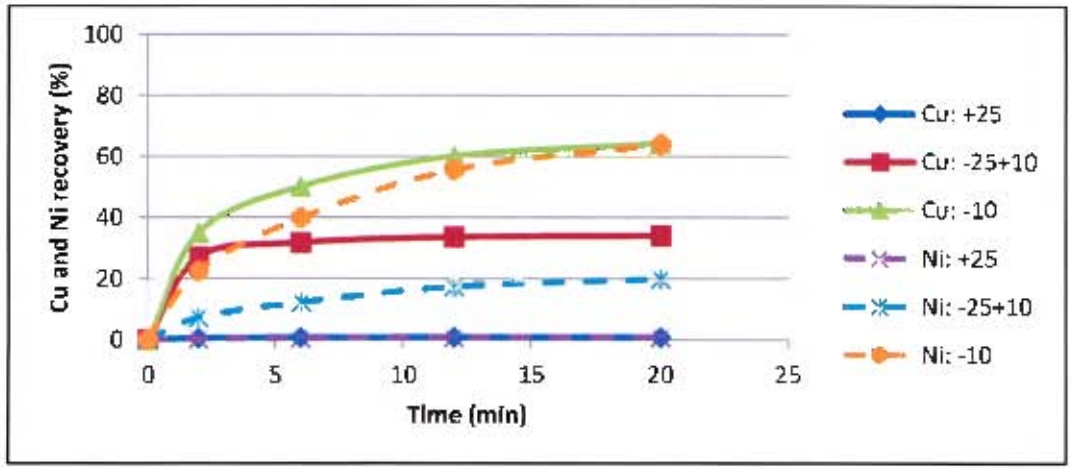

Figure 4.2.17: Cu and Ni recovered into different size fractions during batch flotation of Nkomati ore milled in ball mill (64min)

Figure 4.2.17 shows distribution of recovered copper and nickel by size, for Nkomati ore milled in a ball mill (64min). The distribution of copper and nickel in the concentrate was assessed across the three size fractions viz. -10, +10-25 and +25 µm. This was achieved by screening each of the four batch concentrates into the aforementioned size fractions and then assaying the ore in the fractions for copper and nickel. Copper and nickel recovery were calculated on the basis of the total mass of copper and nickel, respectively, present in the concentrate and tailings. Notable from the figure is the fact that most of the copper and nickel was recovered in the -10 µm fraction. It should also be noted that from Figure 4.2.1, roughly 50 % of the ore was in the -10 µm fraction.

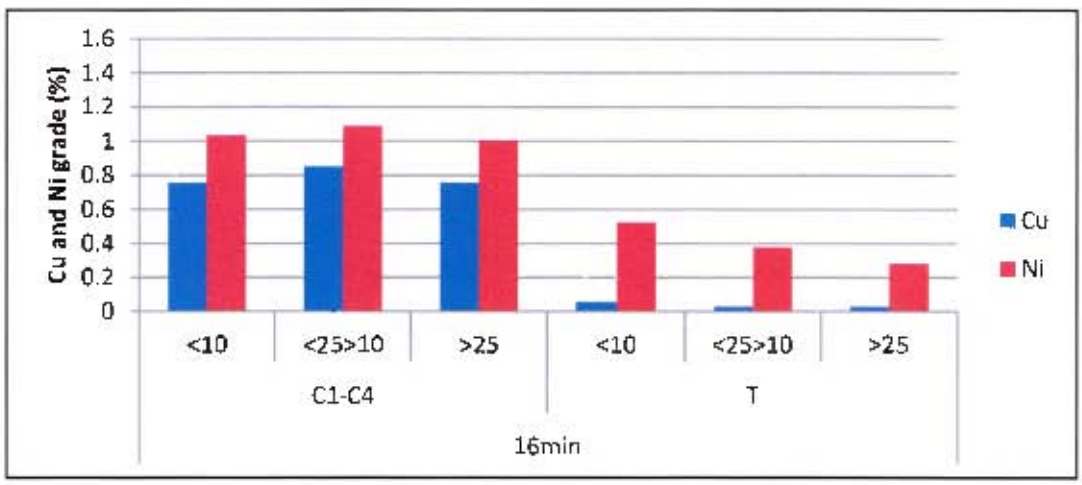

Figure 4.2.18: Cu and Ni grades in different size fractions of concentrates and tailings of Nkomati ore milled in ball mill (16min)

Batch flotation concentrates for ball mill (16min) product were combined and split into three size fractions viz. -10, +10-25 and +25 µm. Copper and nickel grades in these fractions are shown in Figure 4.2.18. The same was done for the tailings. The copper and nickel grades of the tailings were lower than for the concentrates. The highest copper and nickel grades were in the -25+10 µm fraction of the concentrate. The fine (-10 µm) and coarse (+25 µm) fractions had similar copper and nickel grades. Figure 4.2.22 shows that approximately 40 % of the material in the concentrates was below 5 µm. Grade of the nickel lost to the tailings was highest in the -10 µ fraction of the tailings. The grade decreased across the

coarse fractions, reaching the smallest value in the +25 µm fraction of the tailings. Copper grades in the tailings were very low.

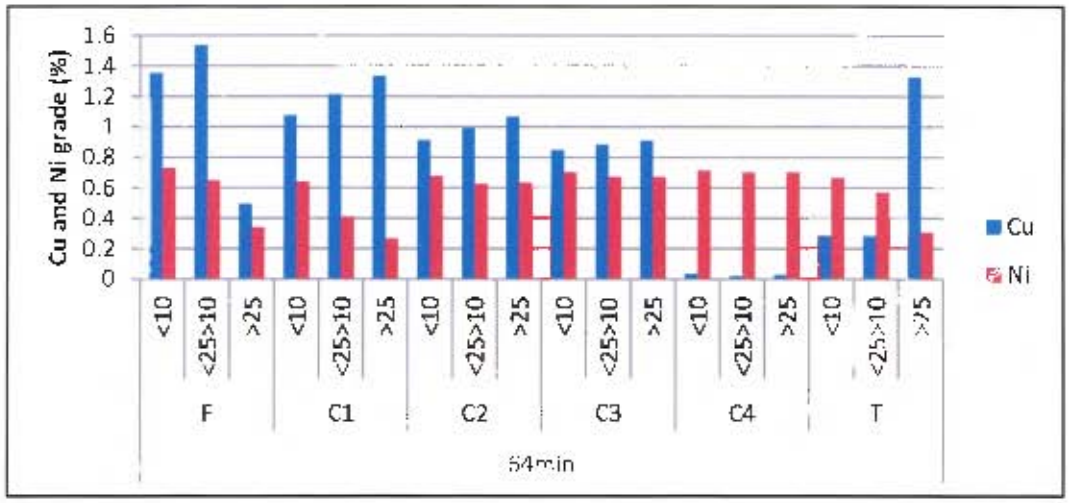

Figure 4.2.19: Cu and Ni grades in different sizes fractions of batch flotation samples of Nkomati ore milled in a ball mill (64min)

Batch flotation concentrates of Nkomati ore milled in a ball mill (64min) were individually separated into three size fractions (-10, +10-25 and +25 µm) and analyzed for copper and nickel. The results of copper and nickel grades in these size fractions are shown in Figure 4.2.19. In the concentrates, the +25 µm fraction had the highest copper grade. Nickel grade was similar in all the size fractions of the concentrates, except for the first concentrate which showed higher grade in the -10 µm fraction. There was a notable trend in the copper and nickel grades of the concentrates across the size fractions. Copper grades increased from fine to coarse size fractions while nickel grades decreased from fine to coarse fractions. However, these differences became less obvious with increasing flotation time. A similar trend was noticed for the tailings.

The full size distributions of the Nkomati feed, concentrates and tailings are shown from Figure 4.2.20 to Figure 4.2.23.

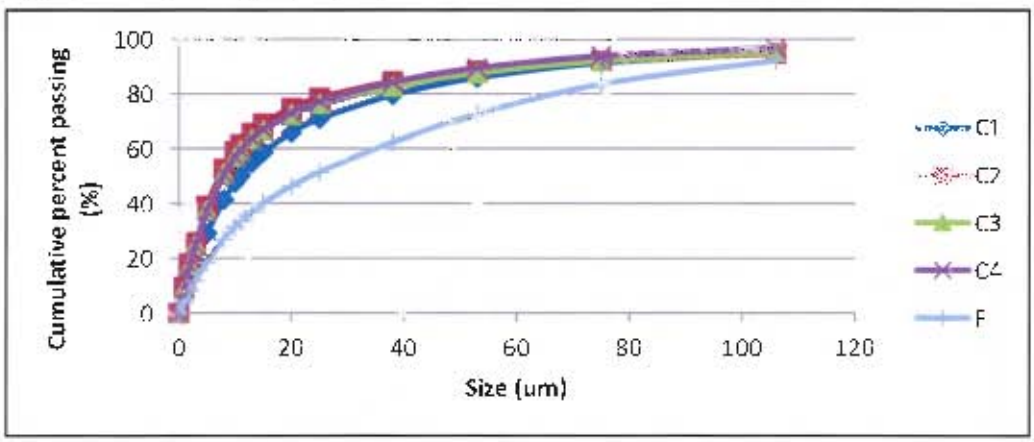

Figure 4.2.20: Size distribution of feed and concentrates of Nkomati ore milled in a ball mill (16min)

Figure 4.2.20 shows the particle size distributions of four batch flotation concentrates from Nkomati ore that was milled in the ball mill (16min). The colour coding differentiates between the size distribution curves for the different concentrates. The curve for

concentrate one (C1) was slightly lower than the curves for other concentrates in the approximate range from 5 µm to 40 µm, indicating presence of coarser particles in this concentrate sample. The size distribution curves for the other concentrates are virtually identical, indicating a similar size distribution of the particles in these concentrate samples.

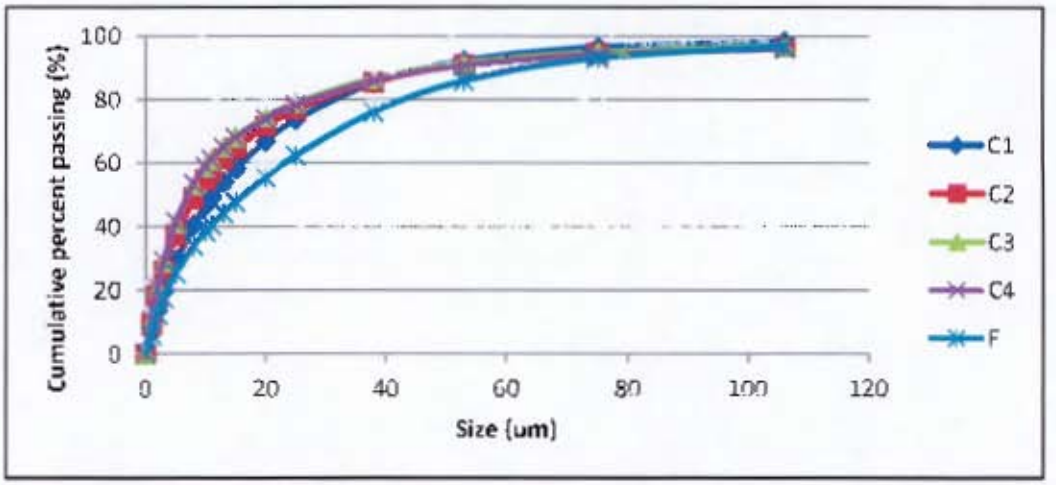

Figure 4.2.21: Size distribution of feed and concentrates of Nkomati ore milled in a ball mill (32min)

Figure 4.2.21 shows particle size distributions of four batch flotation concentrates from Nkomati ore that was milled in the ball mill (32min). It should be noted that in the approximate size range between 10 µm and 30 µm, the percentage of material passing a given size for concentrate one (C1) was lower than for the rest of the concentrates. The size distribution curves for concentrates two (C2), three (C3) and four (C4) were almost identical.

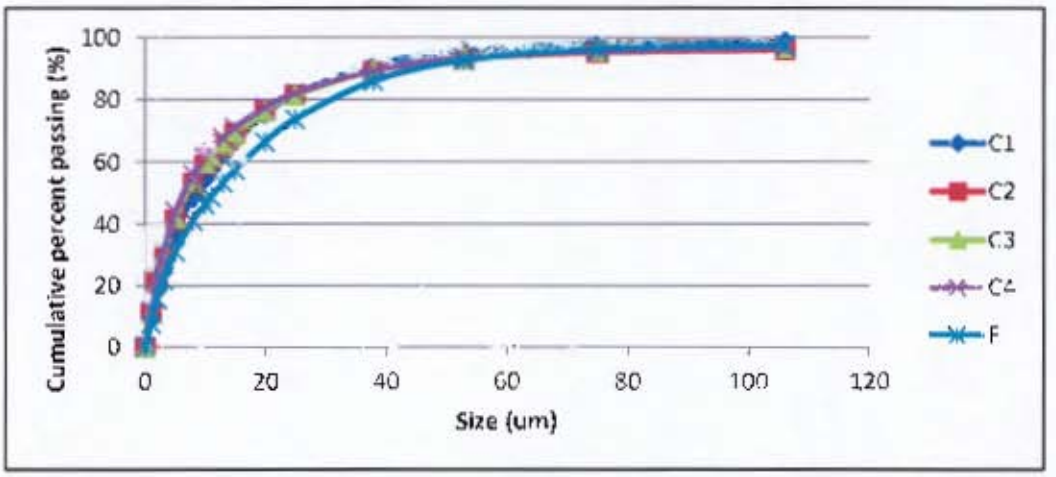

Figure 4.2.22: Size distribution of feed and concentrates of Nkomati ore milled in a ball mill (64min)

Figure 4.2.22 shows the particle size distributions of feed and four batch flotation concentrates of Nkomati ore milled in the ball mill (64min). It should be noted that the curves are very close together, indicating similar size distribution of particles in the concentrate samples. The feed to the float cell is equivalent to mill product. From this figure, it can be seen that approximately 80 % of the material in each concentrate sample is below 20 µm.

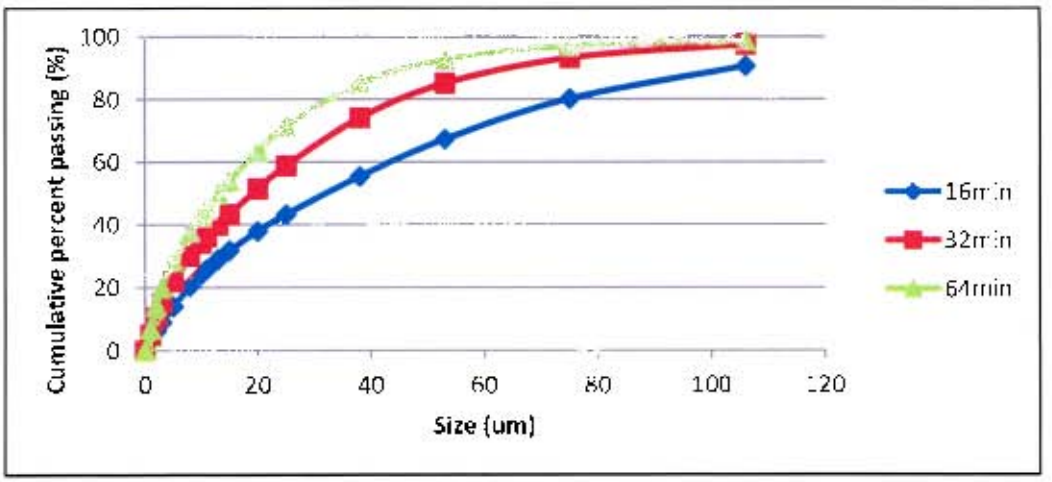

Figure 4.2.23: Size distribution of tailings of Nkomati ore milled in a ball mill (16min, 32min and 64min)

Figure 4.2.23 shows the size distributions of the batch flotation tailings for Nkomati ore that was milled in ball mill (16min, 32min & 64 min). The size distributions of the tailings follow a similar trend to the mill products of the corresponding grinding times.

Table 4.2.2: 50% and 80% passing sizes for flotation feed, concentrates and tailings of Nkomati ore milled in the ball mill (16min & 64min)

	16 min		64 min	
	d50 (µm)	d80 (µm)	d50 (µm)	d80 (µm)
F	24	67	12	31
C1	11	39	8	24
C2	7	28	7	23
C3	8	32	7	23
C4	8	29	6	23
T	32	75	13	32

Table 4.2.2 shows d_{50} and d_{80} sizes for the batch flotation samples of Nkomati ore milled in the ball mill (16min & 64min). Notable from the table is the fact that first concentrates for each of the mill products were slightly coarser than the subsequent concentrates, as indicated by the d_{50} and d_{80} values.

4.2.2 *Platinum group ore (Impala UG2)*

4.2.2.1 *Particle size distribution of ball mill product*

Impala UG2 ore was milled for 16, 32 and 64 minutes in the ball mill. These milled samples provided the feed to float.

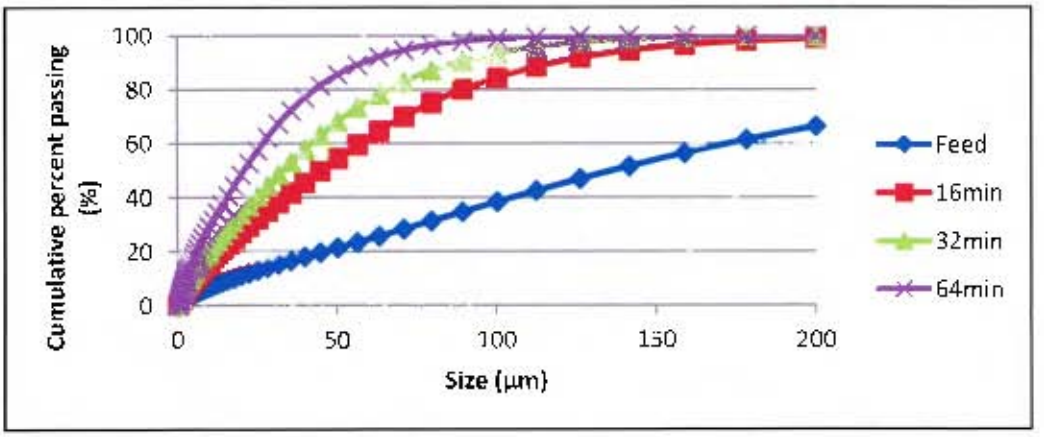

Figure 4.2.24: Size distribution of UG2 ore milled in a ball mill (16min, 32min and 64min)

4.2.2.2 Particle Morphology characterisation

4.2.2.2.1 Scanning electron microscopy (SEM)

The figures shown in this section show the SEM images of the UG2 ore milled for a specified time in the ball mill.

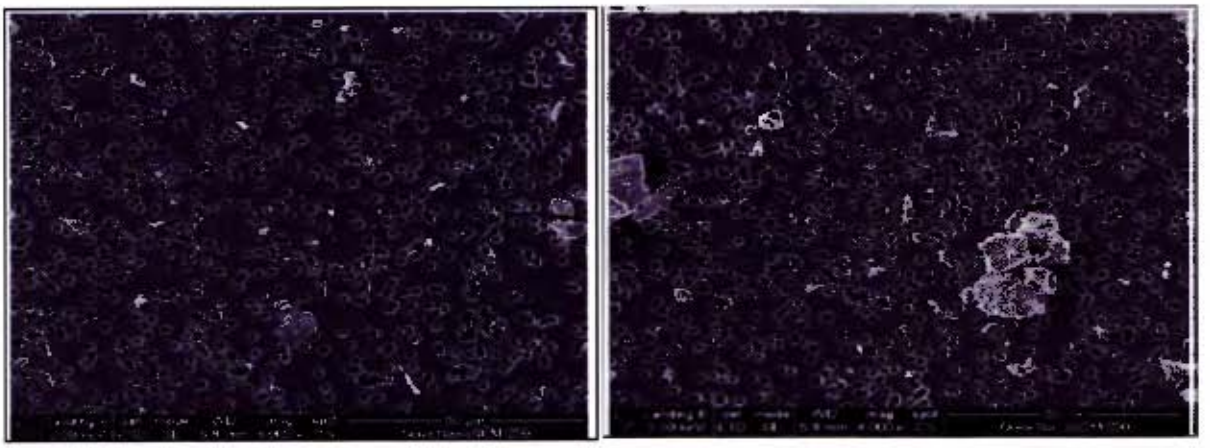

Figure 4.2.25: SEM images of UG2mill feed retained on a 1.2 µm filter (magnification= 4000 x)

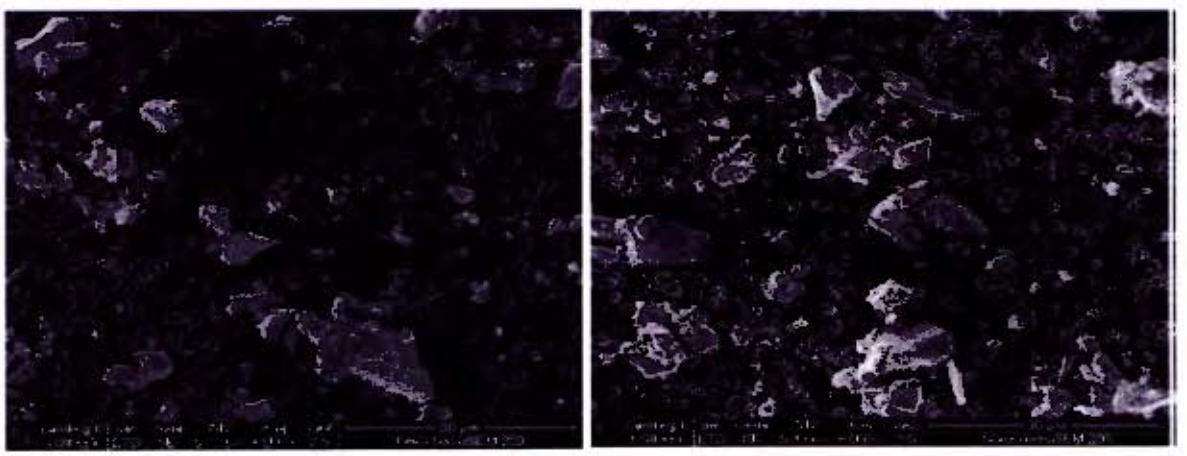

Figure 4.2.26: SEM images of 16 minutes (left) and 64 minutes (right) products of UG2 ore milled in the ball mill, retained on 1.2 µm (magnification= 4000 x)

The SEM images shown in Figure 4.2.25 and Figure 4.2.26 were for -10 µm ore material for each of the conditions. The -10 µm samples were filtered and the material remaining on the filters was imaged to give an average of 10 images for each sample. The filter pore size is included in the figure captions.

4.2.2.2.2 Particle shape characterization

Scatter-diagrams showing aspect ratio and roundness as a function of feret diameter for the particles were compiled. The figures were obtained by analysing the SEM images using proprietary software. The figures are shown in Appendix D.

4.2.2.2.3 Particle Rheology

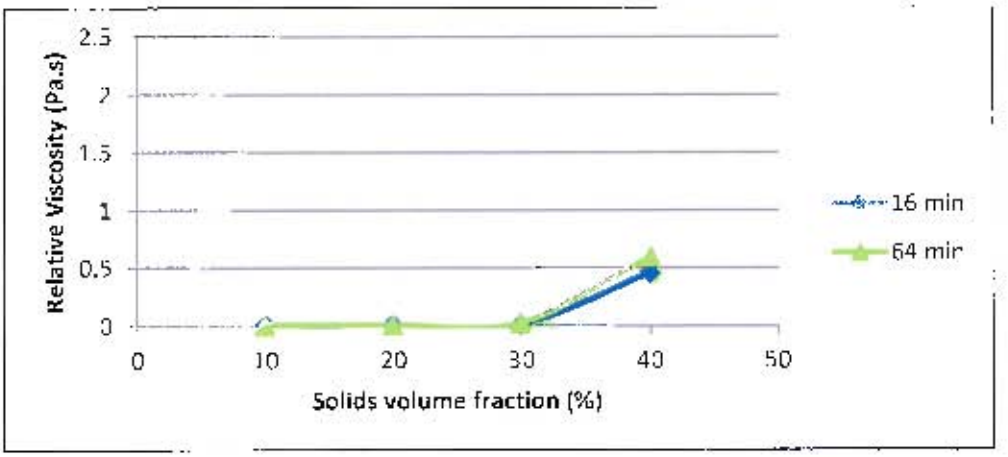

Figure 4.2.27: Relative viscosity as a function of solids volume percentage for -25 µm of UG2 ore milled in ball mill (16min and 64 min)

Figure 4.2.27 shows the relative viscosity of UG2 ore milled in a ball mill for16 and 64 minutes. Ball mill (64min) product shows a slightly higher viscosity than the ball mill (16min) product. It should be noted that differences in viscosity were only noticeable at higher solids volume percent (40 %). Further increases in solids content may have resulted in distinct differences. However, it was not easy to prepare slurry of higher solids content because there was improper mixing of the aqueous solution and the ore. This was largely as a result of the high settling rate of the high density UG2 ore.

4.2.2.3 Mineralogy

X-ray diffraction (XRD) was used to determine structure and mineralogical composition of the ore. There were no differences in structure between ores milled in the two mills.

Table 4.2.3 shows the different phases or minerals and their relative weight percentage in the UG2 ore sample. The composition was determined using XRD. This was determined for the mill feed, ball mill (16min & 64 min) products. Bronzite, chromite, bytownite and diopsite iron were the major components, with significant traces of talc, pyrrhotite and forsterite iron. Bronzite is a member of the orthopyroxene groups. It has the formula, $(Mg,Fe)SiO_3$ (Pillay *et al.*, 2011)

Table 4.2.3: Composition of UG2 ore determined by XRD

Phase number	Mineral	Weight percent (%)		
		Feed	16min	64min
Phase1	Chromite	28.97	26.82	27.82
Phase2	Talc	2.26	2.93	2.53
Phase3	Phlogopite 1M Mica	0.93	1.03	1.18
Phase4	Bytownite	17.02	19.23	18.30
Phase5	Pentlandite	0.00	0.00	0.00
Phase6	Chalcopyrite	0.11	0.16	0.15
Phase7	Pyrite	0.04	0.16	0.09
Phase8	Hornblende magnesian iron	0.96	1.17	0.88
Phase9	Quartz	0.58	0.73	0.50
Phase10	Calcite	0.25	0.33	0.18
Phase11	Forsterite iron	1.60	2.18	2.94
Phase12	Orthoclase	0.62	0.54	0.32
Phase13	Bronzite	36.25	34.68	35.28
Phase14	Pyrrhotite-4C	2.50	2.40	1.62
Phase15	Diopsite iron	7.78	7.54	7.87
Phase16	Chlorite	0.04	0.10	0.40
Phase17	Epidote	0.09	0.00	0.00

4.2.2.4 Batch flotation results

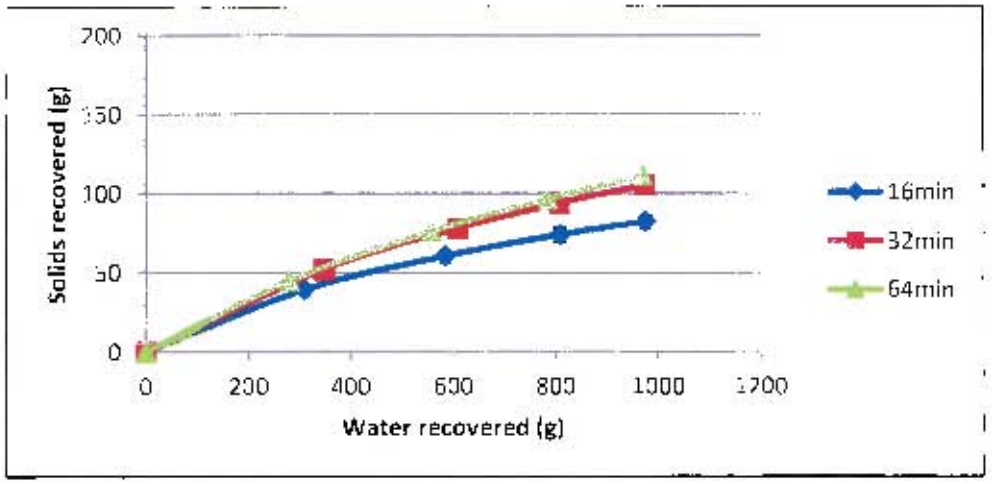

Figure 4.2.28: Solids recovery as a function of water recovery for UG2 ore treated in ball mill (16min, 32min and 64 min)

Figure 4.2.28 shows the amount of solids recovered as a function of water recovery for ball mill products. Relative higher amounts of solids were recovered for the fine (32 and 64 minutes) mill product.

Table 4.2.4: Mass distribution of chromite in the flotation feed, concentrates and tailings of UG2 ore milled in ball mill (16min)

16 min	Mass of Cr_2O_3 (g)			Total	% of feed
Sample name	Size fraction (µm)			mass (g)	Cr_2O_3
	<10	>10<25	>25		
F	26.8	69.2	96.1	192.1	
C	9.0	2.1	0.7	11.7	6.0
T	21.4	53.5	79.5	154.4	80.0

The total concentrate solids recovered were wet screened into three size classes viz. -10 µm, +10-25 µm and +25 µm. Each size class was analysed for chromite.

Table 4.2.4 shows the mass distribution of chromite in the feed to flotation, concentrates and tailings of the ball mill (16min) product. The chromite in the feed was screened into the respective size fractions. The concentrates and tailings were also wet screened into similar size fractions. It should be noted that 6 % of the mass of chromite in the feed to flotation was recovered as flotation concentrates whereas 80 % remained in the tailings. It should be noted from the table that Cr_2O_3 in the concentrates and tailings accounts for only 86 % of the Cr_2O_3 in the feed, making the Cr_2O_3 mass balance not to tie. The 14 % difference can be taken to be a result of experimental error. This is because Cr_2O_3 assays of the tailings are usually difficult to conduct. Furthermore, standard deviation data of the Cr_2O_3 assays could not be obtained. An example of chromite assay results can be seen in Table F.3. The chromite assays were done using different standards, depending on the chrome content of the sample. Each standard had a corresponding range of standard deviation. 1.91 % chrome has +/-8.38 % error; 10.37 % had +/- 1.45 % error and 52.60 % had +/- 0.38 % error.

Different standards could have been used for different samples, which explain the error in the mass balance.

Table 4.2.5: Mass distribution of chromite in flotation feed, concentrates and tailings of UG2 ore milled in ball mill (64min)

64min	Mass of Cr_2O_3 (g)			Total	% of feed
Sample name	Size fraction (µm)			mass (g)	Cr_2O_3
	<10	>10<25	>25		
F	41.9	143.3	14.8	200.0	
C1	2.0	0.0	0.0	2.5	1.0
C2	5.5	0.8	0.0	6.4	3.0
C3	5.4	0.8	0.0	6.2	3.0
C4	17.2	1.0	0.0	18.2	9.0
T	36.1	101.8	12.14	150.1	75.0

Table 4.2.5 shows the mass distribution of chromite in feed to float, flotation concentrates and tailings for UG2 ore milled in a ball mill (64min). The representative samples of feed, concentrates and tailings were wet screened into respective size classes viz. -10 µm, +10-25 µm and +25 µm. The mass of chromite in the feed to flotation in the respective size fractions can be seen from the table. A total of 16 % of this mass was recovered into the concentrates and 75 % remained in the tailings. This accounts for 91 % of the chromite in the feed. The 9 % difference can be taken to be due to experimental error, for the same reasons which were mentioned in the explanation of results Table 4.2.4. Values of chromite mass shown in the two preceding tables were rounded to one decimal place.

Figure 4.2.28 shows total solids recovery of approximately 100 g after 20 minutes of batch flotation. According to Table 4.2.5, almost all of this recovered mass was in the -10 µm fraction, suggesting recovery almost entirely by entrainment.

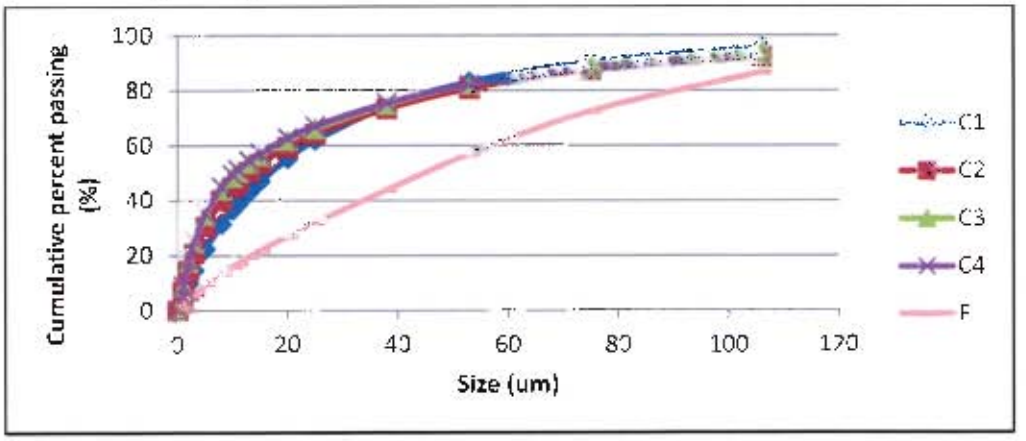

Figure 4.2.29: Size distribution of feed and concentrates for UG2 ore treated in ball mill (16 min)

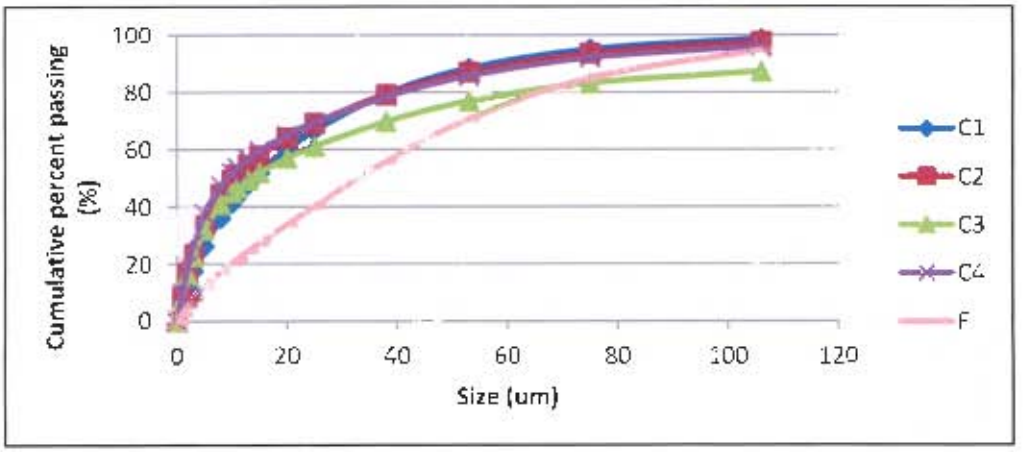

Figure 4.2.30: Size distribution of feed and concentrates for UG2 ore treated in ball mill (32 min)

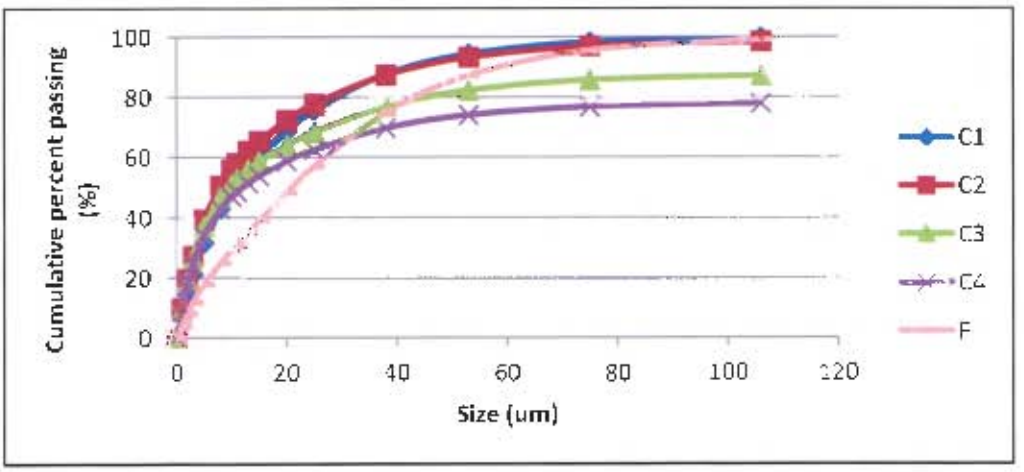

Figure 4.2.31: Size distribution of feed and concentrates for UG2 ore treated in ball mill (32 min)

The particle size distributions of the particles recovered in each concentrate during the batch flotation tests are shown in Figure 4.2.29 to Figure 4.2.31. Relatively fine particles were recovered for ball mill (32min & 64min) products during the early stages of flotation (C1 and C2) and coarse particles were recovered as the flotation time increased (C3 and C4). The d_{80} sizes for third and fourth concentrates were coarser than for the first and second concentrates. However, in the case of the ball mill (16min) sample, flotation resulted in the same size particles being recovered across the flotation time.
Size distributions of the tailings are shown in Figure 4.2.32 and tabulated in Table 4.2.6. The fineness of the tailings increased with increasing milling time.

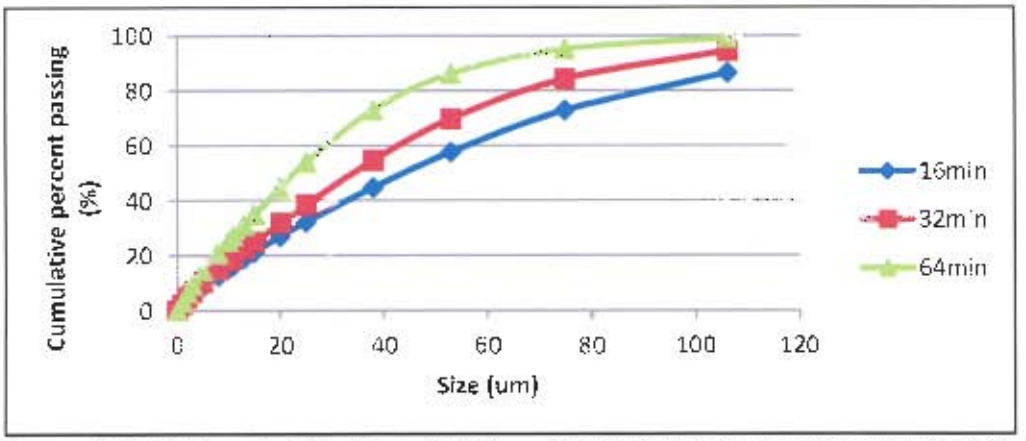

Figure 4.2.32: Size distribution of tailings for UG2 ore treated in ball mill (16min, 32min and 64 min)

Table 4.2.6: 50% and 80% passing sizes for flotation feed, concentrates and tailings of UG2 ore milled for 16 and 64 minutes in the ball mill

	16 min		64 min	
	d50 (µm)	d80 (µm)	d50 (µm)	d80 (µm)
F	45	89	21	43
C1	17	47	10	29
C2	13	52	8	27
C3	11	48	7	26
C4	10	48	7	26
T	44	89	23	45

Coarse particles were recovered in the early stages of flotation and progressively finer particles were recovered as flotation time increased. This is shown by the large d50 and d80 of the first concentrate compared to those of the subsequent concentrates.

4.3 Batch flotation results obtained for treating ores with M4 IsaMill

This section presents the results obtained when treating the two ores in the IsaMill. Section 4.2 focused on the ball mill results.

4.3.1 Base metal sulphide ore (Nkomati ore)

4.3.1.1 Particle size distribution of IsaMill product

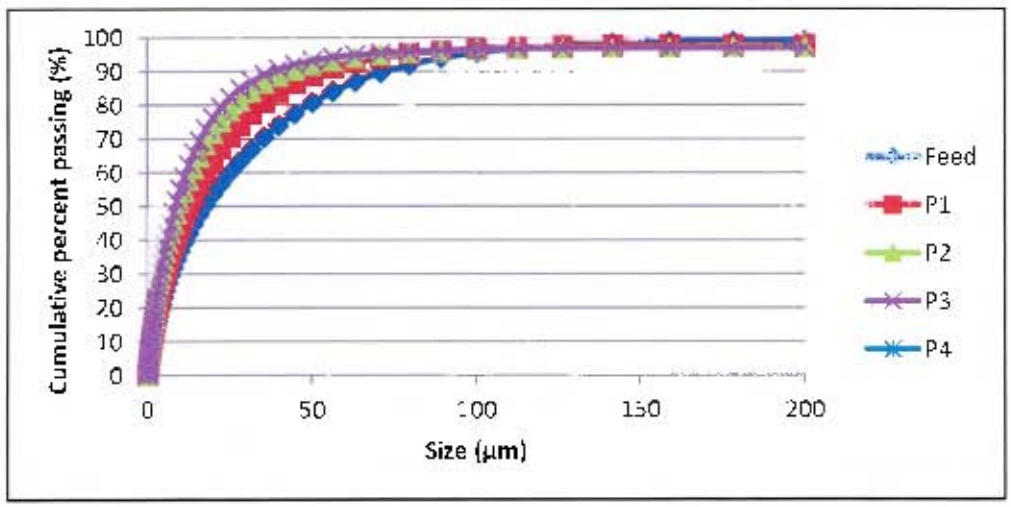

Figure 4.3.1: Size distribution of Nkomati ore milled in the IsaMill (1, 2, 3 & 4 pass)

Figure 4.3.1 shows size distribution of Nkomati ore milled in the IsaMill (1, 2, 3 & 4 pass). There is a respective similarity between the size distributions of ore milled for one and four passes in the IsaMill and same ore milled for 16 and 64 minutes in the ball mill. Size distributions of ore milled in the ball mill were shown in Figure 4.2.1.

4.3.1.2 Particle morphology characterisation

An aspect of particle morphology that was investigated in this work is particle shape. Particle shape was measured using SEM imaging together with proprietary image analysis software for determining shape parameters of the images. Behavioural effect of particle shape was studied by investigating rheological behaviour of ore samples from the two mills.

4.3.1.2.1 Scanning electron microscopy (SEM)

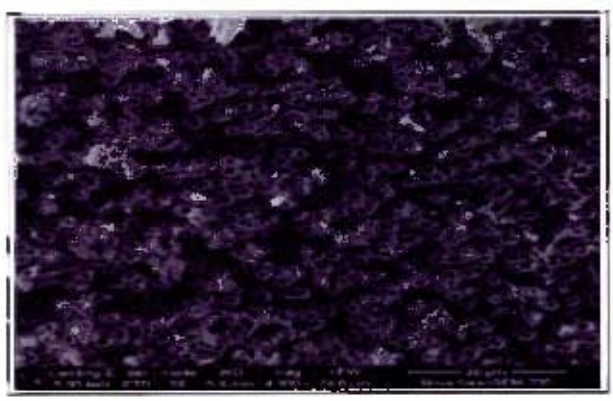

Figure 4.3.2: SEM image of IsaMill (1 pass) product of Nkomati ore retained on a 1 µm filter(magnification= 4000 x)

4.3.1.2.2 Particle Rheology

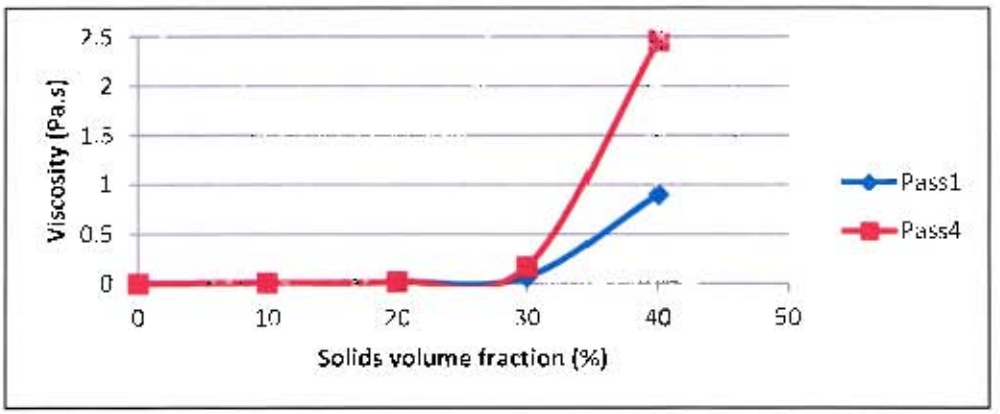

Figure 4.3.3: Relative viscosity as a function of solids volume percentage for -25 µm material of Nkomati ore milled in IsaMill (1 & 4 pass)

Figure 4.3.3 shows the relative viscosity of -25 µm fraction of Nkomati ore milled in the IsaMill (1 & 4 pass). The difference in the viscosity becomes apparent above 30 % solids volume content. Nkomati ore milled in the IsaMill (4 pass) had the highest viscosity. It should be noted here that the viscosity of Nkomati ore milled in ball mill (64min), Figure 4.2.5, was lower than that of the same ore milled in the IsaMill (4 pass), Figure 4.3.3. On the other hand, the ore milled in ball mill (16min) had higher viscosity than ore milled in the IsaMill (1 pass).

4.3.1.3 Mineralogy

Table 4.3.1 shows the composition of Nkomati ore determined by XRD. The samples analysed were the mill feed and ore milled in the IsaMill (1 & 4 pass). It should be noted that there is no significant difference in composition between the feed and IsaMill products. Pyrrhotite is the dominant sulphide mineral, with chalcopyrite and pyrite having equivalent amounts. Pentlandite is less than 1 %.

Table 4.3.1: Composition of Nkomati ore mill feed and IsaMill products determined by XRD

Phase number	Mineral	Weight percent (%)		
		Feed	Pass1	Pass4
Phase1	Enstatite	15.52	15.10	14.51
Phase2	Pyrite	1.62	1.52	1.69
Phase3	Quartz	2.55	2.82	2.75
Phase4	Talc	3.57	3.97	4.92
Phase5	"Biotite 1M Mica"	15.47	14.82	15.39
Phase6	Chalcopyrite	1.29	1.14	1.23
Phase7	Chromite	5.63	4.90	5.37
Phase8	Pyrrhotite-4C	11.77	11.33	10.38
Phase9	Lizardite 1T	5.60	7.23	6.83
Phase10	Diopsite	22.75	24.50	24.61
Phase11	Tremolite	3.22	3.08	2.93
Phase12	Pentlandite	0.53	0.51	0.55
Phase13	Forsternite iron	10.47	9.09	8.85

4.3.1.4 Batch flotation results

In section 4.2.1.4.1, results were presented which showed the reproducibility of the batch flotation procedure. The same flotation procedure was followed in obtaining the results presented in this section and the previous section on ball mill.

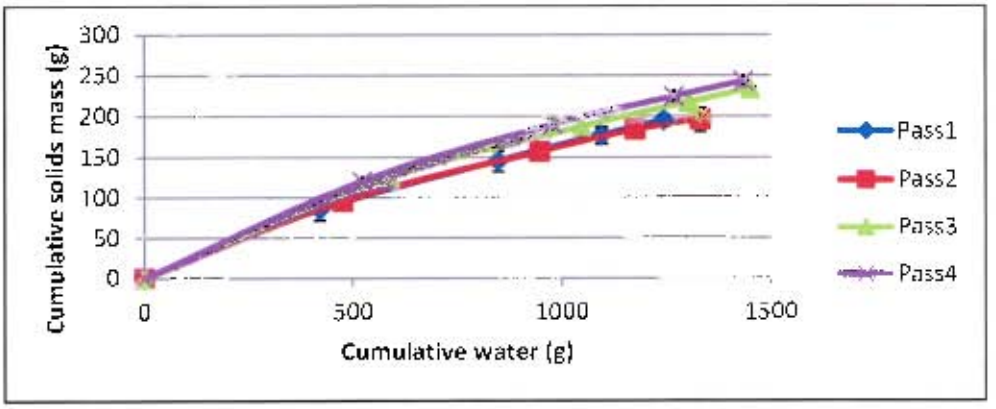

Figure 4.3.4: Solids recovery as a function of water recovery for Nkomati ore milled in IsaMill (1, 2, 3 & 4 pass)

Figure 4.3.4 shows the mass of solids recovered as a function of water recovered during batch flotation tests on Nkomati ore milled in IsaMill (1 & 4 pass). As was seen in Figure 4.3.1, IsaMill (3 & 4 pass) products had the largest fraction of very small particles. It can therefore be noted that a large proportion of these fine particles was recovered together with water during the batch flotation tests. Compared to Figure 4.2.10, more solids were recovered for IsaMill products than for ball mill products after 20 minutes of flotation.

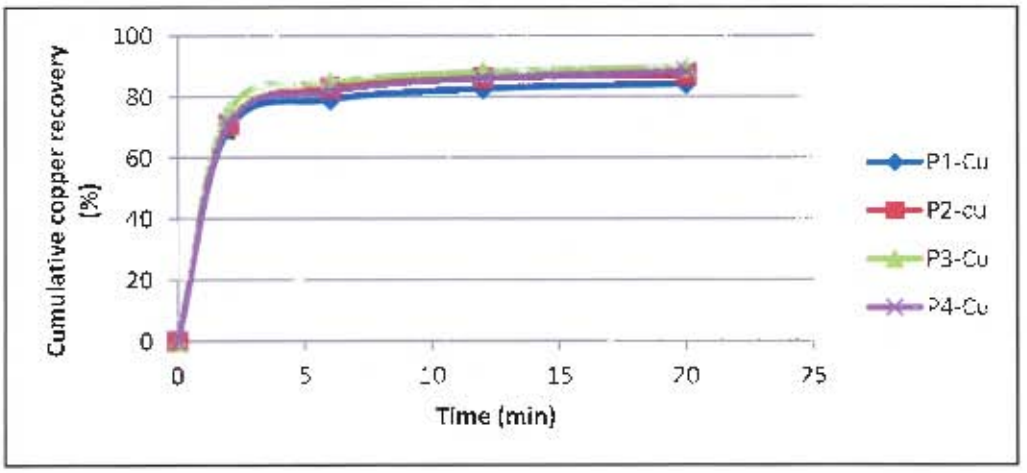

Figure 4.3.5: Cu recovery as a function of flotation time for Nkomati ore milled in IsaMill (1, 2, 3 & 4 pass)

Figure 4.3.5 shows the recovery of copper as a function of flotation time for IsaMill products. It should be noted that the recovery curves lie very close to each other showing little difference in copper recovery for the products obtained after different number of passes in the IsaMill.

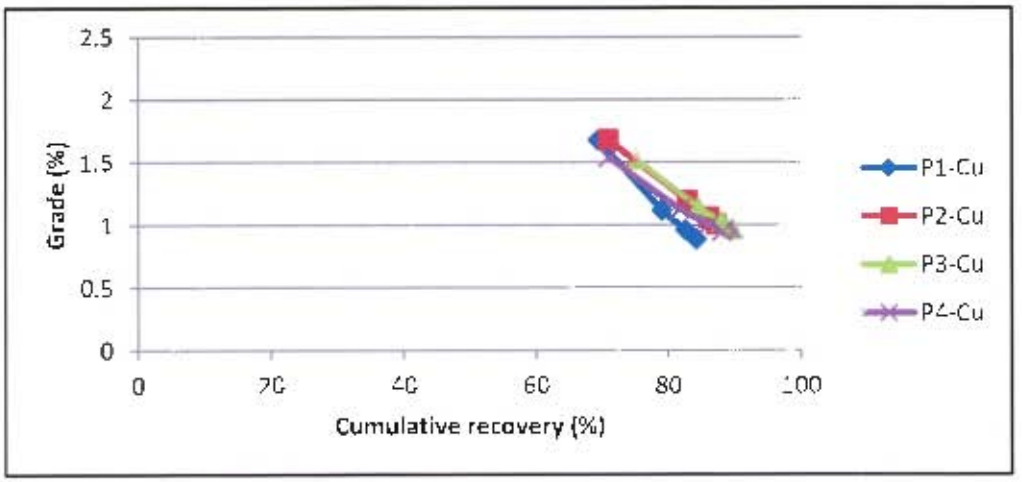

Figure 4.3.6: Cu grade as a function of recovery for Nkomati ore milled in IsaMill (1, 2, 3 & 4 pass)

Figure 4.3.6 shows the relationship between copper grade and recovery for Nkomati ore milled in IsaMill (1, 2, 3 &4 pass). Grade and recovery curves for IsaMill (2 & 3 pass) products were very similar. It can be observed that pass one product had the lowest recovery among all the IsaMill samples. It should be noted that the copper grade was lower than in the case of ore milled in the ball mill as shown in Figure 4.2.12.

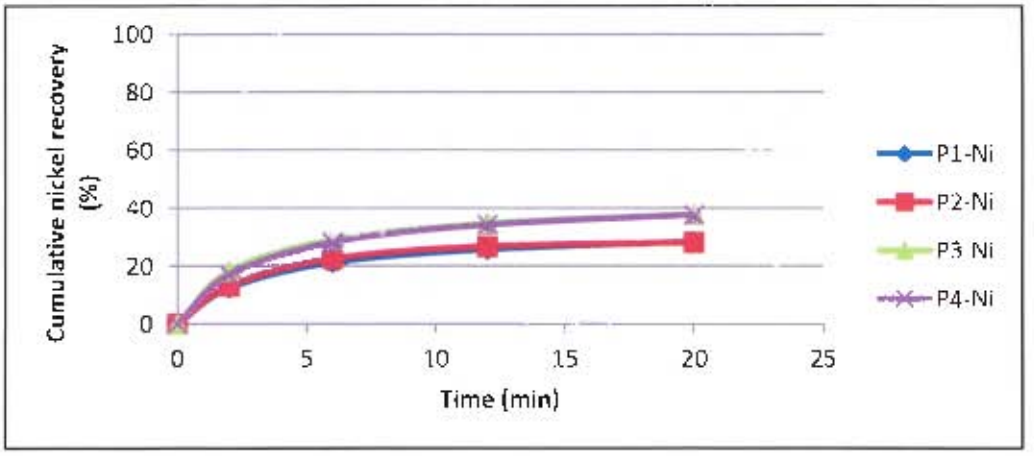

Figure 4.3.7: Ni recovery as a function of flotation time for Nkomati ore milled in IsaMill (1,2 ,3 & 4 pass)

Figure 4.3.7 shows the cumulative recovery of nickel during flotation. It should be noted from the figure that IsaMill (1 & 2 pass) products had the same recovery of nickel as flotation time increased. Similarly, IsaMill (3 & 4 pass) products had similar nickel recovery with time. A total of 28 % nickel was recovered for IsaMill (1 & 2 pass) products. 10% more was recovered for IsaMill (3 & 4 pass) products. Nickel recovery of ball mill products, Figure 4.2.13, showed lower nickel recoveries than those shown in Figure 4.3.7, except for ball mill (16min) product which showed the highest nickel recovery.

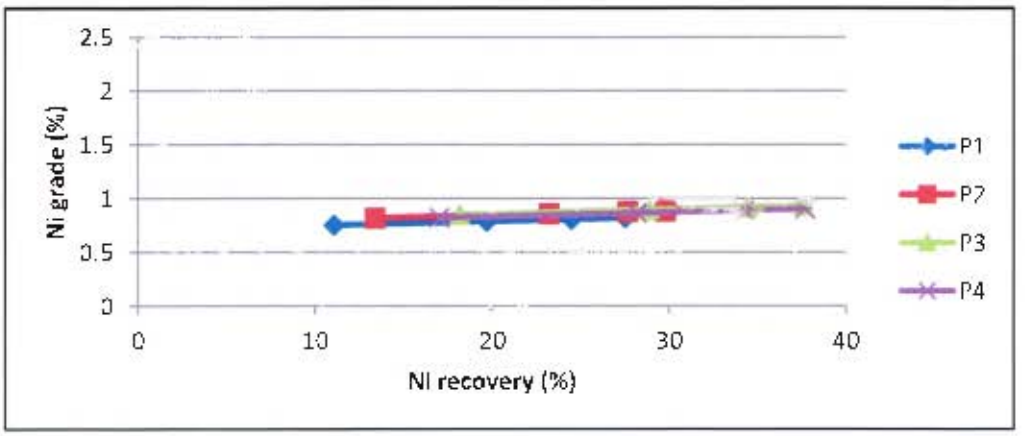

Figure 4.3.8: Ni grade as a function of recovery for Nkomati ore milled in IsaMill (1, 2, 3 & 4 pass)

The grade-recovery curves for nickel shown in Figure 4.3.8 lie very close together showing little differences in grades between different sample concentrates as nickel recovery increases. The overall trend is an increase in nickel grade as recovery increases. This unusual trend was also observed in case of the ball mill in Figure 4.2.14. This is not a typical grade-recovery relationship, which usually has grade decreaseing with increasing recovery.

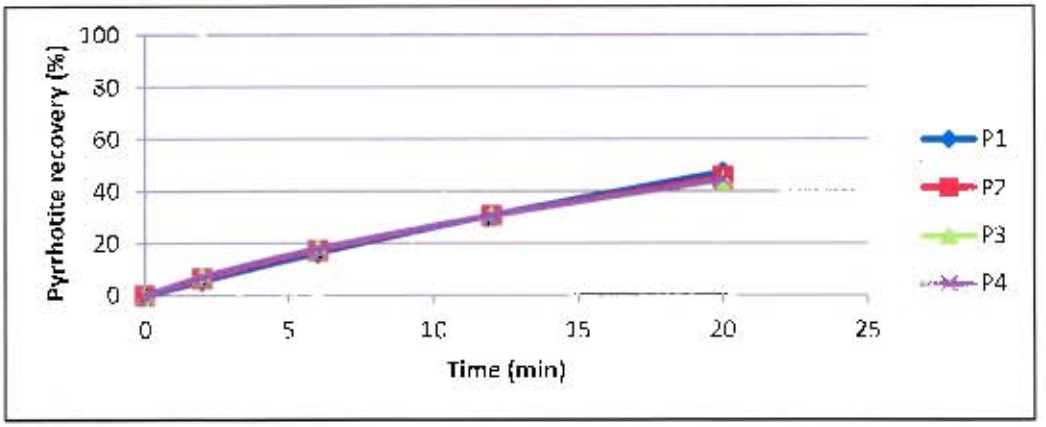

Figure 4.3.9: Pyrrhotite recovery as a function of flotation time for Nkomati ore milled in IsaMill (1, 2, 3 & 4 pass)

Pyrrhotite recovery for each of the IsaMill products is shown in Figure 4.3.9 and is in the range of 50 % after 20 minutes of batch flotation. There is no significant difference observed in the pyrrhotite recovery for the different passes of the IsaMill. It should be noted that pyrrhotite recovery for Nkomati ore milled in ball mill, Figure 4.2.15, was slightly higher than pyrrhotite recovery shown in Figure 4.3.9.

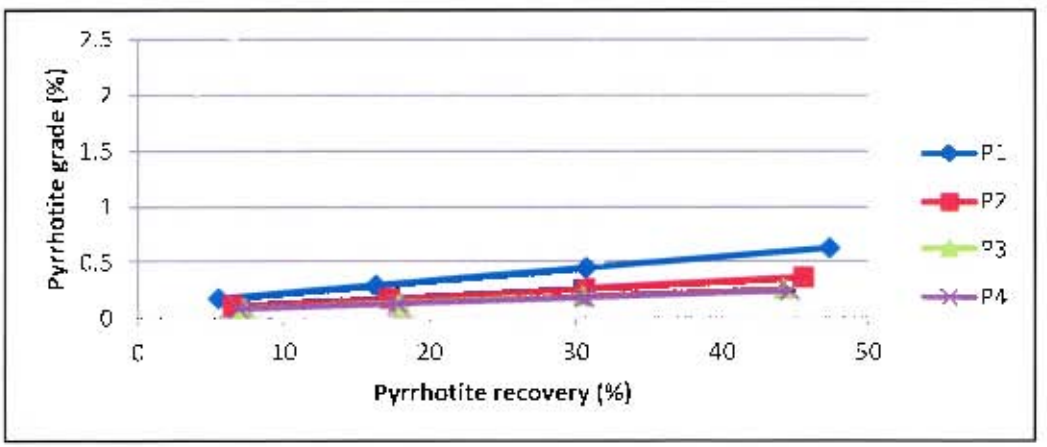

Figure 4.3.10: Pyrrhotite grade as a function of recovery for Nkomati ore milled in IsaMill (1, 2, 3 & 4 pass)

Figure 4.3.10 shows a steady decrease in pyrrhotite grade from the IsaMill (1 pass) through to the IsaMill (4 pass) product. It should be noted that IsaMill (1 & 2 pass) products have slightly higher pyrrhotite recovery than IsaMill (3 & 4 pass) products. Figure 4.2.16 showed higher pyrrhotite grade for ball mill products.

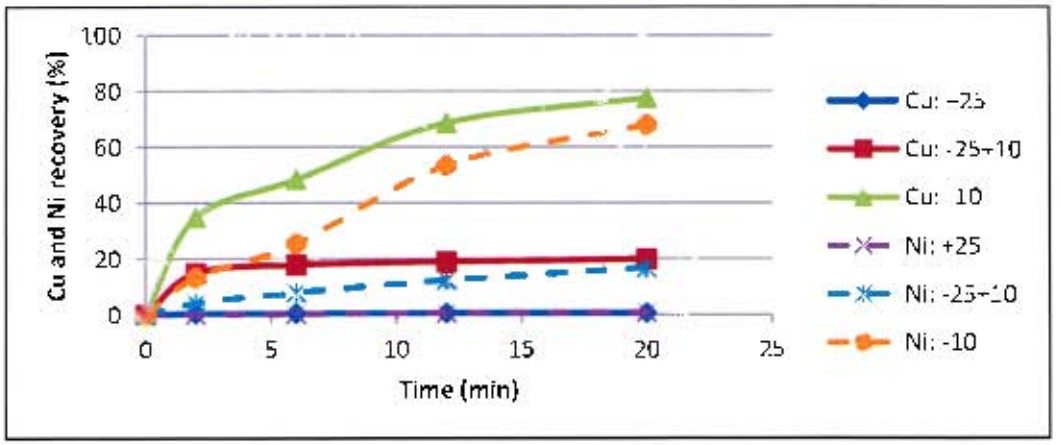

Figure 4.3.11: Cu and Ni recovered into different size fractions during batch flotation of Nkomati ore milled in IsaMill (4 pass)

Figure 4.3.11 shows the distribution of recovered copper and nickel into various size classes. The batch flotation concentrates of Nkomati ore milled in the IsaMill (4 pass) were wet screened to separate them into the given size fractions. The figure shows that most of the copper and nickel that were recovered were in the fine size fractions, especially the -10 µm fraction. It should be noted that there is very little copper and nickel recovery in the -25 µm fraction. The amounts recovered into this fraction are shown in Table 4.3.2 and Table 4.3.3, respectively. Figure 4.3.1 shows that roughly 55 % of the ore milled in IsaMill (4 pass) was in this fraction.

Table 4.3.2: Copper recovered into different size fractions after 20 minutes of batch flotation

Product name	Flotation Time (min)	Recovery into Size class (%)		
		+25 µm	-25 +10 µm	-10 µm
64 min Ball mill	20	0.8	34.1	64.3
Pass 4 IsaMill	20	0.7	19.9	77.6

Table 4.3.3: Nickel recovered into different size fractions after 20 minutes of batch flotation

Product name	Flotation Time (min)	Recovery into Size class (%)		
		+25 µm	-25 +10 µm	10 µm
64 min Ball mill	20	0.9	20.0	64.1
Pass 4 IsaMill	20	0.8	16.8	68.0

Table 4.3.2 and Table 4.3.3 show the numerical values of the mass percentage of copper and nickel, respectively, which was recovered in the three size fractions after twenty minutes of batch flotation for Nkomati ore milled in ball mill (64min) and IsaMill (4 pass).

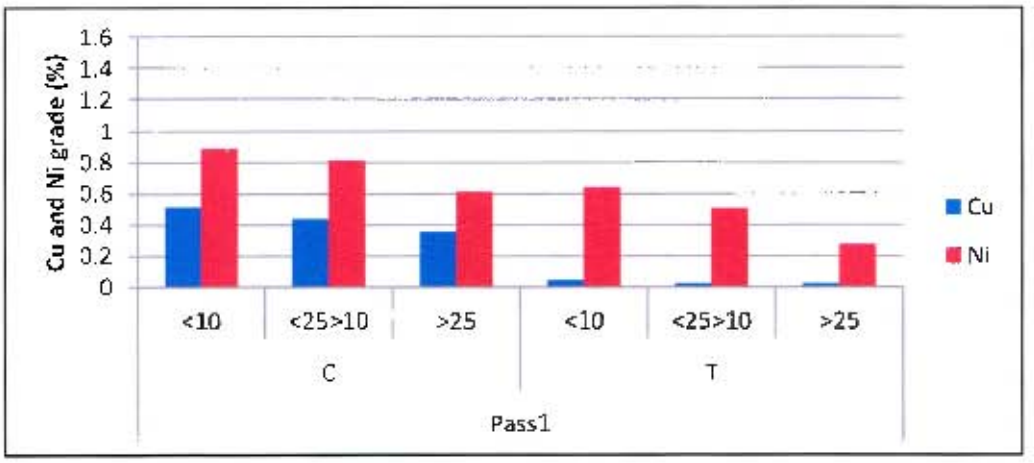

Figure 4.3.12: Cu and Ni grades in different size fractions of concentrates and tailings of Nkomati ore milled in IsaMill (1 pass)

Batch flotation concentrates of Nkomati ore milled in the IsaMill (1 pass) were combined and split into three size classes viz. -10, +10-25 and + 25 µm. The ore in the different size classes was analysed for copper and nickel. The results are shown in Figure 4.3.12. Highest copper and nickel grades are in the -10 µm fraction for both the concentrate and tailings. The grade decreases steadily across the coarse fractions. In the concentrate, the lowest grade is in the +25 µm fraction. The grade of nickel that was lost to the tailings shows a similar trend across the size fractions, decreasing as size increases. Copper grade in the tailings was very small but the nickel grade in the tailings was high. The trends observed for copper and nickel are similar to those observed for ball mill (16min) in Figure 4.2.18.

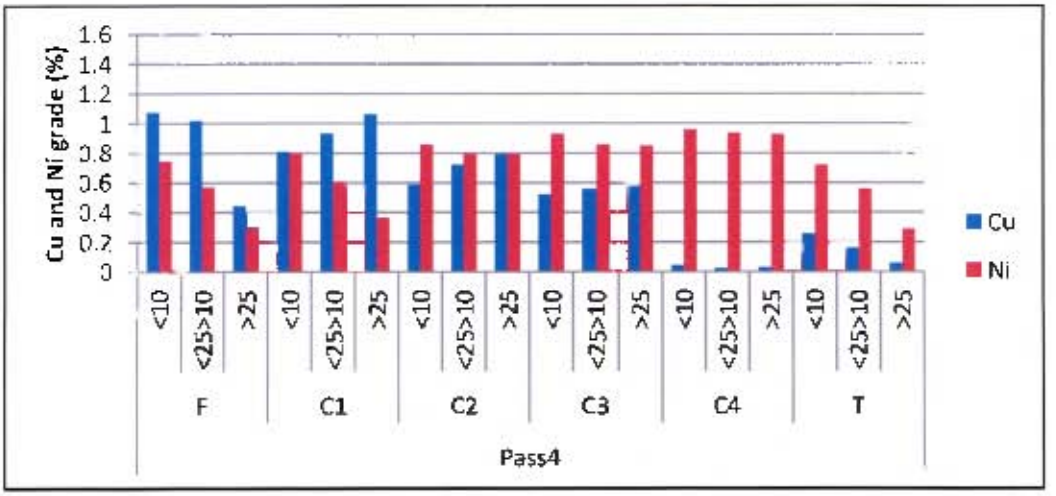

Figure 4.3.13: Cu and Ni grades in different size fractions of batch flotation samples of Nkomati ore milled in IsaMill (4 pass)

Batch flotation concentrates of Nkomati ore milled in the IsaMill (4 pass) were wet screened into three size fractions viz. -10, +10-25 and + 25 µm. Flotation feed and tailings were also split into the same size fractions. The copper and nickel grades are shown in Figure 4.3.13. Comparison of the grades in the -10 µm fractions of the concetrates and tailings ,shows that the tailings had the lowest nickel grade in the -10 µm. Also notable from the figure is that all concentrates, have the highest nickel grade in the -10 µm fraction. Tailings also have the highest nickel grade in the -10 µm. Fourth concentrate (C4) has very low copper grade in the -10 µm fraction.

The concentrates were collected at 2, 6, 12 and 20 minutes flotation time. The concentrate collected at each time interval was dried and riffled. A representative sample of each concentrate was analysed for particle size distribution using a Malvern particle size analyser. The size distribution results of the concentrates and tailings are presented below.

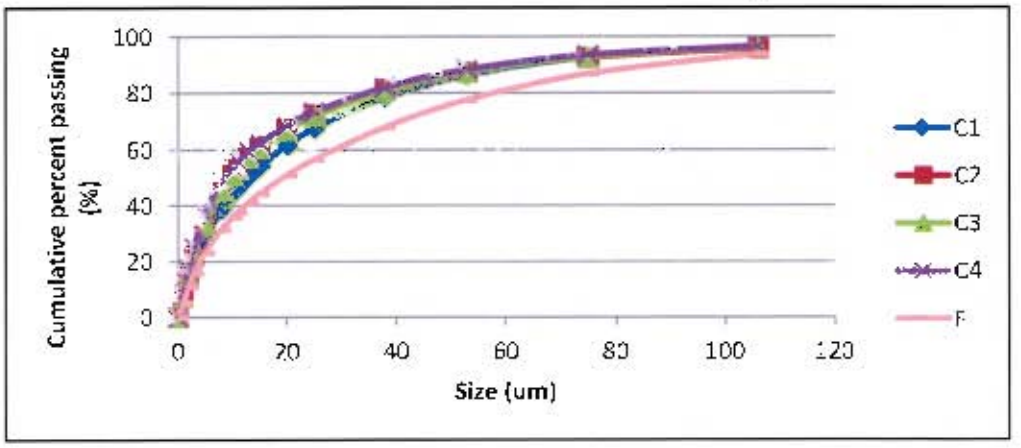

Figure 4.3.14: Size distributions of feed and concentrates of Nkomati ore milled in IsaMill (1 pass)

Figure 4.3.14 shows size distribution of the particles in the four concentrates obtained in the batch flotation of Nkomati ore milled in the IsaMill (1 pass). It should be noted from the figure that the curve for the first concentrate (C1) lies below other concentrates in the approximate size range of 10 µm to 40 µm. This indicates that particles in this concentrate

sample were relatively coarse since the percentage passing any give size, in this range, is lower for C1 than for the rest of the concentrates.

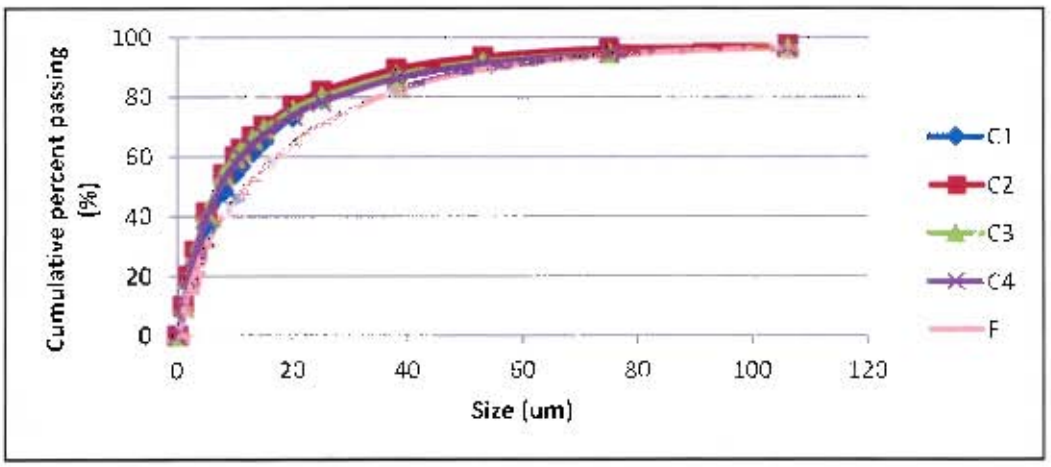

Figure 4.3.15: Size distribution of feed and concentrates of Nkomati ore milled in IsaMill (2 pass)

Figure 4.3.15 shows the size distribution of batch flotation feed and concentrates of Nkomati ore which was milled in the IsaMill (2 pass). There is no significant difference between the curves of the four concentrates. The size distribution of the flotation feed can be noted to be coarser than size distributions of concentrate samples.

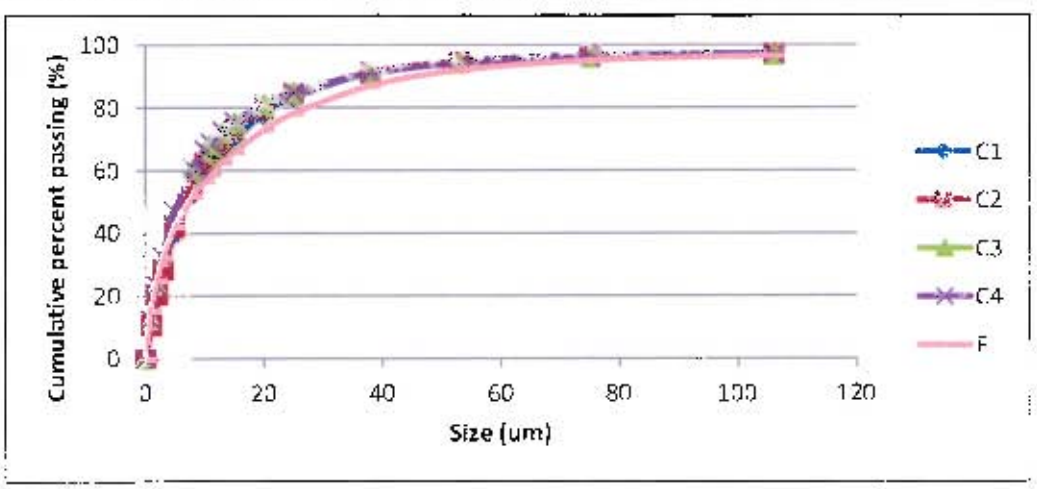

Figure 4.3.16: Size distribution of feed and concentrates of Nkomati ore milled in IsaMill (3 pass)

Figure 4.3.16 shows the size distribution of flotation feed and concentrates for Nkomati ore milled in the IsaMill (3 pass).

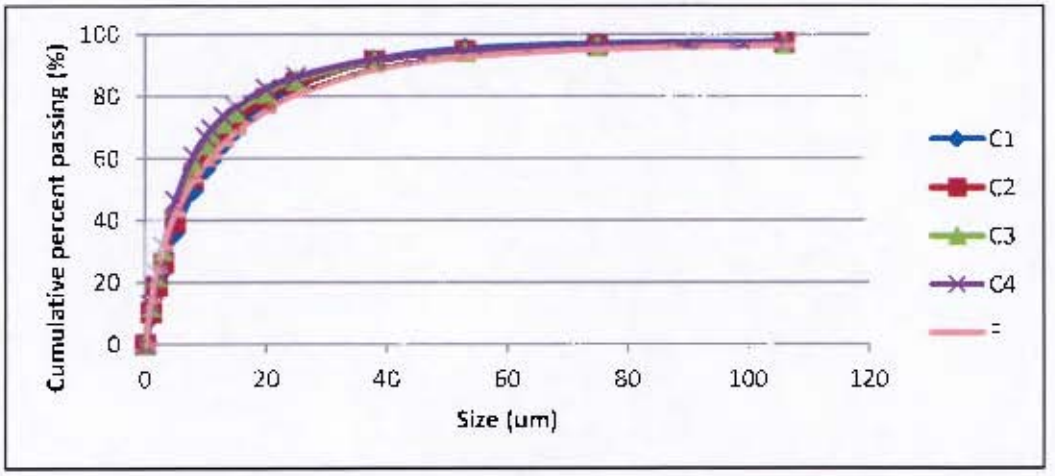

Figure 4.3.17: Size distribution of feed and concentrates of Nkomati ore milled in IsaMill (4 pass)

Figure 4.3.17 shows the size distribution of the batch flotation feed and concentrates of Nkomati ore milled in the IsaMill (4 pass).
It should be noted from Figure 4.3.14 to Figure 4.3.17 that the curves become very similar as the number of passes increases.

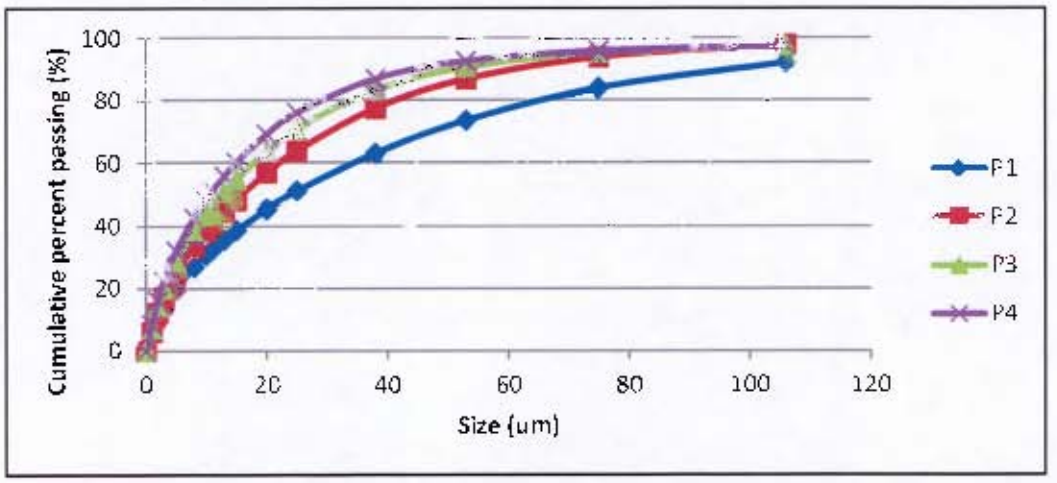

Figure 4.3.18: Size distribution of tailings of Nkomati ore milled in IsaMill (1, 2, 3 & 4 pass)

Figure 4.3.18 shows the size distribution of the flotation tailings of Nkomati ore milled in IsaMill (1, 2, 3 & 4 pass). It should be noted that the trend is similar to the one shown by the size distribution of the feed to float samples. Table 4.3.4 shows the d_{50} and d_{80} values of batch flotation feed, concentrates and tailings of Nkomati ore milled in IsaMill (1 and 4 pass).

Table 4.3.4: 50% and 80% passing sizes for flotation feed, concentrate and tailings samples of Nkomati ore milled in the IsaMill (1 & 4 pass)

	Pass1		Pass4	
	d50 (µm)	d80 (µm)	d50 (µm)	d80 (µm)
F	19	58	7	24
C1	13	40	8	22
C2	10	36	7	21
C3	10	36	6	19
C4	9	34	6	18
T	24	66	11	29

4.3.2 Platinum group ore (Impala UG2)

4.3.2.1 Particle size distribution of IsaMill product

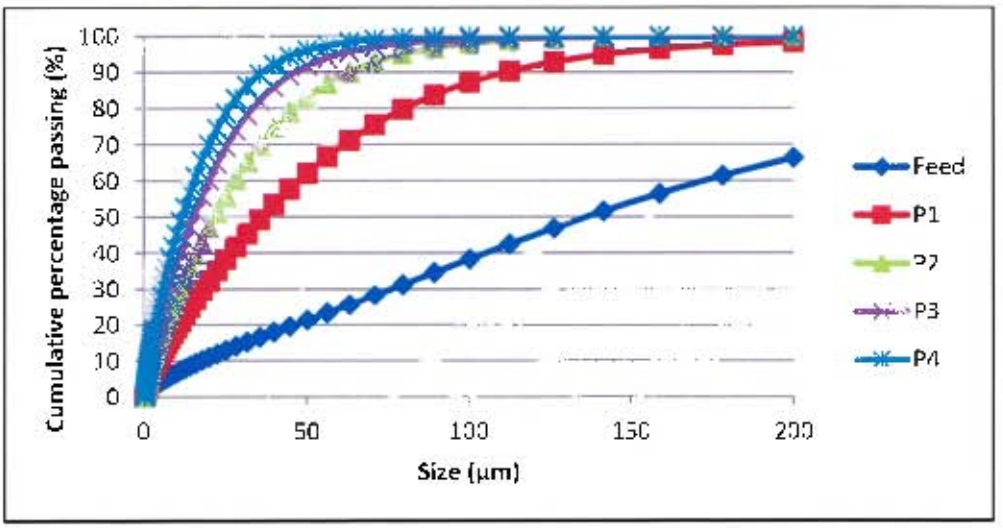

Figure 4.3.19: Size distribution of UG2 ore mill feed and ore milled in the IsaMill (1, 2, 3 & 4 pass)

Particle size distribution of the UG2 ore feed and the same ore milled in the IsaMill (1, 2, 3 & 4 pass) is shown in Figure 4.3.19. The figure was plotted using the default values as obtained from the Malvern, which can be seen in Appendix B. It should be noted here that Nkomati ore milled using the IsaMill was finer than the UG2 ore milled using the same mill.

4.3.2.2 Particle morphology characterisation

4.3.2.2.1 SEM images

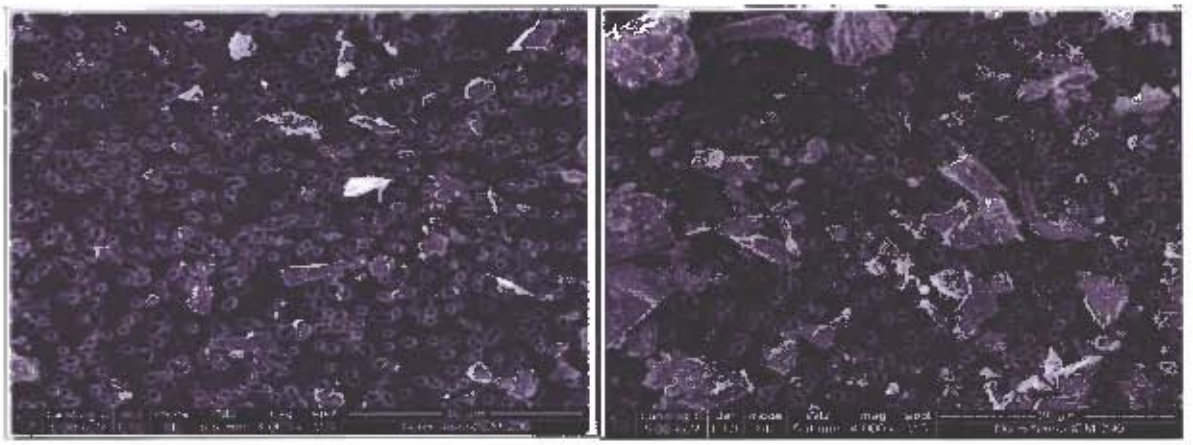

Figure 4.3.20: SEM images of pass one (left) and pass four (right) products of UG2 ore milled the IsaMill retained on a 1.2 µm filter (magnification= 4000 x)

As seen from the SEM images, it is not easy to determine particle shape based on visual analysis alone. This is why image analysis softwares are very important.

4.3.2.2.2 Particle shape characterization

Figures showing aspect ratio as a function of feret diameter for UG2 ore milled in the IsaMill (1 & 4 pass) are shown in Appendix D. The ore was screened to obtain -10 µm material which was then imaged. The bulk of the particles had an aspect ratio between 1 and 6. It should also be noted that the bulk of the particles had a feret diameter around 5.

Roundness values of IsaMill (1 pass) particles had a wide distribution of values between 0.2 and 1. The particles were densely populated around a feret diameter of 6.

Aspect ratio of IsaMill (4 pass) particles was bound between values of 1 and 6. The distribution of feret diameter had a bimodal distribution, with the bulk of the particles around a feret diameter of 6. Roundness values for IsaMill (4 pass) particles ranged between 0.2 and 0.9. The particles had a roughly bimodal distribution of feret diameters, with the bulk of the particles being around 0.7. A general observation was that aspect ratio as a function of feret diameter showed a similar trend for both mill products and the two ores used; they have a bimodal distribution of aspect ratio values. On the other hand, the relationship between roundness and feret diameter differed between the ores but were similar between mill types. An observation was made that roundness values had a wide distribution between 0.2 and 1.

4.3.2.2.3 *Particle Rheology*

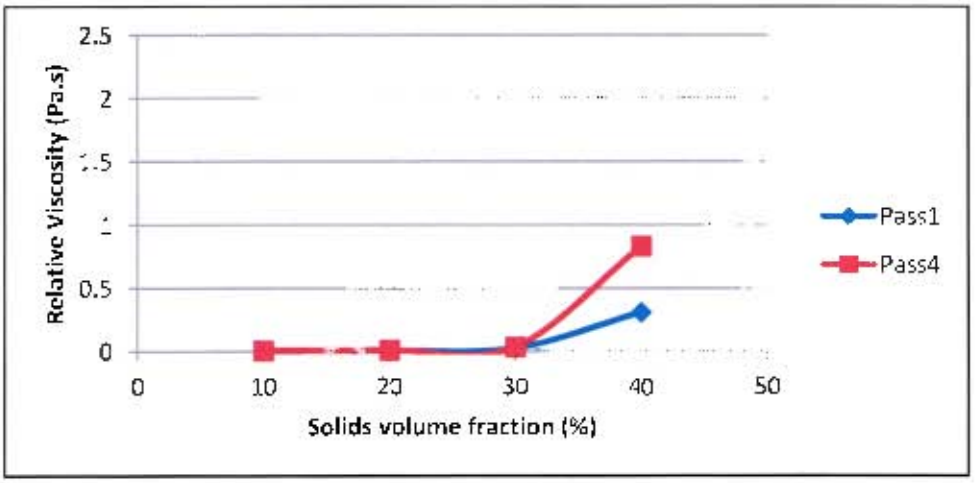

Figure 4.3.21: Relative viscosity as function of solids volume percentage of -25 µm UG2 ore milled in IsaMill (1 & 4 pass)

As seen from Figure 4.3.21, values of relative viscosity of UG2 ore milled in IsaMill (1 & 4 pass) differ as solids volume concentration increases. Slurry of IsaMill (4 pass) product had a higher relative viscosity than that of the IsaMill (1 pass) product at 40 % solids concentration.

Table 4.3.5: Relative viscosity of Nkomati and UG2 ore samples from ball mill and IsaMill at 40 % solids volume

	Relative viscosity	
Sample	Nkomati	UG2
16 min	1.3	0.5
64min	1.3	0.6
Pass1	0.9	0.3
Pass4	2.5	0.8

Table 4.3.5 presents values of relative viscosity, at 40 % solids volume percentage, of Nkomati and UG2 ores milled in ball mill (16min & 64min) and in IsaMill (1 & 4 pass). It should be noted from this table that viscosity values of UG2 ore are lower than those of Nkomati ore. The IsaMill (4 pass) product had the highest viscosity for the two ores, with the Nkomati ore sample having highest viscosity.

4.3.2.3 Mineralogy

Table 4.3.6, shows the composition of Impala UG2 ore determined by XRD. The samples analysed were mill feed and IsaMill (1 & 4 pass) products. There was no significant difference between the compositions of the three samples. The main components were bronzite, chromite, bytowmite and diopsite iron in decreasing percentage. Traces of talc, pyrrhotite and forsterite iron were also present.

Table 4.3.6: Composition of UG2 ore determined using XRD

Phase number	Mineral	Weight percent (%)		
		Feed	Pass1	Pass4
Phase1	Chromite	29.00	26.98	26.52
Phase2	Talc	2.26	2.91	2.86
Phase3	Phlogopite 1M Mica	0.93	2.08	1.33
Phase4	Bytownite	17.02	19.29	18.94
Phase5	Pentlandite	0.00	0.00	0.01
Phase6	Chalcopyrite	0.11	0.11	0.12
Phase7	Pyrite	0.04	0.16	0.16
Phase8	Hornblende magnesian iron	0.96	0.94	0.82
Phase9	Quartz	0.58	0.43	0.53
Phase10	Calcite	0.25	0.22	0.25
Phase11	Forsterite iron	1.60	1.95	2.34
Phase12	Orthoclase	0.62	0.79	0.44
Phase13	Bronzite	36.25	35.07	36.32
Phase14	Pyrrhotite 4C	2.50	2.44	2.61
Phase15	Diopsite iron	7.78	6.64	6.71
Phase16	Chlorite	0.04	0.00	0.00
Phase17	Epidote	0.09	0.00	0.01

4.3.2.4 Batch flotation results

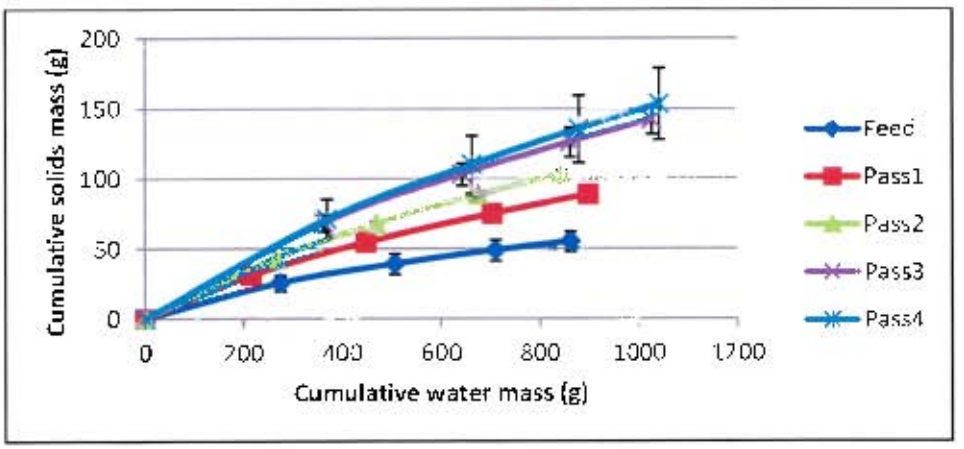

Figure 4.3.22: Solids recovered as a function of water recovered in batch flotation of UG2 feed and ore milled in IsaMill (1, 2, 3 & 4 pass)

Figure 4.3.22 shows mass of UG2 solids that was recovered as a function of water during batch flotation tests of IsaMill products. It should be noted from the figure that an increasing mass of solids was recovered as the product became finer. However, there was no apparent difference between water and solids recoveries of the IsaMill (3 & 4 pass)

products. Water recovered for IsaMill (1 & 2 pass) products was similar. It should also be noted from Figure 4.3.4, that more water and solids were recovered for Nkomati ore milled for the same number of passes in the IsaMill, than for UG2 ore.

Table 4.3.7: Mass distribution of chromite in the flotation feed, concentrates and tailings of UG2 ore milled in IsaMill (1 pass)

1 pass Sample name	Mass of Cr_2O_3 (g) Size fraction (µm)			Total mass (g)	% of feed Cr_2O_3
	<10	>10<25	>25		
F	35.8	79.1	70.5	185.3	
C	14.8	1.5	0.3	16.6	9
T	22.8	70.4	57.4	150.5	81

Table 4.3.7 shows mass distribution of chromite in the flotation feed, concentrates and tailings for UG2 ore milled in the IsaMill (1 pass). The samples were wet screened into three size fractions, viz. +25, -25 +10 and -10 µm and each fraction was analysed for chromite content. It should be noted that the four batch concentrates were combined into one bulk sample which was then screened into the three size fractions. The largest mass of chromite was recovered in the -10 µm fraction and the largest mass of chromite in the tailings was in the -10 µm fraction. The last column of Table 4.3.7 shows the percentage of Cr_2O_3 in the concentrate and tailings relative to the total Cr_2O_3 that was in the feed.

It should be noted that there was more chromite recovered into the concentrates for UG2 ore milled in IsaMill (1 pass) than for the same ore milled in ball mill (16 min), as seen in Table 4.2.4. Cr_2O_3 in the concentrates and tailings accounted for 90 % of the Cr_2O_3 in the feed. The 10 % difference can be taken to be a result of experimental error, for the same reasons that were mentioned in the explanation of results in Table 4.2.4 and Table 4.2.5.

Table 4.3.8: Mass distribution of chromite in the flotation feed, concentrates and tailings of UG2 ore milled in IsaMill (4 pass)

4 pass Sample name	Mass of Cr_2O_3 (g) Size fraction (µm)			Total mass (g)	% of feed Cr_2O_3
	<10	>10<25	>25		
F	127.2	98.4	1.6	227.2	
C1	5.7	2.2	0.0	7.9	3.0
C2	10.4	0.8	0.0	11.2	5.0
C3	13.8	1.0	0.0	14.7	6.0
C4	17.2	1.0	0.0	18.2	8.0
T	70.9	73.6	0.0	144.5	64.0

Table 4.3.8 shows mass distribution of chromite in the flotation samples of UG2 ore milled in the IsaMill (4 pass). A total of 22 % of the mass of chromite in the feed to flotation was recovered in the concentrates. 64 % of the mass was in the tailings. It can be seen from the

figure that the bulk of the recovered chromite mass was in the -10 µm. The values of chromite mass shown in the two preceding tables were rounded to one decimal place.

It should be noted from Table 4.2.5 that more chromite (75%) remained in the tailings for UG2 ore milled in ball mill (64min), compared to the 64 % shown in Table 4.3.8 in the case of ore milled in IsaMill (4 pass). It should also be noted that there was more chromite recovered for each of the concentrates (C1 to C4) in the case of UG2 ore milled in IsaMill (4 pass) as compared to UG2 ore milled in ball mill (64min). It can be seen from Table 4.3.8 that concentrates and tailings account for only 86 % of the Cr_2O_3 in the feed. The 14 % difference can be taken to be a result of the experimental error, for the same reasons which were mentioned in the explanation of the results in Table 4.2.4, Table 4.2.5 and Table 4.3.7.

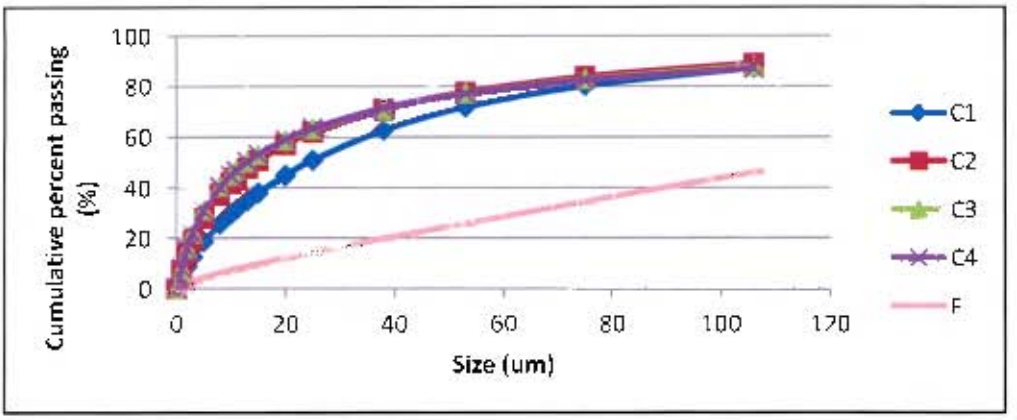

Figure 4.3.23: Size distribution of feed and concentrates of UG2 ore mill feed

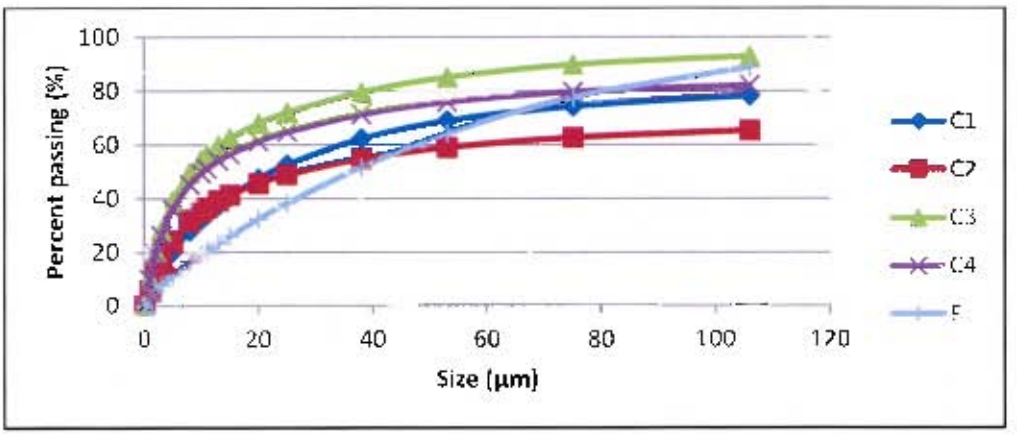

Figure 4.3.24: Size distribution of feed and concentrates UG2 ore milled in IsaMill (1 pass)

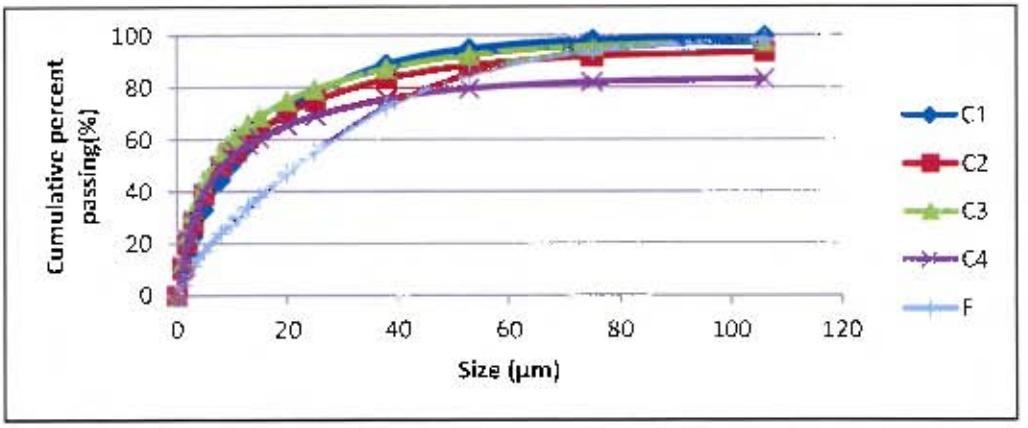

Figure 4.3.25: Size distribution of feed and concentrates of UG2 ore milled in IsaMill (2 pass)

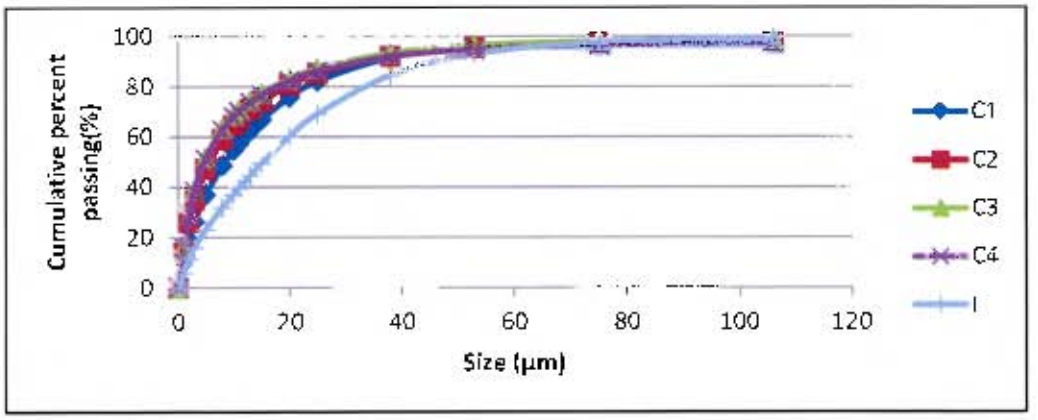

Figure 4.3.26: Size distribution of feed and concentrates of UG2 ore milled in IsaMill (3 pass)

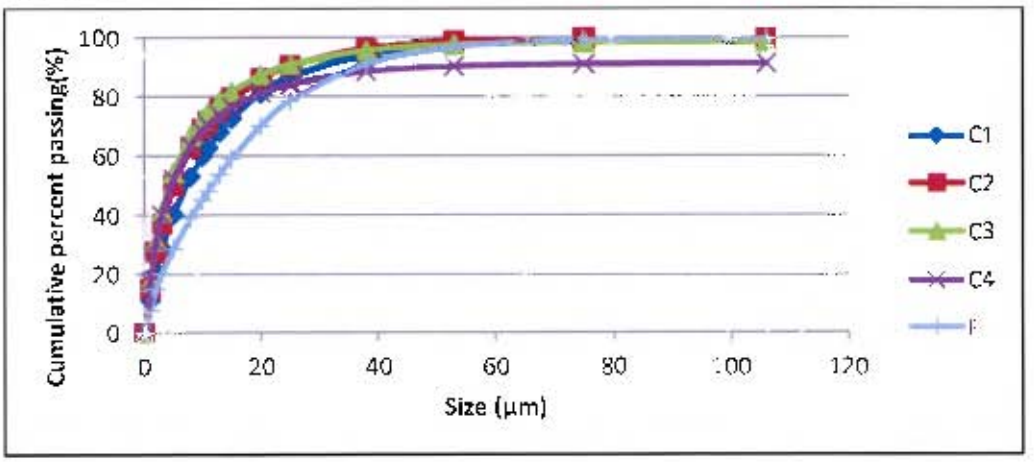

Figure 4.3.27: Size distribution of feed and concentrate of UG2 ore milled in IsaMill (4 pass)

Figures from Figure 4.3.24 to Figure 4.3.27 show size distribution of UG2 ore batch flotation feed and concentrates. The ore was milled in the IsaMill (1, 2, 3 & 4 pass). IsaMill (1 & 2 pass) concentrates were relatively finer than IsaMill (3 & 4 pass) concentrates.

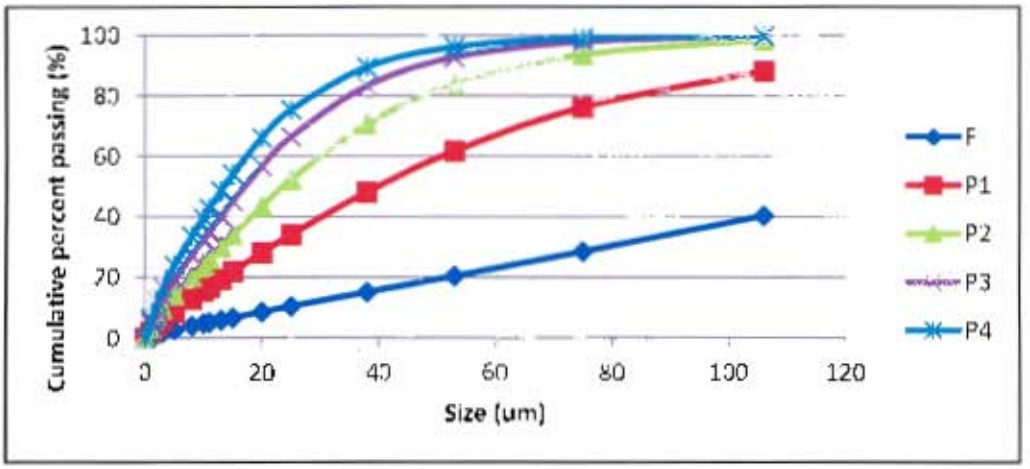

Figure 4.3.28: Size distribution of tailings of batch flotation samples of UG2 ore milled in IsaMill (1, 2, 3 & 4 pass)

Figure 4.3.28 shows the size distribution of the tailings of batch flotation samples of UG2 ore milled in the IsaMill (1, 2, 3 & 4 pass).

Table 4.3.9: 50% and 80% passing sizes for feed, concentrates and tails in the flotation of UG2 ore milled in the IsaMill (1 pass and 4 pass)

	Pass1		Pass4	
	d50 (µm)	d80 (µm)	d50 (µm)	d80 (µm)
F	36	80	13	27
C1	13	40	7	19
C2	8	32	5	15
C3	8	40	4	14
C4	7	35	5	25
T	40	83	12	26

The d_{50} and d_{80} sizes of the batch flotation samples of UG2 ore are shown in Table 4.3.9. Figure 4.3.28 shows the size distribution of tailings of the mill feed and ore milled in the IsaMill (1, 2, 3 & 4 pass).

It was observed from Table 4.3.9, that the concentrate d_{80} sizes were smaller than tailings. This indicates that the coarse particles were not recovered.

As indicated in the earlier sections, the IsaMill produced finer particles than ball mill. More fine particles are present during batch flotation of IsaMill products than for ball mill products.

Chapter 5 DISCUSSION

Grinding is important in any mineral processing operation. The depletion of coarse grained ores has given fine grinding an even greater importance, as ores need to be ground very fine in order to liberate valuable minerals. Most of the research in fine grinding has been concerned with producing particles with a fineness of down to P_{80} of 7 μm, under minimal energy usage. The ability of mills to grind fine and expend energy efficiently has been associated with breakage mechanisms that dominate in a particular type of mill. The two different milling devices selected for this investigation were a horizontal laboratory scale ball mill and an M4 IsaMill. Ball mills have been used for many years in industry. The need for fine grinding has seen ball mills undergo several changes and improvements to make them suitable for the task. On the other hand, IsaMills are a new technology to mineral processing industry, with their first installation in mid-1990's. IsaMill technology was adopted from Netzsch and is suited to fine grinding.

Grinding is known to affect downstream processes such as flotation. The grinding environment in particular has received a very wide attention with extensive research on its influence on downstream processes. Most of the factors associated with grinding environment are chemical and involve chemical interactions between mineral surfaces and grinding media. The physical parameters of milled products that might affect their flotation behaviour have received very limited attention and research. This is with the exception of particle size, which has been fairly intensively investigated. The shape of particles coming out of a mill has been alluded to as one of the physical parameters that play a role in the flotation behaviour of particles. However, research on this phenomenon is limited by the difficulty in determining particle shape. On the research that has been done regarding the effect of grinding on particle shape and the subsequent effect of this shape on flotation behaviour, there are some contradictions. IsaMills have shown benefits in many mineral processing plants where they have been installed, especially in fine grinding. Pease *et al.* (2006) mentioned that recoveries were improved at McArthur River Mine when grinding to P_{80} of 7 μm. Several investigations have been undertaken to study the influence of different comminution devices on flotation behaviour (Chapman, 2010). In most of these studies, a base metal ore was used as a base case for the test work, followed by similar test work on a platinum bearing ore. A similar approach was taken in this investigation.

The test work was set out to investigate the following hypotheses:

- Ore milled in a ball mill and IsaMill will have particles of different shapes. This is because of the different grinding mechanisms that take place in these two mills.
- Ball mill and IsaMill products will show different flotation behaviour. This is because different shapes of particles exhibit different flotation behaviour. Particle shape affects the contact area between particles and bubbles.

The project investigated the effect of comminution on particle shape and the subsequent effect of particle shape on flotation behaviour. The two mills were chosen to provide different grinding mechanisms. SEM images of the products were analysed using proprietary image analysis software to determine the shape parameters. Aspect ratio and roundness of particles were determined. Particles of different shapes have been shown to exhibit

different rheological behaviour (Pabst *et al.*, 2006). In the light of this, rheology of the mill products was investigated to draw further inferences on particle shape.

5.1 Particle characterization of mill products

5.1.1 Particle size distribution of particles to float

Figure 4.2.1 and Figure 4.3.1 show the size distribution of the Nkomati ore after milling for different times in a ball mill and IsaMill respectively. The figures show similar size distributions. This is confirmed by the numerical values presented in Table 4.1.3. This leads to the apparent conclusion that ball mill and IsaMill had similar size reduction abilities on Nkomati ore. However, it should be noted that the Nkomati ore had been processed prior to being fed to the mills. As mentioned in the experimental section, the ore had been milled to 80 % passing 120 µm. The pre-processing step created a considerable amount of fines in the feed to the mills. This is attested to by the similarity of the feed curve to the mills' product curves below 20 µm in Figure 4.2.1 and Figure 4.3.1. Therefore a closer analysis at the fine portion of the size distribution was carried out.

Table 5.1.1: Percentage passing 15, 10 & 5 µm for Nkomati ore milled in ball mill and IsaMill

% passing 15 µm				% passing 10 µm				% passing 5 µm			
IsaMill		Ball Mill		IsaMill		Ball Mill		IsaMill		Ball Mill	
MillFeed	33	MillFeed	33	MillFeed	30	MillFeed	30	MillFeed	21	MillFeed	21
Pass1	41	16min	44	Pass1	32	16min	36	Pass1	20	16min	22
Pass2	52	32min	51	Pass2	41	32min	40	Pass2	26	32min	25
Pass3	60			Pass3	48			Pass3	31		
Pass4	66	64min	63	Pass4	54	64min	51	Pass4	35	64min	33

Table 5.1.1 shows that 33 % of the feed was below 15 µm. This is what went into the mills even before grinding. So the size distribution of the mill products in this case is not a reliable tool for assessing the size reduction ability of the mills. A good measure would be to measure the amount of fines creation by each mill. This could be roughly estimated by subtracting the percentage passing 15 µm in feed from the percentage passing 15 µm for each mill product. This still shows great similarity in the values obtained from ball mill and IsaMill. Hence, Table 5.1.1 shows no significant differences in the volume percentage of solids passing 15, 10 and 5 µm, for both ball and IsaMill products.

Table 5.1.2: Percentage passing 15, 10 & 5 µm for UG2 ore milled in ball mill and IsaMill

% passing 15 µm				% passing 10 µm				% passing 5 µm			
IsaMill		Ball Mill		IsaMill		Ball Mill		IsaMill		Ball Mill	
				MillFeed	7	MillFeed	7	MillFeed	4	MillFeed	4
Pass1	26	16min	22	Pass1	19	16min	16	Pass1	11	16min	9
Pass2	38	32min	27	Pass2	28	32min	20	Pass2	17	32min	12
Pass3	49			Pass3	37			Pass3	23		
Pass4	59	64min	39	Pass4	45	64min	29	Pass4	29	64min	18

On the other hand, Table 5.1.2 shows that for UG2 ore there was a greater percentage of solids passing these sizes for IsaMill products than for ball mill products. For one mill, there is a greater percentage of Nkomati ore passing these sizes than there is UG2 ore. It should be noted that the percentage of feed material passing 15 µm was not included in Table 5.1.2; this is because the values obtained from Malvern were unreasonably high (~90 %), which did not make sense in comparison to the other sizes. This could have been a calculation error in the Malvern software.

Table 5.1.1 and Table 5.1.2 show significant differences between amount of Nkomati and UG2 ores passing the fine fractions. The differences could be due to differences in the hardness of the two ores. Nkomati ore could be a soft ore which breaks easily with minimum amount of stress induced. On the contrary, UG2 ore could be a hard ore which requires large stress intensities in order to break. The exact hardness values of the two ores were difficult to obtain since they vary with composition and area of provenance for real ores. If Nkomati ore breaks easily for any stress intensity, greater than minimum required, it

explains why the volume percentage of solids passing the aforementioned sizes are equal for both mills. By the same token, it explains why IsaMill products have higher volume percentage of UG2 ore passing the sizes since IsaMill is a high energy intensity stirred mill. This trend follows what Kwade *et al.* (1996) noted, viz. that particle fineness increased with stress intensity for the given energy consumption. Bradford *et al.* (1998) carried out tests to determine the operating work index for the Nkomati main concentator. Work index values ranged from 17.9 to 22.2 kWh/t for the various circuits that were proposed. The also noted that the Nkomait ore body was highly variable, resulting in a wide range of ore hardness and grindability. On the other hand, chromite, which consitutes 50 % of Impala UG2 ore, has a hardness of 5.5 to 6.5 on Moh's scale of hardness. This supports the proposition that the diffreence on the amounnt of fines between the two ores could have been a result of the difference in the hardness of the ores.

5.2 Effect of comminution method on particle shape

Particle shape is a fundamental powder property affecting powder packing and bulk density, porosity, permeability, cohesion, flowability, caking behaviour, attrition, interaction with fluids and the covering power of pigments. However, little quantitative work has been carried out on these relationships. Many papers have been written on shape determination but there are few articles which relate the measurements to powder characteristics and end-use concentrator processes (Yekeler *et al.*, 2004).

Yekeler *et al.* (2004) investigated the effect of different grinding methods on particle shape, and the subsequent effect of the given shapes on floatability. They used ball, rod and autogenous mills to grind talc. They postulated that in ball and rod mills, attrition was the main breakage method. They also went further to cite a proceedings paper by Oja and Tuunila (2000) to support the general point that there was a clear difference in the shape of particles ground by different methods. However they added that the character of the material and the type of mill used determine the shape of particles produced.

Vizcarra *et al.*, (2011) described the shape properties of an iron oxide hosted copper-gold ore following comminution in a laboratory scale hammer mill and a piston-die compression unit. They found that particles became less angular as they became smaller. They attributed this trend to more surface attrition events and higher degree of rounding in the smaller size fractions.

The current study was carried out to investigate the flotation behaviour of ball mill and IsaMill products. The shape characterization of the particles using SEM imaging showed no obvious differences between the two mill products. This could be a result of the fact that the grinding methods in these two mills, under the conditions used in this study, were similar. On the other hand, it could be that the nature of the ore played a more important role in determining the shape of the particle. For the two ores investigated in this study, Nkomati and UG2 ores, particle shapes from the two mills were found to be similar when analysed using SEM imaging. However, it should be noted that the shape factors, aspect ratio and roundness or circularity, which were used to characterise particle shape in this study were regarded as simple (Ahmed, 2010). Their simplicity has been shown to give an impression that there were no differences in shape between particles that were being analysed. Advanced shape analyses techniques such as fractal dimension analyses have been shown to give detailed shape analyses and hence showed differences in particle shape

in instances where the simple analyses of particles' aspect ratio and circularity had suggested there were no differences in the shape of particles.

On the other hand, rheological behaviour of the ores milled in the two mills showed differences. This implies differences in particle shape (Barnes, 2000). The shapes of the particles produced by the mills were compared for coarse and fine products of the mills. These correspond to the short and long grinding times respectively. Sixteen minutes of grinding in the ball mill and one pass through the IsaMill were the coarse products. On the one hand, sixty-four minutes of grinding in ball mill and four passes through the IsaMill were the fine products.

The analysis of the SEM images and the size parameter relationships from these images were shown in Appendix D. The similarities in the particle shapes can be observed by comparing the coarse ball mill product with coarse IsaMill product. Similar observations were made by comparing the fine products of the mills. The corresponding figures showed similar results when compared. The figures show shape properties of the -10 µm fraction of the respective ores milled in the given mill for a given time or number of passes.

5.3 Rheology

Rheological behaviour of particles has been used as a diagnostic for the shape properties of the particles (Pabst *et al.*, 2004). Barnes (2000; pp 126) stated that the thickening effect of particles with respect to their shape decreases in the order of rods > plates > cubes/grains > spheres, when the same phase volume of particles is added to the liquid.

This was summarized in a figure which showed the approximate order of thickening power of each shape, with rods/ fibres being the most efficient for any solids volume concentration. Barnes also noted that aspect ratio was the controlling factor in determining the particle's thickening power. This was also illustrated with a figure that showed aspect ratio as a function of solids volume concentration.

The particles that were used for rheology experiments were in the -25 µm material of each of the mill products. This was obtained by wet screening at 25 µm and drying the -25 µm fraction. Barnes (2000) noted that the effect of particle size in dispersions comes through an important mechanism which relates to the spatial arrangement of particles.

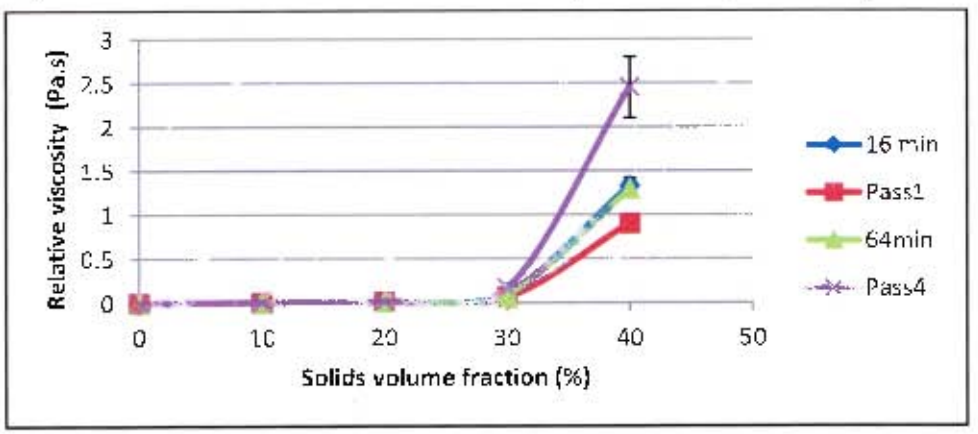

Figure 5.3.1: Relative viscosity as a function of solids volume fraction of Nkomati ore milled in a ball mill (16min & 64min) and IsaMill (1 & 4 pass)

In the light of the expected variation of viscosity with solids volume fraction as demonstrated by Barnes (2000), **Error! Reference source not found.** showed no discernible difference between ball mill products obtained after 16 and 64 minutes of grinding. On the other hand, the same figure showed pass one product of the IsaMill to have more spherical particles than pass four product particles, as shown by the smaller viscosity of pass one product compared to that of pass four. The probable reason for the difference in shape could be the breakage mechanisms employed in breaking the particles. The IsaMill contents in the first pass are mainly coarse particles, which literature suggests are mainly broken by abrasion, whereas when the fourth pass was reached, most of the material in the mill was very fine and broken by impact breakage. Gaudin (1926) as cited by Kaya *et al.* (2002) observed that fine particles were broken by massive fracture which led to angular shapes. Zhang and Kavetsky (1993) developed a method to investigate breakage mechanisms inside a batch ball mill. Their method depended on the size or size distribution of the mill contents. They found that particles of different sizes were broken by different mechanisms. Furthermore, they found that different breakage mechanisms were employed for the same size particles of different materials. Impact breakage produces particles of irregular shapes (Kaya *et al.*, 2002).

Kaya *et al.* (2002) found that high energy grinding machines (IsaMill) produced a large proportion of newly created particles, which favoured irregular shape of product particles. On the other hand mills with low energy (ball mill) used repeated action to reduce particle size and this promoted formation of round particles. Furthermore, Holt (1981) reviewed the effect of comminution devices on particle shape. This led to the conclusion that single-pass devices produced angular particles while retention systems such as ball mills produced more rounded particles. The rounding effect in ball mills was noted to be more pronounced with increased grinding times. However, grinding time did not seem to have an effect on ball mill products in this study.

As mentioned earlier, **Error! Reference source not found.** shows viscosity as a function of solids volume fraction for Nkomati ore milled in a ball mill and IsaMill. Ore milled for sixteen minutes in the ball mill had slightly higher viscosity than ore passed once through the IsaMill. This means that particles from the ball mill were more irregular in shape with those from the IsaMill being more rounded. Sixteen minutes product from the ball mill and pass one product from the IsaMill were regarded as the coarse samples in this project, as confirmed by their size distributions. The irregular shape of particles from the ball mill could be a result of impact breakage which has been said to be a dominant breakage mode in a tumbling ball mill. On the other hand, the round shape of IsaMill pass one product is a result of the attrition events on these coarse particles. As stated earlier, Gaudin (1926) as cited in Kaya *et al.* (2002) observed that large particles were often subject to attrition breakage which accounted for their round shape.

Figure 5.3.1 also shows that pass four product of the IsaMill had higher viscosity than sixty four minutes product from the ball mill as the solids volume fraction increased. With regards to particle shape, this means that particles from the fourth pass of the IsaMill were more fibrous than particles obtained after sixty-four minutes of grinding in the ball mill. These two products represent the fine samples from the mills. These are fine products even though all the samples that were analysed for rheology were below 25 μm, including sixteen minutes and pass one products. As shown by Zhang and Kavetsky (1993) grinding mode depends on the size or size distribution of ore particles in the mill. Mill contents were in the fine size

range for sixty-four minutes and pass four products. According to Holt (1981), retention systems (ball mill) produced rounded particles, with increased grinding times enhancing the rounding effect. On the other hand, fine particles in high energy mills are broken by massive fracture producing irregular particles. Therefore the trends observed in **Error! Reference source not found.** are plausible in the light of the cited literature.

It is evident from Figure 5.3.1 that Nkomati ore milled in the IsaMill (1 pass) had the lowest viscosity, especially as the solids volume fraction increased to 40 %. This means that pass one products were more spherical than others. The pass four products on the other hand had the highest viscosity. This shows that they were the most irregular or needle-shaped particles. Products of the Nkomati milled in the ball mill had similar rheological behaviour and had values between those of the IsaMill ore. This might mean that the same breakage mechanism was employed for grinding Nkomati ore in the ball mill; whereas impact breakage was dominant for breakage of fines (pass four) in the IsaMill and abrasion dominated breakage of coarse (pass one) particles.

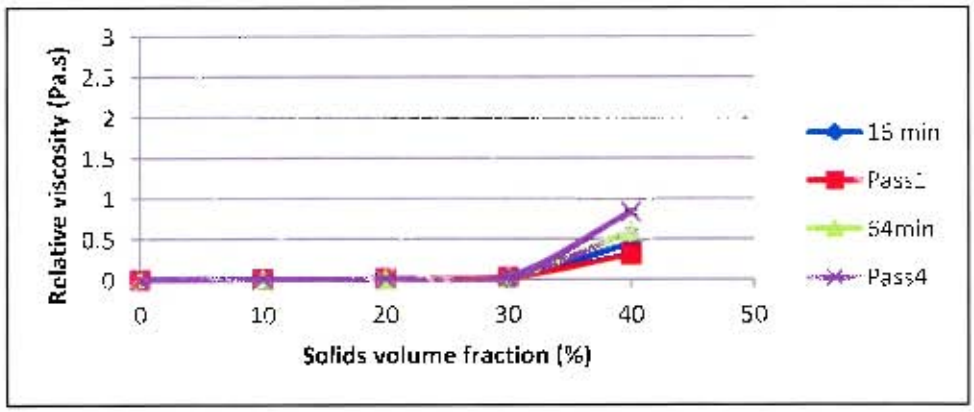

Figure 5.3.2: Relative viscosity as a function of solids volume fraction of UG2 ore milled in a ball mill (16min & 64min) and IsaMill (1 & 4 pass)

Figure 5.3.2 shows viscosity of UG2 ore milled in a ball mill (16min & 64min). On the same figure is shown the viscosity of UG2 ore milled in the IsaMill (1 & 4 pass). The viscosity increases from pass one to pass four products. The 16 minutes product has lower viscosity than 64 minutes product, showing that ore milled in the ball mill (16min) had more rounded particles than ore milled for 64 minutes in the same mill. Ore milled in the IsaMill (1 pass) once again had the roundest particles of all. Particles milled in the IsaMill (4 pass) had the highest viscosity hence most irregular or needle-like in shape.

Mill products were also analysed using x-ray diffraction (XRD). XRD determines the mineral composition of the ore sample and also determines structure. There were no structural differences observed for the two ores types milled by ball mil and IsaMill. However, it should be noted that structural differences between ores milled in different mills have been observed by other researchers (Jones *et al.*, 2011). They used XRD line profile analysis on a sulphide ore milled using a planetary mill and a vibratory mill and observed line broadening effects on samples milled using a planetary mill. They said this showed that more bulk particle-related structural defects were present in the ore milled using planetary mill.

5.4 Flotation behaviour

According to Ahmed (2010), physical and chemical actions occurring on the particle surface during technological processes are highly influenced by the geometry of the particle, and

the exact evaluation of this geometry by means of quantified particle shape factors is important. Particle size, shape and surface roughness are some of the important parameters used to differentiate between particles. Ahmed's (2010) paper was more of a review, discussing various methods that are available for determination of particle shape and referring to studies that have been conducted to correlate particle shape and flotation behaviour.

5.4.1 Base metal sulphides (BMS)

Flotation of base metal sulphides has received much attention over the years. This is due to the various uses of base metals. Another reason is that platinum group metals generally appear to follow similar flotation behaviour to base metal sulphides (Shackleton *et al.*, 2007b; Lekgetho *et al.*, 2009).

Development of hydrophobicity on sulphide minerals arises from an anodic process of collector which is coupled with a cathodic process such as reduction of oxygen (Hintikka & Leppinen, 1995).

The results section showed a general low nickel recovery for all mill samples for both ball and IsaMill products, compared to previous studies (Mishra, 2011). Nickel recovery is important in the flotation of base metal sulphide ores. Sotka *et al.* (2004), highlighted the different types of non-recoverable nickel in a fine-grained base metal sulphide ore. These are non-sulphide nickel-bearing minerals and sulphide nickel locked in difficult particle sizes. A large part of the nickel in the low-grade ores is bound in silicate minerals such as olivine, serpentine, talc, pyroxenes and amphiboles, which are non-sulphide minerals. On the other hand, some nickel is present as very fine possible locked particles, the liberation of which would require uneconomical grinding applications.

Figure 4.2.12 showed a decrease in copper grade as copper recovery increased. This is a typical grade-recovery relationship. Copper recoveries of up to 88 % were realised in the flotation of Nkomati ore. Copper flotation indicates the flotation behaviour of chalcopyrite, since almost all the copper present in the ore is in the chalcopyrite.

Chalcopyrite floatability has been shown to be relatively unaffected by the conditions that prevail in the flotation system and by the changes that occur to the ore before flotation since it usually floats so readily (Newell *et al.*, 2007). In their work they used Nkomati massive sulphide ore. The ore was oxidized for different number of days, after which the recovery of each of chalcopyrite, pyrrhotite and pentlandite was plotted against the oxidation period. Chalcopyrite recovery was found to be virtually unaffected by oxidation whereas recovery of pyrrhotite and pentlandite were heavily reduced. This then shows that chalcopyrite floatability is not a very good indicator of the flotation behaviour of a sulphide ore.

On the other hand, flotation of nickel/pentlandite has been shown to be sensitive to various factors.

Figure 4.2.14 shows the nickel grade-recovery relationship for Nkomati ore milled for various times in the ball mill. The ore milled for 16 minutes showed recovery of up to 45 % while 32 and 64 minutes products had recoveries below 20 %. Notable from the figure is the trend that grade increases as recovery increases for all the products. This is not the typical relationship whereby grade usually decreases with increasing recovery. Kirjavainen *et al.* (2002), observed that collectorless flotation behaviour of a sulphide ore milled in a steel

mill gave low nickel recoveries in the early stages of flotation, up to 4 minutes after which recoveries started to increase. Their explanation for this behaviour was that small iron particles from the steel mill clung to the sulphide particles and anodically protected the sulphide particles from oxidation; such that in the initial stages of flotation, only iron particles were oxidized. However as flotation time increased, most of the iron particles were oxidized from the sulphide surfaces, allowing the sulphide minerals to oxidize and become sulphur rich, non-polar and therefore hydrophobic.

In the light of observations by Kirjavainen *et al.* (2002) and their proposed explanation, maybe mostly gangue or pentlandite coated with gangue was recovered in the initial stages of flotation in the current study. Usually, gangue floats very poorly. However, the lack of depressant usage in this project could explain the flotation of especially naturally floatable gangue. Then as flotation time increased (after 4 minutes), value minerals, such as pentlandite, may start reporting to the concentrate in significant amounts, hence increasing the grade as recovery increased. This is a tenable explanation since mild steel grinding media was used in the ball mill. When ethyl xanthate was added, Kirjavainen *et al.* (2002) saw an increase in recovery nickel and copper sulphides.

As indicated earlier, nickel floatability has been shown to be negatively affected by oxidisation. Newell and Bradshaw (2007) oxidised a massive sulphide Nkomati ore by heating it at 85 ^{0}C for 121 days. Then they applied a sulfidisation process to reverse the effects of oxidation. Sulfidisation increased pentlandite recovery, indicating that pentlandite floatability had been adversely affected by oxidation. In the current work, the wet milled ore was dried in the oven at temperatures above 70 ^{0}C before flotation. Therefore it is likely that during drying, the ore was oxidised, suppressing nickel floatability in the process.

Floatability of pentlandite has been observed to be sensitive to many factors. Firstly, it has been shown to be strongly dependent on particle size, with coarse and particularly fine size fractions having low nickel recoveries. A low recovery in coarse fractions has been attributed to the gravitational detachment of particles from bubbles as the bubble-particle system rises in the flotation system. The poor recovery in the fine fractions has been attributed to both physical and chemical factors. Physically, the fine particles are swept off the bubbles by streamlines of liquid film that move around bubbles. This is why it is believed that adequate recovery of particles by flotation requires that bubbles and particles have equivalent sizes. Chemically, the pentlandite surfaces have been observed to be coated by gangue and/or iron hydroxide layers which suppress nickel recovery.

Secondly, grinding media or mill material has also been seen to affect nickel recovery. Steel media reduces the pulp potential and impedes the adsorption of thiol collectors on sulphide minerals, requiring high collector dosages in order to increase nickel recovery. In this study, 50 g/t collector concentration was used. This is a relatively low collector dosage in comparison to dosages which have been used by other researchers in the batch flotation of sulphide minerals. This could also be another explanation for the low nickel recoveries observed in this study.

In the current study, the parameters mentioned above are relevant and may have played a role in reducing nickel recoveries. The particle size distributions, as seen in Table 5.1.1, show that the ore samples which were floated were very fine, with 36 % and 51 % solids in the -10 µm fraction for ball 16 and 64 minutes, respectively, and 32 % and 54 % material in the -10 µm for IsaMill first and fourth passes, respectively. Particle size might have played a bigger

role in IsaMill samples which have been shown to be finer than ball mill products. However when comparing product milled for 64 minutes in the ball mill and that milled for four passes in the IsaMill, it is should be noted that pass four product gave higher nickel recovery even though pass four product was finer than 64 minutes product as seen from the particle size distributions. This then leads to the discussion on the effect of grinding media used in each of the mills on the flotation of the mill products.

Mild steel media was used in the ball mill and ceramic media was used in the IsaMill. Therefore, pentlandite surfaces of ore milled in the ball mill would have been susceptible to the formation iron hydroxide coatings which impede collector adsorption and result in poor nickel recovery. It should be noted that comparison of the nickel recoveries of products milled in one mill indicates that particle size played a determining role on the nickel recovery. On the other hand, comparison of the products from different mills, shows grinding environment (grinding media) to have been the determining factor in controlling nickel recovery.

Quality of process water (type and strength of ions present) has also been identified as one factor which affects nickel flotation. Kirjavainen *et al.* (2002) cited an electrochemical study which was undertaken by Hodgson and Agar (1989). The study investigated the effect of ions on the surface chemistry of pentlandite (nickel) and pyrrhotite. The observation from hydrophobicity tests was that Ca^{2+} and $S_2O_3^{2-}$ ions competed with xanthate for adsorption on pentlandite surface.

Peng and Seaman (2011) investigated the effect of the ionic strength of process water on the flotation of pentlandite. Borehole water and sea water (brine) were used in their study, with the chosen water type being used in all the stages, i.e. grinding, classification and flotation. The observation was that high ionic strength favoured pentlandite flotation. It should be noted that tap water was used for grinding and wet screening in the current study, whereas synthetic plant water with an ionic strength of 3.5E-0.2M was used for flotation.

Viewing the results of the current study in the light of the effect of process water on pentlandite flotation, it can be seen once again why the observed low nickel recoveries are not unexpected. Synthetic plant water that was used for flotation in this study contained Ca^{2+} ions which have been shown to reduce collector adsorption on pentlandite. Furthermore, the ionic strength of the plant water was not equivalent to ionic strength of brine which was observed to improve pentlandite recovery.

Senior *et al.*, (1995) studied the selective flotation of pentlandite from a nickel ore. They found that the main limitation of nickel recovery was the poor floatability of fine nickel with more than half the unrecovered nickel being less than 8 μm and in the -4 μm fraction. They found that the loss in the fine fractions was 6 times the loss in the +106 μm fraction even though both fractions contained same amount of nickel.

Mineralogy of the ore has also been observed to affect the flotation of pentlandite in a sulphide ore. Serpentine coatings have been observed to depress pentlandite flotation by attaching on pentlandite surfaces. Kirjavainen and Heiskanen (2007) observed this detrimental effect of serpentine slimes, especially chrysotile, on pentlandite flotation. It was also stated that 0.05 g of chrysotile per litre of pulp reduced nickel recovery from 90 % to 5 %. Formation of slime coatings was said to be directly related to the magnitude and sign of the surface charges of the slimes and sulphide particles (Pietrobon *et al.*, 1997). The

mineralogical analysis of the Nkomati ore which was used in the current study, Table 4.2.1, showed that the ore contained 5.6 %, by weight, of serpentine minerals in the form of Lizardite. Therefore, it is possible that their adverse effect on pentlandite flotation went unchecked and hence lowered nickel recovery.

Another parameter which affects flotation of sulphide minerals is pH. Alkaline pHs have been said to be advantageous for the flotation of sulphide minerals. Kirjavainen and Heiskanen (2007) investigated pH when they studied some factors that affect the beneficiation of sulphide nickel-copper ores. Their results further supported the point that alkaline pHs is favourable for sulphide flotation. Their results showed nickel recovery to be less than 20 % around pH 8 and 60 % around pH 11, after which point it dropped.

In the current study, pH was not controlled but monitored; it was found to be in the range 7-8.2. As was seen from Kirjavainen and Heiskanen (2007), nickel recovery is low in this pH range.

The interplay of all of the factors discussed here explains the flotation behaviour observed in the results of this project. The feasibility and scope of the project did not allow for the testing of the extent of the role played by each of these factors. However, in the light of the studies that have been carried out by other researchers on one or several of these factors, it is clear that each of these factors played a certain role which in the end resulted in the observed flotation behaviour. Furthermore, it should be noted there was no attempt to curb the effect of any of these factors which have been shown to depress nickel flotation. The aim of this study was not to determine the parameter which affected pentlandite flotation the most. So the mere presence and relevance of such a parameter in this study was enough to discuss the current results in the context of the available literature. Pentlandite flotation in Nkomati ore milled by the two mills is summarised in Table 5.4.1. It should be noted from the table that there was higher pentlandite recovery and grade for IsaMill (4 pass) product than for ball mill (64min) product. On the other hand, ball mill (16min) product had higher pentlandite recovery and grade than IsaMill (1 pass) product.

Flotation of sulphide minerals is a selective separation of pentlandite from pyrrhotite. Pyrrhotite recovery is generally an undesired concentrate product in the treatment of pentlandite/pyrrhotite ores because pyrrhotite increases sulphur emissions during smelting.

Figure 4.2.16 shows pyrrhotite grade as a function of its recovery for Nkomati ore milled in a ball mill for various grinding times. Pyrrhotite grade increased as pyrrhotite recovery increased as has been observed for pentlandite. Ore milled for 16 minutes showed the highest grade as compared to ore milled for 32 and 64 minutes. However, pyrrhotite recovery of the ore milled for all the three grinding times were similar, reaching up to 55 %. The differences in the grade between the products of the short and long milling times may be due to the interaction between pyrrhotite and mild steel grinding media. Interaction of pyrrhotite with mild steel has been found to have a deleterious impact of the floatability of pyrrhotite (Bozkurt *et al.*, 1998). The effect has been attributed to the formation of hydrophilic iron hydroxide coatings on pyrrhotite which inhibit xanthate adsorption. Therefore it could be that the longer grinding times (32 and 64 minutes) allowed this effect to be more pronounced whereas 16 minutes was short enough to minimise its effect on pyrrhotite recovery. The increasing grade of pyrrhotite with recovery could be a consequence of the pyrrhotite time-recovery as shown in Figure 4.2.15. This figure has near-exponential increase in pyrrhotite recovery as flotation time increases. The typical time-

recovery curve is linear for pyrrhotite, indicating a constant increment of recovery with time.

Figure 4.3.10 shows pyrrhotite grade as a function of recovery for Nkomati ore milled in the IsaMill (1, 2, 3 and 4 pass). The pyrrhotite grade decreased in the order of passes: one > two > three~ four. Notable from this figure is the fact that pyrrhotite grade decreased with increasing particle fineness, even though pyrrhotite recovery is similar despite the varying particle fineness. Ceramic grinding media was used in the IsaMill. The near constant pyrrhotite grade as recovery increases, could be a consequence of the pyrrhotite time-recovery results as shown in Figure 4.3.9, which follows a linear relation with flotation time.

Ball mill products showed higher grades of pyrrhotite than IsaMill products. Pentlandite and pyrrhotite have been found to follow similar flotation behaviour (Miller *et al.*, 2005). A similar behaviour was observed in the current study as shown in Table 5.4.1.

The relative recoveries of chalcopyrite, pentlandite and pyrrhotite follow the trends that have been observed by other researchers (Kirjavainen *et al.*, 2002). This then indicates that the anomalous nickel grade-recovery behaviour that was observed in this study is a result of the various interactions that took place in the system. In this system, none of the flotation variables were controlled, except reagent dosages.

It is interesting to investigate whether, in the flotation of Nkomati ore milled in the two mills for different times, there is a relationship between the shape of the particles (as inferred from the rheological behaviour of the samples) and their flotation behaviour.

Table 5.4.1 summarises the flotation recoveries and grades of chalcopyrite, pentlandite and pyrrhotite for Nkomati ore milled for 16 and 64 minutes in the ball mill and for one and for passes in the IsaMill.

Table 5.4.1: Recovery and grade of chalcopyrite, pentlandite and pyrrhotite for Nkomati ore milled in ball mill and IsaMill

Mill type	Grinding time/ pass number	Recovery (%)			Grade (%)		
		Ch	Pn	Po	Ch	Pn	Po
Ball mill	16min	90	42	60	0.9	1.3	1.6
	64min	90	18	55	1.4	0.7	0.7
IsaMill	1 pass	84	28	48	0.8	0.7	0.6
	4 pass	88	38	43	0.9	0.8	0.3

Figure 4.2.18 and Figure 4.3.12 show the distribution of copper and nickel grade in the batch concentrate and tailings of Nkomati ore milled for 16 minutes in the ball mill and for one pass in the IsaMill, respectively. The grades of the ore milled in the ball mill are higher than those for ore milled in the IsaMill. This could be attributed to the presence of fine particles in the -5 μm. However, Table 5.1.1 shows that the two mill products had similar amounts of material below 5 μm, viz. 20 % for pass one and 22 % for 16 minutes. A noteworthy point is that the nickel grades in the -10 μm and +25 μm fractions, for the ore milled for 16 minutes

are similar, whereas ore milled for one pass in the IsaMill has highest grade in the -10 μm and lowest in the +25 μm.

It has been noted from **Error! Reference source not found.** that Nkomati ore milled in the ball mill for 16 minutes had higher viscosity than the same ore milled for one pass in the IsaMill. This means that particles of the ore milled for one pass in the IsaMill were possibly rounder than those of ore milled for 16 minutes in the ball mill.

Table 5.4.1 shows that 28 % of the nickel was recovered from the ore milled for one pass in the IsaMill, while 42 % was recovered from the ore milled for 16 minutes in the ball mill. This means that there are indications that the more rounded particles exhibited poorer flotation response than the irregular particles for these relatively coarse samples. **Error! Reference source not found.** also shows the viscosity of Nkomati ore milled for 64 minutes in the ball mill and for four passes in the IsaMill. Ore milled using the IsaMill had higher viscosity in this case. This means that the particles of the ore milled in the IsaMill were irregular and rod-like while those of the ore milled in the ball mill were more rounded.

Table 5.4.1 shows that 38 % nickel was recovered from Nkomati ore milled in the IsaMill while 18 % was recovered from that milled in the ball mill. This shows that for fine mill products, irregular or rod-like particles were favourable for flotation as opposed to rounded particles. It may be inferred from these results that one of the effects of using different milling devices is that they produce particles of different morphologies. It is also likely that particles with greater irregularity would have more high energy sites than round particles and these would enhance the particle – bubble attachment. These results may indicate that rheology tests could give a useful indication of the inherent floatability of particles.

Figure 4.2.19 and Figure 4.3.13 show the copper and nickel grade distribution for the batch flotation samples of Nkomati ore milled for 64 minutes in the ball mill and for four passes in the IsaMill, respectively. Grades of the ore milled in the IsaMill are higher than those of the ore milled in the ball mill. In both samples the grades in the -10 μm fraction were the highest for each concentrate and decreased to a minimum value in the +25 μm fraction of that concentrate. It should be noted that the differences in grades amongst the size fractions are significant only in the first concentrate for Nkomati ore milled in both the ball mill and IsaMill. The grades across the size fractions for the subsequent concentrates showed slight decrease as the size fractions became coarser.

It can be concluded that ball mill product of 16 minutes had a better flotation performance, i.e., nickel recovery and grade, than IsaMill pass one product. On the other hand, IsaMill pass four product had higher nickel concentrate grades than ball mill 64 minutes product. The numerical values of copper and nickel recoveries are shown in Table 4.3.2 and Table 4.3.3 respectively. These values were obtained from Figure 4.2.17 and Figure 4.3.11, which show the distribution of recovered copper and nickel during flotation into three size fractions, for 64 minutes and pass four products, respectively.

5.4.2 UG2 ore

5.4.2.1 Particle shape

The shape of UG2 particles milled in the two mills was determined using SEM imaging coupled with proprietary image analysis software to determine the shape parameters from 2-dimensional (2D) SEM images. However, as already mentioned, there was no apparent

difference in the shape of particles determined by SEM imaging. This apparent similarity in the shape of particles could be a limited observation stemming from the use of simple geometric factors of roundness and aspect ratio. Probably, different observations can be made if more rigorous shape analysis methods are used to analyse the same particles. Use of techniques like fractal dimensions would probably reconcile the shape factors results and the rheology results. Brown *et al.* (1994) found that circularity and aspect ratio did not detect differences in particle shape whereas differences were observed when same particles were analysed using structural boundary fractal dimensions.

5.4.2.2 Flotation behaviour

Recovery of chromite with flotation using thiol collectors has been shown to be poor if it happens at all and true flotation of chromite is usually not expected (Maksimainen *et al.*, 2010). Any recovery of chromite has therefore been attributed to entrainment (Mailula *et al.*, 2003). In that light, any recovery of chromite in this study could be viewed as an indication of the degree of entrainment.

Pyrrhotite recovery is desirable in the processing of PGM ores, especially ores from the Bushveld complex. This is because the pyrrhotite may contain significant amounts of PGMs (Miller *et al.*, 2005). There has also been a suggestion that the pyrrhotite recovered in PGM processing provides extra source of sulphur to be used in smelters when treating UG2 ore since the ore is sulphur deficient (Allison & O'Connor, 2011).

Chromitite is the only mineral ore of chromium and has a wide range use of in metals, chemicals and refractories (Souza *et al.*, 2012). In the present instance it is undesirable to recover too much chromitite since it has a deleterious effect on the downstream smelting processes. In this study the mineral was analysed by determining the amount of Cr_2O_3 present in the UG2 ore.

Figure 4.2.28 shows the solids recovery as a function of water recovery for UG2 ore milled in a ball mill for various grinding times. Notable from the figure is the fact that more solids were recovered with water for finer products, i.e. 32 and 64 minutes products. It is well known that fine entrained particles follow the flow of water. This could however also be a result of the gravitational detachment of the coarse 16 minutes product particles from the bubbles during flotation combined with the fact that UG2 ore has a high specific gravity and hence large particles are more likely to be detached from the bubble-particle aggregate.

Figure 4.3.22 shows solids recovery as a function water recovery for UG2 ore milled in IsaMill for four passes. Also included is the solids recovery of the mill feed sample as a function water recovery. The figure shows that more solids were recovered with water as the mill product became finer. This is a similar behaviour to what was seen in Figure 4.2.28. Therefore similar reasons could have given rise to this behaviour.

Batch flotation samples of UG2 ore milled in the two mills were analysed on a size by size basis. The samples that were milled for short grinding times represented coarse and those milled for long grinding times represented fine samples.

Table 4.2.4 shows the mass distribution of chromite in UG2 ore milled in the ball mill (16min). Mass of chromite in the batch flotation concentrates and tailings is also shown. Eighty percent of the chromite that was in the feed to float reported to tailings and 6 % reported to the concentrate. Seventy-seven percent of the chromite that was recovered to the concentrate was in the -10 μm fraction.

Table 4.3.7 shows the mass distribution of chromite in the UG2 ore after it was milled in the IsaMill (1 pass) and in the subsequent concentrate and tailings after the ore was batch floated in a 3 L modified Leeds cell. Eighty-one percent of the chromite in the feed reported to the tailings and 9 % was recovered in the concentrate. Eighty-nine percent of the chromite that was recovered to the concentrate was in the -10 μm fraction. It should be noted here that there was more chromite in the -10 μm of IsaMill (1 pass) than ball mill (16min). The fact that the biggest percentage of the chromite in the concentrates was in the fine fraction, -10 μm, confirms that particle fineness plays a big role in the entrainment of chromite.

A comparison between UG2 ore milled in ball mill (16min) and in the IsaMill (1 pass) shows that IsaMill product had lower viscosity than ball mill product. This means that particles of UG2 ore milled in the IsaMill (1 pass) were more rounded than particles of the same ore milled in the ball mill (16min). As mentioned earlier, chromite recovery of the UG2 milled in the IsaMill (1 pass) was 9 % whereas recovery of UG2 ore milled in ball mill (16min) was 6 %. In terms of particle shape, this means that the more rounded the particles, the more chromite reported to concentrate. The difference in chromite recovery between these two samples is significant even though the difference in their shape as inferred from their rheological response was not very large. This could be an indicator of the role particle shape could play in the floatability or entrainment of particles. It could then be concluded that, for relatively coarse particles, spherical particles are favourable for flotation as opposed to irregular particles. It should be noted at this point that the rheology tests were performed on the -25 μm fractions of the mill products. Zhang and Kavetsky (1993) concluded that the distribution of particles in the mill during grinding determines the breakage mechanisms that dominate in the mill. Breakage mechanisms have also been shown to play a significant role in determining the shape of mill product particles. Therefore, despite the fact that all samples analysed for rheology were -25 μm, ball mill (16min) and IsaMill (1 pass) were regarded as coarse because the overall size distribution of the these products were coarser than products of ball mill (64min) and IsaMill (4 pass).

The observation that more rounded particles show better flotation is similar to what Hoberg and Scheneider (1978) found in their research but contrary to what Forssberg and Zhai (1985) and Hicyilmaz *et al.* (1995) have reported. Wotruba *et al.* (1991) demonstrated that the detachment of rounded particles from a bubble was more likely to occur than the detachment of prismatic particles.

Table 4.2.5 shows the mass distribution of chromite in the UG2 ore milled in the ball mill (64min). Together with this, are shown the mass distributions of chromite in each of the concentrates and the tailings. On average, the -10 μm fractions of the four concentrates each contained more chromite than the other fractions again indicating the dominant role which particle size plays on the recovery of chromite by entrainment. The smallest mass of chromite was recovered in the first concentrate and the largest mass recovered in the fourth concentrate. 6 % of the chromite in the feed was recovered in the concentrates and 75 % remained in the tailings.

Table 4.3.8 shows the mass distribution of chromite in the UG2 ore that was milled in the IsaMill (4 pass). The chromite distribution in the concentrates and tailings after flotation is also shown in the same figure. 22 % of the chromite in the feed was recovered in the concentrates while 64 % was in the tailings. The amount of chromite in the -10 μm fractions

of the concentrates increased as flotation time increased i.e. chromite increased in the order from C1 to C4.

This shows that more chromite was recovered for UG2 ore milled in the IsaMill (4 pass) than for UG2 ore milled in the ball mill (64min). UG2 ore milled in the IsaMill (4 pass) had the greatest amount of chromite recovered in the concentrate. This is presumably because of the greater amount of fines that were in this product, as seen from Table 5.1.2, and hence high entrainment.

Most of the chromite that was recovered into concentrates for all mill products was in the fine fraction of -10 μm. This indicates that chromite is almost entirely recovered by chromite. It has been shown that there is a relationship between particle morphology (shape) and rheology. This could also suggest that there is a strong relationship between entrainment or elutriation and particle morphology (shape).

The primary aim of this study was to investigate whether the use of different milling devices may result in different flotation behaviour and whether any differences observed may be due to difference in morphology resulting from the use of these different devices. Figure 5.3.2 shows the relative viscosity of UG2 ore milled in ball mill and IsaMill as a function of solids volume fraction. Comparing the viscosity of ore milled in the ball mill (64min) and ore milled in the IsaMill (4 pass), the ball mill product had lower viscosity than IsaMill product as the solids fraction increased. This indicates that ball mill (64min) product particles were possibly more spherical that IsaMill (4 pass) product particles. Comparison of the chromite recoveries of the two products showed that more chromite (22 %) was recovered from UG2 ore milled in the IsaMill (4 pass) than was recovered when milled in the ball mill (64min), i.e. 16%. This then shows that for the fine fractions of the ore milled to fine sizes, irregular or rod-shaped particles enhanced chromite recovery in flotation as opposed to spherical particles. This is consistent with what was observed for Nkomati ore. However, it should be noted that in the case Cr_2O_3 recovery, this could provide a basis for assuming that particle shape influences entrainment, assuming, as literature says, that chromite is recovered by entrainment.

Frances et al. (2001) analysed the shape of particles produced by various mills. For all the mills which they used, they found that circularity and the ratio F_{max}/F_{min} increased with decreasing size, indicating that fragments were more elongated than the initial particles. However stirred bead mill products showed this behaviour only down to 10 μm, below which size both circularity and F_{max}/F_{min} decreased, indicating more rounded particles.

The results obtained in the current research point to the fact that the effect of particle shape differ depending on the size of the particles, although there is no absolute certainty on this. A shape that is favourable for flotation in coarse fractions appears to be detrimental for fine fractions.

Chapter 6 CONCLUSIONS

The aim of the study was to investigate whether the flotation behaviour of ball mill and IsaMill products was in any way influenced by the fact that they were milled in different devices. The hypothesis driving this study was that different grinding mechanisms that take place in different types of mills may produce particles with different physical and chemical properties, these differences in turn bringing about different downstream processing behaviour. In this case batch flotation was used to diagnose these differences.

The first conclusion that was drawn from a search of the literature on the grinding mechanisms inside grinding mills was that the study of breakage mechanisms inside grinding mills has largely been approached in a qualitative manner. That is, different breakage modes have been thought to produce particles with different particular properties or physical features. Furthermore, the investigation of breakage mechanisms inside grinding mills is complicated by the fact that there is always more than one grinding mechanisms taking place simultaneously in the mill during grinding. There is no quantitative measure of the extent of each breakage mechanism in a given mill. The most widely proposed particle feature which has been purported to be an indicator of the breakage mechanism that dominates in a given mill is particle shape. However, particle shape assessment also poses problems because its definition is also qualitative; particle shape is a 3-dimensional (3D) property whereas the techniques that are used to measure it are mostly 2-dimensional. Image analysis has been identified as a reliable technique for analysis of particle shape. This technique relies on the analysis of the silhouettes of 3D particles.

Secondly, the effect of the different particle shapes on flotation performance of these particles is not clear from the literature. The conclusions drawn from this study will summarize the results for the two ores in the two milling devices.

Nkomati ore treated in the ball mill and IsaMill under the given conditions had similar size distributions with a P_{80} of 57 µm. Similarly, ore treated for 64 minutes in the ball mill and for four passes in the IsaMill mill had similar size distributions, with a P_{80} of 24 µm.

Ore milled in ball mill (16min) and in IsaMill (1 pass) represented coarse products of the mills while ball mill (64min) and IsaMill (4 pass) products represented fine products. Rheology studies indicated that coarse ball mill products were rounder than IsaMill products whereas ore milled for four passes in IsaMill had higher viscosity than ore milled for 64 minutes in the ball mill from which it can be inferred that IsaMill pass four product was more irregularly or rod-like shaped than those produced after 64 minutes in the ball mill.

From this it was inferred that ball mill products, having similar particle shapes were probably broken by the same mechanisms. On the other hand, ore treated for four passes in the IsaMill had higher viscosity than ore milled for one pass suggesting that the pass four products were more irregular or rod-like in shape and hence impact breakage was dominant in the breakage of this product. This concurs with some findings in the literature which indicate that coarse particles are broken by abrasion while fine particles are broken by impact breakage. The shape analyses results from image analysis showed similar results for products regardless of mill type. The rheological behaviour of UG2 ore treated in the IsaMill (4 pass) gave higher viscosity compared to UG2 ore milled in ball mill (64min). The viscosity values were generally lower for UG2 than they were for BMS.

Chalcopyrite recoveries were, as expected, high for all cases studied and this does not shed any light on the possible effects of shape and size. Pentlandite recovery of Nkomati ore milled in the IsaMill (4 pass) was higher than for ore milled in ball mill (64min). This can be attributed to the cleaning effect of ceramic media used in IsaMill as opposed to mild steel media used in ball mill. However, pentlandite grade of IsaMill (4 pass) product was less than that of ball mill (64min) product. This shows that fine gangue was probably recovered by entrainment with pentlandite in pass four product.

Pentlandite recovery and grade of Nkomati ore milled in the ball mill (16min) were higher than for ore milled in the IsaMill (1 pass). Chalcopyrite recovery and grade was similar for all mill products, which is not surprising given the ease with which chalcopyrite generally floats. Comparison of the nickel recoveries of products milled in one mill indicated that particle size played a determining role on the nickel recovery. On the other hand, comparison of the products from different mills, showed grinding environment (grinding media) to have been the determining factor in controlling nickel recovery.

Correlation of the particle shape characteristics and flotation results showed that, in general, round particles were more favourable for the flotation of coarse particles, whereas irregular particles were more favourable for the flotation of fine particles. This observation was consistent for both BMS and UG2 ores. However it should be noted that in the case of the UG2 ore the chromite is probably mostly recovered by entrainment and hence bubble – particle attachment is not the dominant factor. It could be possible that even the extent to which particles are entrained is affected by their shape. Irregularly shaped particles may be more readily held in the interstices between bubbles in the froth phase.

Chromite recovery for IsaMill products was higher than for ball mill products for both fine and coarse products. This is not a desirable behaviour in the flotation of UG2 ores. However, it should be noted that the performance of these mills on UG2 ore cannot be based on this observation alone since it should be coupled with an analysis of the related PGE recovery and grade data. In this study PGE analyses were not carried out. It should also be noted that, in the context of this study, inert grinding media in the IsaMill did not yield desirable UG2 ore flotation results as compared to mild steel media which was used in the ball mill. More Cr_2O_3 was recovered for IsaMill products than it was for ball mill products. Again it should be noted that surface oxidation phenomena would have a minimal effect on entrained particles.

The batch flotation concentrates were analysed for particles size distribution to determine if recovery of minerals was size dependent. There was no difference in the particle size distributions of the four concentrates of Nkomati ore milled in the two mills. The first concentrate of the UG2 ore had coarser particles than the subsequent concentrates in the products of the two mills, for both the coarse and the fine fractions.

This work indicates that different mill types produce particles of different shapes. These particle shapes then affect flotation and entrainment to varying degrees.

Chapter 7 RECOMMENDATIONS

This work has indicated a relationship between milling procedures and flotation behaviour. This has led to the following recommendations:

- Further work is needed to investigate the relationship between various milling procedures and the rheology of the products of those milling procedures.
- The work has emphasized the importance of integrating comminution and flotation.
- Different types of milling media should be used in the two mills that were used in this study. This could help to decouple the effects of milling media from that of the mill type on the properties of the mill products. PGE recovery and grade data of the UG2 ore should be obtained in order to make more conclusive deductions about the effect of the two mills on flotation performance of UG2 ore.
- An attempt should be made to analyse shape of particles using some of the more advanced analysis techniques like Fourier analysis, delta analysis and fractal geometry. Fractal geometry seems like the simpler of these advanced techniques, and it is highly recommended for further analysis.

Chapter 8 REFERENCES

Ahmad, F. N., Jaafar, M., Palaniandy, S., & Azizli, K. A. (2008). Effect of particle shape of silica mineral on the properties of epoxy composites. *Composites Science and Technology 68* , 346-353.

Ahmed, M. M. (2010). Effect of comminution on particle shape and surface roughness and their relation to flotatio process. *International Journal of Mineral Processing,94* , 180-191.

Allison, S. A., & O'Connor, C. T. (2011). An investigation into the flotation behaviour of pyrrhotite. *International Journal of Mineral Processing 98* , 202-207.

Anfruns, J. F., & Kitchener, J. A. (1977). Rate of capture of small particles in flotation . *Transactions of the Institution of Mining and Metallurgy , Section C: Mineral Processing and Extractive Metallurgy 86* , 9-15.

Barnes, H. A. (2000). *Handbook of elementary rheology.* Wales.

Bernhardt, C., Reinsch, E., & Husemann, K. (1999). The influence of suspension properties on ultra-fine grinding in stirred ball mills . *Powder Technology, 105* , 357-361.

Berthiaux, H., & Dodds, J. (1999). Modelling fine grinding in a fluidized bed opposed jet mill Part I: Batch grinding kinetics. *Powder Technology 106* , 78-87.

Bilgili, E., Hamey, R., & Scarlett, B. (2006). Nano-milling of pigment agglomerates using a wet stirred media mill: Elucidation of the kinetics and breakage mechanisms. *Chemical Engineering Science 61* , 149-157.

Boldyrev, V. V., Pavlov, S. V., & Goldberg, E. L. (1996). Interrelation between fine grinding and mechanical activation. *International Journal of Mineral Processing 44-45* , 181-185.

Bond, F. C. (1952). The third theory of comminution. *Transactions of AIME Mining Engineering 193* , 484-494.

Bozkurt, V., Xu, Z., & Finch, J. A. (1998). Pentlandite/pyrrhoite interaction and xanthate adsorption . *International Journal of Mineral Processing 52* , 203-214.

Bradford, L., McInnes, C., Stange, W., de Beer, C., David, D., & Jardin, A. (1998). The Development of the proposed milling circuit for the Nkomati main concentrator plant. *Minerals Engineering 11(12)* , 1103-1117.

Bradshaw, D. J., Buswell, A. M., Harris, P. J., & Ekmekci, Z. (2006). Interactive effects of the type of milling media and copper sulphate addition on the flotation performance of sulphide minerals from Merensky ore Part I:Pulp chemistry. *International Journal of Mineral Processing,78* , 153-163.

Brown, G. J., Miles, N. J., & Hall, S. T. (1994). Fractal assessment of finely ground limestone for flue gas desulphurization. *Minerals Engineering 7 (8)* , 1057–1067.

Bulatovic, S. M. (2007). *Handbook of flotation reagents- Chemistry, Theory and Practice: Flotation of Sulfide Ores.* Elsevier .

Burford, B. D., & Clark, L. W. (2007). *IsaMill technology used in efficient grinding cirtcuits.*

Carter, R. M., & Yan, Y. (2005). Measurement of particle shape using digital imaging techniques. *Journal of Physics: Conference Series 15* , 177-182.

Cawthorn, R. G. (1999). The platinum and palladium resources of the Bushveld complex. *South African Journal of Science 95* , 481-489.

Cawthorn, R. G., & Webb, S. J. (2001). Connectivity between western and eastern limbs of the Bushveld Complex. *Tectonophysics 330 (3-4)* , 195-209.

Chamber of mines. (2010). *Facts anf Figures.* Retrieved February 9, 2012, from Chamber of Mines South Africa: http://www.bullion.org.za/content/?pid=71&pagename=Facts+and+Figures

Chapman, N. A. (2010). *A study of the effect of different comminution procedures on the recovery of platinum group elements: MSc Thesis.* Cape Town: University of Cape Town.

Choi, H. K., & Choi, W. S. (2003). Ultra-Fine Grinding Mechanism of Inorganic Powders in a Stirred Ball Mill -The effect of grinding aids-. *Korean Journal of Chemical Engineering 20(3)*, 554-559.

Clark, L. W., & Burford, B. D. (2004). *Fine Grinding and Project Enhancement.*

Clark, N. N. (1986). Three Techniques for Implementing Digital Fractal Analysis of Particle Shape. *Powder Technology 46*, 45-52.

Coulson, J. M., Richardson, J. F., Backhurst, J. R., & Harker, J. H. (1991). *Chemical Engineering volume 2 : Particle Technology and Separation Processes.*

Deglon, D. A. (2005). The effect of agitation on the flotation of platinum ores. *Minerals Engineering 18*, 839-844.

Ding, Z., Yin, Z., Liu, L., & Chen, Q. (2007). Effect of grinding parameters on the rheology of pyrite-heptane slurry in a laboratory stirred media mill. *Minerals Engineering 20*, 701-709.

El-Shall, H. (1984). Mechanisms of Grinding Modification by Chemical Additives: Organic Reagents. *Powder Technology 38*, 267-273.

Erdem, A. S., & Ergün, S. L. (2009). The effect of ball size on breakage rate parameter in a pilot scale ball mill. *Minerals Engineering 22*, 660-664.

Fahlstrom, P. H. (1974). Autogenous grinding of base metal ores at Boliden Aktiebolag . *CIM Bulletin 78*, 127-141.

Farber, B. Y., Knopjes, L., & Bedesi, N. (2009). Advances in ceramic media for high energy milling applications. *Minerals Engineering 22*, 704-709.

Filippov, Y. M. (1998). Flotation of fine particles and intergrowths by small air bubbles. *Journal of Mining Science 34*, 466-470.

Forssberg, E., & Zhai, H. (1985). Shape and surface properties of the particles liberated by autogenous grinding . *Scandinavian Journal of Metallurgy 14 (1)*, 25-32.

Frances, C., Le Bolay, N., Belaroui, K., & Pons, M. N. (2001). Particle morphology of ground gibbsite in different grinding environments. *International Journal of Mineral Processing,61*, 41-56.

Fuerstenau, D. W., Kapur, P. C., & De, A. (2003). Modelling breakage kinetics in various dry comminution systems. *KONA*, 121-132.

Gao, M., & Forssberg, E. (1995). Prediction of size distributions for stirred ball mill. *Powder Technology 84*, 101-106.

Gao, M., Young, M., & Allum, P. (2002). *IsaMill fine Grinding Technology and its Industrial Applications at Mt Isa Mines.*

Gaudin, A. M., & Malozemoff, P. (1932). Recovery by Flotation of Mineral Particles of Colloidal Size. *The Journal of Physical Chemistry 37 (5)*, 597-607.

George, P., Nguyen, A. V., & Jameson, G. J. (2004). Assessment of true flotation and entrainment in the flotation of submicron particles by fine bubbles. *Minerals Engineering 17*, 847-853.

Goncalves, K. L., Andrade, V. L., & Peres, A. E. (2003). The effect of grinding condition on the flotation of a sulphide copper ore. *Minerals Engineering 16*, 1213-1216.

Gottlieb, P., Wilkie, G., Sutherland, D., Ho-Tun, E., Suthers, S., Perera, K., (2000). Using Quantitative Electron Microscopy for Process Mineralogy Applications . *Journal of Minerals, Metals and Materials 52* , 24-25.

Grano, S. (2009). The critical importance fo the grinding environment on fine partilce recovery in flotation. *Minerals Engineering 22* , 386-394.

Greenwood, R., Luckham, R. F., & Gregory, T. (1997). The Effect of Diameter Ratio and Volume Ratio on the Viscosity of Bimodal Suspensions of Polymer Latices. *Journal of Colloid and Interface Science* , 11-21.

Harbort, G., Hourn, M., & Murphy, A. (1998). *IsaMill Ultrafine grinding for a sulphide leach process.* MIM Proces Technologies.

He, M., & Forssberg, E. (2006). Influence of slurry rheology on stirred media milling of limestone. In S. K. Kawatra, *Advances in Comminution* (pp. 243-260). Littleton: Society for Mining, Metallurgy and Exploration, Inc. (SME).

He, M., & Forssberg, E. (2007). Influence of slurry rheology on stirred media milling of quartzite. *International Journal of Mineral Processing* , 240-251.

He, M., Wang, Y., & Forssberg, E. (2006). Parameter effects on wet ultrafine grinding of limestone through slurry rheology in a stirred media mill. *Powder Technology, 161* , 10-21.

He, M., Wang, Y., & Forssberg, E. (2004). Slurry Rheology in wet ultrafine grinding of industrial minerals: A Review. *Powder Technology 147* , 94-112.

Heine, D. R., Petersen, M. V., & Grest, G. S. (2010). Effect of particle shape and charge on bulk rheology of nanoparticle suspensions. *The Journal of chemical physics 132, 1-6* .

Hennart, S. L., Wildeboer, W. J., van Hee, P., & Meesters, G. M. (2009). Identification of the grinding mechanisms and their origin in a stirred ball mill using population balances. *Chemical Engineering Science 64* , 4123-4130.

Herna´inz, F., & Calero, M. (2001). Froth flotation:kinetic models based on chemical analogy. *Chemical Engineering and Processing 40* , 269275.

Hic¸yilmaz, C., Ulusoy, U., & Yekeler, M. (2004). Effects of the shape properties of talc and quartz particles on the wettability based separation processes. *Applied Surface Science 233* , 204-212.

Hicyilmaz, C., Bilgen, S., Atalay, U., & Ulusoy, U. (1995). Effect of shape characteristics of particles on flotation. *Fizykochemizne Problemy Mineralurgii 29* , 31-38.

Hicyilmaz, C., Ulusoy, U., Bilgen, S., & Yekeler, M. (2005). Flotation responses to the morphological properties of particles measured with three-dimensional approach. *International Journal of Mineral Processing 75* , 229-236.

Hintikka, V. V., & Leppinen, J. O. (1995). Potential control in the flotation of sulphide minerals and precious metals. *Minerals Engineering 8 (10)* , 1151-1158.

Hoberg, H., & Schneider, F. U. (1978). Zur flotation feints verteilter metallphasen aus vorre duzierten. *Erzen. Freib. Forsch. HA., 593* , 149-160.

Hodgson, M., & Agar, G. E. (1989). Electrochemical investigation into the flotation chemistry of pentlandite and pyrrhotite: process water and xanthate interactions. *Canadian Metallurgical Quarterly 28 (3)* , 189– 198.

Hogg, R. (1999). Breakage mechanisms and mill performance in ultrafine grinding. *Powder Technology 105* , 135-140.

Hogg, R., Turek, M. L., & Kaya, E. (2004). The Role of Particle Shape in Size Analysis and the Evalutation of Comminution Processes. *Particulate Science and Technology 22 (4)*, 355-366.

Holt, C. B. (1981). The shape of particles produced by comminution- A review. *Powder Technology 28*, 59-63.

Huang, G., & Grano, S. (2006). Galvanic interaction between grinding media and arsenopyrite and its effect on flotation Part 1. Quantifying galvanic interaction during grinding. *International Journal of Mineral Processing 78* , 182-197.

Huh, C., & Mason, S. G. (1974). The flotation of axisymmetric particles at horizontal liquid interfaces. *Journal of Colloid and Interface Science 2 (47)* , 271-289.

Jankovic, A. (2005). A review of regrinding and fine grinding technology - the facts and myths. *IRR Crushing and Grinding Conference.* Perth: Metso Minerals Process Technology .

Jankovic, A. (2003). Variables affecting the fine grinding of minerals using stirred mills. *Minerals Engineering 16* , 337-345.

Jankovic, A., Dundart, H., & Mehta, R. (2010). Relationships between comminution energy and product size for a magnetite ore. *The Journal of The Southern African Institute of Mining and Metallurgy 110*, 141-146.

Jones, G., Corin, K. C., van Hille, R. P., & Harrison, S. T. (2011). The generation of toxic reactive oxygen species (ROS) from mechanically activated sulphide concentrates and its effect on thermophilic bioleaching. *Minerals Engineering 24*, 1198-1208.

Kaya, E., Hogg, R., & Kumar, S. R. (2002). Particle Shape Modification in Comminution. *KONA 20*, 188-195.

Kelly, E. G., & Spottiswood, D. J. (1990). The breakage function; what is it really? *Minerals Engineering 3*, 405-414.

Kirjavainen, V., & Heiskanen, K. (2007). Some factors that affect beneficiation of sulphide nickel–copper ores. *Minerals Engineering 20* , 629–633.

Kirjavainen, V., Schreithofer, N., & Heiskanen, K. (2002). Effect of some process variables on flotability of sulfide nickel ores. *International Journal of Mineral Processing 65* , 59-72.

Klimpel, R. R. (1999). The selection of wet grinding chemical additives based on slurry rheology control. *Powder Technology 105* , 430-435.

Knieke, C., Steinborn, C., Romeis, S., Peukert, W., Breitung-Faes, S., & Kwade, A. (2010). Nanoparticle production with stirred-media mills: Opportunities and limits. *Chemical Engineering Technology 33 (9)* , 1401-1411.

Konert, M., & Vandenberghe, J. (1997). Comparison of laser grain size analysis with pipette and sieve analysis: a solution for the underestimation of the clay fraction. *Sedimentology 44* , 523-535.

Konopacka, Z., & Drzymala, J. (2010). Types of particles recovery-water recovery entrainment plots useful in flotation recovery. *Adsorption 16* (4-5), 313-320.

Kwade, A. (1999). Wet comminution in stirred media mills-research and its practical application. *Powder Technology 105* , 14-20.

Kwade, A., & Schwedes, J. (2002). Breaking characteristics of different materials and their effect on stress intensity and stress number in stirred media mills. *Powder Technology 122* , 109-121.

Lange, A. G., Skinner, W. M., & Smart, R. S. (1997). Fine:Coarse particle interactions and aggregation in sphalerite flotaiton. *Minerals Engineering 10* , 681-693.

Laskowski, J. S., Liu, Q., & O'Connor, C. T. (2007). Current understanding of the mechanism of polysaccharide adsorption at the mineral/aqueous solution interface . *International Journal of Mineral Processing 84* , 59-68.

Lekgetho, T. B., Chetty, D., & Tredoux, M. (2009). *Investigation of the behaviour of platinum-group minerals and base metals during flotation of UG2 ore.* Swaziland: 11th SAGA Biennial Technical Meeting and Exhibition.

Lin, I. (1998). Implications of fine grinding in mineral processing: a mechanochemical approach. *Journal of Thermal analysis 52* , 453-461.

Lynch, A. J., & Rowland, C. A. (2005). *The History of Grinding.* Society for Mining, Metallurgy and Exploration.

Mailula, T. D., Bradshaw, D. J., & Harris, P. J. (2003). The effect of copper sulphate addition on the recovery of chromite in the flotation of UG2 ore. *The Journal of the South African Institute of Mining and Metallurgy* , 143-146.

Maksimainen, T., Luukkanen, S., Morsky, P., & Kalapadus, R. (2010). The effect of grinding environment on flotation of sulphide poor PGE ores. *Minerals Engineering 23* , 908-914.

Martinez-Carrillo, D., & Uribe-Salas, A. (2008). Experimental study of the recovery of hydrophilic silica fines in column flotation. *Minerals Engineering 21* , 1102-1108.

Meloy, T. P., Durney, T. E., & Eppler, D. T. (1979). Sophisticated shape analysis of green pellets from a balling drum. *13th International Mineral Processing Congress*, (pp. 1619- 1641). Warsaw.

Miettinen, T., Ralston, J., & Fornasiero, D. (2010). The limits of fine particle flotation. *Minerals Engineering 23* , 420-437.

Miller, J. D., Li, J., Davidtz, J. C., & Vos, F. (2005). A review of pyrrhotite flotation chemistry in the processing of PGM ores. *Minerals Engineering 18* , 855-865.

Mishra, J. (2011). *Investigating the role of pulp chemistry on the floatability of the Cu-Ni sulfide ore. MSc Thesis.* Cape Town: University of Cape Town.

Mondal, S. K., & Mathez, E. A. (2007). Origin of the UG2 chromitite later, Bushveld complex. *Journal of Petrology 48 (3)* , 495-510.

Napier-Munn, T., Morrell, S., Morrison, R., & Kojovic, T. (2005). *Mineral Comminution Circuits.* Queensland: Julius Kruttschnitt Mineral Research Centre.

Nel, E., Theron, J., Martin, C., & Raabe, H. (2004). PGM Ore Processing at Impala's UG-2 Concentrator in Rustenburg, South Africa. *34th Annual Meeting of the Canadian Mineral Processors.* Ontario.

Nel, E., Valenta, M., & Naude, N. (2005). Influence of open circuit regring milling on UG2 ore composition and mineralogy at Impala's UG2 concentrator. *Minerals Engineering 18* , 785-790.

Newell, A. J., & Bradshaw, D. J. (2007). The development of a sulfidisation technique to restore the flotation of oxidised pentlandite. *Minerals Engineering 20* , 1039-1046.

Newell, A. J., Skinner, W. M., & Bradshaw, D. J. (2007). Restoring floatability of oxidised sulfides using sulfidisation. *International Journal of Mineral Processing 84* , 108-117.

Nguyen, A. V., & Schulze, H. J. (2004). *Colloidal Science of Flotation.* New York: Marcel Dekker Inc .

Oja, M., & Tuunila, R. (2000). The influence of comminution method to particle shape. In: *Proceedings of the XXI International Mineral Processing Congress* , (pp. 64-74).

Pabst, W. (2004). Fundamental considerations on suspension rheology. *Ceramics 48 (1)* , 6-13.

Pabst, W., & Gregorová, E. (2007). *Characterisation of particles and particle systems.* Prague: ICT Prague.

Pabst, W., Berthold, C., & Gregorov´a, E. (2007). Size and shape characterisation of oblate and prolate particles. *Journal of the European Ceramic Society 27* , 1759-1762.

Pabst, W., Gregorov´a, E., & Berthold, C. (2006). Particle shape and suspension rheology of short-fiber systems. *Journal of the European Ceramic Society 26* , 149-160.

Palaniandy, S., Azizli, K. A., Hussin, H., & Hashim, S. F. (2008). Effect of operational parameters on the breakage mechanism of silica in a jet mill. *Minerals Engineering 21* , 380-388.

Parry, J. M. (2006). *Ultrafine grinding for improved mineral liberation in flotation concentrates: Master af Applied Science Thesis.* The University of British Columbia.

Partyka, T., & Yan, D. (2007). Fine grinding in horizontal ball mills. *Minerals Engineering 20* , 320-326.

Pease, J. A. (2006). Autogenous and inert miling at fine sizes- the IsaMill. *SAG 2006 Conference UBC/CIM.* Vancouver.

Pease, J., Curry, D., & Young, M. (2006). Designing flotation circuits for high fines recovery. *Minerals Engineering 19* , 831-840.

Peng, Y., & Seaman, D. (2011). The flotation of slime-fine fractions of Mt.Keith pentlandite ore in de-ionised and saline water. *Mlnerals Engineering 24* , 479-481.

Peng, Y., Grano, S., Fornasiero, D., & Ralston, J. (2003). Control of grinding conditions in the flotation of galena and its separation from pyrite. *International Journal of Mineral Processing 70* , 67-82.

Pentberthy, C. J., Oosthuyzen, E. J., & Merkle, R. W. (2000). The recovery of platinum-group elements from UG-2 chromitite, Bushveld Complex- a mineralogical perspective. *Mineralogy and Petrology 68* , 213-222.

Petruk, W. (2000). *Applied Mineralogy in the Mining Industry.* Ottawa, Ontario: Elsevier.

Pietrobon, M. C., Grano, S. R., Sobieraj, S., & Raltson, J. (1997). Recovery mechanisms for pentlandite and MgO-bearing gangue minerals in nickel ores from Western Australia. *Minerals Engineering 10 (8)* , 775-786.

Pilevneli, C. C., Kızgut, S., Torog˘lu, I., Cuhadarog˘ lu, D., & Yig˘ it, E. (2004). Open and closed circuit dry grinding of cement rejects in a pilot scale vertical stirred mill. *Powder Technology 139* , 165-174.

Pillay, K., Becker, M., Chetty, D., & Thiele, H. (2011). The effect of gangue mineralogy on the density separation of low grade nickel ore. *The Southern African Institute of Mining and Metallurgy* , 493-510.

Podczeck, F. (1997). A shape factor to assess the shape of particles using image analysis. *Powder Technology 93* , 47-53.

Pourghahramani, P., & Forssberg, E. (2005). Review of applied particle shape descriptors and produced particle shapes in grinding environments.Part1.Particle Shape Descriptors. *Mineral Processing and Extractive Metallurgy Review 26* , 145-166.

Prasher, C. L. (1987). *Crushing and Grinding Process Handbook.* Chichester: John Wiley & Sons Limited.

Rahal, D., Erasmus, D., & Major, K. (2011). Knelson-Deswik Milling Technology: Bridging the Gap between Low and High Speed. *Proceedings of the 43rd Annual Canadian Mineral Processors Conference* , (pp. 557-587). Ontario.

Rao, K. H., & Chernyshov, I. V. (2011). Challenges in sulphide mineral processing. *The Open Mineral Processing Journal 4* , 7-13.

Reay, D., & Ratcliff, G. A. (1975). Experimental testing of the hydrodynamic collision model of fine particle flotation . *Canadian Journal of Chemical Engineering 53 (5)* , 481-486.

Riley, G. S. (1968). An Examination of the Separation of Differently Shaped Particles. *Powder Technology 2* , 315-319.

Robins, W. H. (1954). The significance and application of shape factors in particle size analysis. *British journal of Applied Physics 5* , 82-85.

Santana, R. C., Farnese, A. C., Fortes, M. C., Ataíde, C. H., & Barrozo, M. A. (2008). Influence of particle size and reagent dosage on the performance of apatite flotation. *Separation and Purification Technology 64* , 8-15.

Savassi, O. N. (2006). Estimating the recovery of size-liberation classes in industrial flotation cells: A simple technique for minimizing the propagation of the experimental error. *International Journal of Mineral Processing 78* , 85-92.

Schouwstra, R. P., Kinloch, E. D., & Lee, C. A. (2000). A Short Geological Review of the Bushveld Complex. *Platinum Metals Review, 44* , 33-39.

Schuhmann, R. J. (1942). *Flotation kinetics: Methods for the steady-state study of flotation problems.* Cambridge, Massachusetts: Department of Metallurgy, Massachusetts Intsitute of Technology.

Senior, G. D., Trahar, W. J., & Guy, P. J. (1995). The selective flotation of pentlandite from a nickel ore. *International Journal of Mineral Processing 43* , 209-234.

Shackleton, N. J., Malysiak, V., & O'Connor, C. T. (2007a). Surface characteristics and flotation behaviour of platinum and palladium tellurides. *Minerals Engineering 20* , 1232-1245.

Shackleton, N. J., Malysiak, V., & O'Connor, C. T. (2007b). Surface characteristics and flotation behaviour of platinum and palladium arsenides. *International Journal of Mineral Processing 85* , 25-40.

Shi, F., Morrison, R., Cervellin, A., Burns, F., & Musa, F. (2009). Comparison of energy efficiency between ball mills and stirred mills in coarse grinding. *Minerals Engineering 22* , 673-680.

Sotka, P., Lamberg, P., & Lahtinen, M. (2004). *Non-recoverable metals- do you know how much you have?* Retrieved 02 17, 2012, from http://www.outotec.com/19494.epibrw

Souza, R. F., Brandao, P. R., & Paulo, J. B. (2012). Effect of chemical composition on the z-potential of chromite: In Press. *Minerals Engineering* .

Stamboliadis, E. T. (2007). The Energy Distribution Theory of Comminution Specific Surface Energy, mill efficiency and distribution mode. *Minerals Engineering 20* , 140-145.

Sutherland, K. L. (1948). Physical chemistry of flotation. XI: Kinetics of the flotation process. *Journal of Physical and Colloid Chemistry 52.* 394-425.

Tangsathitkulchai, C. (2002). Acceleration of particle breakage rates in wet batch ball milling. *Powder Technology 124* , 67-75.

Tinke, A. P., Govoreanu, R., Weuts, I., Vanhoutte, K., & De Smaele, D. (2009). A review of underlying fundamentals in a wet dispersion size analysis of powders. *Powder Technology 196* , 102-114.

Ulusoy, U., & Kursun, I. (2011). Comparison of different 2D image analysis measurement techniques for shape of talc particles produced by different media milling. *Minerals Egineering 24* , 91-97.

Ulusoy, U., Yekeler, M., & Hicyalmaz, C. (2003). Determinnation of the shape, morphological and wettability properties of quartz and their correlations. *Minerals Engineering 16 (10)* , 951-964.

Unland, G., & Al-Khasawneh, Y. (2009). The influence of particle shape on parameters of impact crushing. *Minerals Engineering 22* , 220-228.

van Schoor, M. (2005). The application of in-mine electrical resistance tomography (ERT) for mapping potholes and other disruptive features ahead of mining. *The Journal of the South African Institute of Mining and Metallurgy 105* , 447-452.

Varinot, C., Hiltgun, S., Pons, M. N., & Dodds, J. (1997). Identification of the fragmentation mechanisms in wet-phase fine grinding in a stirred bead mill . *Chemical Engineering Science 52 (20)* , 3605-3612.

Venkataraman, K. S., & Narayanan, K. S. (1998). Energetics of collision between grinding media in ball mills and mechanochemical effects. *Powder Technology 96* , 190-201.

Viscarra, T. G., Wightman, E. M., Johnson, N. W., & Manlapig, E. V. (2010). The effect of breakage mechanism on the mineral liberation properties of sulphide ores. *Minerals Engineering 23* , 374-382.

Vizcarra, T. G., Wightman, E. M., Johnson, N. W., & Manlapig, E. V. (2011). The effect of breakage method on the shape properties of an iron-oxide hosted copper-gold ore. *Minerals Engineering 24* , 1454-1458.

Walker, W. H., Lewis, W. K., McAdams, W. H., & Gilliland, E. R. (1937). *Priciples of Chemical Engineering.* NY, USA: McGraw-Hill.

Wang, Y., & Forssberg, E. (2000). Technical Note: Product size distribution in stirred media mills. *Minerals Engineering 13* , 459-465.

Weiss. (1985). *SME Mineral Processing Handbook.*

Weller, K. R., & Gao, M. (2000). *Ultra-fine Grinding.* Brisbane: CSIRO.

Wilson, A., & Chunnett, G. (2006). Trace Element and Platinum Group Element Distributions and Genesis of the Merensky Reef, Western Bushvel Complex, South Africa. *Journal of Petrology 47 (12)* , 2369-2403.

Wolmarans, E., & Morgan, P. (2009). Milling circuit selection for the Nkomati 375 ktpm concentrator. *The Journal af South African Institute of Mning and Metallurgy 109* , 653-664.

Wotruba, H., Hoberg, H., & Schneider, F. U. (1991). Investigation on the separation of microlithe and zircon. The influence of particle shape on floatability. Preprints. *XVII Internatianal Mineral Processing Congress IV*, (p. 83). Dresden, Germany.

Xiao, Z., & Laplante, A. R. (2004). Characterizing and recovering the platinum group minerals- a review. *Minerals Engineering 17* , 961-979.

Xu, R., & Di Guida, O. A. (2003). Comparison of sizing small particles using different technologies. *Powder Technolgy 132* , 145-153.

Ye, X., Gredelj, S., Skinner, W., & Grano, S. R. (2010). Regrinding sulphide minerals- Breakage mechanisms in milling and their influence on surface properties and flotation behaviour. *Powder Technology 203* , 133-147.

Yekeler, M., Ulusoy, U., & Hicyilmaz, C. (2004). Effect of particle shape and roughness of talc mineral ground by different mills on the wettability and floatability. *Powder Technology 140* , 68-78.

Yue, J. (2003). *Rheological effects on ultra-fine grinding in stirred mills: Master of Applied Science Thesis.* The University of British Columbia

Yue, J., & Klein, B. (2005). Particle breakage kinetics in horizontal stirred mills. *Minerals Engineering 18* , 325-331.

Zhang, Y. M., & Kavetsky, A. (1993). Investigation of particle breakage mechanisms in a batch ball mill using back-calculation. *International Journal of Mineral Processing 39* , 41-60.

Zheng, X., Johnson, N., & Franzidis, J.-P. (2006). Modelling of etrainment in industrial flotation cells: water recovery and degree of entrainment. *Minerals Engineering 19* , 1191-1203.

Appendix A : Ore preparation and milling

This section contains all the details and figures that were not included in the experimental and results section.

Nkomati ore to be prepared as feed for both ball mill and IsaMill was wet screened to determine its size distribution.

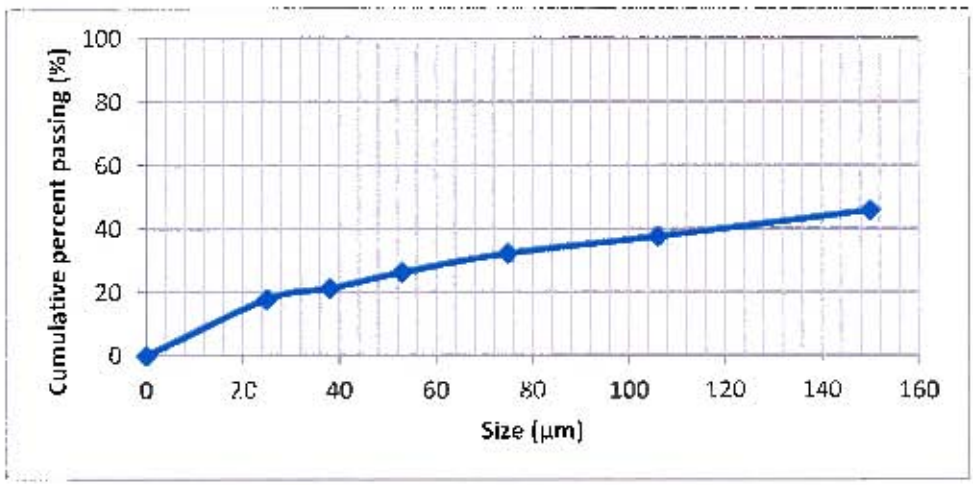

Figure A.1.1: Size distribution of the Nkomati ore stock

Nkomati ore was milled to 80 % passing 106 µm to provide feed for ball mill and IsaMill tests. Determination of the feed size distribution, i.e. 80 % -106 µm, was achieved by crash stopping the mill and taking out a sample for wet screening at 106 µm. The dry sample was weighed to determine the mass passing 106 µm. This was a rough and quick method of determining the time needed to get to 80 % 106 µm. A double check was made after the ore was milled, by wet screening a representative sample though a stack of sieves.

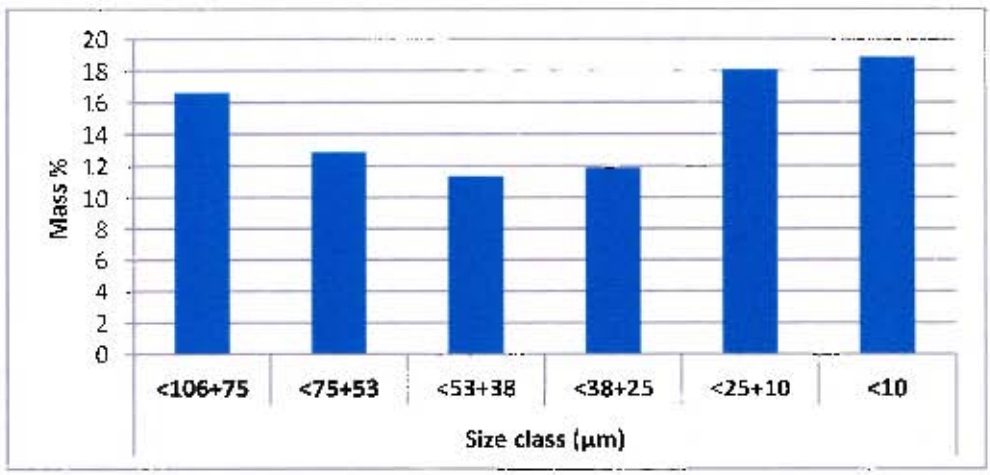

Figure A.1.2: Mass distribution of Nkomati feed into various size classes

A.1 The raw data of the IsaMill runs

Table A.1: Raw data for IsaMill run 1 on Nkomati ore

PASS 1						PASS 2					
Time (minutes)	HH:MM	kWh	Power (kW)	Temp (oC)	Pressure (bar)	Time (minutes)	HH:MM	kWh	Power (kW)	Temp (oC)	Pressure (bar)
0	0.50	18.4	1.9	23.0	0.3	0	0.52	19.07	1.8	33.5	0.5
5	0.50	18.55	2.0	27.0	0.4	5	0.52	19.18	1.9	32.5	0.4
10	0.51	18.7	2.0	27.5	0.4	10	0.52	19.32	1.9	32.5	0.4
15	0.52	18.85	1.9	27.5	0.4	15	0.53	19.46	1.8	32.5	0.4
20	0.52	19	1.9	27.5	0.3	20	0.53	19.6	1.8	32.5	0.4
PASS 3						PASS 4					
Time (minutes)	HH:MM	kWh	Power (kW)	Temp (°C)	Pressure (bar)	Time (minutes)	HH:MM	kWh	Power (kW)	Temp (oC)	Pressure (bar)
0	0.53	19.70	2.2	37.0	0.4	0	0.55	20.30	1.8	38	0.40
5	0.54	19.84	1.8	36.0	0.35	5	0.55	20.43	1.8	38	0.15
10	0.54	19.97	1.8	36.0	0.35	10	0.56	20.53	1.8	38	0.15
15	0.54	20.11	1.8	36.0	0.35	15	0.56	20.66	1.8	38	0.15
20	0.55	20.26	1.8	36.0	0.3	20	0.57	20.79	1.8	37.5	0.15
25						25	0.57	20.89	1.8	36	0.20

Table A.2: Conditions for IsaMill operation

Run number:	1	2	3
Date:	22/ 06/ 2010	31/08/2010	19/08/2011
Media type:	MT1	MT1	MT1
Initial Media Mass (kg):	4.642	4.704	5.754
Final Media mass (kg):			
Qslurry (l/min):	1.5	27.115	
Pump speed (?):	65		
Mill speed (rpm?):	1528	66	
Slurry SG:	1.03	1529	

Table A.3: Raw data for IsaMill run 2 on Nkomati ore

Pass 1					Pass 2				
Time (minutes)	kWh	Power (kW)	Temp (0C)	Pressure (bar)	Time (minutes)	kWh	Power (kW)	Temp (0C)	Pressure (bar)
0	23.90	1.4	20	0.3	0	24.75	1.9	35	0.5
5	24.02	2	30	0.6	5	24.78	1.8	35	0.4
10	24.17	1.9	30	0.6	10	24.92	1.9	35	0.5
15	24.32	2	30	0.6	15	25.07	1.9	35	0.5
20	24.47	2	30	0.6	20	25.22	1.9	35	0.5
25	24.7	2.2	33	0.2	25	25.37	1.9	35	0.5
Avg.	24.26	1.9	28.8	0.5	Avg.	25.02	1.9	35	0.5
Pass 3					Pass 4				
Time (minutes)	kWh	Power (kW)	Temp (0C)	Pressure (bar)	Time (minutes)	kWh	Power (kW)	Temp (0C)	Pressure (bar)
0	25.48	1.9	35.0	0.4	0	26.19	1.9	38.5	0.3
5	25.54	2.1	40.0	0.3	5	26.23	2.0	40.0	0.3
10	25.67	1.8	38.0	0.4	10	26.40	1.8	40.0	0.4
15	25.81	1.9	38.0	0.4	15	26.54	1.8	40.0	0.4
20	25.96	1.8	38.0	0.4	20	26.68	1.8	40.0	0.4
25	26.1	1.8	37.0	0.4	25	26.82	1.8	38.0	0.3
Avg.	25.816	1.9	38.2	0.4	Avg.	26.47667	1.85	39.42	0.4

Table A.4: Raw data for IsaMill Run 3 on Nkomati ore

Pass 1							Pass 2						
Time (min)	HH: MM	Wh	Power (kW)	Temp (C)	Pressure (bar)	RPM	Time (min)	HH: MM	Wh	Power (kW)	Temp (C)	Pressure (bar)	RPM
0	0.52	6432	2.0	25.0	0.45	1529	0	0.54	7018	2.1	25	0.40	1529
5	0.52	6587	2.3	26.0	0.60	1529	5	0.54	7186	2.1	31	0.55	1529
10	0.53	6763	2.2	26.5	0.60	1529	10	0.54	7346	2.1	32	0.55	1529
15	0.53	6924	2.2	26.5	0.59	1529	15	0.54	7465	2.1	36	0.50	1529
20	0.53	7018	2.1	26.5	0.55	1529	20						
Pass 3							Pass 4						
Time (min)	HH: MM	Wh	Power (kW)	Temp (C)	Pressure (bar)	RPM	Time (min)	HH: MM	Wh	Power (kW)	Temp (C)	Pressure (bar)	RPM
0	0.54	7465	2.1	36.0	0.5	1529	0	0.55	7788	2.2	37	0.50	1529
5	0.55	7527	2.1	37.5	0.5	1529	5	0.56	7943	2.0	36	0.50	1529
10	0.55	7754	2.1	37.5	0.5	1529	10						
15	0.55	7788	2.2	37.5	0.5	1529	15						
20							20						

Table A.5: Raw data for IsaMill Run 1 on UG2 ore

Pass1							Pass 2						
Time (min)	HH: MM	Wh	Power (kW)	Temp (C)	Pressure (bar)	RPM	Time (min)	HH: MM	Wh	Power (kW)	Temp (C)	Pressure (bar)	RPM
0	0.57	1746	1.3	22.0	0.1	1512	0	0.59	2446	2.3	29.0	0.59	1529
5	0.58	1899	2.4	27.0	0.56	1529	5	0.59	2690	2.2	33.0	0.5	1529
10	0.58	2090	2.6	29.0	0.8	1529	10	0.60	2858	2.3	29.0	0.5	1529
15	0.58	2275	2.5	29.0	0.6	1529	15	0.60	3030	2.2	29.0	0.5	1529
20	0.59	2446	2.3	29.0	0.59	1529	20	0.60	3215	2.1	29.0	0.5	1529
Pass 3							Pass 4						
Time (min)	HH: MM	Wh	Power (kW)	Temp (C)	Pressure (bar)	RPM	Time (min)	HH: MM	Wh	Power (kW)	Temp (C)	Pressure (bar)	RPM
0	0.54	7465	2.1	36.0	0.5	1529	0	0.55	7788	2.2	37.0	0.5	1529
5	0.55	7527	2.1	37.5	0.5	1529	5	0.56	7943	2	36.0	0.5	1529
10	0.55	7754	2.1	37.5	0.5	1529	10						
15	0.55	7788	2.2	37.5	0.5	1529	15						
20							20						

A.2 IsaMill signature plots

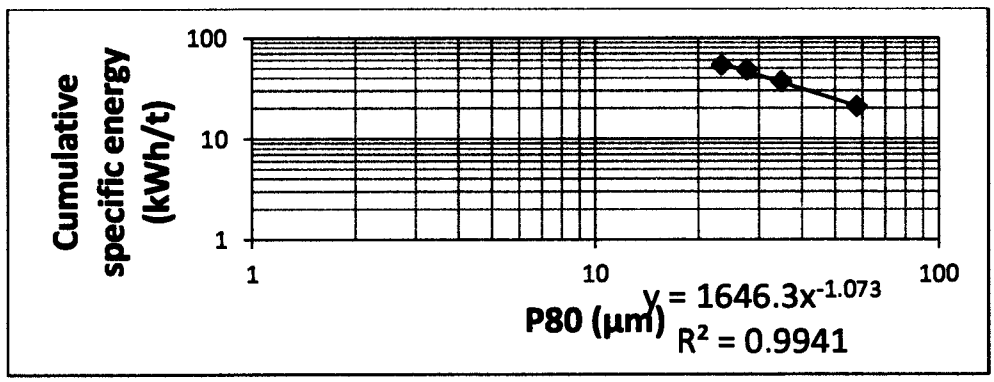

Figure A.2.1: Specific energy for grinding Nkomati ore to a given P80 size

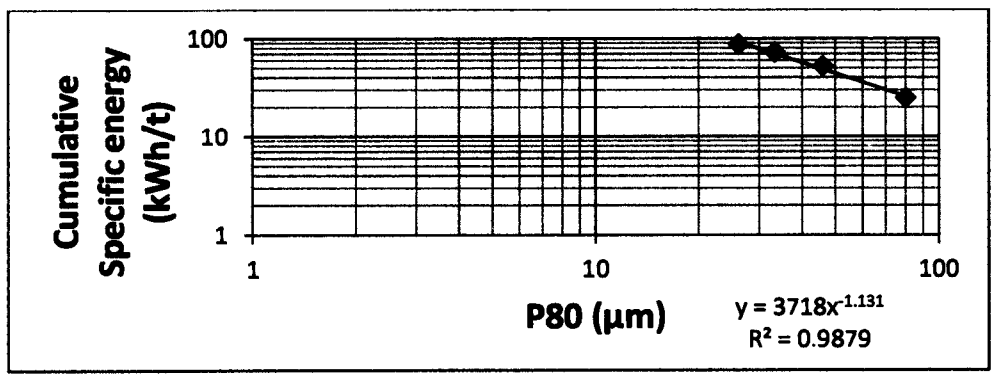

Figure A.2.2: Specific energy for grinding UG2 ore to a given P80 size

Table A.6: PSD data as from Malvern Mastersizer 2000

IsaMill-Nkomati						Ball Mill-Nkomati ore		
Size (μm)	Feed	Pass1	Pass2	Pass3	Pass4	16min	32min	64min
0	0	0	0	0	0	0	0	0
1	1	2	3	4	4	2	2	4
1	1	2	3	4	4	2	3	4
1	1	3	4	5	5	3	3	5
1	2	4	5	6	6	3	4	6
1	2	4	5	7	7	4	5	7
1	2	5	6	8	8	5	5	8
1	3	5	7	9	9	5	6	9
1	3	6	8	10	10	6	7	10
1	4	7	9	11	12	7	8	11
1	4	8	10	13	13	7	9	13
2	4	9	11	14	14	8	10	14
2	5	10	12	15	16	9	11	15
2	5	11	14	17	18	10	12	17
2	6	12	15	18	19	11	13	18
3	7	13	16	20	21	12	14	20
3	7	14	18	22	23	14	16	22
3	8	16	20	24	26	15	17	24
4	9	18	22	26	28	17	19	26
4	11	19	24	29	30	18	21	28
4	12	21	26	31	33	20	23	31
5	13	23	28	34	36	22	25	33
6	15	25	31	36	39	24	27	36
6	17	27	33	39	42	26	30	39
7	19	30	36	42	45	29	32	42
8	21	32	38	45	48	31	35	45
9	23	34	41	48	52	33	38	48
10	25	37	44	51	55	36	40	51
11	27	39	47	54	59	38	43	54
13	29	42	50	58	62	40	46	58
14	32	45	53	61	66	43	49	62
16	34	48	56	65	69	45	52	65
18	36	51	60	68	73	48	56	69
20	38	54	63	72	76	51	59	73
22	40	57	67	75	79	53	63	76
25	42	60	71	78	82	56	66	80

Investigation of the flotation behaviour of ball mill and IsaMill products

IsaMill-Nkomati						Ball Mill-Nkomati ore		
28	45	63	74	81	85	59	70	83
32	47	67	78	84	87	62	74	86
36	49	70	81	86	89	66	77	88
40	51	74	84	89	91	69	81	91
45	54	77	86	90	92	73	84	92
50	56	81	89	92	93	76	87	94
56	59	84	91	93	94	80	90	95
63	62	87	93	94	95	83	92	96
71	65	90	94	95	95	86	94	97
80	68	92	95	96	96	89	96	97
89	71	94	96	96	96	92	97	97
100	74	96	97	96	96	94	98	98
112	78	97	97	97	97	96	98	98
126	81	98	97	97	97	97	99	98
142	84	98	98	97	97	98	99	98
159	87	99	98	97	97	98	99	98
178	89	99	98	97	97	99	99	98
200	91	99	98	97	97	99	99	98

Table A.7: PSD data for UG2 ore as from Malvern Mastersizer 2000

IsaMill- UG2						Ball Mill-UG2		
Size (µm)	Feed	Pass1	Pass2	Pass3	Pass4	16min	32min	64min
0	0	0	0	0	0	0	0	0
1	0	1	1	2	3	1	1	1
1	0	1	2	3	4	1	1	2
1	0	1	2	3	4	1	1	2
1	0	2	3	4	5	1	2	2
1	1	2	3	4	6	1	2	3
1	1	2	4	5	7	2	2	3
1	1	3	4	6	8	2	3	4
1	1	3	5	7	9	2	3	5
1	1	3	5	7	10	3	3	5
1	1	4	6	8	11	3	4	6
2	1	4	7	9	12	3	4	7
2	2	5	7	10	13	4	5	7
2	2	5	8	11	15	4	6	8
2	2	6	9	13	16	5	6	9
3	2	7	10	14	18	5	7	10
3	3	7	11	15	19	6	8	11
3	3	8	12	17	21	7	8	12
4	3	9	13	18	23	7	9	14
4	4	10	14	20	25	8	10	15
4	4	11	16	21	27	9	11	16
5	4	11	17	23	29	10	12	18
6	5	13	19	25	31	10	13	19
6	5	14	20	27	33	11	15	21
7	5	15	22	29	36	12	16	23
8	6	16	24	32	39	14	17	25
9	6	18	26	34	42	15	19	27
10	7	19	28	37	45	16	20	29
11	7	21	31	40	49	18	22	32
13	8	23	33	44	53	19	24	34
14	9	25	36	47	57	21	26	37
16	9	27	40	51	61	23	28	41
18	10	30	43	56	66	25	31	44
20	11	32	47	60	70	27	34	48
22	12	35	51	65	74	29	37	53
25	13	38	56	69	79	32	40	57

IsaMill- UG2						Ball Mill-UG2		
28	14	42	60	74	83	35	44	62
32	15	45	65	78	86	38	48	67
36	17	49	70	82	89	42	53	72
40	18	53	75	86	92	46	58	77
45	20	58	79	89	94	50	63	81
50	21	62	83	92	96	55	68	85
56	23	67	87	94	97	59	73	89
63	26	71	90	96	98	65	78	92
71	28	76	93	97	99	70	83	95
80	31	80	95	98	99	75	87	96
89	35	84	97	99	100	80	91	98
100	38	87	98	99	100	85	94	99
112	42	90	99	99	100	89	96	100
126	47	93	99	100	100	92	98	100
142	52	95	100	100	100	95	99	100
159	56	96	100	100	100	97	99	100
178	61	98	100	100	100	98	100	100
200	66	98	100	100	100	99	100	100

Appendix B : Particle size distribution in the size classes

Nkomati ore milled in the two mills was wet screened to different size classes. These classes were then analysed for particle size distribution to determine the narrowness of the size classes from the two mills.

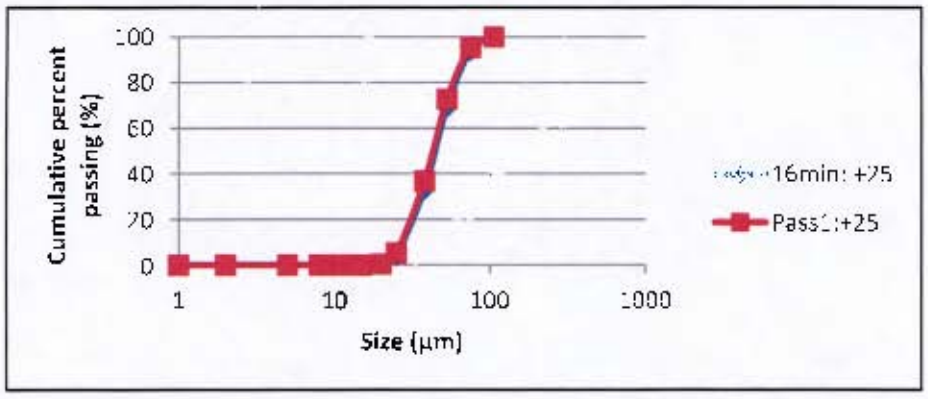

Figure A.2.1: Particle size distribution in the +25 micron fraction for 16 minutes and pass one products

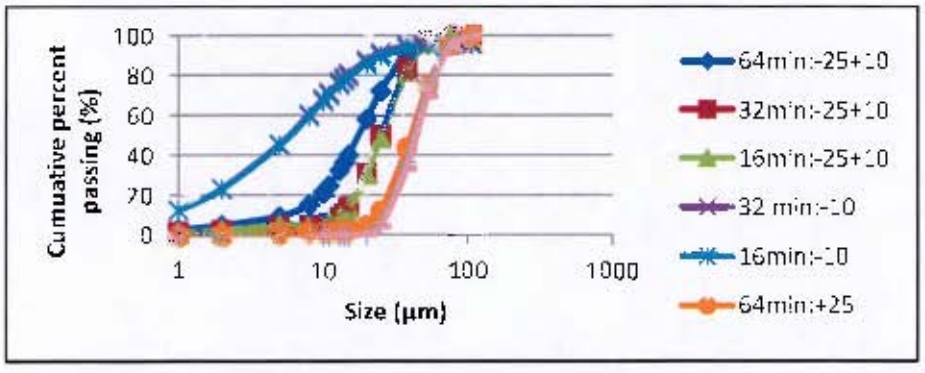

Figure A.2.2: Size distribution within size classes

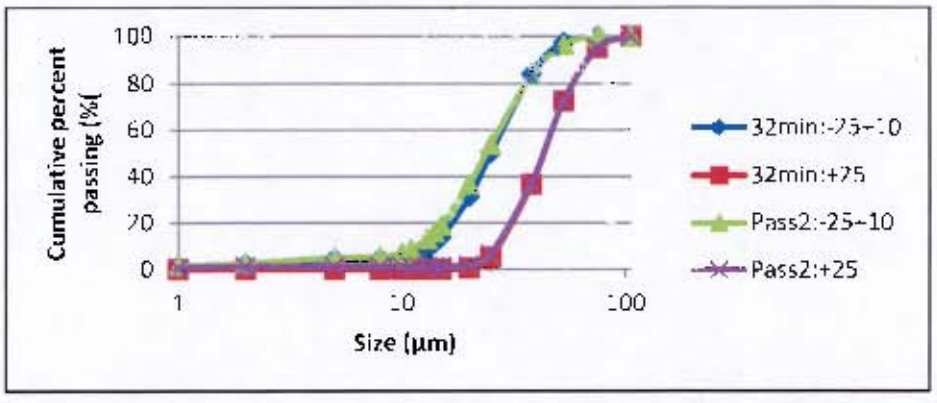

Figure A.2.3: PSD in size fractions of Nkomati ore milled for 32 minutes in ball mill and for two passes in IsaMill

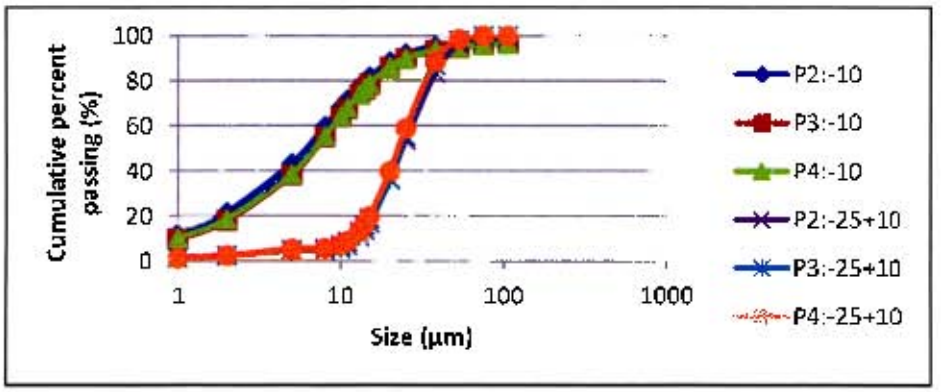

Figure A.2.4: PSD in the size fractions of Nkomati ore milled for different passes in the IsaMill

Appendix C : Particle shape characterisation

Ore samples were filtered through a series of filter papers of varying size. The number of particles was then counting using software. These particles were imaged using SEM.

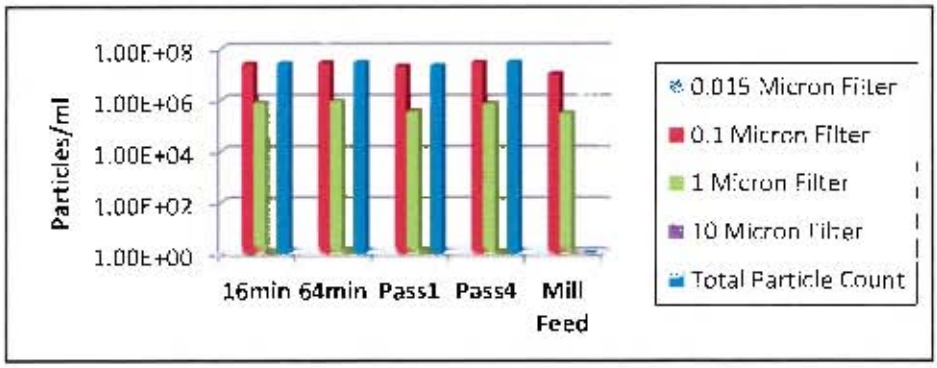

Figure A.2.1: Particle counting of UG2 ore samples filtered through varying filter sizes

Distribution of particle sizes was then represented as a function of the number of particles with that size.

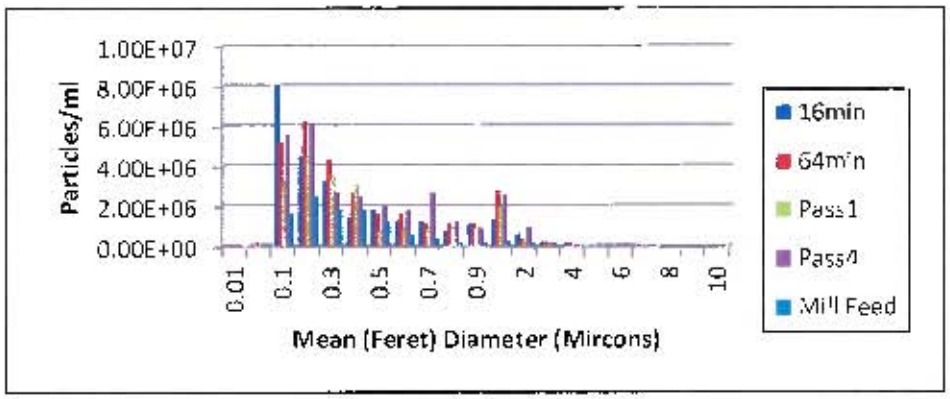

Figure A.2.2: Particle number as a function of particle size

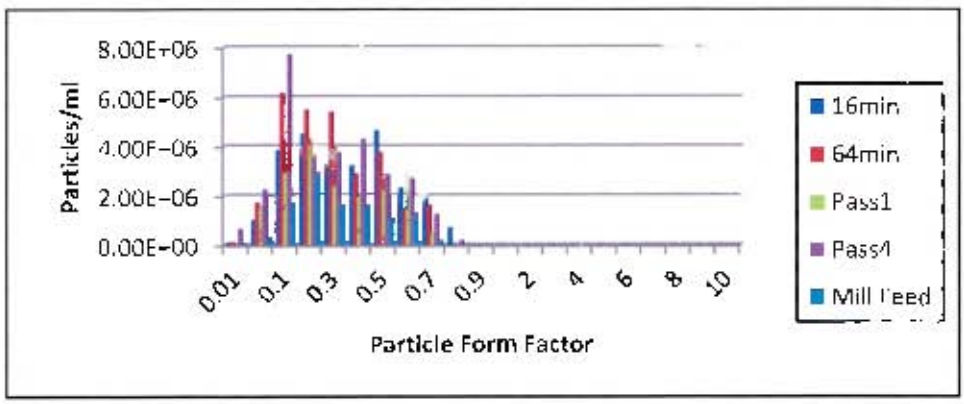

Figure A.2.3: Number of particles as a function of form factor

Appendix D : Scatter diagrams relating the size parameters to each other

D.1 Ball mill Nkomati ore

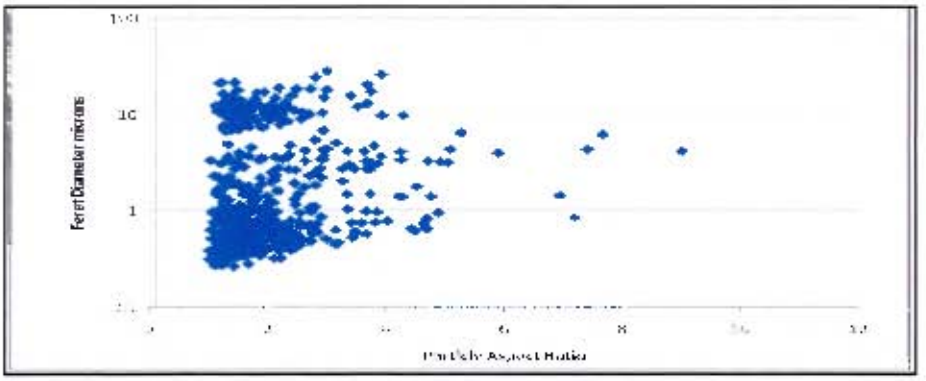

Figure D.1.1: Aspect ratio as a function of feret diameter for Nkomati ore treated in ball mill (16 minutes)

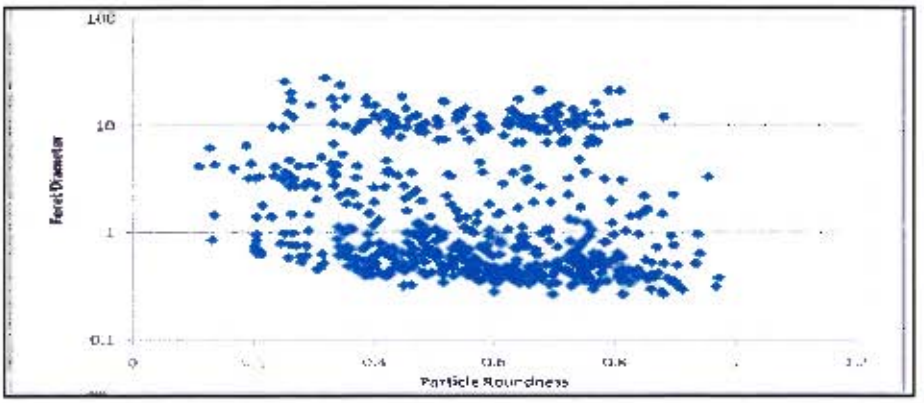

Figure D.1.2: Roundness as a function of feret diameter for Nkomati ore treated in ball mill (16 minutes)

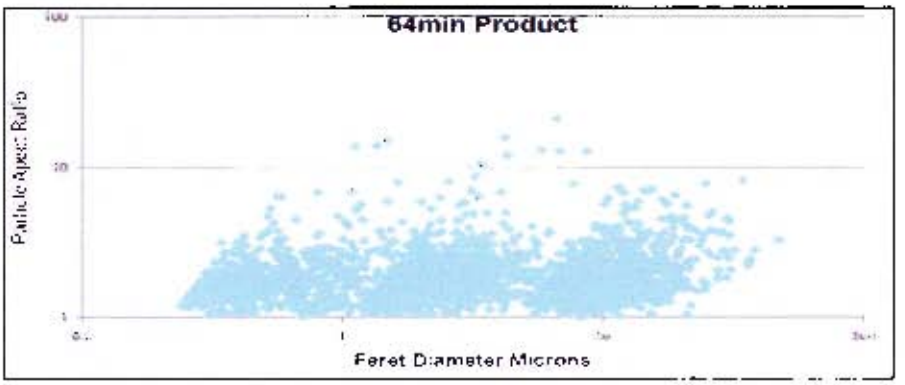

Figure D.1.3: Aspect ratio as a function of feret diameter for Nkomati ore treated in ball mill (64 minutes)

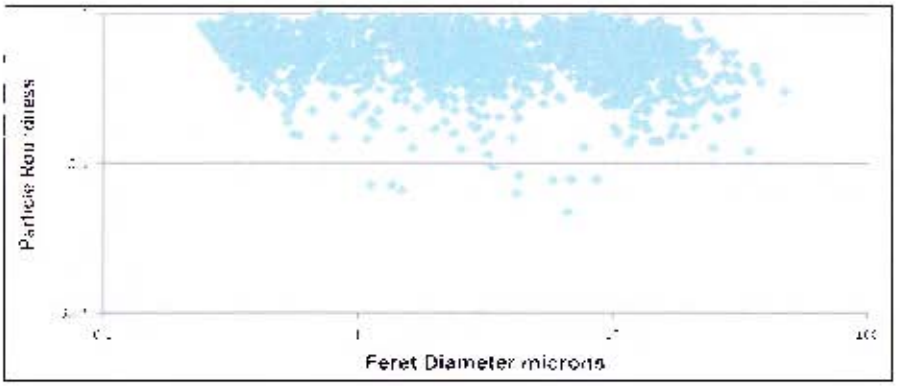

Figure D.1.4: Roundness as a function of feret diameter for Nkomati ore treated in ball mill (64 minutes)

D.2 UG2 ore treated with a ball mill

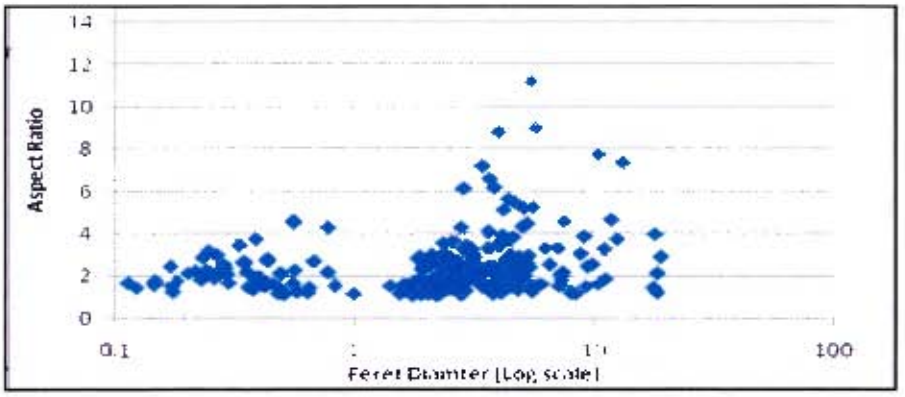

Figure D.2.1: Aspect ratio as a function of feret for UG2 mill feed

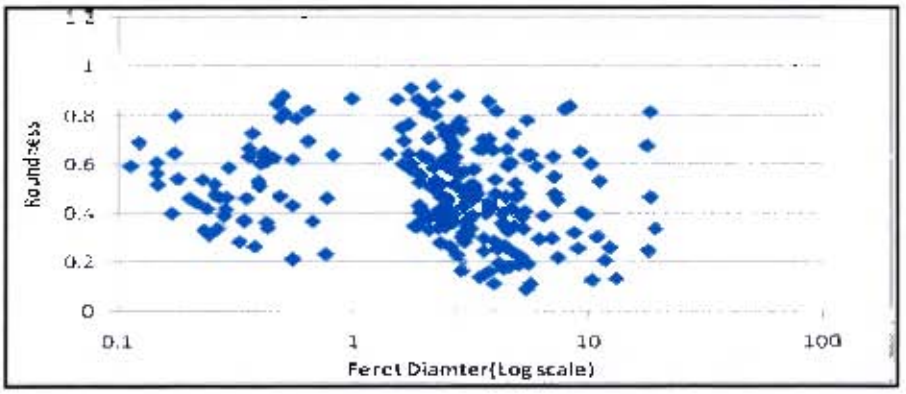

Figure D.2.2: Roundness as a function of feret diameter for UG2 mill feed

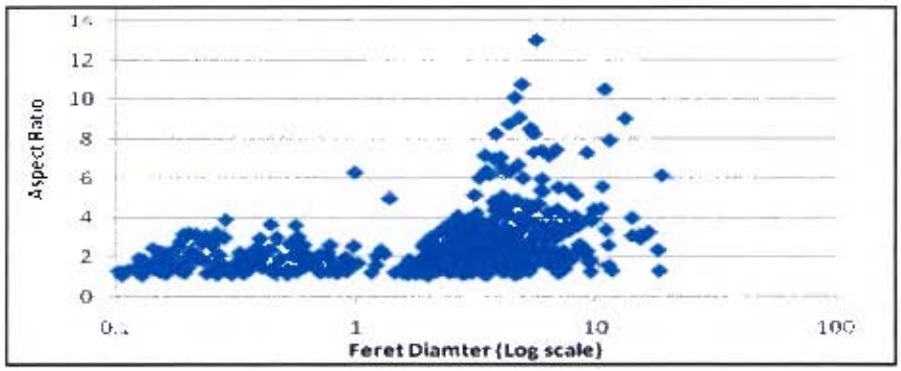

Figure D.2.3: Aspect ratio as a function of feret diameter for UG2 ore treated in a ball mill (16min)

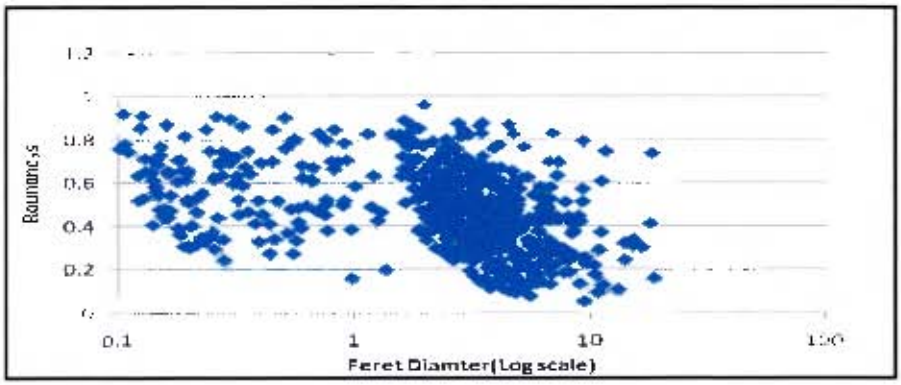

Figure D.2.4: Roundness as a function of feret diameter for UG2 ore treated in a ball mill (16 minutes

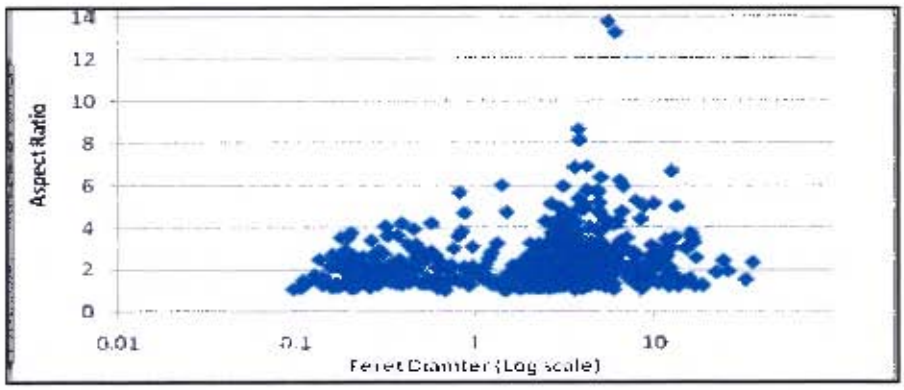

Figure D.2.5: Aspect ratio as a function of feret diameter for UG2 treated in ball mill (64 minutes)

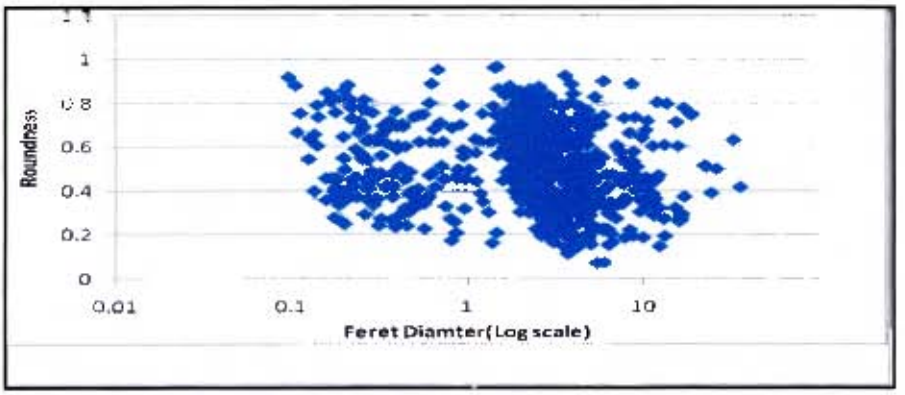

Figure D.2.6: Roundness as a function of feret diameter for UG2 treated in ball mill (64 minutes)

D.3 Nkomati ore treated with M4 IsaMill

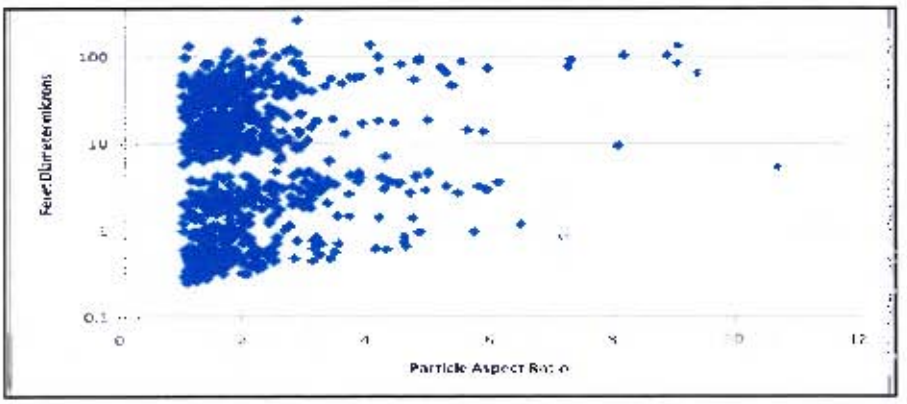

Figure D.3.1: Aspect ratio as a function of feret diameter for Nkomati ore treated with IsaMill (1 pass)

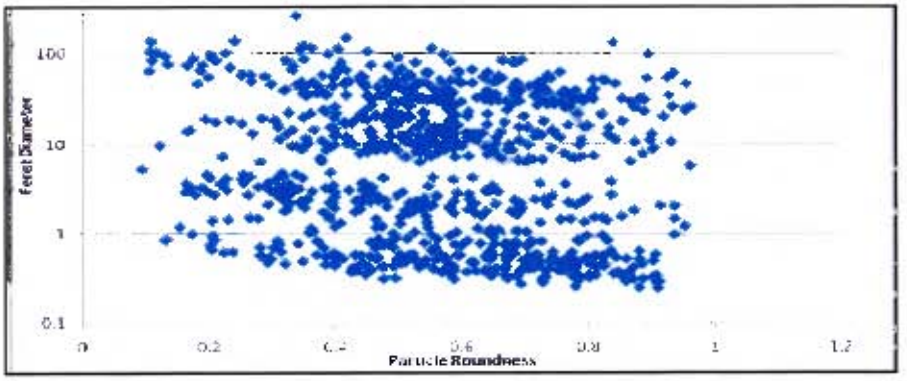

Figure D.3.2: Roundness as a function of feret diameter for Nkomati ore treated in IsaMill (1 pass)

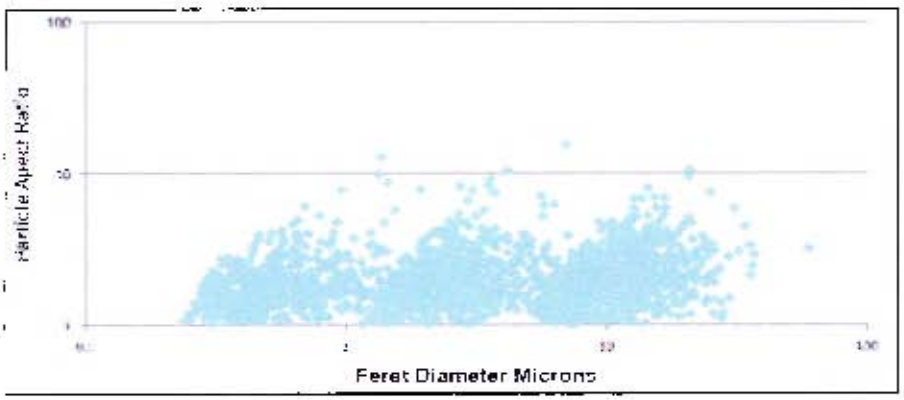

Figure D.3.3: Aspect ratio as a function of feret diameter for Nkomati ore treated with IsaMill (4 pass)

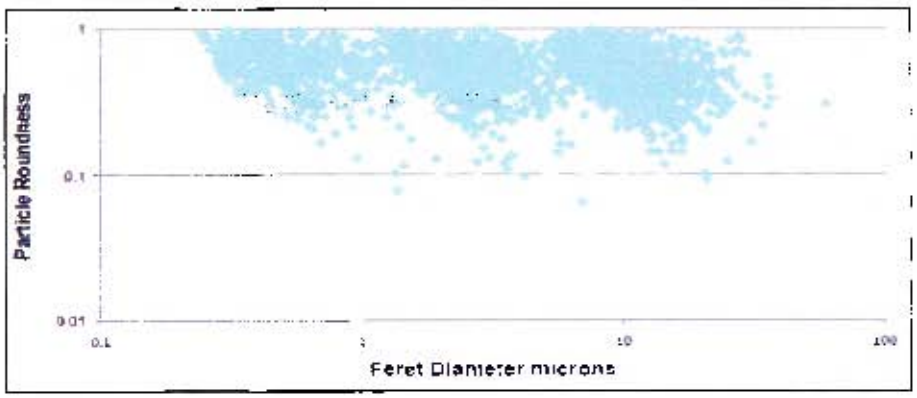

Figure D.3.4: Roundness as a function of feret diameter for Nkomati ore treated with IsaMill (4 pass)

D.4 UG2 ore treated with IsaMill

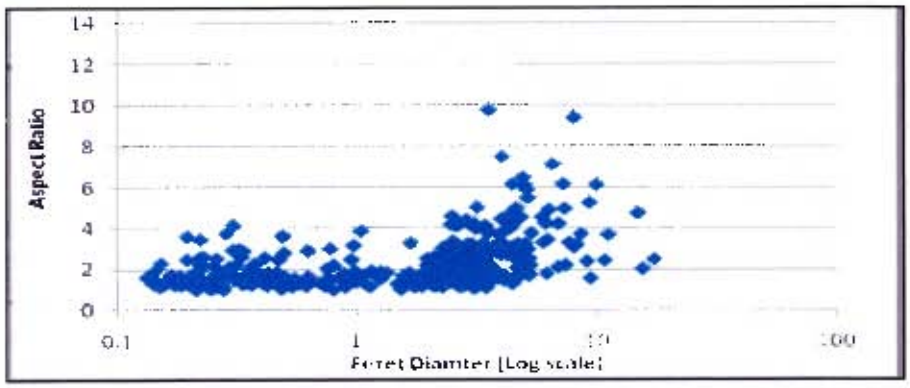

Figure D.4.1: Aspect as a function of feret diameter for UG2 ore treated with IsaMill (1 pass)

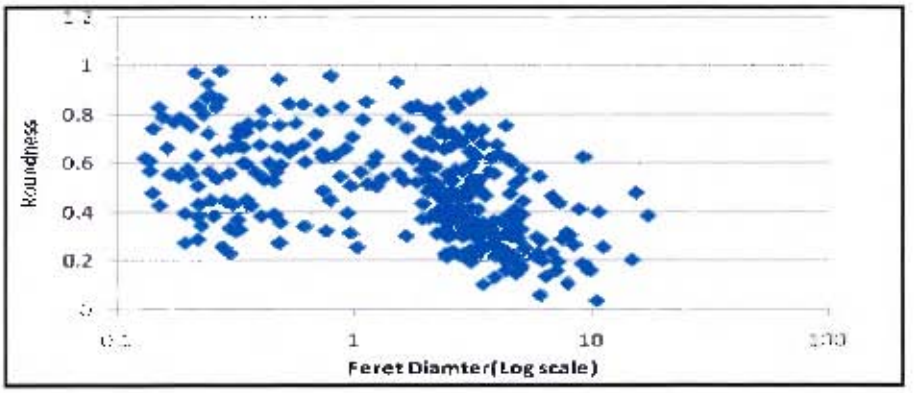

Figure D.4.2: Roundness as a function of feret diameter for UG2 ore treated with IsaMill (1 pass)

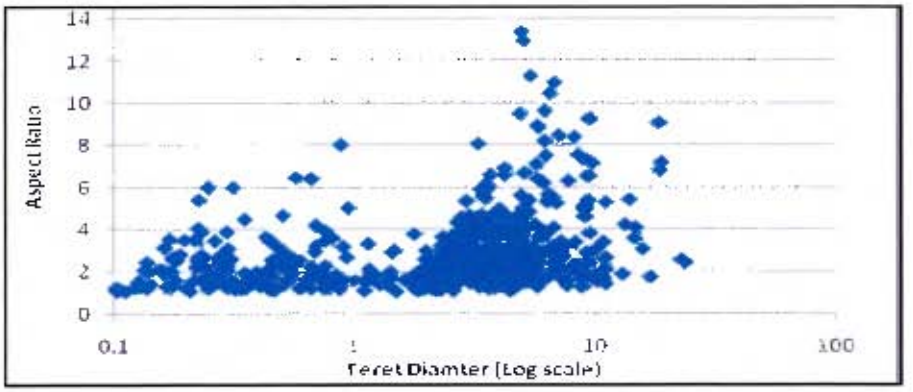

Figure D.4.3: Aspect ratio as a function of feret diameter for UG2 ore treated with IsaMill (4 pass)

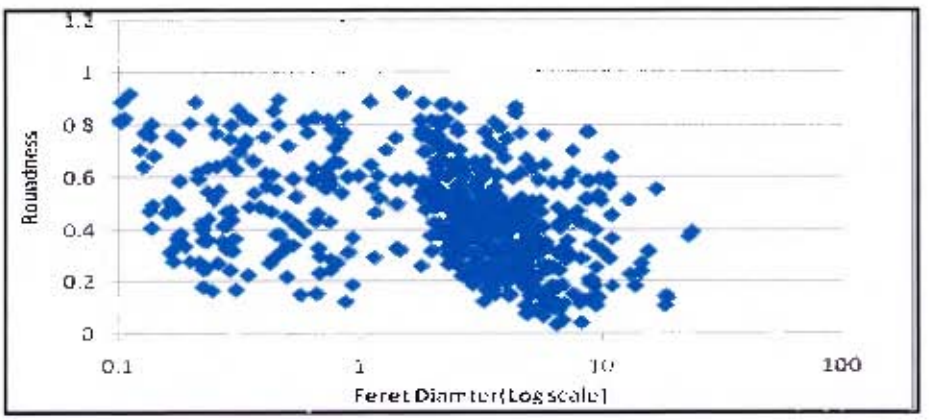

Figure D.4.4: Roundness as a function of feret diameter for UG2 ore treated with IsaMill (4 pass)

Appendix E : Rheology

E.1 Particle size distribution of ore samples used for rheology tests

The mill product were wet screened at 25 µm and the – 25 µm material were used for rheology tests. The sieved samples were analysed for particle size distribution using laser diffraction (Malvern Mastersizer 2000). The size distributions are shown here.

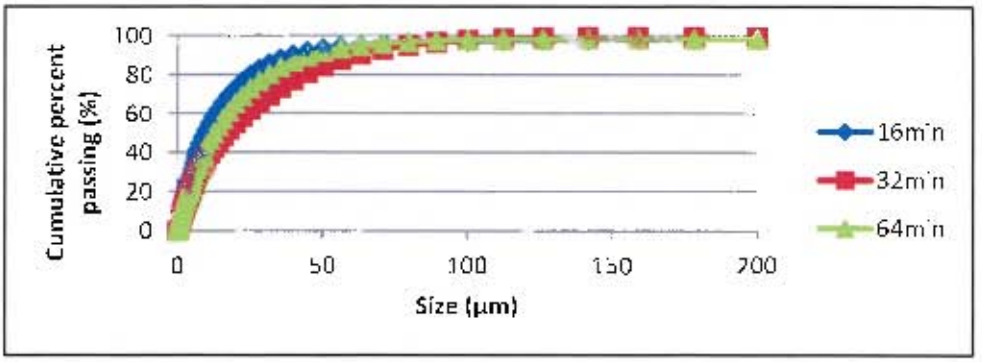

Figure E.1.1: PSD of the -25 um material of Nkomati ore milled in the ball mill for different times

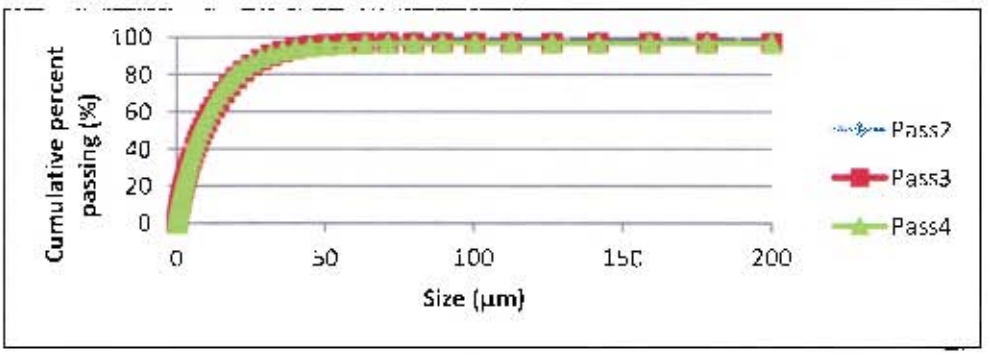

Figure E.1.2: PSD of the -25 um material of Nkomati ore milled in the IsaMill for different passes

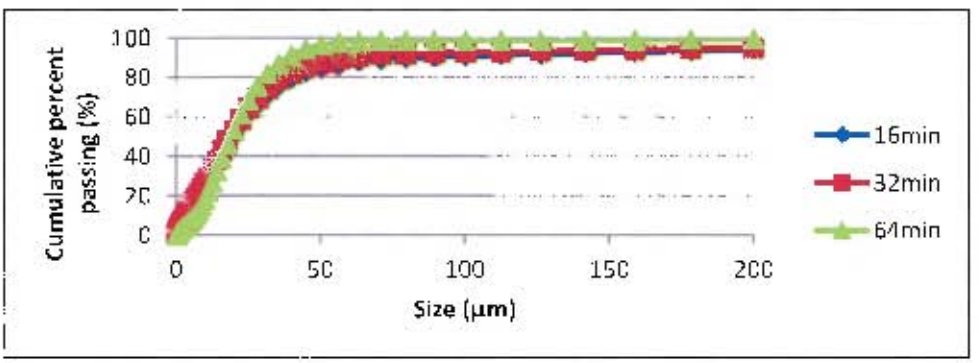

Figure E.1.3: PSD of the -25 um material of UG2 ore milled in the ball mill for different times

Nkomati ore milled for one pass in the IsaMill was not analysed for PSD in the -25 µm. UG2 ore milled for one to four passes in the IsaMill were also not analysed for PSD in the -25 µm. The figures shown in this section illustrate that the PSDs in this fraction were similar for ores milled for different grinding times.

E.2 Flow curves

The flow curves of the slurry samples at 10, 20, 30 and 40 % solids volume concentration were obtained for the products of the two mills. Flow curves show the variation of shear stress as a function of shear rate. In the following figures, the shear stress was plotted on the logarithmic scale in order to maintain clarity.

E.3 Flow curves of Ball Mill products

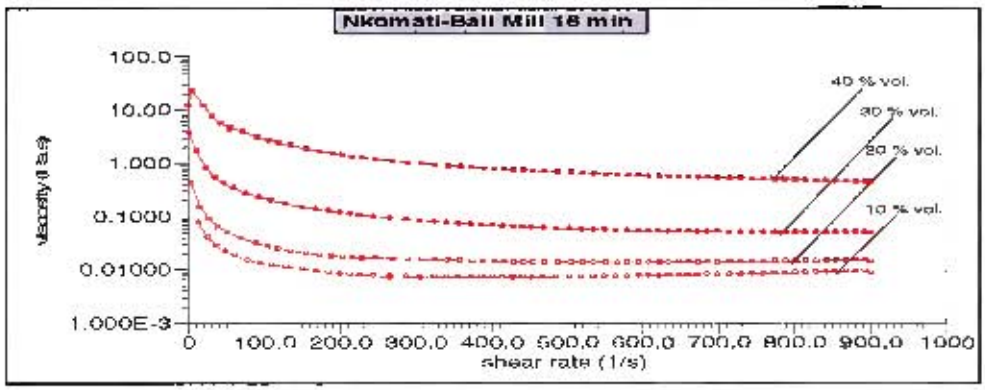

Figure E.3.1: Viscosity as a function of shear rate for Nkomati ore milled for 16 minutes in a ball mill

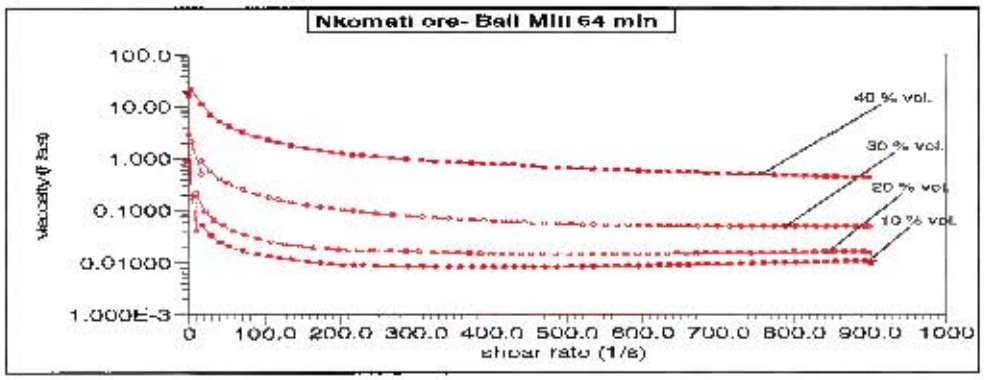

Figure E.3.2: Viscosity as a function of shear rate for Nkomati ore milled for 64 minutes in a ball mill

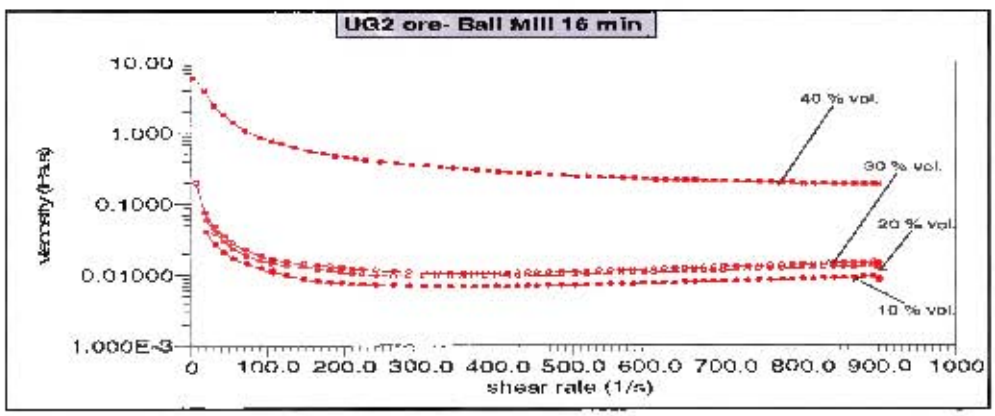

Figure E.3.3: Viscosity as a function of shear rate for UG2 ore milled in a ball mill for 16 minutes

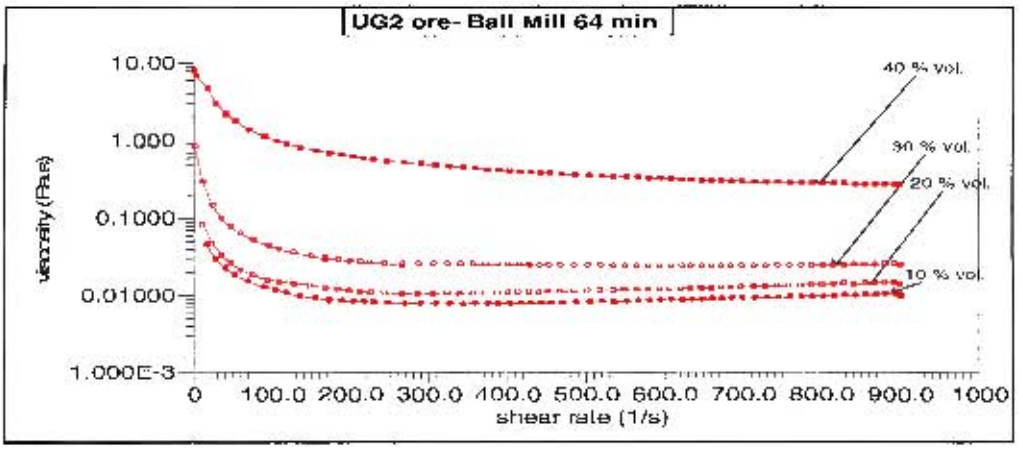

Figure E.3.4: Viscosity as a function of shear rate for UG2 ore milled for 64 minutes in a ball mill

E.4 Flow curves of IsaMill products

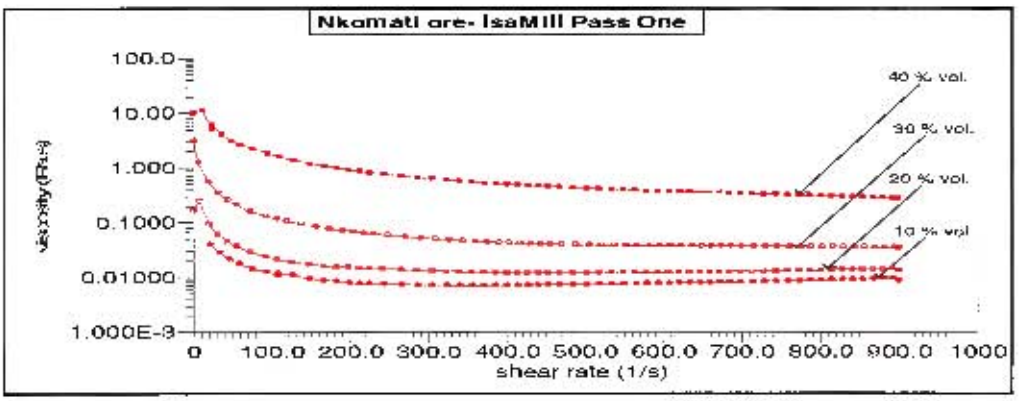

Figure E.4.1: Viscosity as a function of shear rate for Nkomati ore milled for one pass in the IsaMill

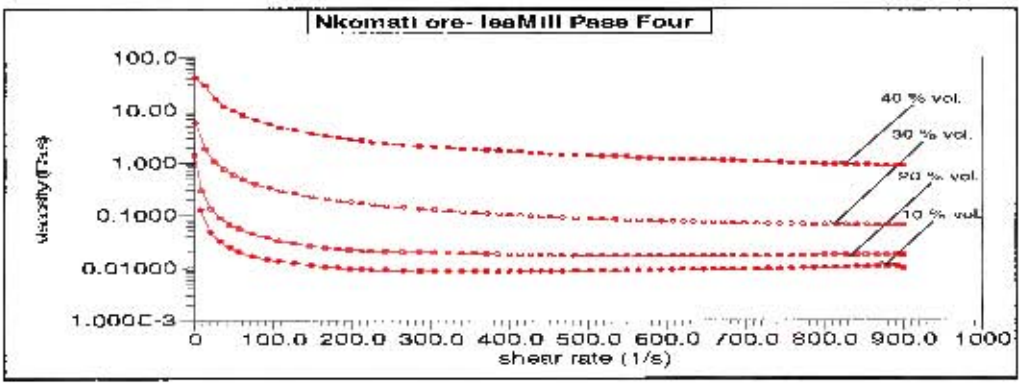

Figure E.4.2: Viscosity as a function of shear rate for Nkomati ore milled for four passes in the IsaMill

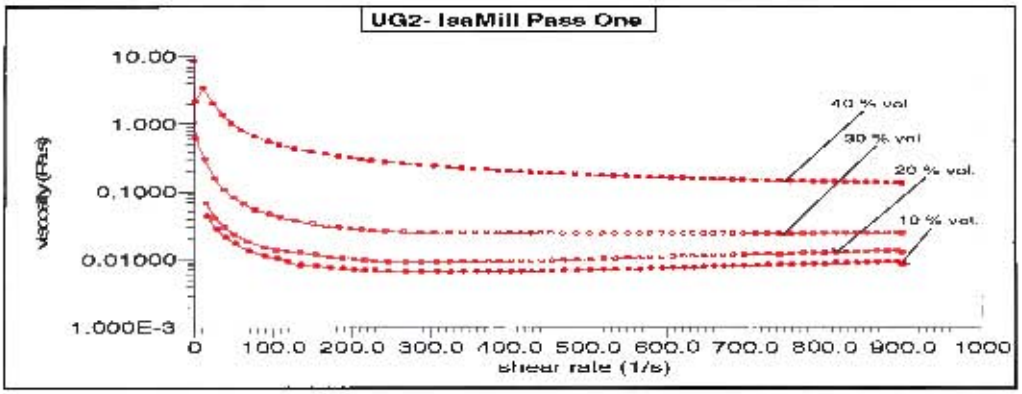

Figure E.4.3: Viscosity as a function of shear rate for UG2 ore milled for one pass in the IsaMill

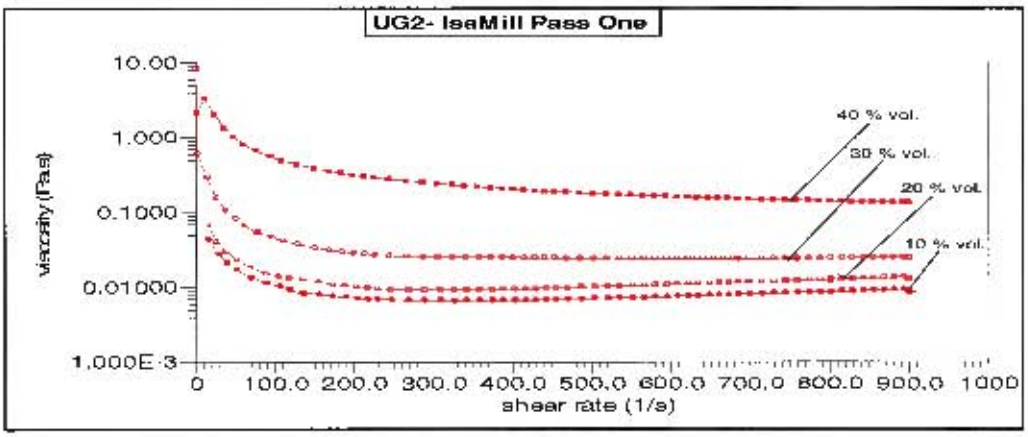

Figure E.4.4: Viscosity as a function of shear rate for UG2 ore milled for one pass in the IsaMill

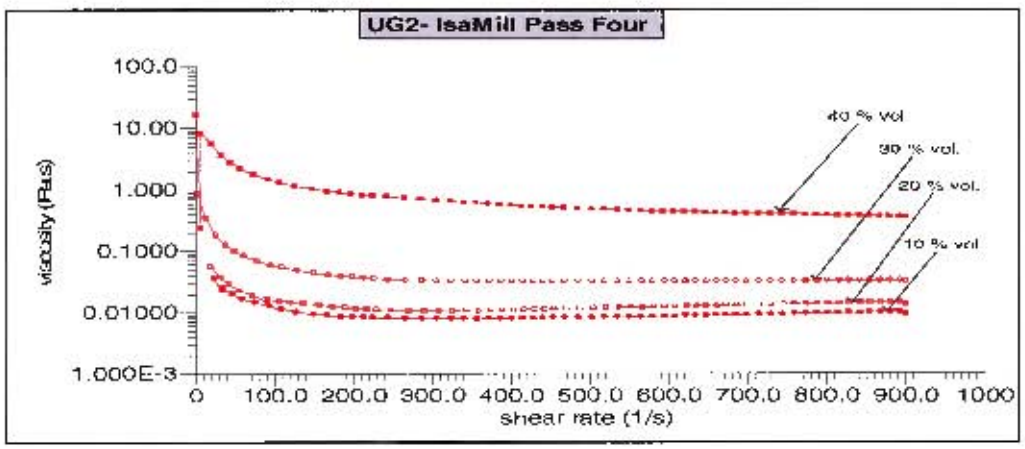

Figure E.4.5: Viscosity as a function of shear rate for UG2 ore milled for four passes in the IsaMill

Appendix F: Flotation

F.1 Raw data

Table F.1: Example of Batch flotation raw data (Ball mill (64min), Nkomati ore)

Tota	1000.7							
	C1	C2	C3	C4	FEED	TAILS1	TAILS2	TAILS3
C + PAPER	87.57	55.07	26.65	17.88	17.75	18.84	18.64	779.1
PAPER	3.38	3.29	3.28	3.28	3.46	3.42	3.29	7.53
CONC.	84.14	51.73	23.37	14.1	14.29	15.42	15.35	771.57
B + H2O	572.09	576.21	576.15	579.2				
BOTTLE	440.28	457	365.77	197.33				
H20	131.81	119.21	210.38	381.27				
D + C + H20	877	820.3	716.2	804.7				
DISH	250.11	236.19	237.45	248.34				
C + H20	626.89	584.11	478.75	555.76				
H20 REC.	410.94	413.17	245.00	160.39				

Table F.2: Example of Batch flotation raw data (Ball mill (64min), UG2 ore)

Total	1000.23							
	C1	C2	C3	C4	FEED	TAILS1	TAILS2	TAILS3
C + PAPER	48.38	34.47	23.39	17.78	21.3	17.18	20.09	842.5
PAPER	3.21	3.25	3.15	3.26	3.2	3.08	3.41	7.5
CONC.	45.17	31.22	20.24	14.52	18.1	14.09	16.68	835
B + H2O	576.76	549.22	561.98	575.02				
BOTTLE	496.53	331.08	394.57	301.24				
H20	80.23	218.14	167.41	273.78				
D + C + H20	653.6	777.48	664.54	706.91				
DISH	249.17	249.79	251.38	236.94				
C + H20	404.43	527.69	413.16	469.97				
H20 REC.	273.03	278.33	225.51	181.67				

Table F.3: Example of chromite assay results

				METHOD USED	
				Fire assay	Wet Chem
				ELEMENT	
				4E-Pgm	Cr_2O_3
SAMPLE ID	GRADE	SDATE	LAB ID	g/t	%
16min-C:-25		26-Sep	No.: 61968		1.26
16min-C:-25+10		26-Sep	No.: 61969		2.61
16min-C:-10		26-Sep	No.: 61970		7.26
16min-T3:+25		26-Sep	No : 61971		15.89
16min-T3:-25+10		26-Sep	No.: 61972		18.37
16min-T3:-10		26-Sep	No.: 61973		14.46
Pass1-C:-25		26-Sep	No.: 61974		0.91
Pass1-C:-25-10		26-Sep	No.: 61975		2.54
Pass1-C:-10		26-Sep	No.: 61976		9.54
Pass1-T3:-25		26-Sep	No.: 61977		13.70
Pass1-T3:-25+10		26-Sep	No.: 61978		19.28
Pass1-T3:-10		26-Sep	No.: 61979		14.78
64min-C1:-25		26-Sep	No.: 61980		0.98
64min-C1:-25-10		26-Sep	No.: 61981		2.67
64min-C1:-10		26-Sep	No.: 61982		8.04
64min-C2:-25		26-Sep	No.: 61983		1.00
64min-C2:-25-10		26-Sep	No.: 61984		2.32
64min-C2:-10		26-Sep	No.: 61985		8.50
64min-C3:-25		26-Sep	No.: 61986		0.94
64min-C3:-25+10		26-Sep	No.: 61987		2.35
64min-C3:-10		26-Sep	No.: 61988		8.95
64min-C4:+25		26-Sep	No.: 61989		1.1
64min-C4:-25+10		26-Sep	No.: 61990		3.02
64min-C4:-10		26-Sep	No.: 61991		10.39
64min-T3:-25		26-Sep	No.: 61992		11.73
64min-T3:-25-10		26-Sep	No.: 61993		17.87
64min-T3:-10		26-Sep	No.: 61994		15.31
Pass4-C1:-25-10		26-Sep	No.: 61995		8.27
Pass4-C1:-10		26-Sep	No.: 61996		12.73
Pass4-C2:-25-10		26-Sep	No.: 61997		3.57
Pass4-C2:-10		26-Sep	No.: 61998		11.81
Pass4-C3:-25-10		26-Sep	No.: 61999		3.70
Pass4-C3:-10		26-Sep	No.: 62000		12.53
Pass4-C4:-25+10		26-Sep	No.: 62001		3.96
Pass4-C4:-10		26-Sep	No.: 62002		13.43
Pass4-T3:-25-10		26-Sep	No.: 62003		16.04

Pass4-T3:-10		26-Sep	No.: 62004		17.35

F.2 Recovery and grade calculations

The recovery and grade equations used in the calculations were as shown in the experimental section.

F.3 Chalcopyrite, pentlandite and pyrrhotite calculations

The mass of the sulphide minerals were calculated based on the following molecular formulae of the minerals: $CuFeS_2$ (chalcopyrite), Fe Ni S or $(Fe, Ni)_9S_8$ (Pentlandite) and Fe S or $FeS_{1.06}$ (pyrrhotite).

The mass of copper and the stoichiometric ratio of copper and sulphur in chalcopyrite were used to calculate the mass of sulphur in chalcopyrite. Mass of copper, nickel and sulphur was obtained using XRF analysis results together with batch flotation mass pull data.

$$m_{Cu,Ch} = \frac{M_{Cu}}{M_{Ch}} * m_{Ch}$$

$$m_{S,Ch} = 2 * \frac{M_S}{M_{Ch}} * m_{Ch}$$

In a similar manner, the mass of nickel was used together with the stoichiometry between nickel and sulphur in pentlandite to calculate the amount of sulphur in pentlandite.

$$m_{Ni,Pn} = 9 * \frac{M_{Ni}}{M_{Pn}} * m_{Pn}$$

$$m_{S,Pn} = 8 * \frac{M_S}{M_{Pn}} * m_{Pn}$$

The mass of sulphur in pyrrhotite was calculated as the difference between total mass of sulphur and the mass of sulphur in both chalcopyrite and pentlandite.

$$m_{S,Po} = m_{S,tot-}(m_{S,Ch} + m_{S,Pn})$$

The fraction of sulphur in pyrrhotite was then used to calculate the mass of pyrrhotite.

$$m_{S,Po} = 1.06 * \frac{M_S}{M_{Po}} * m_{Po}$$

The symbols are as follows: $m_{x,y}$ indicates mass of element x in mineral y; M_z indicates molar mass of element or mineral z; m_i indicates mass of mineral i; Ch is chalcopyrite; Pn is pentlandite; Po is pyrrhotite. The elements retain their universal symbols.

Thereafter the grade and recovery for each mineral were calculated as outlined in the experimental section.